TRANSIENT FREQUENCY DEVIATION CONSIDERATIONS IN POWER SYSTEM STABILITY STUDIES

M. Y. AKHTAR, B.Sc. (Eng.), B.E. (Hons.),
C. Eng., M.I.E.E.

Submitted in partial fulfilment of the requirements
for the Degree of Doctor of Philosophy in
The Australian National University

October 1968

Department of Engineering Physics,
Research School of Physical Sciences,
THE AUSTRALIAN NATIONAL UNIVERSITY,
CANBERRA. A.C.T.

DECLARATION

I declare that this thesis reports my own original work, that no part of the thesis has been accepted or presented for the award of any degree or diploma by any university, and that to the best of my knowledge the thesis contains no material previously published or written by another person except where due reference is given by direct credit in the text or in the bibliography.

....

M. Y. Akhtar,
Canberra.
October, 1968.

PREFACE

This thesis is concerned with the development of suitable methods to represent power system elements as frequency-dependent in system stability studies, employing digital computers. The object has been to bring calculated performance closer to actual performance. The methods developed are applicable to both transient stability (first swing) and dynamic stability (multi-swing) studies, but, due to lack of appropriate information, the studies presented herein have been restricted to transient intervals.

Regarding the contents of the various sections: section 1 presents a historical development of the problem of transient stability and its solution; section 2 describes the assessment of instantaneous frequency; section 3 deals with the detailed representation of synchronous machines, including the effect of instantaneous frequency deviations on machine e.m.f., stored energy and machine reactance, as well as on transient torques; section 4 deals with a treatment of transmission network damping; section 5 presents a frequency-dependent representation of system loads; section 6 integrates the work of the previous four sections to produce a comprehensive transient stability study incorporating all refinements; section 7 presents a general discussion; section 8 gives recommendations for further work; section 9 concludes the main thesis presentation; section 10 presents the mathematical derivations involved in sections 2 to 5, and section 11 presents key references and selected bibliography.

Regarding the originality of the material presented herein; the methods developed in section 2.2.2 (determining the instantaneous frequency); section 3.2.1 (considering variations of machine e.m.f., angular momentum and machine reactance); section 3.2.2 (considering the transient torques); section 4.1 (considering transmission network damping); section 5.1 (representing induction motors as frequency-dependent loads); and in section

5.2 (representing static frequency-dependent loads) are claimed to be original, and have resulted in the following papers: -

Published:

AKHTAR, M. Y., "Frequency-dependent dynamic representation of induction motor loads." Proc. IEE, Vol. 115, No. 6, June 1968, pp. 802-812.

Accepted for Publication by IEE (London):

AKHTAR, M. Y., "Frequency-dependent power-system static-load characterics."

AKHTAR, M. Y., "Transient damping torques in synchronous machines during disturbances."

AKHTAR, M. Y. and KANEFF, S., "Damping in transmission systems under transient conditions."

AKHTAR, M. Y., "A comprehensive consideration of instantaneous frequency deviations in power system transient stability studies."

Submitted for Publication to IEE (London):

KANEFF, S. and AKHTAR, M. Y., "Influence of synchronous machine rotor angular velocity variations in transient stability studies."

ACKNOWLEDGEMENTS

The author is highly indebted to his supervisor, Dr. S. Kaneff, for proposing the research study and for valuable suggestions, guidance, discussion and encouragement throughout the project. The author would like to record appreciation to Prof. G. Newstead, Department of Engineering Physics, Australian National University, and Prof. J. L. Woodward, Department of Electrical Engineering, University of Adelaide, for providing facilities in their respective departments; to the Electricity Trust of South Australia for providing useful information on power system parameters; to the Commonwealth of Australia and Pakistan Governments for providing the opportunity of scholarship; and to the West Pakistan University of Engineering and Technology for granting study leave since March 1965.

CONTENTS

SUMMARY

In comprehensive transient and dynamic power system stability studies, the effects of change in instantaneous operating frequency have been hitherto neglected, partly due to lack of adequate methods of treatment, and partly due to considering (erroneously) such effects as insignificant. The present study has shown that neglect of changes in instantaneous frequency in transient stability studies can at the worst give an erroneous assessment of stability and even at best can result in a substantially different picture of current and voltage distribution throughout the system when compared with calculations including transient frequency changes.

Methods have been developed to include transient frequency effects in the various power system elements as follows:-

> A simple vector method, employing the various synchronous machine e.m.f's behind their saturated quadrature axis reactances, in conjunction with the instantaneous system admittance matrix, evaluates the instantaneous frequencies of the various bus voltages and branch currents.
>
> Synchronous machine e.m.f's and angular momenta are modified in a manner directly proportional to the instantaneous rotor speed to take account of instantaneous rotor angular velocity variations.
>
> Synchronous machine damping torques (which may be positive or negative depending on rotor slip with respect to the resultant air gap flux) are treated by employing asynchronous characteristics in conjunction with the rotor slip while taking the asynchronous output as proportional to the square of the instantaneous magnitude of the resultant air gap flux.

Transmission network parameter variations due to transient frequency excursions are adjusted on the basis of the instantaneous frequencies of bus voltages for shunt branches and of branch currents for series branches.

To handle induction motor loads on a dynamic and frequency-dependent basis, a method employing the property of linearity of the operating characteristics of an induction motor (within the normal operating range of slip) has been developed. This method allows single motors or groups of induction motors to be represented through the use of the more commonly available parameters - horsepower, inertia factor, full load slip, power factor, magnetising current and efficiency. As a consequence of this approach, a reasonable accuracy in predicted performance is achieved in the absence of accurate equivalent circuit parameters, even when using groups of assembled curves of representative machine parameters.

Static frequency-dependent loads (for example, mercury arc rectifiers, arc furnaces, discharge lamps and electric welders), are taken account of by a method which employs current-dependent instantaneous effective resistance and frequency-dependent inductive reactance, which conforms to the appropriate practical characteristics.

When the above refinements are added in transient stability studies, it has been found that assessment of power system behaviour differs significantly from studies which ignore transient frequency deviation effects. Depending on system configuration and parameters, the refinements introduced in this report can show a system to have a greater or lesser margin of stability than that assessed for the system if the refinements are not included. Even in a case where, when including the refinements, the system appears still to have an enhanced margin of stability, network current and voltage distributions calculated without the refinements can nevertheless cause erroneous protective relay settings. Consequently, it is recommended that in spite of the added computing time necessary, instantaneous frequency deviation effects are well worth incorporating in accurate power system transient stability studies.

LIST OF SYMBOLS

ac	-	Specific electric loading in Amp. Cond./m.
B	-	Specific magnetic loading in Wb./Sq.m.
C	-	Series compensating capacitance.
C'&C'_j	-	Slope of the stator current-slip characteristic.
d	-	Rotor diameter of an induction motor.
E_m	-	E.M.F. of machine m.
E_o	-	Load terminal voltage.
E_Q	-	E.M.F. behind X_q.
E_q	-	Internal machine voltage proportional to field current.
E_d	-	Internal machine voltage proportional to quadrature axis rotor current.
E'_d	-	Internal machine voltage proportional to quadrature axis flux linkages.
E'_q	-	Internal machine voltage proportional to direct axis flux linkages.
E_p	-	Voltage behind Potier reactance (X_p).
E_i	-	Voltage behind direct axis transient reactance (X'_d).
f	-	Instantaneous frequency.
f_o	-	System nominal frequency.
f_r	-	Instantaneous frequency corresponding to actual speed of synchronous machine rotor.
f_k	-	Instantaneous frequency of voltage at bus k.
$f_{k\ell}$	-	Instantaneous frequency of current through branch, $k-\ell$.

H - Inertia factor - stored energy constant.

hp - Horse power.

I - Instantaneous current.

I_2 - Negative sequence current component.

I_{dc} - Direct current component.

I_{om} - Magnetising current drawn by an induction motor.

I_r & I_s - Receiving end and sending end currents, respectively.

I_d & I_q - Direct and quadrature axes components of I, respectively.

I_m - Current supplied to machine m.

I_k - Current input to node k with the estimated voltage.

$I_{k\ell}$ - Branch current between nodes k and ℓ .

i - Iteration just completed.

$i-1$ - Iteration preceding to i.

J - Moment of inertia.

K_d & K_q - Direct and quadrature axes saturation factors, respectively.

K - Constant.

K_g - Governor gain.

K_w - Winding factor.

K_D - Slope of the synchronous m/c. asynchronous torque-slip characteristic.

L - Inductance of a circuit.

M - Instantaneous angular momentum.

M_o - Angular momentum at system nominal frequency.

m - Number of phases.

n_o - Speed at the end of the time interval "Δt".

n - Instantaneous speed in R.P.M.

n_1 - Synchronous speed in R.P.M.

n_{oo} - Full load speed in R.P.M.

P - Instantaneous active power input.

P.U. - Per unit quantities.

P_m - Mechanical power input to machine m.

P_e - Electrical power output.

P_D - Damping power.

P_{Dn} - Braking power due to negative sequence current.

P_{Dc} - Braking power due to d.c. rapidly decaying component.

P_{KVA} - Synchronous machine rating in KVA.

P_{os} - Position of main valve.

p - Number of pairs of poles and an operator $(\frac{d}{dt})$.

Q - Instantaneous reactive power input.

Q_L & Q_C - Inductive and capacitive vars, respectively.

R - Instantaneous effective resistance; equivalent resistance corresponding to active power input to an induction motor at a given supply voltage.

R' & X' - Transmission line resistance and reactance, respectively.

R_a - Armature resistance.

R_A - Arc resistance.

R_1 & R_2 - Positive and negative sequence resistances, respectively.

r_o	-	Resistance equivalent to no - load losses.
r_1 & x_1	-	Stator resistance and reactance, respectively.
r_2 & x_2	-	Rotor resistance & reactance as referred to stator, respectively.
s	-	Instantaneous slip.
s_{maxT}	-	Slip at maximum torque.
s_1	-	Slip at the beginning of time interval "Δt".
s_2	-	Slip at the end of the time interval "Δt".
s_{oo}	-	Full load slip.
T	-	Instantaneous motor torque.
T_g	-	Overall generator time constant.
T_ℓ	-	Load torque.
T_{max}	-	Maximum torque.
T_t	-	Overall turbine time constant.
T_D	-	Damping torque coefficient.
T_{do} & T_{qo}	-	Direct & quadrature axes open circuit time constants, respectively.
T'_{do} & T'_{qo}	-	Direct & quadrature axes open circuit transient time constants, respectively.
T''_{do} & T''_{qo}	-	Direct & quadrature axes open circuit subtransient time constants, respectively.
V'	-	Infinite bus voltage.
V_k	-	Voltage at node k.
ΔV_k	-	Voltage correction for node k.
V	-	Supply voltage per phase.
V_f	-	Field voltage.

V_r - Receiving end voltage and reference voltage.

V_s - Sending end voltage and stabilizing voltage.

V_t - Machine terminal voltage.

V_{dp} & V_{dq} - Direct & quadrature axes components of E_p, respectively.

X - Equivalent reactance corresponding to reactive power input to an induction motor at a given supply voltage.

X_e - External reactance.

X_d & X_q - Direct & quadrature axes reactances, respectively.

X'_d & X'_q - Direct & quadrature axes transient reactances, respectively.

X''_d & X''_q - Direct & quadrature axes subtransient reactances, respectively.

x_3 - Magnetising reactance.

$Y_{k\ell}$ - Self and mutual admittance between nodes k and ℓ .

a_k, c_k, e_k, $G_{k\ell}$, $r_{k\ell}$ - Real components.

b_k, d_k, g_k, $B_{k\ell}$, $r'_{k\ell}$ - Imaginary components.

V_d & V_q - Direct & quadrature axes components of V_t, respectively.

α - Slope of torque-slip and torque-speed characteristics.

γ_j - Magnetising current as fraction of full load current.

ρ - Density of the rotor material.

η - Efficiency of the motor.

ϵ - Instantaneous deviation in angular velocity.

ω - Instantaneous angular velocity.

ω_o - Angular velocity at the end of time interval "Δt"; System nominal angular velocity.

ω_1	-	Synchronous angular velocity.
$\Delta\omega_m$	-	Angular velocity of phasor E_m on the X-Y plane.
$\Delta\omega'_m$	-	" " " I_m " "
$\Delta\omega'_{k\ell}$	-	" " " $I_{k\ell}$ " "
Δt	-	Time interval.
δ_m	-	Power angle of machine "m".
Φ	-	Resultant air gap flux.
Φ_s	-	Flux produced by stator currents.
Φ_r	-	" " " the rotor magnetising winding.
Ψ	-	Phase angle between V_r & I_r and E_Q & Φ.
Cos ϕ	-	Power factor of an induction motor.
θ_α	-	Phase angle of Φ at the beginning of time interval "Δt".
θ	-	" " " " end " " "
θ_k	-	Instantaneous phase angle of voltage phasor at the node k at the end of time interval "Δt".
θ_{ok}	-	Instantaneous phase angle of voltage phasor at the node k at the beginning of the time interval "Δt".
$\theta_{k\ell}$	-	Instantaneous phase angle of branch current, $k-\ell$ at the end of the time interval "Δt".
$\theta_{ok\ell}$	-	Instantaneous phase angle of branch current, $k-\ell$ at the beginning of the time interval "Δt".
Φ_{ad} & Φ_{aq}	-	Direct & quadrature axes components of Φ_s, respectively.

$P_{\ell k}$&$Q_{\ell k}$ - Active and reactive powers at the load bus k (for variable terminal voltage), respectively.

P'_k&Q'_k - Active and reactive power loads at node k for frequency-dependence, respectively.

Z_{jj} - Driving point impedance for machine j including X_q.

Z_{jk} - Transfer impedance between machines j and k including X_q.

i_1, i_2&i_{34} - Instantaneous values of currents through branches 1, 2 and between nodes 3 & 4, respectively.

I_{max} - Maximum value of current.

t - Time in seconds.

μ - Voltage regulator forward path gain.

T_e - " " " " time constant.

K_s - " " stabilizing path gain.

T_s - " " " " time constant.

E^i_m, f^i_m&M^i_m - Quantities pertaining to machine m at iteration i.

k' - An integer.

V_a - Voltage per phase across an induction motor (in Fig. 10.1).

$R'_1+jX'_1$ - Equivalent impedance of $r_1 + jx_1$ and jx_3 in parallel.

$p\theta$ - Instantaneous deviation in the bus voltage frequency.

$p\delta$ - Rate of change of power angle.

$f(V_{dp})$ - Function of (V_{dp}).

α_d&α_q - Direct and quadrature axes amortisseur decrement factors, respectively.

ℓ - Length of an induction motor rotor.

j&k	-	The subscripts denoting machine j and machine k, respectively.
β	-	Phase angle.
—	-	Bars under the symbols indicate vector quantities.
A'	-	Constant.

1. INTRODUCTION

Concurrent with the increase in complexity and size of electric power systems, there has arisen the increasing need for more refined methods of system planning and assessment. Advances in electronic computing methods and capabilities have made possible successively improved methods of calculation, so much so, that it might be expected that not a great deal more can be achieved without a careful relating of analytical techniques to the results obtained from full scale tests conducted on power systems, in order to assess the degree of agreement between the predicted and actual system behaviour. (Unfortunately few such realistic tests have been conducted).

In spite of the great amount of effort devoted to calculation refinements, however, there seems to have been little attention given to the study of power system behaviour at frequencies different from normal, whether during steady-state operation or during transient and dynamic electro-mechanical excursions - the assumption has been that instantaneous frequency changes have negligible consequence, particularly in transient and dynamic stability studies[195].

1.1 Historical Development of Power Systems

Prior to 1890, parallel operation of alternators was established in isolated instances[1, 2]. Since the first enunciation of the principles of interconnection by Merz and McLellan (in an address to the British Association in 1904[75]), isolated power stations and isolated electric companies started interconnections, and as a result, the problem of hunting of synchronous machines under sudden load changes emerged. This problem did not assume importance until after the change from belt driven machines to direct coupled machines and from smooth to slotted armature construction[84]. Probably the most successful method for minimising hunting was the introduction of dampers proposed by Leblanc[4, 5] in France in connection with alternators, and independently by Lamme[84] in the United States in connection with synchronous converters.

Small isolated power systems faced the problem of heavy short-circuit currents, and in order to reduce their severity and the duty of the circuit breakers which had to deal with such heavy abnormal currents, the solution proposed by various authors[10, 14, 15, 17], was the use of series current-limiting reactors at various points in the system. These reactors could localize the faults[16], thus maintaining the continuity of supply. With gradual expansion of the small isolated systems, they were interconnected and integrated into larger systems for the sake of continuity, economy, reliability and pooling of technical knowledge and finances, this process requiring high voltage transmission links for mutual transfer of power[8].

High voltage transmission lines transferring power to distant load centres and allowing mutual transfer of power between two electric power systems, have limited capacity, depending upon the sending end voltage, current, power factor and line impedance. To improve the maximum limits of power transfer, synchronous condensers were suggested[32,33] to be installed on the transmission line routes (for example, ref. 33, shows an increase of 42% in maximum power limit for a typical high voltage transmission line in the presence of synchronous condensers). Later, series resistors were suggested for the same purpose[64].

High voltage lines, because of their excessive charging currents, created a further problem by requiring too low an excitation of the synchronous machines under light loads supplied over long distances, thereby causing pole slipping, leading to instability[31]. To solve this problem, excitation levels of synchronous machines were adjusted in practice to produce operation at or near unity power factor[117, 144], and in order to control system voltages, shunt reactors were employed to overcome the excessive charging currents[113].

With the growth of power system capacities and the increase in physical distances between generating stations and load centres, extra-high-voltage transmission lines have been introduced. These are series compensated by capacitors to overcome their excessive inductive reactances[102, 106, 113, 133, 147]. The problem of physical distance has been handled in two ways:-

(a) By employing d.c. transmission links (which have zero synchronous length[84, 157]).

(b) By employing tuned transmission lines (i.e. the electrical length is increased to more than half wave length[220]).

Synchronous machines can develop a limited maximum electrical power depending on the excitation voltage, machine terminal voltage, machine reactance, and the phase difference between the excitation voltage and the machine terminal voltage. In the last decade, the average output of generating sets installed has increased rapidly, and with improvements in manufacturing techniques, synchronous machines have become physically smaller for a given output. In turn, this has resulted in an increase in the natural reactance of the alternators and a reduction in the inertia factor of the sets as a whole[198]. Such trends seem likely to continue in the future[200], and will tend to make the stability problems more acute. On the other hand, regulating devices, such as voltage regulators and speed governors, have undergone spectacular improvements in their performance. For example, voltage regulators can maintain voltage regulation in the system under normal operation to within $\pm$ 0.1%, and present day regulators employing static excitation systems (instead of d.c. exciters) have resulted in operation of synchronous machines with equivalent to zero reactance under disturbed conditions[251]. Voltage regulators have made substantial contributions towards the increase in stability limits of synchronous machines by their quick response and higher ceiling voltages (reported in the literature from 1928 to date). Speed governors have also contributed towards stability of synchronous machines[63, 210] - particularly displacement governors[181]. Recently, braking resistors have been employed at the synchronous machine terminals, in order to ensure stable operation during disturbances[237].

In order to supply system load requirements, maximum power limits for synchronous machines as well as for transmission links must be taken into consideration for future planning of the power system. The stability limit, i.e. the maximum power transfer from the generating station to the load centres via the transmission lines, is usually reached when the power which can be transmitted over a line or obtained from an alternator, is a maximum. (As stability and voltage regulation are very closely associated, stability may also be defined as an ability to maintain voltage under varying conditions of load for which a system is designed).

In order to meet the system load requirements at all times under normal and abnormal situations for both the present and the future, extensive and precise planning is essential, involving knowledge of the system load requirements from time to time. For this purpose, load surveys[127] are carried out at regular intervals and load trends are studied[201] at various key points in the power system to assess the future demands. Such comprehensive surveys can reveal the correct loading pattern of the system if based on:-

(a) Population estimates, housing requirements, commercial and industrial requirements, and past load trends at various key load centres.

(b) The demand ascertained by the type of area; high density, low density, and future saturation.

(c) Various types of utilization equipment and increasing lighting intensities.

With the aid of qualitative and quantitative load information at the various loading centres, the generation, transmission and distribution system capacities can be made available at the actual required time as far as possible; otherwise earlier provision of excess capacity will put an extra burden of untimely investment, while late availability will cause losses in revenue and inability to meet increasing load demands.

Present day electric power systems include the following elements:-

(i) Synchronous machines - main source of electrical energy, equipped with: dampers to overcome hunting, to increase the negative sequence reactance and to overcome the excessive high voltages under asymmetrical faults; excitation system to control the wattless current, maintain system voltages within the declared limits and to improve the steady-state and transient stability limits; governors to adjust the active power needed by the machine at the system nominal frequency and to facilitate the stable operation of the entire system under disturbed conditions.

(ii) Transmission lines - to transfer powers from distant plants economically, and also to interconnect the isolated systems, keeping them in synchronism by mutual power transfer as needed.

(iii) Series reactors - to reduce the magnitude of short circuit currents with which the circuit breakers have to deal; to localize faults for continuity purposes; to reduce lamp flicker caused by violently fluctuating loads (for example caused by arc furnaces).

(iv) Shunt reactors - to neutralise the excessive charging currents drawn by high voltage lines.

(v) Series capacitors - to neutralise partly the excessive inductive reactance of extra high voltage lines; to increase their power-carrying capacities, and to reduce the violent fluctuations in reactive power drawn by apparatus such as electric welders.

(vi) Shunt capacitors - to improve the operating power factor of the loads at the load centres and to regulate the load voltages.

(vii) Synchronous condensers - to supply the wattless current at the load centres, to regulate the load voltages and to increase the power transfer limits of high voltage lines.

(viii) Shunt resistors - for synchronous machine braking under disturbed conditions.

(ix) Series resistors - to increase the maximum power transfer limits of transmission lines.

(x) System loads - the main consumers of electrical energy for which the entire system has been planned. Such loads involve: synchronous motors, synchronous converters, induction motors, arc furnaces, electric welders, mercury-arc rectifiers, heating and lighting appliances.

1.2 Power System Studies

From the viewpoint of economy, safety and reliability of supply under actual conditions of loading for both present and future system requirements, knowledge of the performance of the various power system elements is essential. For assessments of performance under the worst predicted situations, practical tests are very expensive and difficult to carry out, so that model testing has to be relied upon to a very large extent. Such models may be physical or mathematical.

Power system performance assessment involves: load flow in key transmission lines and feeders; stability under steady-state and disturbed conditions - the stability of a power system is its capability to ride through a change in system demand which may be gradual or instantaneous, and may also be defined as its ability to respond to the power demands for which it has been designed.

Series current limiting reactors made their way into power systems as the only solution for reduction of short-circuit currents. In order to evaluate the magnitudes of short-circuit currents, analytical techniques, together with practical tests were presented by Diamant[19], but there was marked disagreement between theory and practice. Doherty and Shirley[23] subsequently introduced refinements, for example, by including leakage factors in calculating the transient reactances for the synchronous machines for treatment in short-circuit studies - this produced better agreement between theory and practice.

Small interconnected power systems faced the problem of steady-state stability limits, whereas the transient stability problem was almost absent. Brooks presented a graphical solution[7] in 1907 with the aid of a phasor diagram to determine the maximum power transfer between two synchronous machines running in parallel. Such interconnected systems involved high voltage transmission links for mutual transfer of power, and the problem of limited power transfer through a given line was soon met. Philip presented a circle diagram[9] in 1911 to determine the maximum power transfer over a transmission line with varying R:X ratios. Subsequent calculations were presented also by Steinmetz[25]. The transmission problem was tackled analytically by employing generalized transmission line constants[32, 33], and the calculations compared with measurements on a 2300V and 625 KVA line with good agreement between theory and practice; the authors also suggested the use of synchronous condensers, to improve the maximum power transfer limit (as indicated in section 1.1).

In 1917, Johnson[21] pointed out the latent introduction of instability due to the excessive use of series reactors to reduce the magnitude of short-circuit currents in a system under disturbed conditions. In the same year, Juhnke[22] also mentioned the transient stability problem in relation to the use of series current limiting reactors. In 1920, Schuchardt[24], described some instances of unstable operation of certain alternators on American systems, and suggested the elimination of series reactors used for current limiting purposes. In Britain, the power system grid was expanding and the deficiency of synchronising power able to be carried by transmission lines was causing problems[27].

A simplified representation of a synchronous machine by a fixed e.m.f. acting behind transient reactance followed from the constant flux-linkage theorem put forward by Doherty and Shirley[23] in 1918, and was proved by Rogowski[27], with respect to an explanation of short-circuit phenomena in synchronous machines. This method in conjunction with assumed zero electrical resistance of various circuits proved very useful for short-circuit current calculations, as employed by Franklin[39] in 1925. On the other hand, Spencer and Hazen[37] felt the analytical techniques too difficult and tedious, and consequently in 1925, they built a small scale model of a power system, representing the sources by phase shifting transformers, transformers by their equivalent circuits, and transmission lines and system loads by lumped impedances at system nominal frequency.

By this time, power systems had become quite complex, and engineers were meeting problems with the transient stability limits for the entire system[42, 47]. In 1926, Shirley[45] pointed out the practical stability limits in supplying certain classes of load, even with short lines. The loads were classified as:-

(1) Constant power output - induction motors with practically constant shaft output, such as those driving fans, pumps, compressors, direct-current generators; synchronous motors for the same classes of service as for induction motors.

(2) Variable impedance - synchronous converters supplying power to series motors for railway service.

(3) Constant impedance - lighting, heating, electric furnaces, welders, and synchronous converters for lighting load.

(4) Miscellaneous - combination of constant power, variable impedance, and constant impedance loads.

The emphasis was placed on active and reactive power demands as affected by the terminal voltage and not on the instantaneous frequency influence. Such loads were further described by Clough[47] in 1927, with the aid of volt-ampere characteristics, and showed the possibility of unstable operation when the alternators were operated at constant excitation.

Analytical solutions regarding the behaviour of synchronous machines under steady-state and transient conditions, such as cyclic variations of impressed torque, sudden angular displacement, synchronising out of phase and short-circuits, were presented by Doherty and Nickle[46] and Ku[52]. Subsequently, a complete 2-reaction theory of synchronous machines, first enunciated by Blondel, was presented by Park[53] in 1929. A simplified step-by-step method suggested by Park and Bancker[50] for synchronous machine calculations was developed in detail by Longley[61(1930)], on the basis of Park's two reaction theory, to calculate the swing curves for synchronous machines under disturbed conditions for symmetrical 3-phase faults. Following this, Clarke[65] introduced symmetrical components for asymmetrical and simultaneous faults by developing special equivalent circuits for such faults. The two reaction theory for the synchronous machine was further extended to include saturation, armature circuit capacitance, dampers and a balanced terminal impedance by Park[68], Crary[81], Concordia[83, 85] and Ku[86] respectively.

The increased complexity of electric power systems demanded a complete analysis, but due to computing difficulties, analytical techniques were based on the following simplifying assumptions[57] :-

(a) Resistance and capacitance were neglected.

(b) Reactances in the direct and quadrature axes were considered equal.

(c) Normal voltage was maintained under steady-state conditions on the high-tension side of transformers at the generator end.

(d) The power factor at the high tension side was normally 0.98 lagging.

(e) Flux linkages behind transient reactance of the generator and motor were considered to remain constant during the first swing.

(f) Magnetic saturation was neglected.

(g) Damping torques were neglected.

(h) Results were based on the first swing only.

(i) Faults were considered only on the high tension side of the unit transformer.

(j) Constant shaft torque assumed.

(k) Governor, voltage regulator action and load-speed characteristics were neglected.

(ℓ) Changes in instantaneous synchronous machine speeds were neglected.

All the above assumptions provided simplified mathematical models to carry out power system studies, in particular neglecting the change in speed of the synchronous machines, which permitted treating the transmission and distribution networks and the power system loads at system nominal frequency. Since the development of the 2-reaction theory, the assessment of performance for power system elements by physical models was preferred in the face of difficult analytical techniques. These techniques were continually refined for various individual elements : for example, synchronous machines - refined to include damping and synchronizing torques, and the characteristics of automatic voltage regulators and governors; induction motors - including damping and transient analysis during switching and faults; high voltage direct current transmission systems.

Most of the analytical studies were based on a single machine supplying an infinite bus, either directly or through an external impedance, with possible extensions to two or three machines[74, 76].

At this stage, the power system studies were classified as:-

(1) Load flow studies.

(2) Steady-state stability studies.

(3) Transient stability studies.

The load flow studies did not present many problems and could easily be carried out on A.C. and D.C. calculating boards[99, 104, 132], and on A.C. network analyzers[60, 88, 89, 111, 120, 150, 155], with the synchronous machines being represented by e.m.f's acting behind equivalent reactances[71], and treating the rest of the system by equivalent circuits at system nominal frequency.

Regarding stability studies, improved models were developed, in which the synchronous machines were represented by simulation techniques [60, 116], (with e.m.f's corresponding to the excitation, and their phase angles corresponding to the governor settings). Such models were quite satisfactory for carrying out steady-state stability studies, but for transient stability, the necessary step-by-step adjustments of the magnitudes and phases of the machine e.m.f's were time consuming and tedious. In 1950, a modified model system was developed in which the synchronous machine units were replaced by micro-machines[121, 149] of very low power (1-10 KVA), in which the operating characteristics of the models were intended to correspond to those of the full size machines; however, there was still a marked difference in results when compared to actual tests on a system[173]. In 1955, a dynamic analyzer was built by Kaneff[150], which offered a range of scaling by changing the value of capacitor in the machine units and the results agreed with the step-by-step integration methods of the swing equation. Full-scale stability tests carried out in 1958 on the 132 KV Britain grid[173] confirmed the general accuracy of the usual network analyzer studies for transient stability.

Since the beginning of the era of digital computers, mathematical models for complex power systems have been rapidly developing, as they offer as detailed a treatment of power system elements as one has the ingenuity and the information to include; moreover, physical models have their own inherent limitations which make them in many respects less attractive than digital methods. Stability studies on high speed digital computers have taken into account all the simplifying assumptions (a to k above) which were adopted in the past due to computing difficulties. Comprehensive digital computer programs have been developed to carry out such stability studies[214, 216, 229, 246].

1.3 The Importance of Power System Frequency

As already mentioned, present day stability studies make use of modern high speed digital computers, which offer as detailed a representation of the various power system elements as the state of knowledge and practice permit. Limitations are in fact due to the absence of adequate methods for detailed representation and the lack of necessary information on appropriate system data.

Of the simplifying assumptions mentioned in the previous sections, only (ℓ), that is, changes in instantaneous synchronous machine speeds, has hitherto been ignored in calculation refinements.

Under conditions of operation with given operating capacity constraints, the power controller has two parameters available for adjustment to meet the system load requirements : system operating frequency, and voltage. Loads such as induction motors are affected predominantly by the operating frequency, whereas others, for example, mercury arc rectifiers, arc furnaces, discharge lamps, electric welders, filament lamps and element heaters, are affected predominantly by the operating voltage. Thus, depending upon the composition of the system loads, the power controller will take the necessary action under normal and emergency conditions when there is a shortage of spinning reserve. In general, induction motor loads predominate in a power system, and consequently the operating frequency of the system has proved to be a very powerful adjustable parameter available to the power controller[119, 156].

Under transient disturbance conditions, the rotors of the various synchronous machines will be subjected to deviations in speed from the normal steady-state system nominal value, giving rise to transient changes in instantaneous frequencies of voltages and currents throughout the system. The magnitude of these frequency changes may amount to several percent of system frequency as discussed in Section 2. Transient variations in frequency throughout the system affect the performance of the various power system elements as follows:

(i) The instantaneous stored energy in the rotating parts of the synchronous machines and the machine e.m.f's vary. The effect on machine e.m.f. has been dismissed in a purely inductive circuit in reference 195, even though the constant magnitude of current at a changed value of machine e.m.f. will be followed by a change in active and reactive power. This neglect of change in instantaneous frequency has permitted the equating of P.U. torque to the P.U. power (which is not in fact true).

(ii) Produce a relative speed between the synchronous machine rotors and the resultant air gap fluxes, and in addition, cause a rapidly decaying d.c. magnetic field (in the case where the fault is close to the machine), and a flux produced by negative sequence currents (in the case of asymmetrical faults). Under these circumstances, the synchronous machines develop various damping and opposing torques (due to interaction of the rotor and the resultant air gap flux) in addition to their electrical output torques. The damping torques may be positive or negative depending upon the slip of the rotor with respect to the resultant air gap flux. The existing practice has been to consider such damping torques as directly proportional to the instantaneous slip of a synchronous machine rotor with respect to an infinite bus voltage in the case of a single machine connected to an infinite bus, (whether through an external reactance or not), whereas in a multi-machine case, the instantaneous slip has been considered with respect to the Thevenin's equivalent e.m.f. in series with the short circuit impedance when the machine under consideration is disconnected[163]. This treatment will always give damping in the positive direction whether the machine starts accelerating or decelerating under disturbed conditions. The treatment presented in ref. (224) considers the damping torque as proportional to the rotor slip with respect to the terminal voltage, on the basis of the argument that the machine views the remaining power system network through its terminals : this is erroneous because the damping torque in fact depends on the relative speed between the rotor and the resultant air gap flux.

(iii) The transmission and distribution network parameters vary, thus introducing negative damping by effectively reducing the mutual synchronising coefficients for the various synchronous machines. The change in system network parameters will upset the current and voltage distributions in the entire system, resulting in erroneous settings of protective relays and of tap-settings of various power and distribution transformers.

(iv) The active and reactive power demands of the power system loads (which determine the system performance under normal and abnormal situations) vary. The more usual loads met in practice include : induction motors, synchronous motors, filament lamps, element heaters, discharge lamps, arc-furnaces, electric welders, and mercury-arc rectifiers; all of which are voltage-dependent, and except for filament lamps and element heaters, are also frequency-dependent. The power system loads have previously been represented in transient and dynamic stability studies in various ways, for example by:-

(1) Constant shunt impedance at system nominal frequency, giving active and reactive power directly proportional to the square of the terminal voltage.

(2) Constant current sinks, giving active and reactive powers directly proportional to the terminal voltage.

(3) Non-linear loads.

Loads have been represented in a very detailed manner in reference 247, by:-

$$P_{\ell k} = a + b V_k + c V_k^2$$
$$Q_{\ell k} = d + e V_k + f' V_k^2$$

for their instantaneous terminal voltage-dependence, (where (a, b, c, d, e and f') are the constants as determined by the load data and the load characteristics); and by

$$P'_k = P_{\ell k}(1 + k_1 (p\theta)'_k)$$
$$Q'_k = Q_{\ell k}(1 + k_2 (p\theta)'_k)$$

for their instantaneous frequency-dependence, where k_1 and k_2 are constants and $(p\theta)$ is the instantaneous deviation in the bus voltage frequency from its nominal value.

All the usual representations of power system loads have hitherto treated the loads as static and independent of frequency, except in the case of ref. 247, in which it is suggested that the loads may be represented as in the relations P'_k and Q'_k above - that is, linearly dependent on frequency deviation. However, although some loads may depend linearly on frequency deviations, others (for example, arc-furnaces and electric welders) do not. Clearly, a more complex relationship between the frequency deviation and load deviations must be introduced.

1.4 Objective of the Present Project

In view of the previous neglect of transient frequency deviations in power system stability studies, and particularly because of trends towards low inertia and high natural reactance synchronous machines, it is considered important to investigate the effect of transient frequency deviations on the various components of a power system (both separately and in an integrated manner) in order to ascertain the magnitude of the various effects. This has formed the motivation for the present project.

2. INSTANTANEOUS FREQUENCY VARIATIONS ON A POWER SYSTEM

Under disturbed conditions, the various synchronous machines on a power system move at varying angular velocities, different from their steady-state values, thereby producing instantaneous frequency deviations, from system nominal values, of the voltages and currents throughout the system. Such transient deviations of frequency affect the performance of the various power system elements, as has already been suggested in Section 1.

2.1 Magnitude of Frequency Excursions

It can be shown by a simple approximate argument that in extreme cases, frequency excursions on power systems of up to $\pm$ 5% of synchronous frequency can occur[142]. More commonly, however, excursions of up to $\pm$ 2% may be expected in normal configurations (see, for example, ref. (195), page 6); this figure has been confirmed by the author for various different systems which have been studied by the methods presented herein. (For example, see figure 3.6 (c)).

The general magnitude of instantaneous frequency excursions has been long appreciated; however, awareness of the order of quantitative effects produced on the system, particularly in relation to transient and dynamic stability, has been lacking - indeed, the effect has been considered negligible[195]. It will later be evident that including instantaneous frequency excursions in calculations of transient stability can have an important significance.

2.2 Assessment of Instantaneous Frequency

Consider the power system of Figure 2.1, where two machines supply a common load through a transmission line. Transient conditions may be produced by applying a fault on load bus No. 4, and as a result of application of the fault, the instantaneous rotor angular velocities of each machine will deviate from ω_o, the synchronous value.

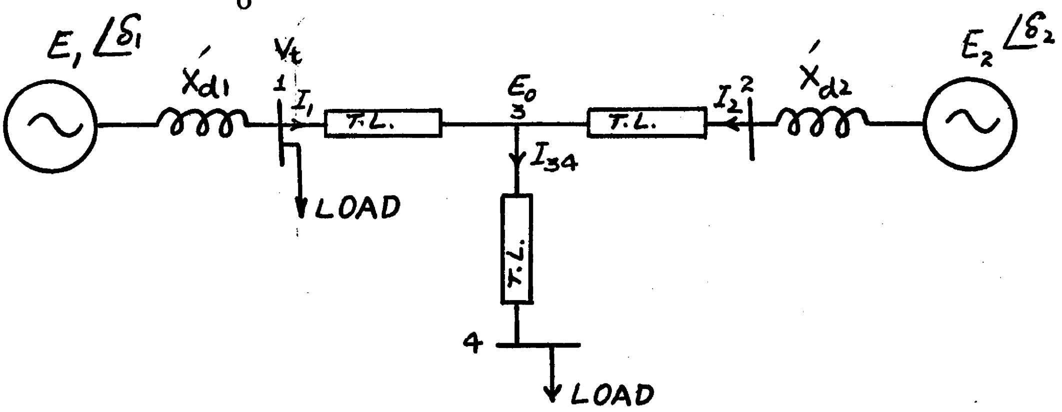

Fig. 2.1 Power system illustrating assessment of instantaneous frequency.

Under disturbed conditions, the e.m.f. and current phasors will move with respect to a reference phasor moving with synchronous angular velocity, as shown in fig. 2.2, by small, and in general different, angular velocities. Thus phasors I_1, I_2, I_{34}, E_o, and V_t will follow E_1 and E_2 with different relative angular velocities depending on the instantaneous values of reactance voltages in the circuit : these values can be found from a knowledge of the instantaneous frequency of the current passing through the various parts of the system, and in general under disturbed conditions, the instantaneous frequency of the above quantities will be different from synchronous.

In figure 2.1, the machines may swing either in the same direction, in which case the frequency of all phasors follows these swings at different rates, or they may swing in opposite directions, when phasors I_1 and I_2 will follow their respective machines, with I_{34} following either I_1 or I_2 depending on whether machine 1 or machine 2 respectively is dominant.

$$\text{Let} \quad i_1 = I_{max1} \sin \omega t$$

$$i_2 = I_{max2} \sin (\omega + \epsilon) t$$

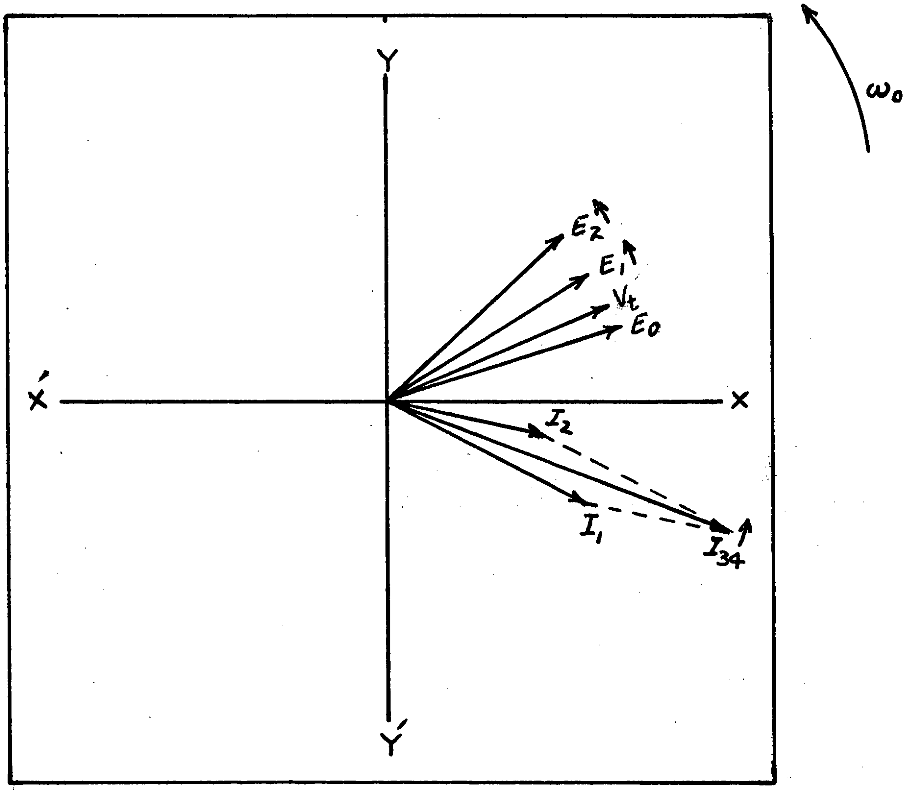

Fig. 2.2 Phasor diagram on X-Y plane.

Where ω and $\omega + \epsilon$ are the instantaneous angular velocities of phasors I_{max1} and I_{max2}, respectively,

assuming $I_{max1} = I_{max2} = 1$,

then $\quad i_{34} = \sin \omega t + \sin (\omega + \epsilon) t$

$$= 2 \sin (\omega + \epsilon/2)\, t \,.\, \cos (\epsilon/2)\, t \qquad (2.1)$$

The term $\cos (\epsilon/2)\, t$ in equation (2.1) modulates the amplitude of the sine wave of instantaneous angular velocity $(\omega + \epsilon/2)$, and its contribution to change the amplitude is quite small during the time interval "Δt" which is usually of the order of 0.05 sec. For example, if $\epsilon = \pi$, i.e. deviation in instantaneous angular velocity is 1% from its nominal value, the contribution by the term $\cos\ \epsilon/_2\ t$ during the time interval of 0.05 sec. is to reduce the magnitude of the sine wave by 0.3%, whereas when $\epsilon = \pi/_2$, the reduction is 0.07%.

For zeros of i_{34},

$$\sin(\omega + \epsilon)t = -\sin \omega t \tag{2.2}$$

The equation (2.2) will be satisfied if,

$$(\omega + \epsilon)t = 2\pi k' + \beta \tag{2.3}$$

and $$\omega t = 2\pi k' - \beta \tag{2.4}$$

Adding equations (2.3) and (2.4) and dividing by 2,

$$\omega t + \epsilon\ t/_2 = 2\pi k'$$

or the instantaneous angular velocity of the phasor I_{34}

$$= \omega + \epsilon/_2 \tag{2.5}$$

On the basis of the assumption that $I_{max1} = I_{max2}$, the additional term $\epsilon/_2$ in equation (2.5) represents the average deviation. In the case where I_1 is dominant, the contribution by the additional term will be very small, whereas a dominant contribution of I_2 will bring this additional contribution in equation (2.5) close to ϵ when $I_1 \rightarrow o$. The instantaneous variations of I_{34} will follow approximately a sine law but with changing frequency. Therefore, the difference in instantaneous frequencies can be evaluated as "(incremental phase displacement/incremental time)". Thus the rate of change of instantaneous time phase of the resultant current flowing in a branch, divided by 2π, will give the instantaneous frequency of the current.

In order to account for the situation arising on an actual power system where, during transient disturbances, changes in instantaneous frequency of voltages and currents occur on different parts of the system as a result of acceleration and deceleration of the synchronous machines, it is possible to determine the instantaneous contribution of current in each particular branch of the system made by each machine or machine group.

2.2.1 Partial Differentiation Method

In order to determine the instantaneous resultant current both in magnitude and phase in a branch of the transmission network, the contributions of current by individual machines towards the total current in a particular branch should be known. Then, by applying the principles of superposition, the resultant currents can be evaluated both in magnitude and phase. The instantaneous current in the branch between buses k and l is,

$$I_{k\ell} = \sum_j \frac{\partial I_{k\ell}}{\partial I_j} \times I_j \tag{2.6}$$

This information is required many times for each branch (as shown in section (4.1.1.2)), at each interval of time during a transient stability study, and this becomes a very time consuming part of the calculation procedure on a digital computer.

2.2.2 Rotating Phasor Method

A reference X-Y plane is selected to move at an angular velocity ω_o in an anticlockwise direction, at the system nominal frequency. All voltage and current phasors are first placed on the X-Y plane under the steady-state conditions satisfied just prior to a disturbance. This may be achieved as follows:

(a) Take a reference bus, which may be a load or machine bus in the network, and establish its voltage phasor along the X axis of the X-Y plane.

(b) Carry out a normal load flow study under steady state conditions. This gives complete steady state information on all voltage and current phasors in the system (and in particular provides the magnitudes and relative positions of the machine e.m.f. phasors on the X-Y plane).

The above steps (a) and (b) are performed at the beginning of a study only. Subsequently, in order to be able to handle transient conditions in which the various quantities such as voltages, currents, admittances, and instantaneous frequencies vary, the following steps must be carried out at the beginning of each new operation (for example, the occurrence of a fault, fault clearance and so on). In each such instance, all phasors (except the synchronous machine e.m.f. phasors which necessarily cannot suddenly change position) must be relocated on the X-Y plane, using the following steps:

(c) Resolve the machine bus e.m.f's on the X-Y plane in complex form as,

$$\underline{V}_k = E_m \cos \delta_m + j E_m \sin \delta_m$$

assuming the other bus voltages to be $1 + j0$, as a first approximation.

(d) Replace all loads by their equivalent admittances at the system nominal frequency.

(e) Form the admittance matrix for the entire system at the system nominal frequency in the first instance, or for subsequent operations, form the matrix at the appropriate new instantaneous frequencies.

(f) Calculate the various node voltages, branch currents and their phase angles on the X-Y plane as outlined in the Appendix 10.1, whereby an iterative process corrects the node voltages, one by one, assuming the others as constant, and rapidly provides the quantities required to within a predetermined index of accuracy.

By the above process, the voltage phasors for all the system nodes may be represented on the X-Y plane under steady-state conditions. The various branch currents of the transmission network can also be represented on the same X-Y plane. When the system is subjected to a transient disturbance, all phasors will adjust their instantaneous positions depending upon the self and mutual admittance of the various nodes. In order to exclude the purely electrical transients, all phasors are relocated on the X-Y plane in the manner described above, each time a change of operation (e.g. switching of loads or of components of the transmission and distribution network and the occurrence or removal of faults) takes place.

During the solution of the power system differential equations for transient stability studies, instantaneous angular positions for each phasor (voltage or current) are available at the beginning and end of each step time interval, Δt. Then the instantaneous frequency of the voltage at the bus k is given by,

$$f_k = \frac{\theta_k - \theta_{ok}}{2\pi\Delta t} + f_o \tag{2.7}$$

and the instantaneous frequency of the current through the line between buses k and ℓ is,

$$f_{k\ell} = \frac{\theta_{k\ell} - \theta_{ok\ell}}{2\pi\Delta t} + f_o \tag{2.8}$$

When applied to a digital computer program which takes instantaneous frequency effects into account, solution for each step can be made to converge rapidly to an acceptable accuracy as outlined in section (3.2.1.6). In this way, instantaneous frequency variations at any point of the system may readily be found. Identical values for the variations in instantaneous frequency can of course be derived from the slopes of the angle-time curves (when expressed in cycles per second).

3. SYNCHRONOUS MACHINE REPRESENTATION AND BEHAVIOUR

The basic 2-axis theory of the synchronous machine first enunciated by Blondel was further developed by Park[53] in the 1920's, and extended by Concordia, Crary, Ku, and Park to include : the effect of magnetic saturation[71]; armature resistance[58]; armature circuit capacitance[81]; balanced terminal impedance[85]; synchronous machine damping (offered by the eddy currents induced in the rotor structure and by the dampers provided to overcome the earlier hunting problems, as well as to increase the negative sequence reactance of the alternators and to suppress the excessive voltages during asymmetrical faults on the alternators[66]); extension to n-phase synchronous machines[86] and the analysis of asymmetrical faults by symmetrical components[65]; methods for assessing the performance of synchronous machines under various conditions of operation.

In the early 1930's, the advantages of quick acting voltage regulators[54], and governors[63] were also realised, but in view of the computing difficulties with analytical techniques, the following simplifying assumptions have previously been employed in transient stability studies carried out to predict the performance of synchronous machines under disturbed conditions : -

(a) Constant flux linkages.

(b) Transient saliency neglected.

(c) Damping torques neglected.

(d) Voltage regulator and speed governor effects neglected.

(e) Saturation neglected.

(f) Stability determined by the first swing.

(g) Changes in instantaneous speed of synchronous machine rotors neglected.

Many of the above assumptions are to a degree self-compensating and it is possible to obtain results which are reasonably close to those existing in practice[173], by representing the synchronous machine by an e. m. f. acting behind the direct axis transient reactance, with the mechanical input power held constant, while treating the entire system at system nominal frequency.

In the light of developments and performance achieved by automatic voltage regulators and governors, the results obtained on the basis of the above assumptions have been considered to be safe[214], and synchronous machine damping has been considered to be positive and to give safe results[195]. In practice, however, synchronous machine damping can be positive or negative, depending upon the synchronous machine slip with respect to the resultant air gap flux under disturbed conditions, as discussed further in Section 3. 1. 4.

From the viewpoint of economy, power systems should be designed close to their transient stability limits, and for normal operation, a knowledge of the true behaviour of the synchronous machines under the most extreme conditions is essential. In the last decade, the development of high speed digital computers has facilitated the analytical solution of power systems, and consequently, comprehensive digital computer programs have been developed[214, 216, 229]: the present study extends this work.

3. 1 Synchronous Machine Representation

In comprehensive stability studies of power systems, the synchronous machine has been generally represented in 2-axis form, as shown in Figure 3. 1. The machine equations have been derived[214] on the basis of the following assumptions: -

(a) The transformatory terms in the machine equations are ignored. (This is equivalent to neglect of d. c. components of the machine currents which are taken into account by the braking torques).

(b) Amortisseur currents are neglected in the voltage equations. (The amortisseur currents are indirectly included in the machine damping).

(c) Unbalanced faults are represented by symmetrical component methods, and the machine equations represent positive phase sequence components only.

The set of equations for each machine in its own reference frame may be written in the form:-

$$E_Q = E_q - I_d (X_d - X_q) \tag{3.1}$$

$$V_d = E_d - I_d R_a + X_q I_q \tag{3.2}$$

$$V_q = E_q - R_a I_q - I_d X_d \tag{3.3}$$

$$E'_q = E_q - I_d (X_d - X'_d) \tag{3.4}$$

$$E'_d = E_d + I_q (X_q - X'_q) \tag{3.5}$$

The above representation of synchronous machines allows for saliency; the e. m. f. E_Q has to be calculated during each time interval so that the e. m. f. behind the direct axis transient reactance may be treated as constant for the constant flux linkage assumption. The decay of flux linkages on both direct and quadrature axes depends upon the transient open-circuit field time constants, that is on T'_{do} and T'_{qo}.

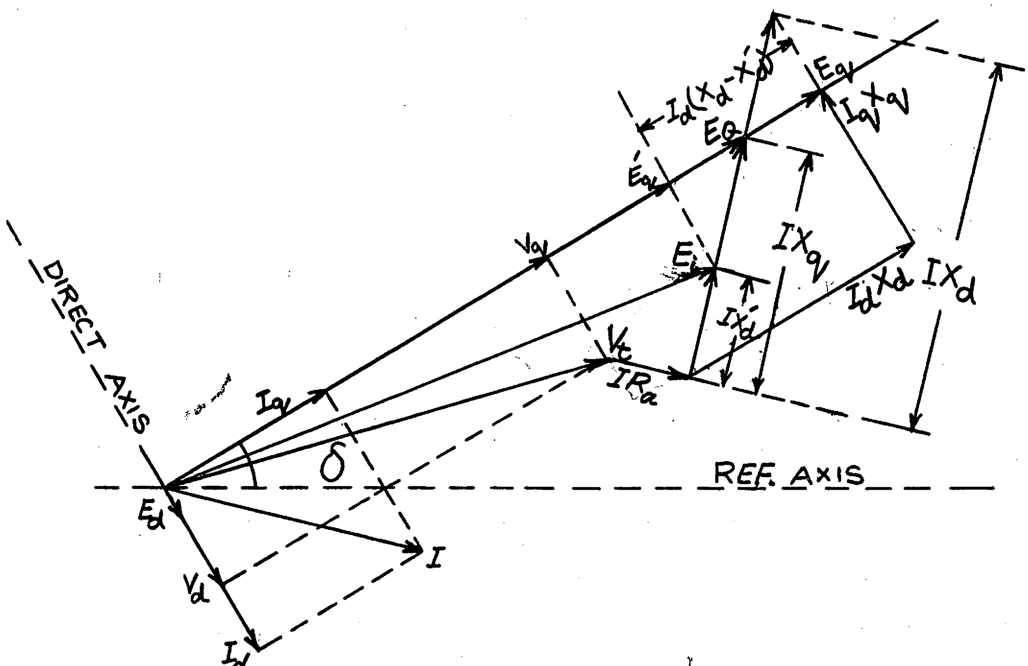

Fig. 3.1 Synchronous machine phasor diagram.

$$\frac{dE'_q}{dt} = \frac{(V_f - E_q)}{T'_{do}} \tag{3.6}$$

$$\frac{dE'_d}{dt} = -\frac{E_d}{T'_{qo}} \tag{3.7}$$

Where V_f is the per unit exciter voltage.

Electrical output of a single machine:-

$$= P_e = E_Q \cdot I_q$$

The equation of motion of the machine when damping and braking torques are neglected is :-

$$\frac{H}{\pi f}\,\frac{d^2\delta}{dt^2} = P_m - P_e \tag{3.8}$$

In the case of multi-machine systems,

$$P_{ej} = \frac{E_{Qj}^2}{Z_{jj}} \operatorname{Cos} \theta_{jj} - \sum_{k=1}^{n} \frac{E_{Qj}\, E_{Qk}}{Z_{jk}} \operatorname{Cos} (\delta_j - \delta_k + \theta_{jk}) \qquad j \neq k \tag{3.9}$$

where Z_{jk} includes the reactance X_q.

$$\text{And } I_{dj} = \frac{E_{Qj}}{Z_{jj}} \operatorname{Sin} \theta_{jj} - \sum_{k=1}^{n} \frac{E_{Qk}}{Z_{jk}} \operatorname{Sin} (\delta_j - \delta_k + \theta_{jk}) \qquad j \neq k \tag{3.10}$$

From the phasor diagram of figure 3.1,

$$E_{Qj} = E'_{qj} + I_{dj} (X_{qj} - X'_{dj}) \tag{3.11}$$

By substituting equation (3.10) in (3.11),

$$E'_{qj} = \left(1 + \frac{(X'_{dj} - X_{qj})}{Z_{jj}} \operatorname{Sin} \theta_{jj}\right) E_{Qj} - \sum_{k=1}^{n} E_{Qk} \frac{(X'_{dj} - X_{qj})}{Z_{jk}} \operatorname{Sin} (\delta_j - \delta_k + \theta_{jk}) \qquad j \neq k \tag{3.12}$$

The set of equations represented by (3.12) can be conveniently written in matrix form:-

$$\begin{bmatrix} E'_{q1} \\ E'_{q2} \\ - \\ - \\ - \\ - \\ E'_{qn} \end{bmatrix} = \begin{bmatrix} K_{11} & K_{12} & - & - & - & K_{1n} \\ K_{21} & - & - & - & - & - \\ - & & & & & - \\ - & & & & & - \\ - & & & & & - \\ - & & & & & - \\ K_{n1} & - & - & - & - & K_{nn} \end{bmatrix} . \begin{bmatrix} E_{Q1} \\ E_{Q2} \\ - \\ - \\ - \\ - \\ E_{Qn} \end{bmatrix} \tag{3.13}$$

Where $$K_{jj} = 1 + \frac{(X'_{dj} - X_{qj})}{Z_{jj}} \operatorname{Sin} \theta_{jj}$$

and $$K_{jk} = - \frac{(X'_{dj} - X_{qj})}{Z_{jk}} \operatorname{Sin} (\delta_j - \delta_k + \theta_{jk}) \qquad j \neq k$$

From equation (3.13),

$$\left[E_Q\right] = \left[K\right]^{-1} \cdot \left[E'_q\right] \tag{3.14}$$

The matrix can be inverted to obtain the instantaneous values of E_{Qj}, which is to be used in equation (3.9) to give the electrical outputs.

The driving point and transfer impedances can be conveniently determined by a digital computer for all the machines by carrying out a load flow study for the system in the presence of the machine concerned, when all the other machines are replaced by their quadrature axis saturated reactances, and by employing the definitions of Z_{jj} and Z_{jk} as outlined in ref. (195).

3.1.1 Machine Saturation

The procedure adopted here involves a correction of the flux linkages within the machine[229]. The method is approximate because it is assumed that the flux linkage is known for the stator circuits only and is taken as zero for the rotor circuits. This approach tends to indicate a higher degree of rotor saturation than would actually exist, but has the advantage that it reduces to the method for saturation correction in the A.I.E.E. test code for synchronous machines[107].

The following assumptions are employed:-

(a) The difference in reluctances of the direct and quadrature axes paths is due only to difference in the length of the air gap in each axis.

(b) The degree of saturation in an axis is proportional to the components of the voltage behind the Potier reactance. This saturation level exists for all rotor and stator circuits in that axis.

(c) The distortion of any air gap flux waves does not change the unsaturated inductance values or destroy the sinusoidal variations assumed for rotor and stator inductances.

The saturation factor at any specified voltage for the direct or quadrature axis, K_d or K_q, is defined as:-

$$\frac{\text{Field current to give that voltage on the magnetisation curve}}{\text{Field current to give that voltage on the air gap line}} - 1$$

The direct axis saturation factor may be obtained directly from the machine open circuit characteristic corresponding to the value of the quadrature axis component of the Potier voltage, or at:-

$$V_{qp} = V_q + R_a I_q + I_d X_p \tag{3.15}$$

$$\text{and} \quad K_d = f(V_{qp}) \tag{3.16}$$

and, as a consequence of the first assumption, the value of the quadrature axis saturation factor may also be obtained from the same open circuit characteristic, by multiplying the value found at the direct axis component of Potier voltage by the ratio X_q/X_d.

$$\text{Then} \quad V_{dp} = V_d + R_a I_d - X_p I_q \tag{3.17}$$

$$\text{and } K_q = \frac{X_q}{X_d} \cdot f(V_{dp}) \tag{3.18}$$

It is assumed that the linkages of the direct and quadrature axes are composed of two parts; one due to mutual flux and the other due to leakage flux. The former is subjected to saturation and the latter is not. Then the machine per unit equations are modified as:-

$$V_q = E_q - R_a I_q - \left[\frac{X_d - X_p}{1 + K_d} + X_p\right] I_d \tag{3.19}$$

$$V_d = E_d - R_a I_d + \left[\frac{X_q - X_p}{1 + K_q} + X_p\right] I_q \tag{3.20}$$

$$E'_q = E_q - \left(\frac{X_d - X'_d}{1 + K_d}\right) I_d \tag{3.21}$$

$$E'_d = E_d + \left(\frac{X_q - X'_q}{1 + K_q}\right) I_q \tag{3.22}$$

$$\frac{dE'_q}{dt} = \frac{1}{T'_{do}} (V_f - (1 + K_d) E_q) \tag{3.23}$$

$$\frac{dE'_d}{dt} = \frac{-1}{T'_{qo}} (1 + K_q) E_d \tag{3.24}$$

The above equations (3. 19 to 3. 24) have been used in the phasor diagram shown in figure (3. 2) representing machine behaviour at some specific time.

The equations (3. 19 to 3. 24) reduce to equations (3. 3 to 3. 7) if saturation is neglected; that is if $K_d = K_q = o$.

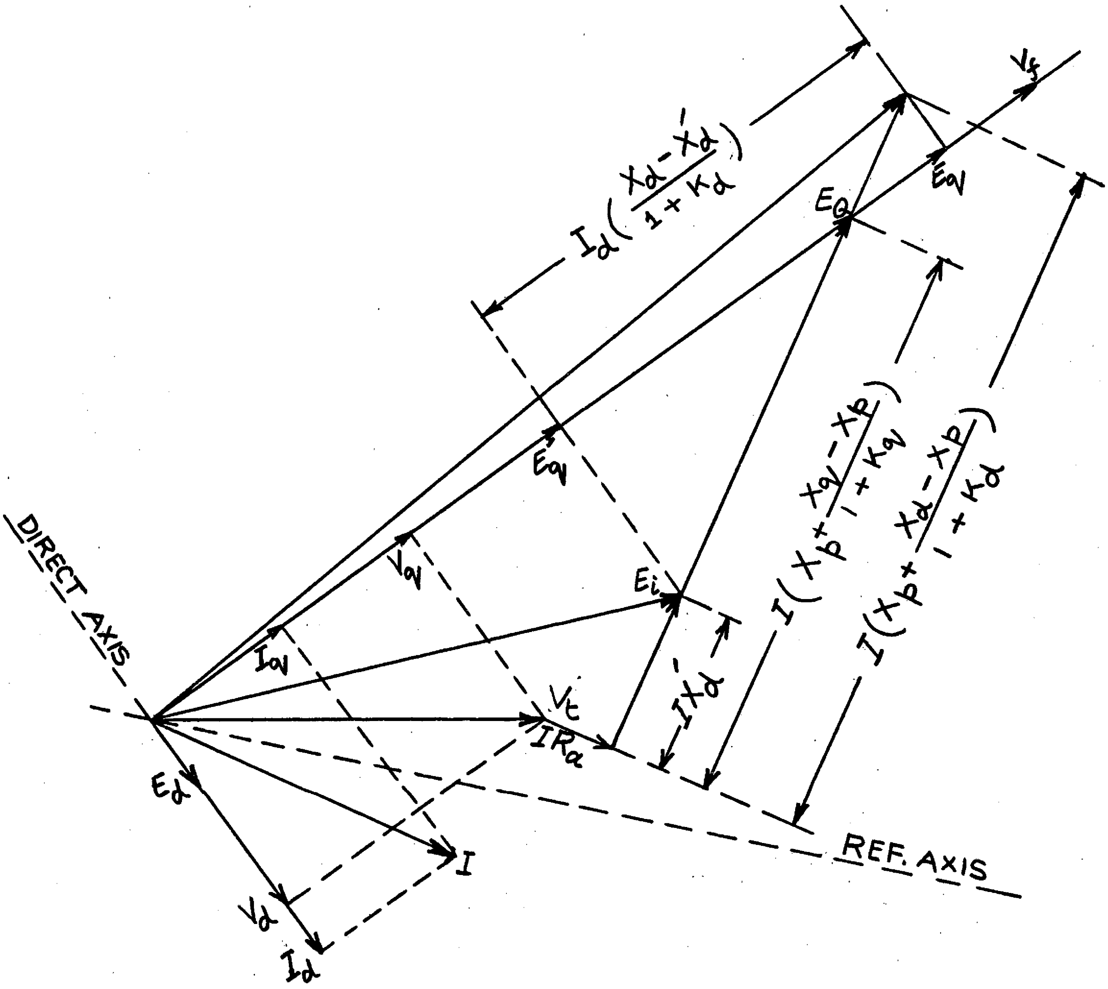

$$V_f = (1 + K_d)\,E_q$$

Fig. 3.2 Phasor diagram of a saturated synchronous machine in the transient state.

The saturation curve derived from an open circuit characteristic can be conveniently represented by polynomials[214] to evaluate $(1 + K_d)$ and $(1 + K_q)$ directly for given components of Potier voltage on the direct and quadrature axes.

3.1.2 Automatic Voltage Regulator

It has been demonstrated[176] that the presence of high speed, continuously acting voltage regulators improves the steady-state and transient stability limits of a synchronous machine. The representation of voltage regulator effects is particularly important in single machine studies where optimum evaluation of the various parameters is desired but, in multi-machine studies, considerable simplification can be made in representation, while preserving the same overall effect[214]. As an example of practical operation, tests on a particular power system indicated that normal voltage regulator adjustment was such as to just overcome the flux decay in the synchronous machines during disturbed conditions[198].

The details of high speed voltage regulators in general follow a common pattern, consisting of one or more stages of power amplification, preceded by one or more stages of magnetic amplifiers, before being fed to the main exciter. In addition to this forward loop, various feedback signals are used for stabilising purposes. These elements may be represented by simple gains and time constants; a typical system is shown in figure 3.3(a)[214]. Many of the time constants are very small and the same form of response can be obtained by the simplified system shown in figure 3.3(b).

There are limits imposed on the maximum output voltage of the main exciter and, in most designs, the input magnetic amplifier has input limits set by the saturation of the iron. A typical step response on open circuit is shown in figure 3.3(c).

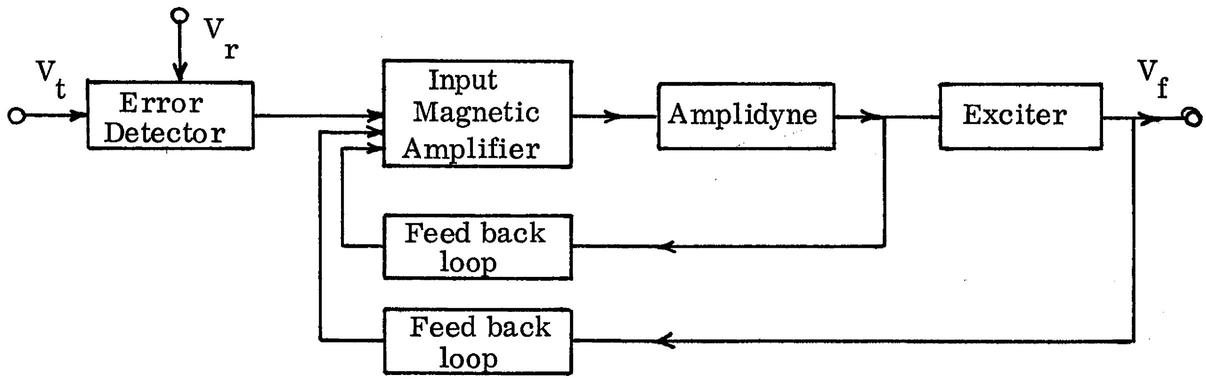

Fig. 3.3(a) Typical voltage regulator block diagram.

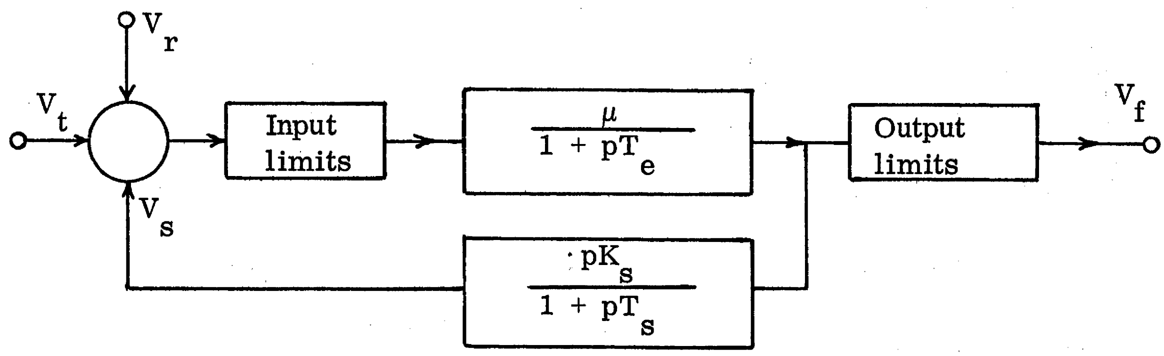

Fig. 3.3(b) Reduced voltage regulator block diagram.

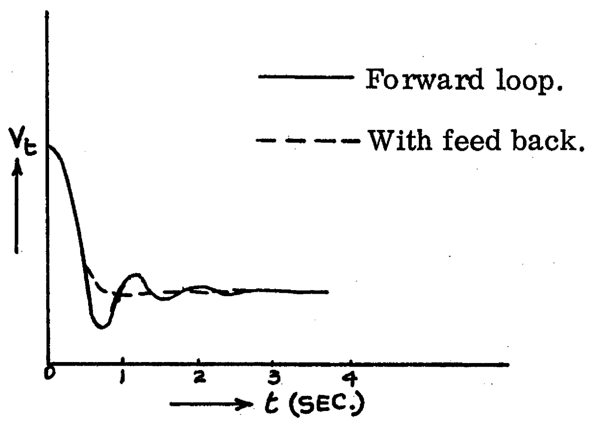

Fig. 3.3(c) Voltage regulator step response.

From the block diagram in figure 3.3(b),

$$V_f = \frac{\mu}{1 + pT_e} (V_r - V_t - V_s) \tag{3.25}$$

$$V_s = \frac{p\,V_f\,K_s}{1 + pT_s} \tag{3.26}$$

The example worked out in section (5.1.2.2) indicates that a conventional voltage regulator which is sensitive only to terminal voltage is not suitable for machine no. 3, because during the disturbance the raised machine voltage will promote deceleration, whereas if the voltage regulator happens to be sensitive to instantaneous speed changes, then the performance of machine no. 3 might have been improved; this example dictates that the voltage regulators should also be sensitive to speed changes (this trend is noted in latest developments[251]).

3.1.3 Speed Governor

Speed governors are difficult to simulate in power system stability studies. From the control system point of view, it is desirable that the characteristics should be reduced to simple gains and time constants for mathematical analysis. The mechanisms and oil systems appear to possess marked dead band and time delay characteristics, which drastically alter the response in comparison with an idealised representation[214]. It has been considered more appropriate to represent the governing system by a gain, fixed to give the required regulation, and by two time constants, one for the mechanism, and one effective time constant for the flow of steam through the turbine, as this is consistent with field tests[173, 199] and other studies carried out[183]. There are limits imposed on the response of the governor by the fact that both the steam input and the governor travel can never become negative.

The block diagram is shown in figure 3.4 and the equations governing performance are:-

$$P_{os} = \frac{K_g (p\,\delta)}{1 + pT_g} \tag{3.27}$$

$$P_m = \frac{P_{os}}{1 + pT_t} \tag{3.28}$$

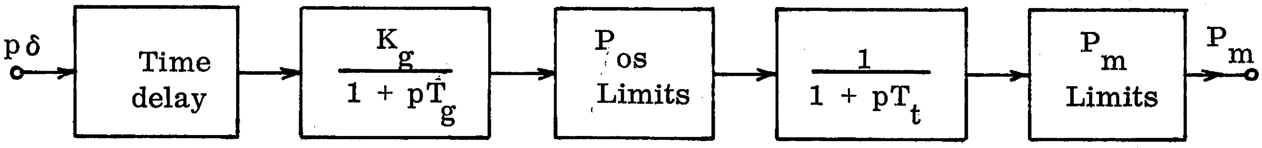

Fig. 3.4 Block diagram of governor simulation.

3.1.4 Transient Torques

Under disturbed conditions, the synchronous machines move at speeds different from nominal synchronous speed. This brings a relative speed between the synchronous machine rotors and the resultant air gap fluxes, which is responsible for the presence of e. m. f's in the amortisseur winding and rotor body, causing an induction torque (which may be motoring or generating depending upon whether the resultant air gap flux leads or lags the rotor respectively), to come into play as soon as the instantaneous speed of the rotor deviates from that of the air gap flux. In this situation, synchronous machines develop various opposing torques (due to the interaction of rotor and air gap fluxes) in addition to electrical output torque. The torques which always oppose the direction of motion are called the braking torques and the torque which depends upon electro-mechanical oscillations is termed a damping torque. Reference 214 has indicated that machine damping has a spectacular effect, while the regulating devices have comparatively little effect, whereas reference 163 indicates only a small machine damping effect in the presence of flux decay and references 195, 224, also indicate only a slight improvement in transient stability limit due to amortisseur windings (a typical low resistance amortisseur is stated to produce an improvement in power limit of 2%).

3.1.4.1 Braking Torques

In a synchronous machine, under steady-state conditions, the flux produced by the rotor magnetising winding and that produced by the stator currents move simultaneously intact in the same direction at synchronous speed with a fixed phase difference, depending upon the machine excitation and the output as shown in figure 3.5. In order to overcome electro-mechanical oscillations, an amortisseur winding is provided on the rotor in the form of a squirrel cage. If, in some manner, a steady magnetic field is introduced in the air gap, the rotor structure moving at synchronous speed will have eddy currents induced in its iron, as well as an induction motor torque induced in its amortisseur and magnetising windings; this is equivalent to an ordinary induction motor at standstill with the supply switched on. The torques developed under these circumstances will always act in opposition to the direction of motion of the rotor and are called braking torques. Such torques in practice, exist only under fault conditions, and are of two types:-

(a) Direct-Current Braking - A fault close to the synchronous machine gives rise to a rapidly decaying direct current component in the stator winding, which has been confirmed by practical tests[198]. The stator resistance losses due to this direct current and the interaction of the d.c. flux with the rotor windings produce a braking

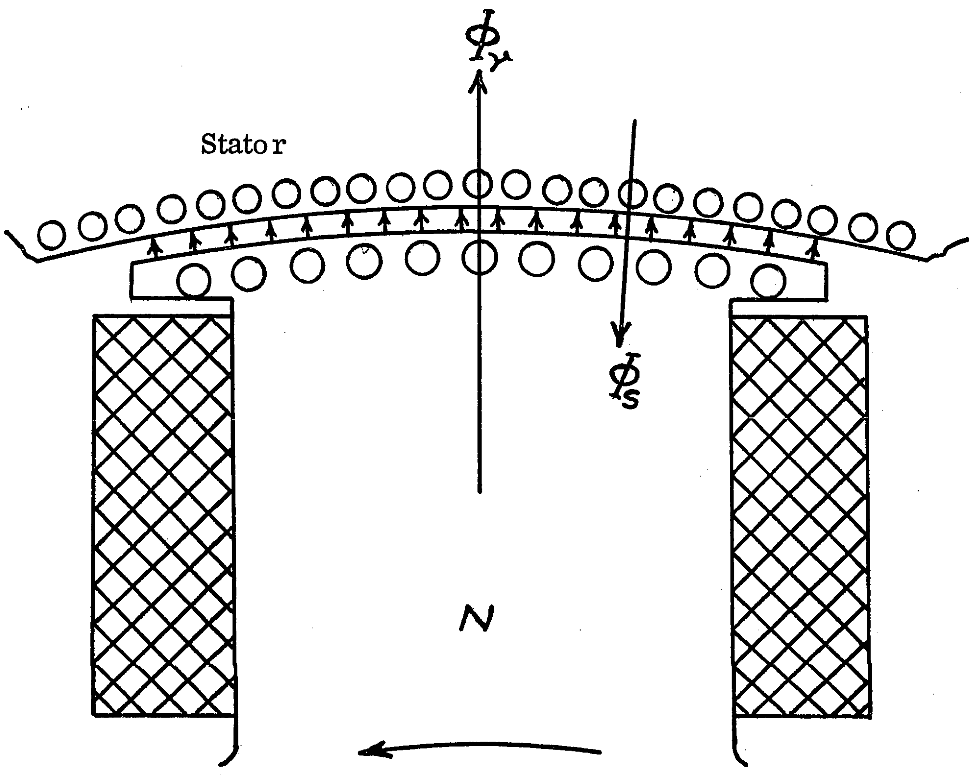

Fig. 3.5 One pole of a salient-pole synchronous machine with damper winding indicating the relative positions of stator flux (Φ_s) and rotor flux (Φ_r).

torque in the synchronous machine, which has been represented by the equation[229],

$$P_{Dd} = \frac{I_{dc}^2}{2} (4 R_2 - 3 R_1) \tag{3.29}$$

This relation can be used to correct the nett accelerating power of the synchronous machine.

(b) Negative-Sequence Braking - In the presence of asymmetrical faults, such as single line to ground, double line to ground, line to line, opening of single and double lines, there exists a negative sequence current which flows through the stator conductors of the machine, thus producing a magnetic field in the air gap, which moves at twice the synchronous speed with respect to the rotor windings. The interaction of this magnetic field with the rotor windings and iron structure, creates a torque which always tends to slow the machine. This torque has been represented by the equation[163],

$$P_{Dn} = I_2^2 (R_2 - R_1), \tag{3.30}$$

and the nett out-of-balance power available for the synchronous machine can be corrected accordingly.

3.1.4.2 Damping Torques

As pointed out earlier in section (3.1.4), the damping torques in synchronous machines are the outcome of the relative speed between the rotor and the resultant flux in the air gap. These torques play an important role in damping out oscillations. The relation to evaluate damping torque has been derived from Park's equations[195], as well as from the view point of induction motor theory[163] as,

$$T_{(amort)} = \frac{(V')^2 \; (X'_d - X''_d)}{(X'_d + X_e)\,(X''_d + X_e)} \cdot \frac{s}{\alpha_d} \cdot \mathrm{Sin}^2\delta$$

$$+ \frac{(V')^2 \; (X_q - X''_q)}{(X_q + X_e)(X''_q + X_e)} \cdot \frac{s}{\alpha_q} \cdot \mathrm{Cos}^2\delta \qquad (3.31)$$

where s = per unit slip

α_d = direct axis amortisseur decrement factor

$$= \frac{(X'_d + X_e)}{(X''_d + X_e)} \cdot \frac{1}{T''_{do}}$$

α_q = quadrature axis amortisseur decrement factor

$$= \frac{(X_q + X_e)}{(X''_q + X_e)} \cdot \frac{1}{T''_{qo}}$$

The damping torque coefficient from equation (3.31),

$$T_D = \frac{dT}{ds} = a\ \sin^2\delta + b\ \cos^2\delta \qquad (3.32)$$

or $$T_{D(ave)} \cong \frac{a + b}{2}$$

where $$a = \frac{(V')^2 \; (X'_d - X''_d)}{(X'_d + X_e)\,(X''_d + X_e)} \cdot \frac{1}{\alpha_d}$$

and $$b = \frac{(V')^2 \, (X_q - X''_q)}{(X_q + X_e)\,(X''_q + X_e)} \cdot \frac{1}{\alpha_q}$$

In the above, strictly speaking, s should be the slip between the resultant air gap flux and the rotor, but the damping torque coefficient has been modified with the direct and quadrature axes amortisseur decrement factors, thus enabling us to use the slip of the rotor with respect to the infinite bus instead of the slip with respect to the resultant flux. In addition to the above induction motor torque, the relative speed between the stator flux and the rotor induces eddy currents in the iron structure of the rotor, thus producing eddy current damping as confirmed by actual tests[195]. Bahrali and Adkin[199], have investigated such eddy current damping in synchronous machines with the aid of operational impedances and curves of magnetisation for the machines. For lower frequencies of oscillation, the Bahrali and Adkin result reduces to Crary's formula as in equation (3.32).

The treatment of damping torques as presented by Bahrali and Adkin gives approximately the asynchronous torque, and this allows the derivation of the overall damping coefficient T_D from the asynchronous torque/speed characteristics.

Then the damping torque $= T_D \cdot s$

where s is the P. U. deviation in the speed of the synchronous machine. For synchronous generators, s has been taken as positive when the machine experiences an induction generator torque.

An extension of damping torque consideration to a multi-machine system has been made in reference 163 in which the infinite bus voltage is chosen to correspond to the Thevenin's equivalent e.m.f. when the machine under consideration is disconnected, whereas the external reactance corresponds to the short circuit reactance (because the resistance is usually small, and the instantaneous slip of the machine under consideration will be with respect to the instantaneous phase of the Thevenin equivalent e.m.f.).

Hore[224], suggests the measurement of s with respect to the terminal voltage, because, he argues, the machine views the whole network from its terminals - this procedure is quite time saving (but not precise). Hore concludes that the neglect of damping torques is safe because the damping contributed is positive (and of the order of 1% improvement in fault clearance time).

The above considerations of damping torque will produce effects which always work only in the positive direction (and never in the negative direction), whether the synchronous machine is accelerating or decelerating, which does not correspond to the situation in practice, where the damping in fact can be positive or negative (as shown in Section 3.2.2).

3.2 Behaviour Under Disturbed Conditions

Under disturbed conditions, the various synchronous machine rotors move at different instantaneous speeds with respect to the steady-state synchronous speed, resulting in deviations in instantaneous frequency of the voltages and currents in the various parts of the power system. The change in instantaneous speed brings about:-

(a) A change in the kinetic energy stored in the synchronous machine rotating parts.

(b) A change in machine e.m.f's depending upon the type of excitation system.

(c) A change in the synchronous machine reactance.

(d) A relative speed between the rotors of the synchronous machines and their resultant air gap fluxes.

(e) Prime Mover Damping : the inherent prime mover torque-speed characteristic with constant valve opening causes positive damping as a result of change in shaft torque consequent on a change in speed. This effect is less than that produced by the amortisseur damping windings and is accordingly considered as having relatively small significance on the first-swing transient stability limits (reference 195, Chapter 7).

3.2.1 Consideration of Instantaneous Frequency Effects

As pointed out above, the prime mover damping has relatively small significance during the first-swing transient stability periods, and will not be considered here. The effects (a) to (c) have been hitherto neglected - these will be treated in detail in the next sections. Effect (d) has been incorrectly represented in the past, and is considered in Section (3.2.2).

3.2.1.1 Representation of Angular Momentum

Transient stability calculations take account of angular momentum usually through a Stored Energy Factor, H, given by:-

$$H = \frac{5.48 \times 10^{-6} \, Jn_1^2}{P_{kVA}} \text{ kW - secs/kVA} \tag{3.34}$$

or sometimes through a Factor, $M_o = \dfrac{P_{kVA} \cdot H}{180 \, f_o}$ (3.35)

Clearly, M depends on the machine instantaneous rotor angular velocity (or instantaneous frequency) and, for a given machine, may be expressed:-

$$M = K \cdot f_r$$

$$\text{or} \quad M = \frac{M_o \cdot f_r}{f_o} \tag{3.36}$$

Accurate representation of angular momentum effects therefore requires appropriate modification of M in the step by step calculations to take account of instantaneous frequency in the manner suggested by Equation (3.36).

3.2.1.2 Representation of Machine e.m.f.

The synchronous machine e.m.f. depends upon the instantaneous rotor speed, and for a separately excited alternator (i.e. the main exciter not driven by the main alternator shaft), the instantaneous e.m.f. induced is directly proportional to the instantaneous speed of the machine rotor, whereas in the case where the main exciter is common shaft driven, the alternator e.m.f. induced will be approximately proportional to the square of the rotor instantaneous speed. Present day high output machines on power systems do not usually employ common shaft driven exciters due to commutator problems, and for these machines, the instantaneous machine e.m.f. is given by,

$$E_m = \frac{E_{mo} \, f_m^i}{f_o} \tag{3.37}$$

3.2.1.3 Representation of Machine Reactance

Reactances of synchronous machines are normally specified at system nominal frequency, but their actual instantaneous values depend upon the instantaneous frequency of the machine current, which, during transient disturbances, deviates from that of the machine e.m.f. as shown in figure 3.6(c). The instantaneous frequencies of the stator currents can be equal to those of the e.m.f's only when there is a very close symmetrical fault (see Section 3.2.2). The instantaneous values of all machine reactances are directly proportional to the stator current instantaneous frequency, but their consideration involves considerable increase in computing time with negligible overall benefit (as discussed in Section 3.2.1.6, and illustrated in figure 3.6(b)).

3.2.1.4 Representation of Unit Transformers

Unit transformers have previously been considered by their equivalent impedances at system nominal frequency. A recent report[234] on damages caused by overfluxing the unit transformers under various conditions of operation suggests that the machine terminal voltage should not exceed more than 105% of the rated value, otherwise there will be permanent damage to the transformer due to excessive eddy currents in the iron core, winding conductors and the steel structure. (This 5% over-excitation is according to the design specifications for power transformers (ASA standard C57.12-00.400 (1958))). In the present studies, as the adjustment of the automatic voltage regulator gain is such as just to overcome the flux decay under disturbed conditions, there will be no possibility of over-excitation, and therefore the transformer representation by an equivalent impedance at the instantaneous frequency of the current passing through it will be adequate.

In the case where there is in fact over-excitation of the unit transformers under disturbed conditions, their leakage reactance will increase, with the consequent appearance of a shunt load due to excessive eddy currents. This matter clearly requires further study before accurate representations of the effects can be achieved.

3.2.1.5 Procedure for Transient Stability Calculations

The following procedure satisfies the requirements of the present method, providing swing curves and other relevant information:-

(1) Form the admittance matrix for the entire power system at system nominal frequency for load flow studies.

(2) Determine the overall power balance for the system.

(3) Replace all the loads by their shunt admittances.

(4) Apply the appropriate disturbance.

(5) Determine the driving point and transfer admittances for the various machines.

(6) Determine the new angular positions of the various synchronous machines by solving their differential equations.

(7) Determine the instantaneous frequency for all the machines as,

$$f_m^i = \frac{\delta_m^i - \delta_{om}^i}{2\pi \cdot \Delta t} + f_o$$

(8) Modify the instantaneous frequency by an accelerating factor as,

$$f_m^i = f_m^{i-1} + (f_m^i - f_m^{i-1}) \times \text{Accelerating factor}$$

(9) Modify the e.m.f's. of the synchronous machines as,

$$E_m^i = \frac{E_{mo} \times f_m^i}{f_o}$$

(10) Calculate the instantaneous angular momentums as,

$$M_m^i = M_{om} \cdot \frac{f_{rm}^i}{f_o}$$

(11) Modify the machine reactances for the instantaneous frequency.

(12) Form the new admittance matrix for the entire system at the current values of instantaneous frequency, adjusting machine reactances appropriately.

(13) Determine the new driving point and transfer admittances for the various machines.

(14) Determine the new angular positions of the various synchronous

machines by solving their differential equations.

(15) Test for convergence,

(a) instantaneous frequency should be within (say) 10^{-6} cycles.

(b) instantaneous machine power angles to be within (say) 10^{-3} degrees.

If the tests are not satisfied, go to step (7) and recycle.

(16) Write the required quantities.

Solution proceeds iteratively. An accelerating factor of 1.35 has been found suitable for operation (8), giving convergence to within the tolerances of operation (15) in 6 to 7 iterations. It may be noted that smaller values of accelerating factor produce too slow a convergence, while larger values produce overcorrections, leading to instability of the solution. A time interval for each step, $\Delta t = 0.05$ sec. has been found suitable (as in the case of the usual transient stability calculations).

3.2.1.6 Problem Illustrating Instantaneous Frequency Effects

In order to highlight the frequency-dependent effects of the synchronous machines, a 4-machine problem, figure 3.6(a)* (based on an

* Note. This problem is basically the same as an example presented in reference 195, except that H factors of the synchronous machines have been modified to correspond more closely to those of modern machines. In addition, the load at bus 7 remains of constant configuration, whereas in the original case a section of it (0.153 P.U. at unity power factor) was disconnected with occurrence of the fault.

example from ref. 195) has been chosen to illustrate the magnitude and significance of the effects introduced herein. The transmission network and the system loads are in this case represented at system nominal frequency. A 3-phase fault is applied on the line connecting buses 10 and 11, close to bus 11; breaker 1 disconnects this line from bus 11, and subsequently, the fault is cleared completely by breaker 2 isolating the faulty line.

Further information relating to the illustrative problem shown in figure 3.6(a) is given in Table I, and figure 3.7 indicates the saturation curve which has been approximated by a third degree Polynomial for all the synchronous machines in the system.

TABLE I

Details for Figure 3.6(a)

Machine	Saturated Synchronous Reactance (Xd) (P.U.)	Potier Reactance = Direct Axis Transient Reactance (Xd') (P.U.)	Direct Axis Open Circuit Field Time Constant (seconds)	Voltage Regulator Characteristics* (Conventional, Continuously Acting)
1	1.0	0.13	7.5	Exponential Response Voltage Gain = 20
2	1.8	0.28	7.5	Total Excitation Time
3	1.8	0.259	7.5	Constant = 0.5 secs. (Exciter + Main
4	0.95	0.15	7.5	Generator Field winding).

The machines have no transient saliency (that is, X'_q is taken as equal to X'_d).

* Voltage regulator gain for each machine has been adjusted so as just to overcome changes in e.m.f. due to flux decay, in conformity with reasonable practice (as, for example, suggested in Ref. 198).

Selected significant results are shown plotted in figures 3.6(b), (c), (d) and (e). In all of the above cases, the transmission networks and loads have been considered at system nominal frequency for reasons outlined above.

For the purposes of comparison, swing curves have been obtained for the different methods of representation of the synchronous machines as outlined in Table II.

TABLE II

Methods Employed in Representing Synchronous Machines

Type of Synchronous Machine Representation	Calculation Time in minutes using an IBM 360/50 Computer
(i) e.m.f. behind transient reactance (using standard procedure of long standing[195])	0.4
(ii) as for (i), plus variations of "M" with instantaneous frequency	0.6
(iii) as for (i), plus variations of machine e.m.f. with instantaneous frequency	0.6
(iv) as for (i), plus variations of machine reactance with instantaneous frequency	6.0
(v) as for (i), plus variations of "M" and machine e.m.f. with instantaneous frequency	0.6
(vi) as for (i), plus variations of "M", machine e.m.f. and reactance with instantaneous frequency	6.0
(vii) inclusion of voltage regulator, saturation and flux decay effects (without transient frequency considerations)	0.7
(viii) as for (vii), plus variations of "M" and machine e.m.f. with instantaneous frequency	0.8
(ix) as for (vii), plus variations of "M", machine e.m.f. and reactance with instantaneous frequency	6.3

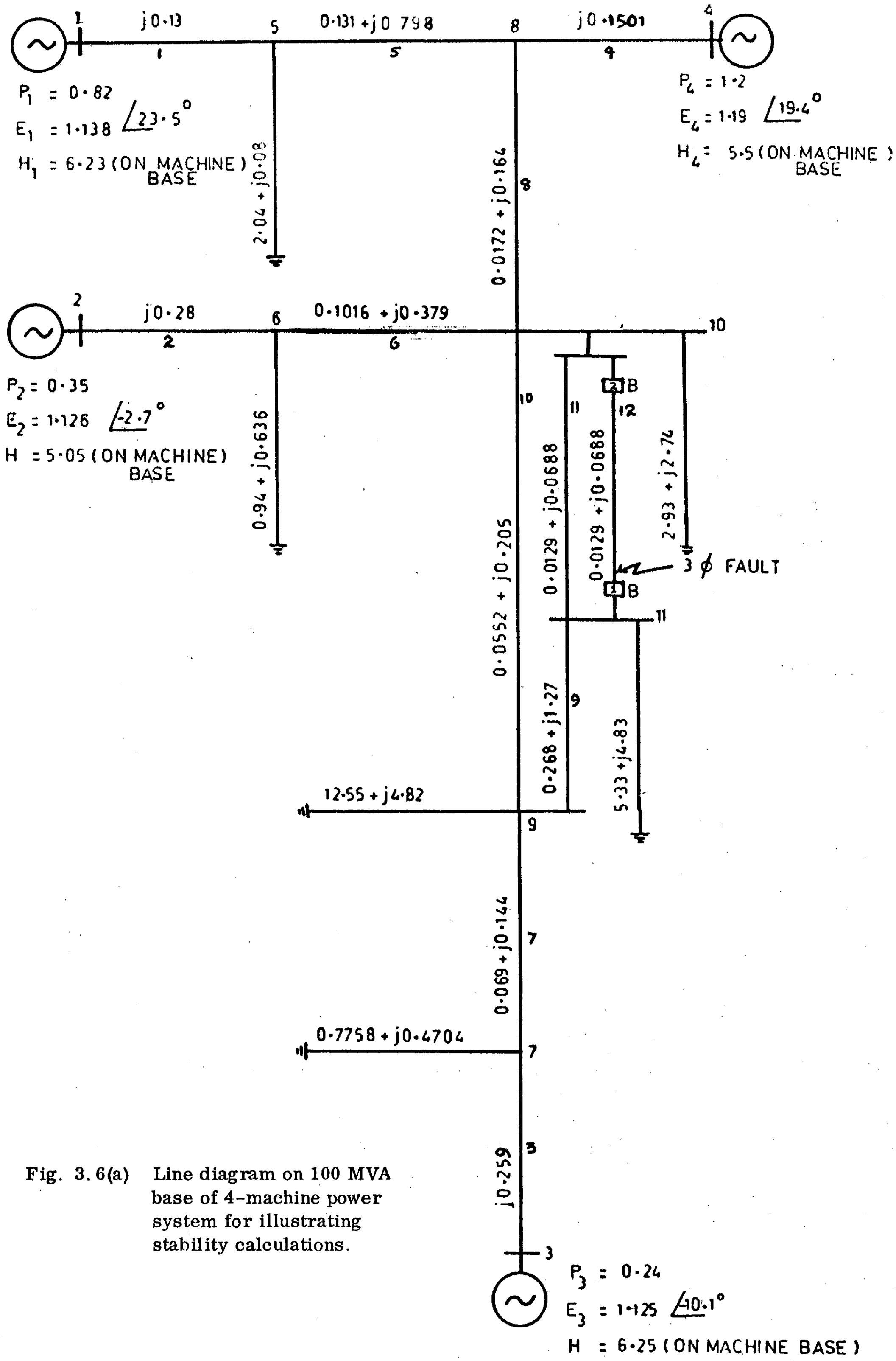

Fig. 3.6(a) Line diagram on 100 MVA base of 4-machine power system for illustrating stability calculations.

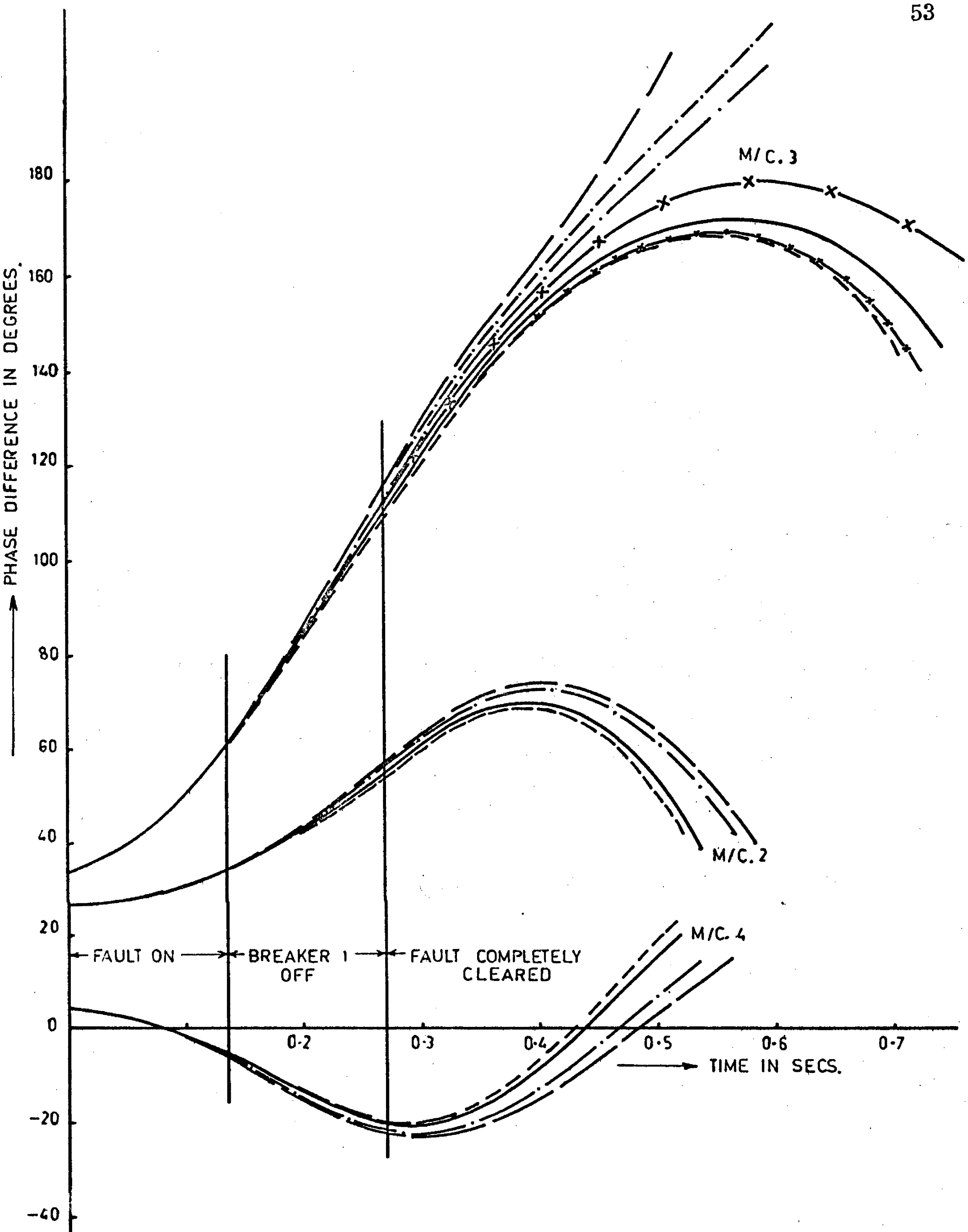

Fig. 3. 6(b) Relative swing curves with respect to machine 1 for a near unstable case when total fault clearance time=270 m sec.

————	with e. m. f. behind transient reactance.
—·—·—	" " " " " + variations of M with f.
—x—	" " " " " + " " E " "
————	" " " " " + " " E & M with f.
——·——	" voltage regulator, saturation and flux decay.
– – – – –	" " " " " " " + variations of E & H with f.
—x—x—x—	" " " " " " " " and reactance.

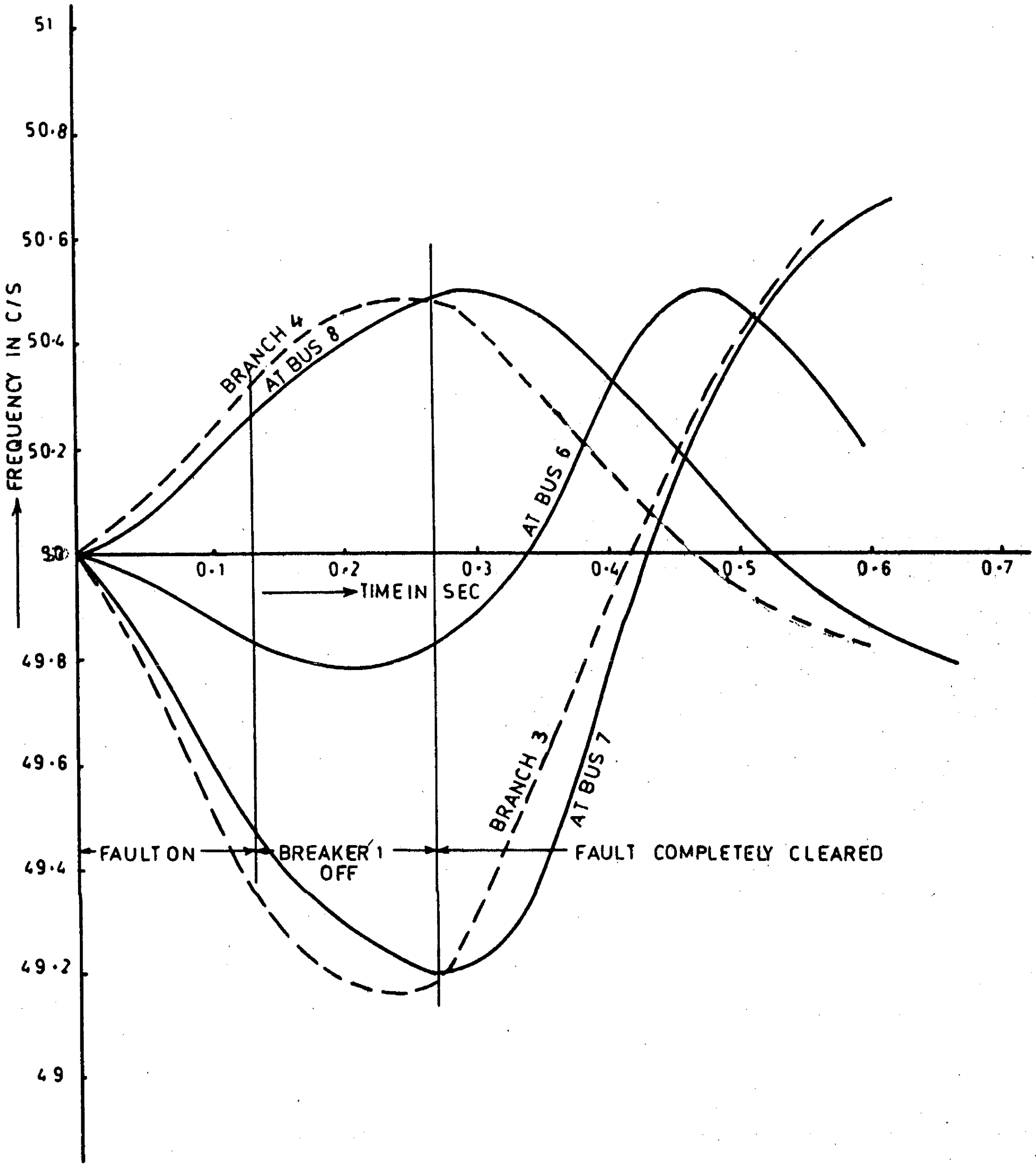

Fig. 3.6(c) Instantaneous frequency at specified points in the system with the most detailed representation of the synchronous machines. (Total fault clearance time = 270 m sec.).

———— Instantaneous frequency of voltage.
– – – – " " " current.

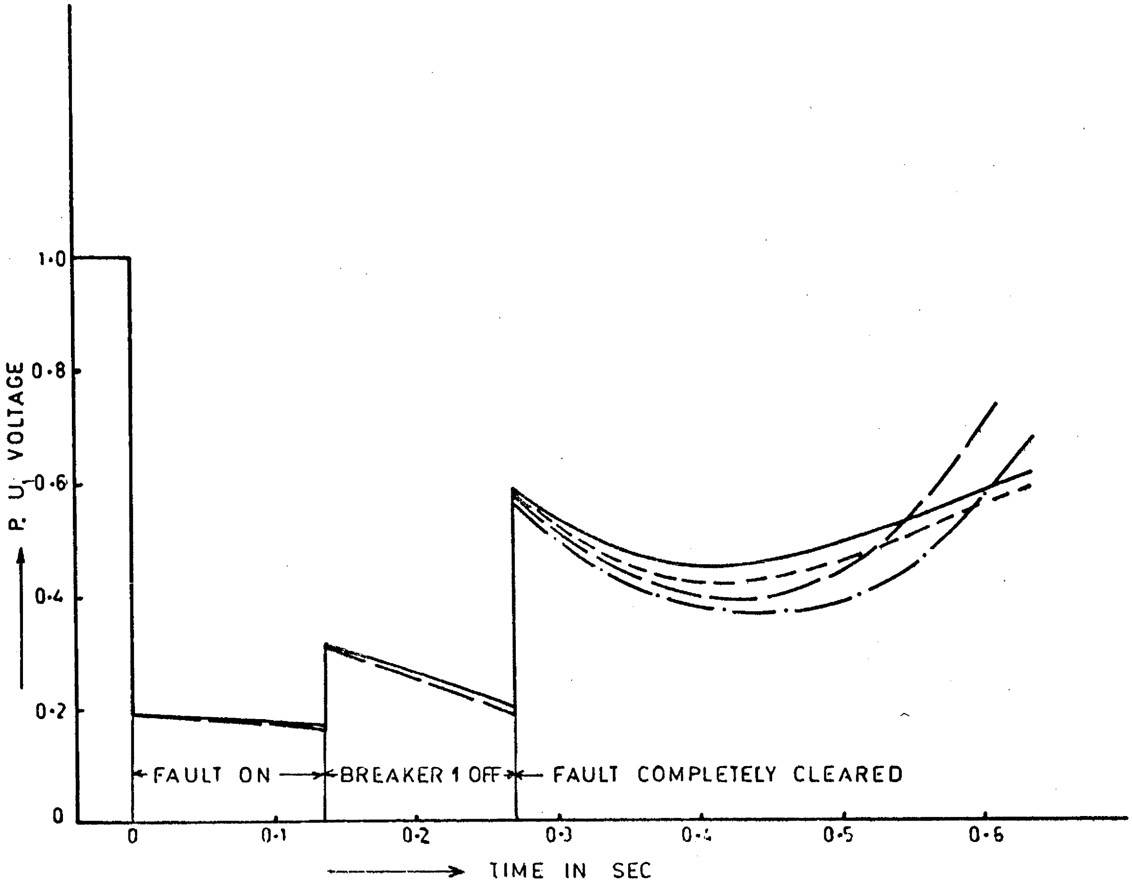

Fig. 3.6(d) Voltage variations at bus no. 10. (Total fault clearance time ≈270 m sec.).

——— ——— with e.m.f. behind transient reactance.
————— " " " " " + variation of E & M with f.
———·——— " voltage regulator, saturation and flux decay.
– – – – – – " " " " " " " + variation of E & M with f.

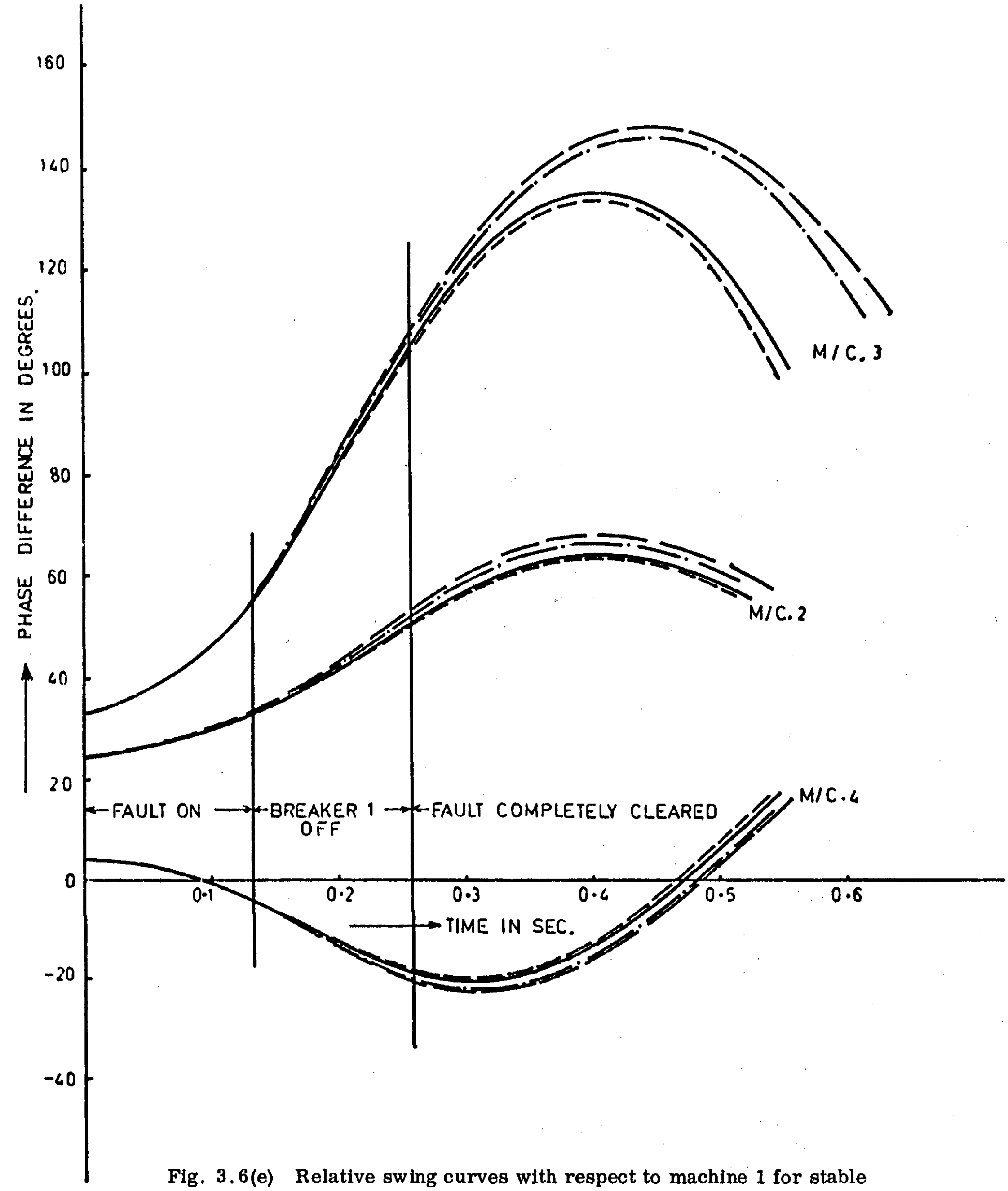

Fig. 3.6(e) Relative swing curves with respect to machine 1 for stable conditions when total fault clearance time is 258 m sec.

—— —— with e. m. f. behind transient reactance.
———— " " " " " + variation of E & M with f.
—— —— " voltage regulator, saturation and flux decay.
– – – – – " " " " " " " + variations of E & M with f.

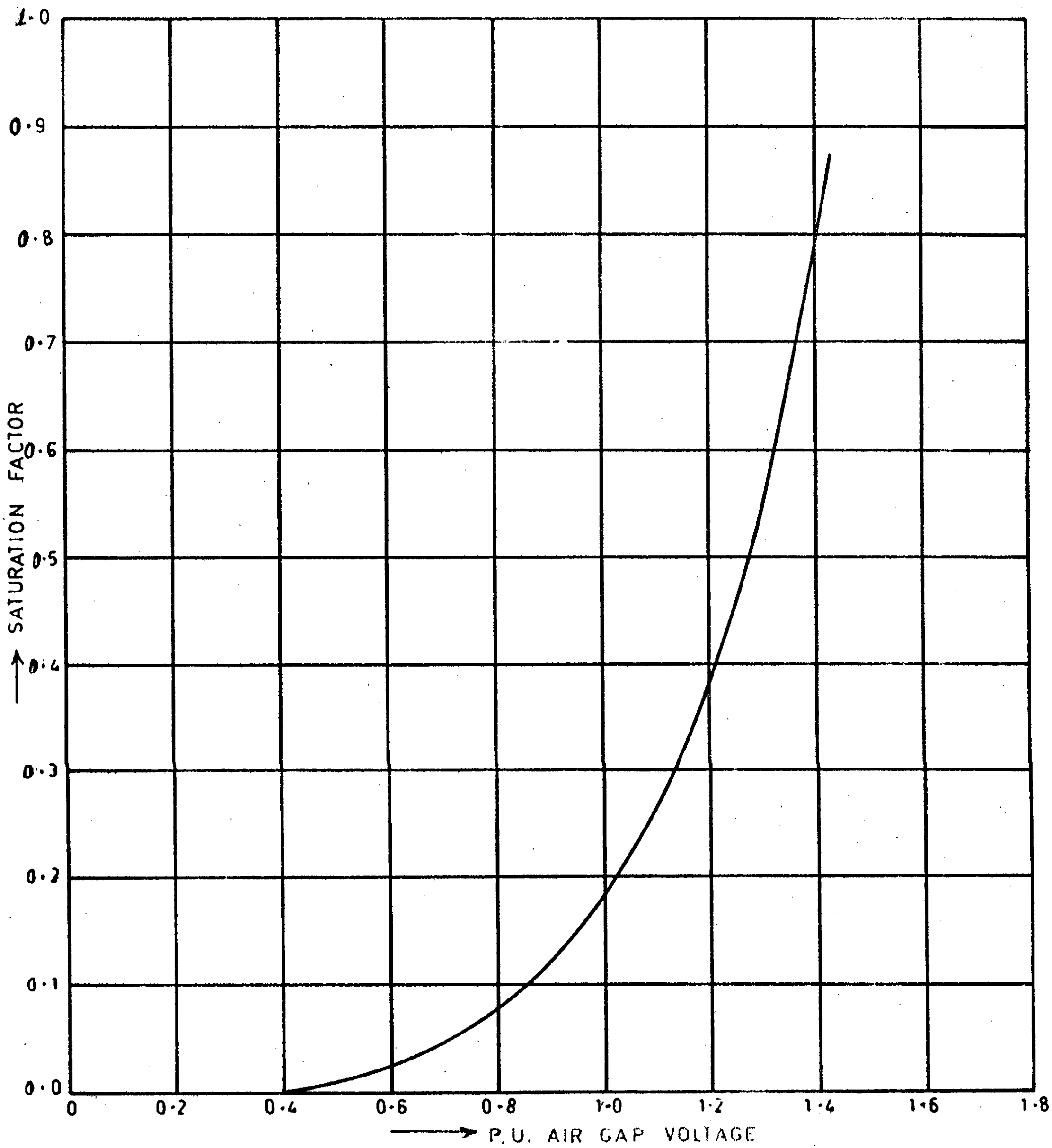

Fig. 3.7 Saturation curve for synchronous machine.

3.2.2 Treatment of Damping Torques

Figure (3.8b) indicates the phasor diagram for the system shown in Figure (3.8a), just after a 3-phase symmetrical fault. The flux produced by the stator current will be in phase with the stator current, and consequently the resultant air-gap flux can be evaluated and positioned with respect to reference phasor V'. The instantaneous position of the rotor conductors can be conveniently referenced by the e.m.f. phasor E_Q, because the direct axis of the rotor is always 90^o ahead of quadrature axis, indicated by E_Q (e.m.f. behind the quadrature axis reactance). During the disturbance period, the phasor E_Q swings forward or backward, depending upon the nett out of balance power available to the synchronous machine. The current I will follow the phasor E_Q; it may follow at the same angular velocity (above or below the synchronous speed) at which E_Q is moving, or it may follow at an angular velocity above or below that of E_Q. The damping power will depend on the relative speed between the phasors E_Q and Φ and not on the slip of phasor E_Q with respect to the infinite bus voltage phasor V', as has been used in references 214 and 229. The resultant air-gap flux can conveniently be evaluated as the P.U. e.m.f. behind the Potier reactance (X_p) of the machine. The situation in the following cases is considered:-

(a) During the Fault Period

During this period there will be a d.c. rapidly decaying component if the fault is very close to the machine and is symmetrical. This can be handled conveniently[229] as explained in Section (3.1.4.1). The current I phasor, which is responsible in changing the phase difference between E_Q and Φ, follows the E_Q phasor at the same speed and consequently there will be no damping torque of the type discussed in Section (3.1.4.2), except the d.c. braking.

During asymmetrical faults, negative sequence braking is present but the positive sequence current component will create damping because it will not follow the phasor E_Q at the same speed. Negative sequence braking can be handled[229] as explained in Section (3.1.4.1).

(b) After the Fault Clearance

During this period, the system is in a normal configuration but oscillatory; there will be no braking, and the damping torques present will damp out the oscillations if the system remains in step. The damping torque is equal to $\frac{K_D}{\omega_1} \cdot \frac{d\Psi}{dt}$, where K_D^* is the slope of the asynchronous torque-slip characteristic of the synchronous machine under consideration, and Ψ is the phase difference between the phasors E_Q and Φ.

In the case where the synchronous generator is accelerating, (that is the phasor E_Q has higher instantaneous frequency than base frequency of the system, and consequently the phasor Φ follows E_Q), if the phasor Φ moves at a higher instantaneous frequency than E_Q, then there will be negative damping, due to induction motor torque, whereas if phasor Φ moves at a lower instantaneous frequency than E_Q, then there will be positive damping due to induction generating torque as shown by the illustrative examples in Sections (3.2.2.2 and 3.2.2.3). For a decelerating synchronous generator, the generating torque developed due to the interaction of the resultant air-gap flux and rotor structure, will promote the deceleration, thus acting as

---

* K_D is equal to P.U. asynchronous torque/P.U. slip, and is used as a damping coefficient in the proposed approach to consider synchronous machine damping while employing the rotor slip w.r.t. the resultant air-gap flux Φ, whereas T_D is the damping coefficient for the existing approach when the rotor slip used is w.r.t. the infinite bus voltage.

negative damping, whereas the motoring torque will act as positive damping under these circumstances.

3.2.2.1 Transient Stability Calculation Procedure to Include Damping

(a) Form the admittance matrix for the entire system at system nominal frequency for load flow studies.

(b) Determine the overall power balance for the system and the resultant air-gap fluxes for all the synchronous machines quantitatively.

(c) Apply the appropriate disturbance.

(d) Determine the driving point and transfer admittances for the various machines.

(e) Determine the resultant air-gap fluxes for all the synchronous machines both in magnitude and phase.

(f) Determine the direct current components and the negative phase sequence current components for all the synchronous machines at the beginning of the time interval "Δt".

(g) Calculate the new angular positions of the various synchronous machines by solving their differential equations.

(h) Determine the machine currents, such as d.c. component, negative and positive phase sequence in magnitude and phase.

(i) Calculate the resultant air-gap fluxes both in magnitude and phase.

(j) Determine the instantaneous frequencies of the e.m.f's. E_Q and of resultant air-gap fluxes "Φ", as

$$f_{\Phi} = \frac{\theta - \theta_o}{2\pi \Delta t} + f_o$$

$$f_{E_Q} = \frac{\delta - \delta_o}{2\pi \Delta t} + f_o$$

(k) Determine the average frequencies of E_Q and Φ during the time interval "Δt".

(ℓ) Determine the slip between E_Q and Φ.

(m) Determine the average damping powers during the time interval "Δt",

$$= K_D \cdot s \left[\frac{\text{average magnitude of } \Phi \text{ during } \Delta t}{\text{normal magnitude of } \Phi}\right]^2 \times \text{P. U. speed.}$$

(n) Determine the average braking powers during the time interval "Δt".

(o) Determine the nett out-of-balance power available to the various synchronous machines.

(p) Determine the new angular positions for the synchronous machines by solving their differential equations.

(q) Test for convergence of instantaneous machine power angles to be within (say) 10^{-3} of a degree. If the test is not satisfied, go to step (h) and repeat.

(r) Write the various quantities.

The solution proceeds iteratively.

3.2.2.2 Single - Machine Study

The line diagram for a single-machine supplying an infinite bus is shown in Figure (3.8a). The constants used for this machine are those of a 9 MVA, 13.8 KV, salient pole synchronous machine reported in reference 195, for which the damping coefficient has been determined by field tests. Figure (3.9) indicates the instantaneous frequency of the phasors E_Q and the resultant flux for a case which is assessed as unstable when damping is ignored, but which becomes stable in the presence of damping, as shown in Figure (3.12b). From the instantaneous slip variations of the phasor E_Q, shown in Figure (3.10), it is obvious that the damping is always positive during the fault, when the machine accelerates, both for rotor slip considerations with respect to the infinite bus voltage and machine terminal voltage (V_t), whereas Figure (3.9) indicates that the damping is positive up to the point F, (because up to this point, the machine develops extra generating torque due to the slip speed between E_Q and Φ), but after the point F, the damping in fact becomes negative, as shown by the instantaneous slip between the resultant flux and the rotor in Figure (3.11). This negative damping continues until the fault is cleared and the machine starts decelerating. In these calculations, a figure of $K_D = 250$ has been used, based on asynchronous torque-slip characteristics which have been determined experimentally, for example, in Reference 192, which gives the slope as 1.0 P.U. power output/0.004 P.U. slip, i.e. $K_D = 250$.

Figures (3.12) (a andb) indicate the swing curves obtained under different conditions: during the fault, the reduced Thevenin's equivalent e.m.f. available to the machine provides very little damping when considered with respect to the synchronous speed, whereas consideration of damping with respect to the resultant air-gap flux indicates a relatively larger effect. The consideration of damping with respect to the instantaneous

$E_Q = 1.64 \angle 23.85^{\circ}$

$P = 0.8$ P. U.

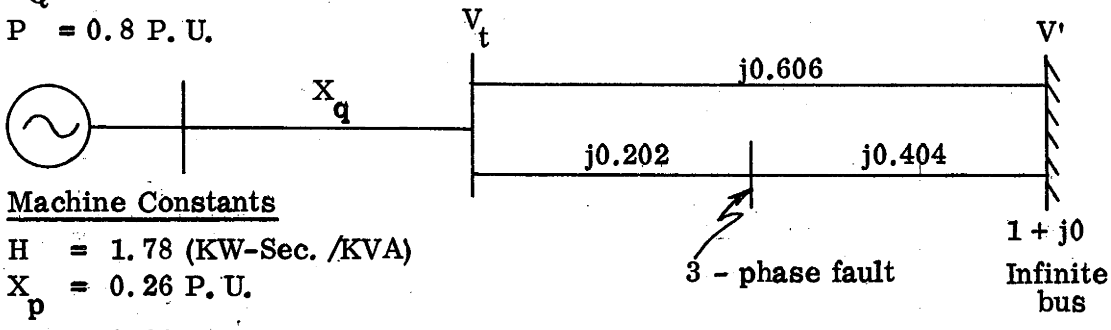

<u>Machine Constants</u>

$H = 1.78$ (KW-Sec. /KVA)

$X_p = 0.26$ P. U.

$X_d' = 0.26$ "

$T_{do} = 10$ Sec.

$T_D = 5.6$ P. U. /P. U. Slip

$X_d = 1.1$ P. U.

$X_q = 0.524$ "

Fig. 3.8(a) Line diagram for single machine transient stability study.

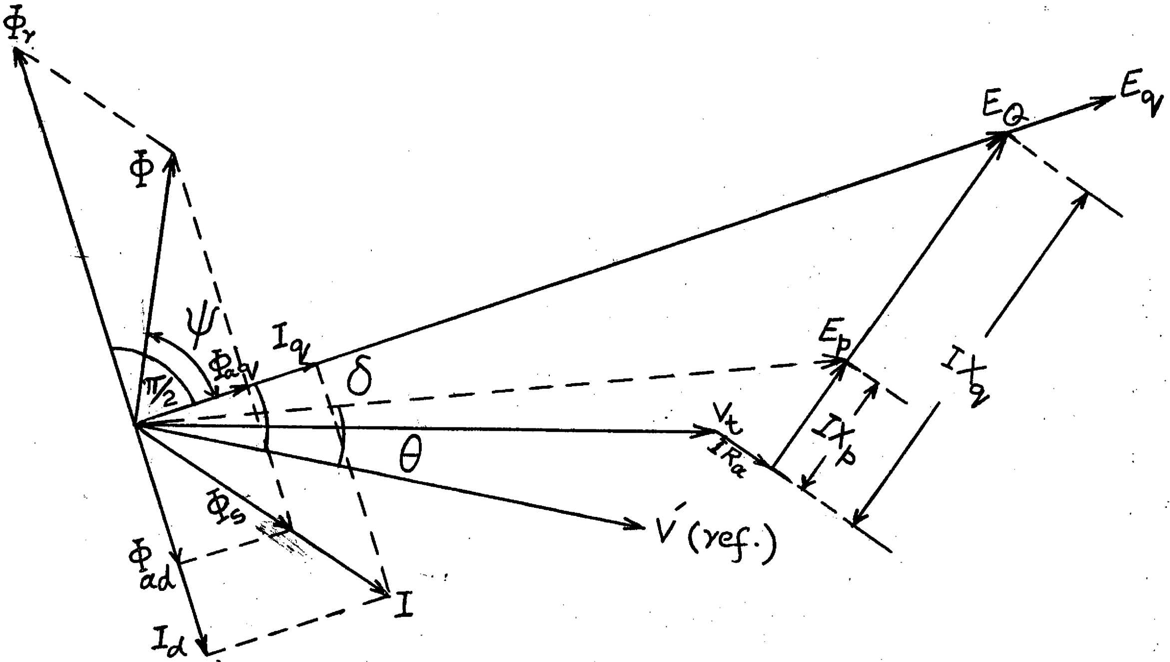

Fig. 3.8(b) Phasor diagram for the synchronous machine of Fig. 3.8(a).

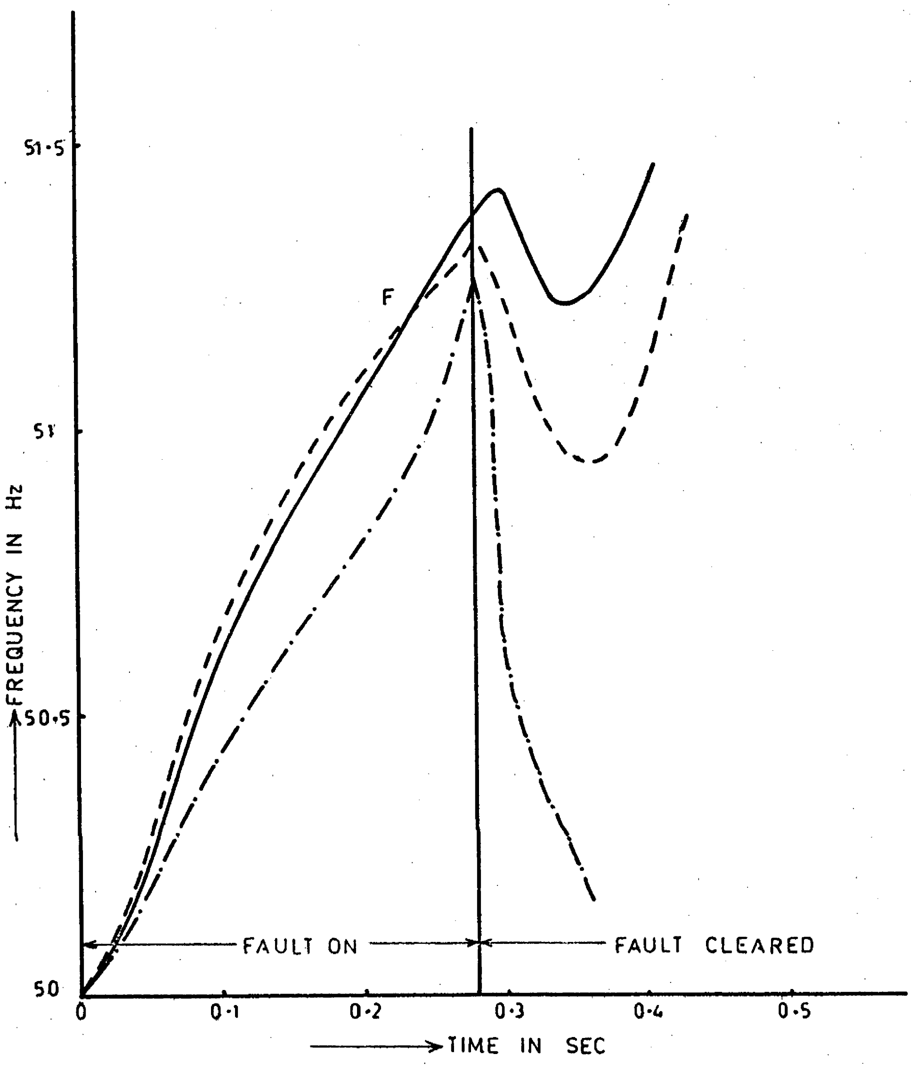

Fig. 3. 9 Instantaneous frequencies for the case shown in Fig 3.12 (b).

– – – – – – Frequency of E_Q (voltage behind X_q).

——————— " " ϕ (resultant air gap flux).

—·—·—·— " " V_t (M/c terminal voltage).

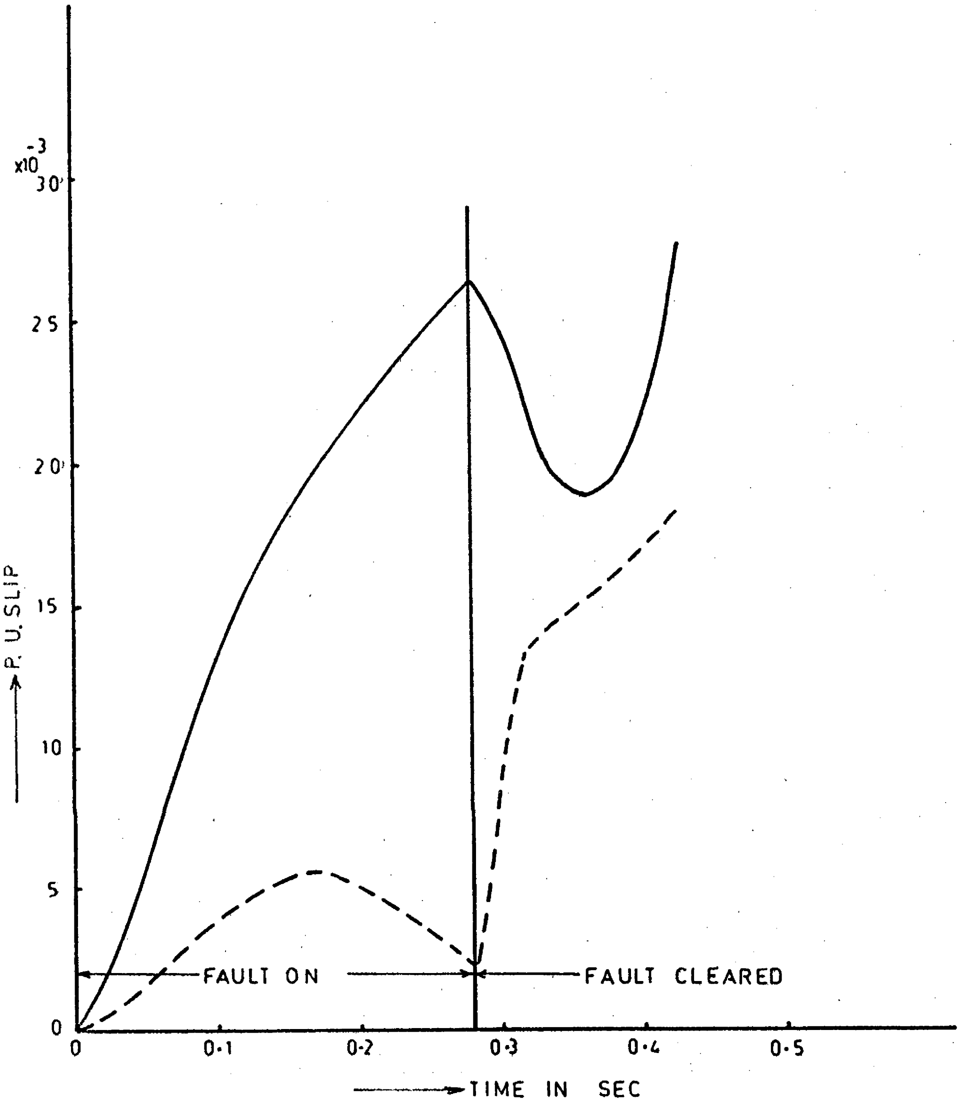

Fig. 3.10 Instantaneous slip of rotor.

——— with respect to infinite bus, V'.

– – – " " " m/c terminal voltage, V_t.

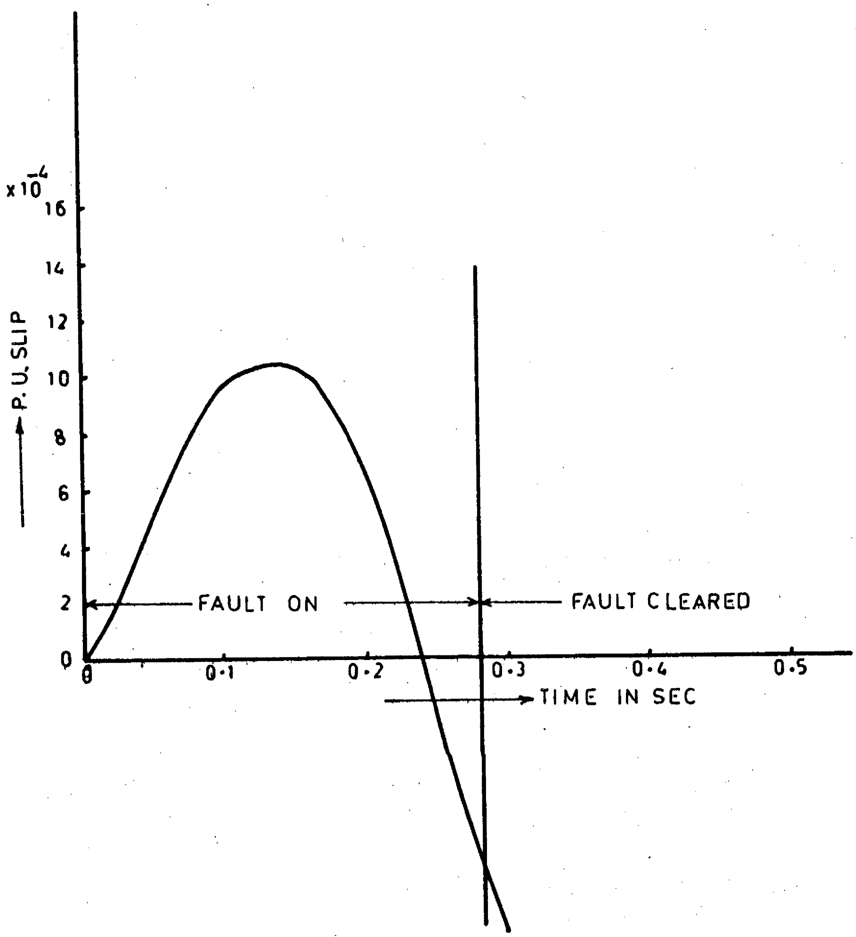

Fig. 3.11 Instantaneous slip of rotor with respect to resultant air gap flux, i.e. Φ

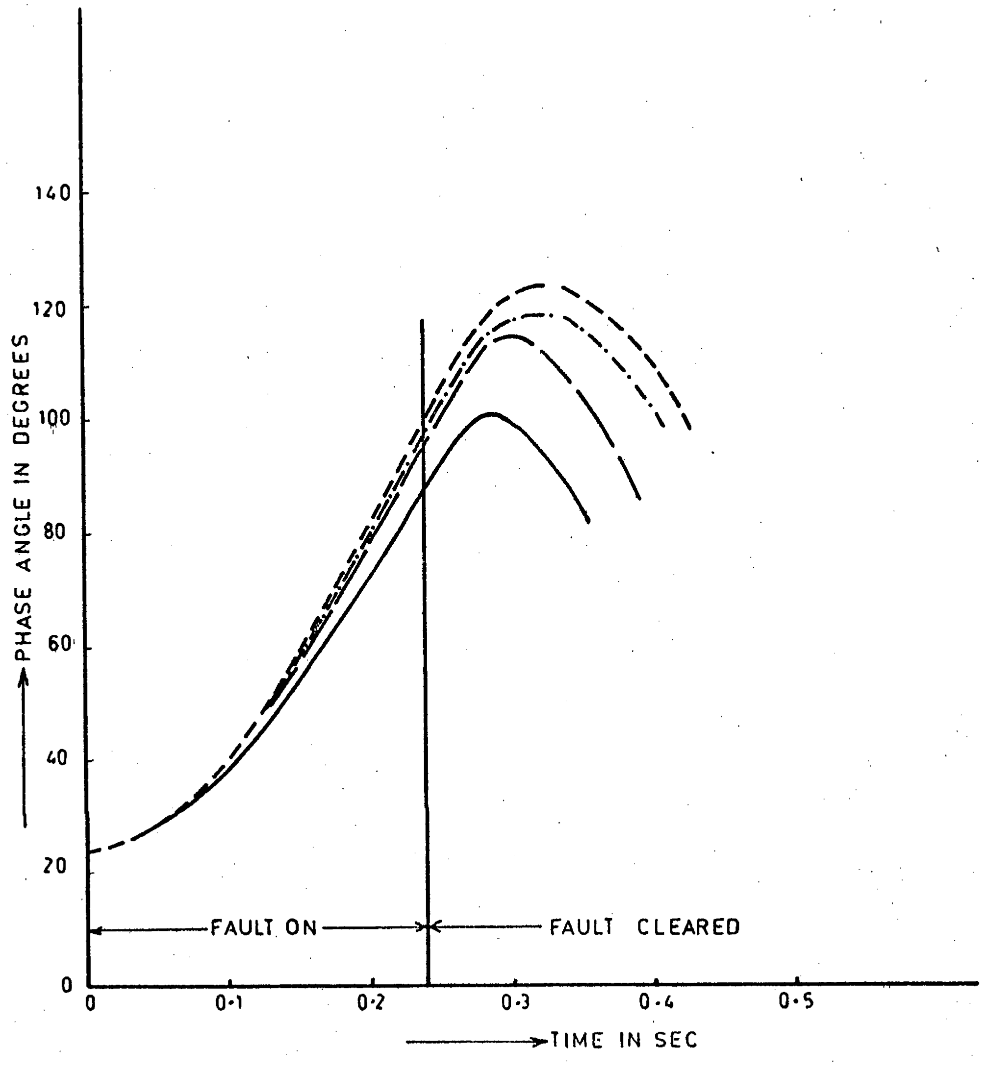

Fig. 3.12(a) Swing curves for synchronous machine of Fig.3.8(a) [For a case which is stable when damping is neglected].

- – – – – with no damping.
- –·–·– " damping when rotor slip used is w.r.t. V_t,
- —— —— " " " " " " " " V',
- ———— " " " " " " " " ϕ

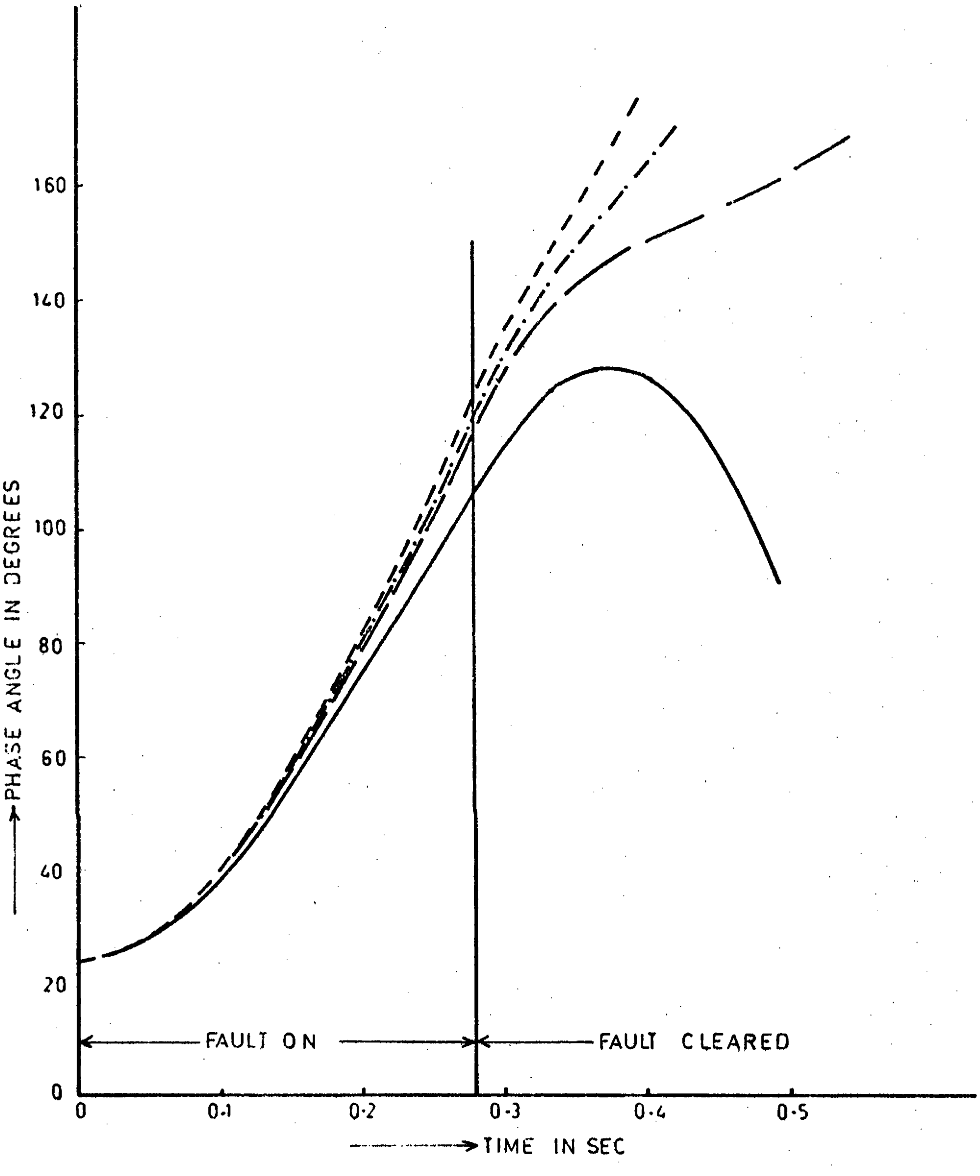

Fig. 3.12(b) Swing curves for synchronous machine of Fig. 3.8(a) [for a case which is unstable when damping is neglected].

– – – – with no damping.

–·–·–·– " damping when rotor slip used is w.r.t. V_t

—— —— " " " " " " " " V'

———— " " " " " " " " Φ

terminal voltage as suggested in Reference 224, indicates only a very small effect as shown in Figure (3.12) (a and b).

3.2.2.3 Multi-Machine Study

In this case, the Thevenin's equivalent e.m.f's must be determined in both magnitude and phase during each interval when using the existing methods of calculation[163]. As shown in Section 3.1.4.2, the damping torque is proportional to the square of the voltage of the infinite bus, and also as reported in Reference 192, the asynchronous output power varies directly with the square of the terminal voltage, but the method presented here considers the asynchronous torque as being proportional to the square of the instantaneous resultant air-gap flux.

In order to illustrate the inherent differences between the proposed and existing methods of treating damping, a 4-machine problem based on an example in Reference 195, (line diagram shown in Fig. (3.6a)), is presented. In order to illustrate the effect of transient saliency, the appropriate parameters have been included in the problem of Fig. 3.6(a), as given in Table III.

TABLE III Details for Figure (3.6a)

Machine	Saturated Synchronous Reactance		Potier Reactance = Direct Axis Transient Reactance X'_d (P.U.)	Direct Axis Open Circuit Field Time Constant Secs.	Remarks
	X_d(P.U.)	X_q(P.U.)			
1	0.6	0.13	0.09	7.5	Voltage regulator gain = 20. Total excitation time constant = 0.5 sec.
2	1.5	0.28	0.2	7.5	
3	1.0	0.259	0.18	7.5	
4	0.6	0.15	0.1	7.5	

The damping coefficient T_D used has been taken as 10, as reported in Reference 198, whereas K_D is the same as for a single machine study, that is, 250. The system has been investigated for conditions close to instability, but in fact remains stable. Figures (3.13) (a, b, c and d) indicate the instantaneous frequencies of E_Q, resultant flux, and of Thevenin's equivalent e.m.f., and Figure (3.14) indicates the swing curves for all the four machines under the following conditions :- without damping; damping assessed by an existing method; and damping calculated by the proposed method. The fault is a symmetrical 3-phase fault, on one line of the two-circuit line between nodes 10, 11 (Figure (3.6a)), remaining on for 123 m sec., then breaker 1 trips; after 246 m secs., the fault is completely cleared by removing the faulty line.

From the calculated results shown in Figures (3.13) (a-d), considering the synchronous machines individually:-

Machine No. 1 - Has negative damping up to the point F_1 and subsequently positive, when the rotor slip is taken with respect to the Thevenin's equivalent e.m.f., whereas the machine experiences negative damping up to F_2 only, and positive subsequently when the rotor slip is considered with respect to the resultant air-gap flux.

Machine No. 2 - Indicates positive damping during the decelerating period, and negative, after the fault has been completely cleared, up to the point F_3, when the slip is considered with respect to the Thevenin's equivalent e.m.f.; whereas the machine has positive damping during the fault period and negative after the fault has been cleared up to the point F_4, when the slip is taken with respect to the resultant air-gap flux.

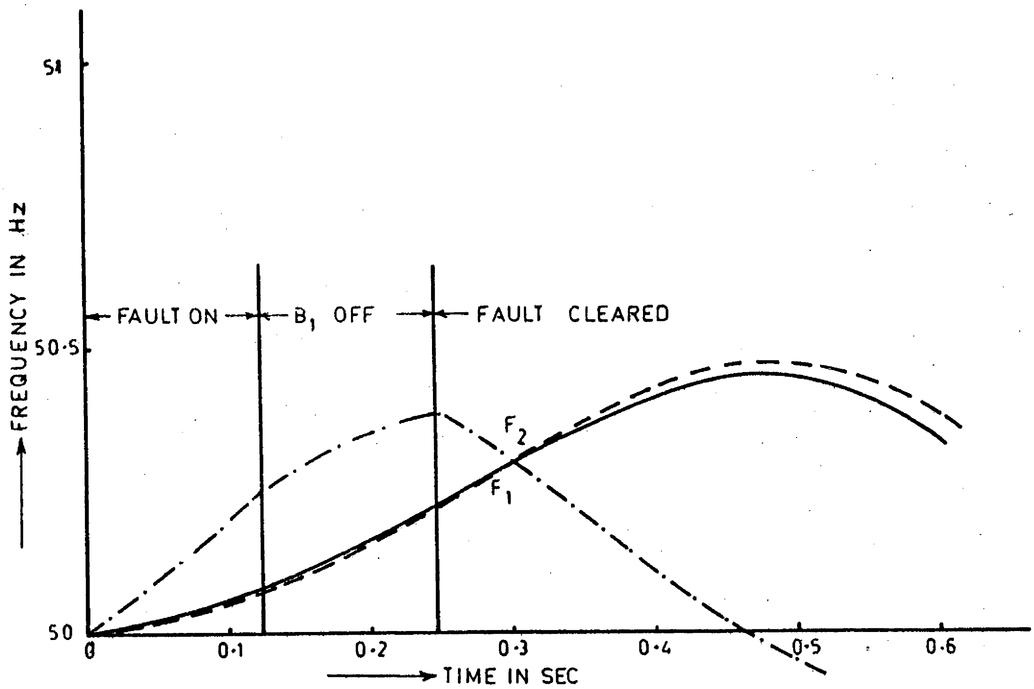

Fig. 3.13(a) Instantaneous frequencies of E_Q, Φ , and Thevenin's equivalent e.m.f. for machine no. 1.

- - - - - - Frequency of E_Q

———— " " Φ

—·—·—·— " " Thevenin's equivalent e.m.f.

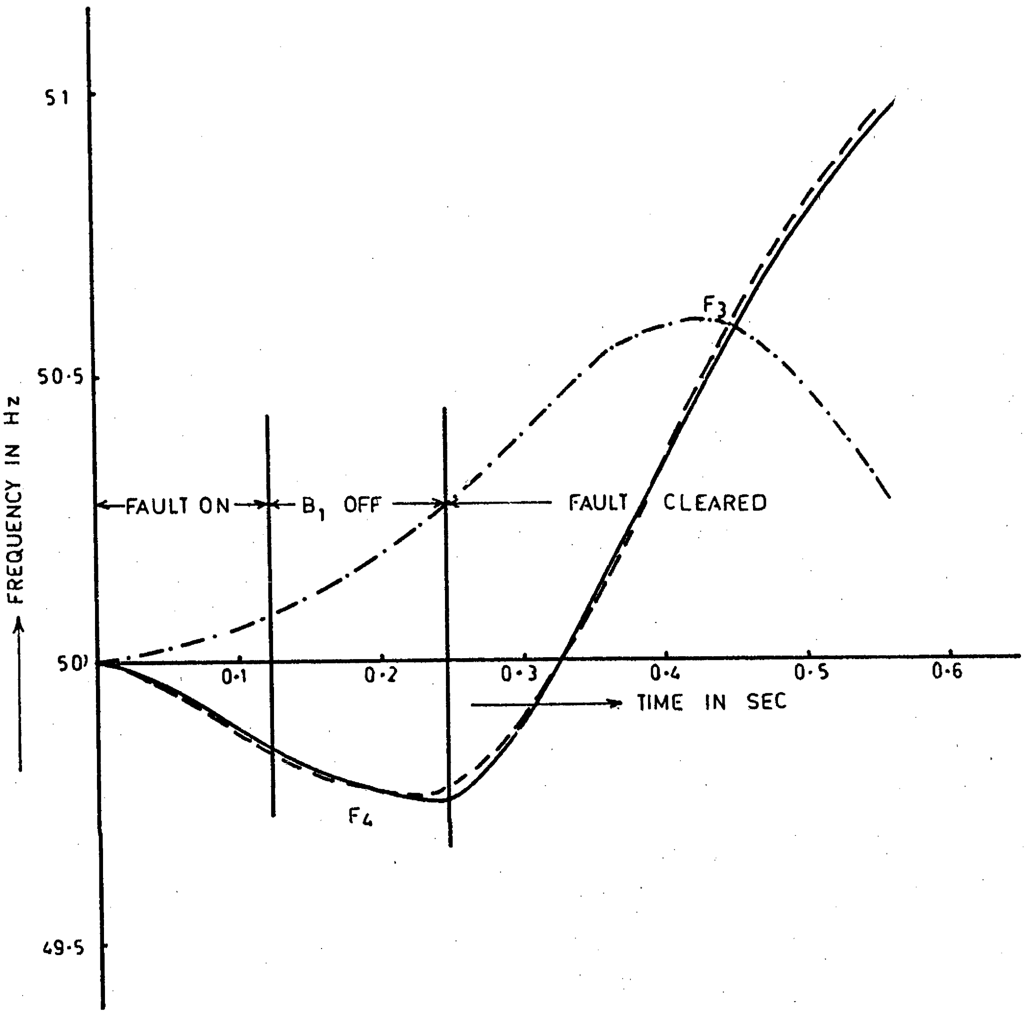

Fig. 3.13(b) Instantaneous frequencies of E_Q, Φ, and Thevenin's equivalent e.m.f. for machine no. 2.

— — — — — Frequency of E_Q
———————— " " Φ
—·—·—·— " " Thevenin's equivalent e.m.f.

Machine No. 3 - Experiences positive damping throughout, up to the point F_5 when the machine decelerates during the fault, and accelerates after fault clearance if the slip is considered with respect to the resultant air-gap flux; whereas the rotor slip with respect to the Thevenin's equivalent e.m.f. indicates positive damping during the fault and negative after fault clearance up to the point F_6, and then again positive.

Machine No. 4 - Has positive damping during the fault and subsequently negative up to the point F_7, when the rotor slip is considered with respect to the Thevenin's equivalent e.m.f.; whereas the machine has positive damping during the fault and negative subsequently, up to the point F_8, and then again positive, when the rotor slip is considered with respect to the resultant air-gap flux.

3.2.2.4 Availability of Relevant Data

The method of treatment of damping forces as employed in Section (3.2.2) involves an approximation in deriving the coefficient "K_D" (which depends on the asynchronous characteristics of the various synchronous machines) due to lack of specific information about each synchronous generator. The value of $K_D = 250$ is based on the assumption that the machine or the equivalent machine representing a group of synchronous generators, will run at a slip of 0.4% if it is to be run as an asynchronous machine - this average value has been assessed from the meagre literature available[192]. The asynchronous characteristics of course differ for different capacity machines, and a more accurate way to assess K_D for a group of machines

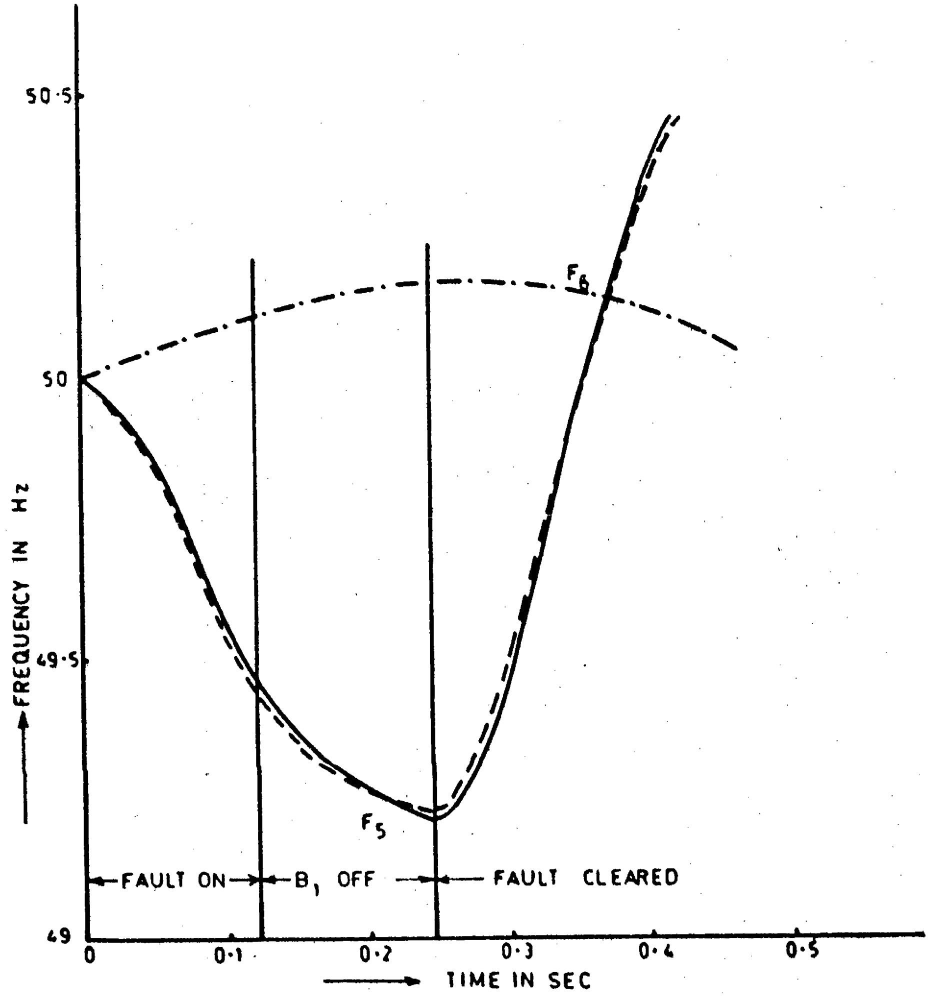

Fig. 3.13(c) Instantaneous frequencies of E_Q, Φ, and Thevenin's equivalent e.m.f. for machine no. 3.

– – – – – – Frequency of E_Q
———— " " Φ
—·—·—· " " Thevenin's equivalent e.m.f.

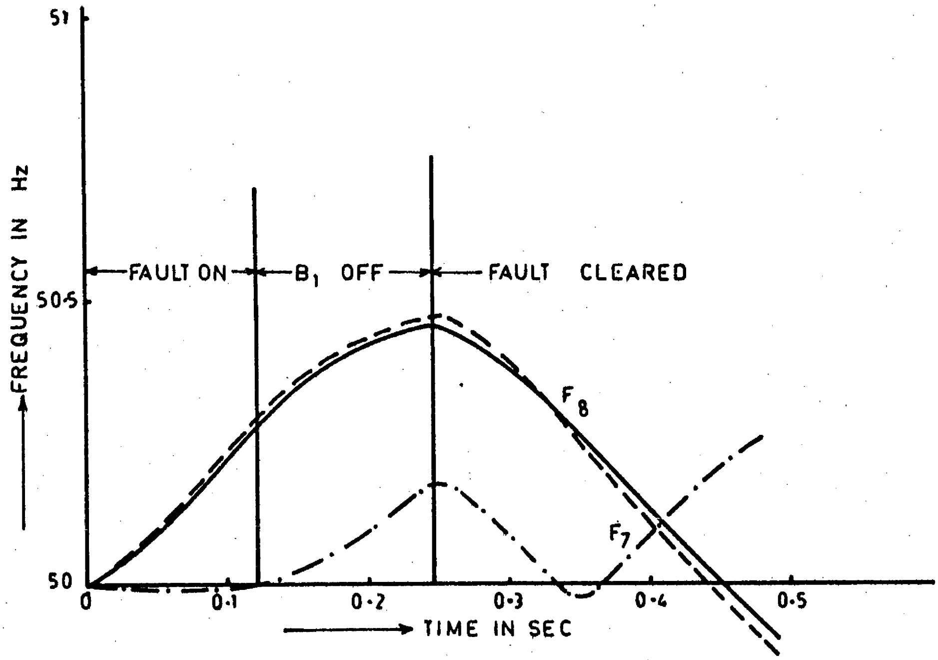

Fig. 3.13(d) Instantaneous frequencies of E_Q, Φ, and Thevenin's equivalent e.m.f. for machine no. 4.

– – – – – Frequency of E_Q

———— " " Φ

—·—·—·— " " Thevenin's equivalent e.m.f.

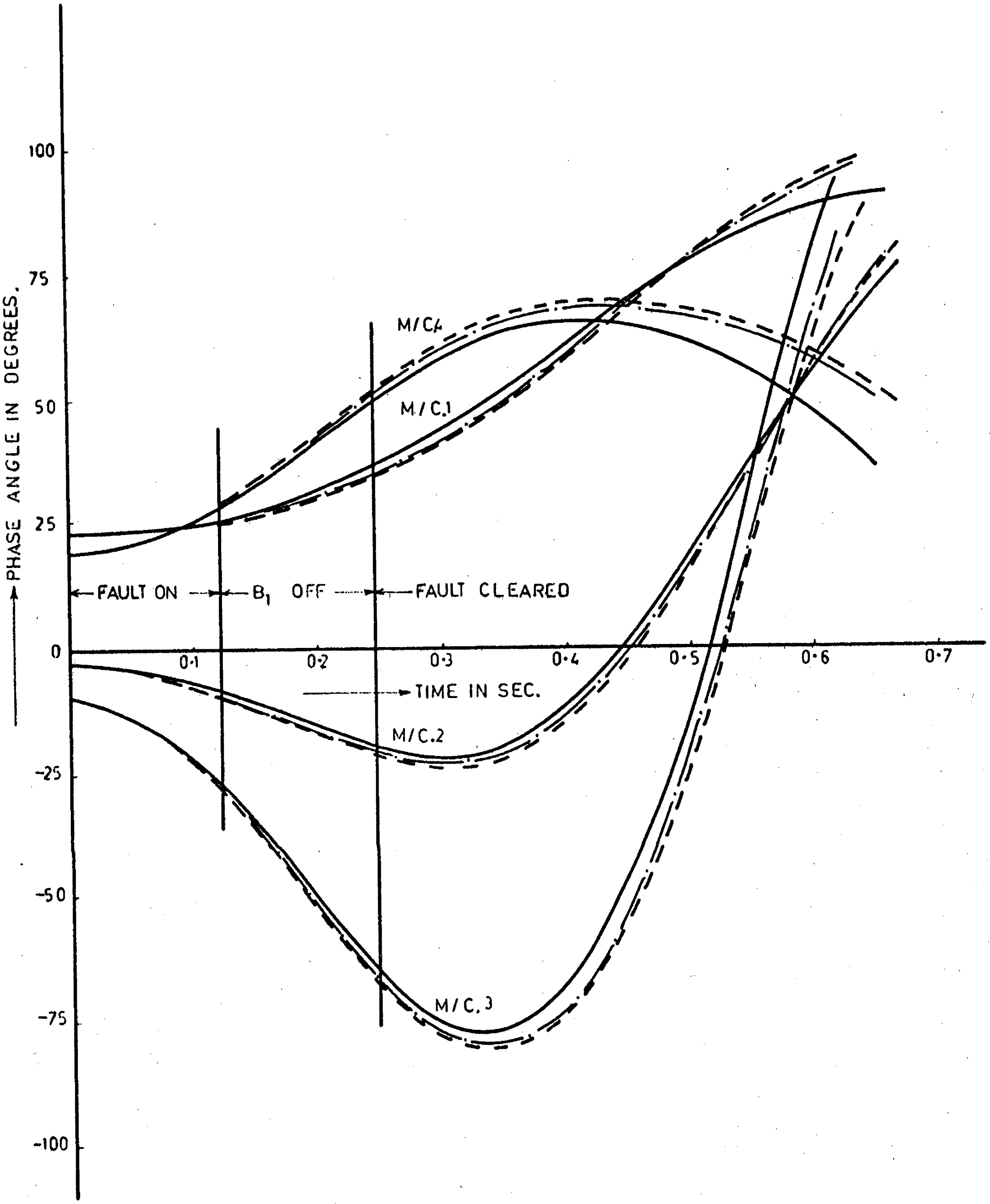

Fig. 3.14 Swing curves for all machines.

– – – – – Without damping.
———— With " by the proposed method.
——·—— " " " " existing "

(represented by an equivalent machine), is to obtain the asynchronous characteristics of all machines and find the value of the equivalent slope of the total asynchronous characteristic, as has been employed for the treatment of induction motors in appendix (10.5).

Although in the illustrative examples an average value has been used for K_D, the method for assessing the effects of damping torques is itself accurate in the presence of adequate information regarding asynchronous characteristics.

3.3 Discussion

3.3.1 Influence of e.m.f., Stored Energy, and Internal Reactances

It is clear from the results of Figure (3.6b) (supported by many other similar calculations) that as regards the relative importance of the effects on power system behaviour resulting from transient frequency considerations involving angular momentum, machine e.m.f., and machine reactance, the most significant effect results from machine e.m.f., with a somewhat smaller influence due to angular momentum. Changes in machine reactance with frequency in the above problem produce only very slight effects.

Compared with the influence of voltage regulators, saturation, transient saliency and flux decay on the performance of a synchronous machine, variation of instantaneous frequency produces a comparable influence only from variation in machine e.m.f. It should be noted however, that the degree of influence of the respective factors affecting machine e.m.f., apart from instantaneous frequency, will depend on the properties and parameters of the machine components, for example, voltage regulator gain; other situations could, therefore, arise in which the relative significance of the appropriate factors may be different from the results recorded here.

From Figure (3.6b), for a total fault clearance time of 270 milliseconds, the system appears stable when instantaneous frequency is taken into consideration in the synchronous machines (except when the influence of instantaneous frequency on "M" and/or machine reactance only is included) and unstable otherwise, even when voltage regulator, saturation, and flux decay effects are included (without instantaneous frequency). For a stable case, with reasonable margin of stability as in Figure (3.6e), differences between the various methods of representation are less spectacular but still significant.

Comparison between the results based on the various representations will be made on:-

(1) Load changes distributed at the terminals of all four machines;*

and (2) Changes in fault clearance time;

to cause a given curve in Figure (3.6b) to coincide with another. On the basis of (1),

adding a total of 6 MW, causes the curve obtained by the inclusion of voltage regulator, saturation and flux decay effects (Table II, (vii)) to coincide substantially with that corresponding to e.m.f. behind transient reactance (Table II, (i)). Similarly, adding a total of 12 MW, causes the curve of (v) or (vi) to coincide with (i), and by adding 18 MW, (viii) or (ix) coincides with (i).

---

* Total machine terminal loads = 215 MW.

On the basis of (2),

> increasing the fault clearance time by 5 milliseconds causes (vii) to coincide with (i); increasing fault clearance time by 12 milliseconds causes (v) or (vi) to coincide with (i), and increasing fault clearance time by 17 milliseconds causes (viii) or (ix) to coincide with (i)*.

The voltage variations at bus 10 indicated in Figure (3.6d), throw further light on the differing degrees of stability calculated in the individual cases.

Instantaneous frequency variations at various points in the power system network for the conditions of (viii) or (ix) of Table II and Figure (3.6b), are plotted in Figure (3.6c). A maximum frequency deviation of approximately 1.6% is apparent for machine 3 (which in this case remains stable).

Table II records the respective calculation times taken for the various cases. It will be apparent that best returns on computing time are obtained for cases (v) and (viii). In view of the only relatively slight effect due to inclusion of variation of machine reactance with frequency, and the somewhat excessive computing time involved, there seems little justification for considering this effect in the present study.

With the representation of e.m.f. behind transient reactance for transient stability studies during the first swing as comparison : Figure (3.6b) shows this case to be calculated as unstable; adding the refinements of voltage regulator, saturation and flux decay effects still indicates an unstable system. On the other hand, adding, in either case, the refinement of instantaneous frequency dependence of machine e.m.f. (with or without modification of angular momentum and machine reactance with frequency), indicates stability.

---

* That is, 6% increase required.

Moreover, the marginal effects of the instantaneous frequency refinements are in this problem greater than those due to the inclusion of voltage regulator, saturation and flux decay; although this favourable balance may not be so great in other possible situations, it is considered that instantaneous frequency effects are worthy of inclusion in precise studies involving synchronous machines operating under transient conditions.

On the measure of magnitude of influence and computing time involved, incorporation of instantaneous frequency influence on angular momentum and machine e.m.f. seems justified in the representation of synchronous machines, but modification of machine reactance with frequency appears unwarranted because of its slight influence and comparatively excessive demand on computing time.

3.3.2 Influence of Transient Torques

Considering the single-machine problem, inclusion of damping when treated with respect to the infinite bus, as in the existing methods of calculation, gives an assessment of machine performance which differs from that obtained by the author's treatment. For example, fault clearance time increases from 270 m sec. when damping is ignored, to 275 m sec. when the damping is included by the existing methods; that is, an increase of 1.85%. On the other hand, inclusion of damping with respect to the resultant air-gap flux gives a corresponding increase of 9.3%, which seems to be more reasonable in the light of qualitative discussions in the literature, for example, in References 163 and 195.

In the case of a multi-machine study, it is possible to have positive damping for some machines and negative damping for others at a particular instant as shown by Figures (3.13) (a, b, c and d). It is just possible that the positive damping period of one machine may not be overlapped by the negative damping of the other; under such circumstances, the nett outcome of damping does not seem to be significant, but the current and voltage distribution will be different in the system. In the case where positive damping periods or negative damping periods may coincide, then the nett outcome will be quite significant as shown by the angular swings of the various synchronous machines in Figure (3.14). Machine no. 1 has predominantly negative damping which overlaps partly the negative damping experienced by machine no. 3 towards the end of fault clearance. Machine no. 4 being the largest in capacity with a higher value of inertia factor, indicates mostly positive damping, thereby overcoming the enhanced negative damping experienced by other small capacity machines in the system. The overall positive damping under these circumstances raises the margin of stability by 10 MW, that is 3.7% of the total system output, and the fault clearance time increases from 270 to 280 m sec. when damping torques are considered with respect to the resultant air gap flux. On the other hand, damping, when considered with respect to the Thevenin's equivalent e.m.f. has very small effect in this example, as shown in Fig. (3.14).

Considering the overall picture of the instantaneous angular velocity deviation effects on the performance of the synchronous generators, there will always be a positive contribution* by the change in machine e.m.f. and angular momentum, which should be given due consideration in the light of the present trend towards reduction in inertia constants and increase in machine natural reactances[200]. The influence of transient frequency variation on the machine reactance seems only small, however, and moreover involves excessive computing time.

Synchronous machine damping plays an important role during oscillatory conditions, and as it cannot be stated with confidence whether damping will be positive or negative, its inclusion in transient stability studies seems essential.

---

* That is, improvement of stability.

4. TRANSMISSION NETWORK CONSIDERATIONS

In modern high voltage interconnected power systems, the transmission network has acquired prime importance in linking generation centres with distribution centres. These networks need special consideration for their precise representation in power system studies (for example, load flow studies for normal operations and stability studies under steady-state and abnormal conditions), because of the large phase difference between the sending end and receiving end voltages. From the view point of stability this phase difference is the limiting factor which sets the practicable upper limit of transmission line length. In recent years, this limiting factor has been extended in three ways:-

(a) Employment of series capacitors for high voltage transmission lines at appropriate locations[134].

(b) Tuned lines in which the electrical line length is made to be more than its physical length; for example, more than half wave length, by employing tuning circuits[220].

(c) D. C. transmission lines which have zero synchronous length.

4.1 Transmission System Damping

As soon as the frequency in any part of a power system network deviates from its steady-state value, damping forces come into play. In the past, it has been assumed that these damping forces are positive and improve stability, so that their neglect in calculations must produce results which are safe. Positive damping forces have been used in various refined computer programmes to date, but because of lack of adequate data and suitable methods of approach, consideration has not been thorough; for example, in one report, all damping forces have been lumped into a sysyem damping coefficient of "2"[219].

It may be readily seen, however that damping can be negative as well as positive. In Figure (4.1), a synchronous machine with e.m.f. E_1 acting behind the machine's transient reactance, supplies a constant impedance load, (for example, a pure resistance), through a series-compensated transmission line of inductance L, with line resistance and charging capacitance neglected. C is a series compensating capacitor. A transient condition is created by changing load impedance (suddenly). Assuming the same instantaneous frequency for all branches and for all bus voltages,

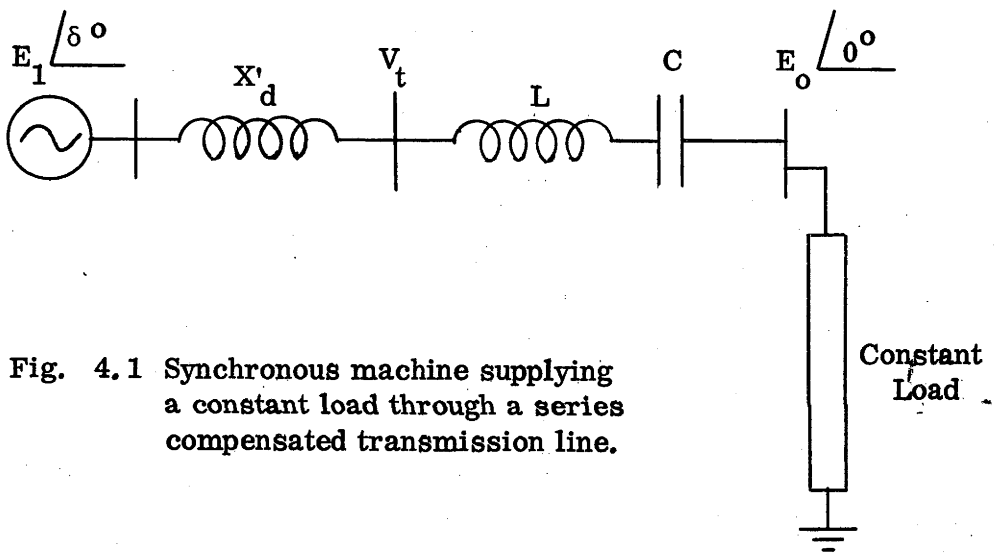

Fig. 4.1 Synchronous machine supplying a constant load through a series compensated transmission line.

Line current just after the disturbance (from Figure 4.1),

$$= \frac{|\underline{V}_t - \underline{E}_o|}{\omega_o L - \frac{1}{\omega_o C}}$$

If the machine moves with an instantaneous angular velocity ω_1, then

$$\text{Line current} \doteqdot \frac{\left| V_t - E_o \right| \dfrac{\omega_1}{\omega_o}}{\omega_1 L - \dfrac{1}{\omega_1 C}}$$

$$= \frac{1}{\omega_o} \cdot \frac{\left| V_t - E_o \right|}{L - \dfrac{1}{\omega_1^{\,2} C}} \qquad (4.1)$$

When the synchronous machine accelerates, ω_1 increases from its nominal value of ω_o and the current falls, reducing E_o as the load is of constant impedance : consequently, the effective load on the machine is slightly reduced, so providing an enhanced accelerating force. (The above occurs during a transient interval for which the machine governor setting is assumed not to change.)

Then $$P_e = \frac{E_1 E_o}{X'_d + X_e} \sin \delta$$

where $$X_e = \left(\omega L - \frac{1}{\omega C} \right)$$

and accelerating power, $$\Delta P = P_m - P_e \qquad (4.2)$$

If the machine initially decelerates, then by similar reasoning the current increases, resulting in an increased load on the machine and enhancing the decelerating force. The above form of system behaviour may be termed negative damping, as increase in the amplitude of electromechanical oscillations is promoted.

In the absence of the series line compensating capacitor C, the line current becomes independent of the instantaneous angular velocity of the machine, and the voltage E_o increases and decreases with instantaneous frequency. Consequently, with fixed impedance load, more load is placed on the machine when it accelerates and less when it decelerates, so that oscillations tend to be reduced in amplitude and the effect is that of positive damping.

When the actual system load is not a constant impedance or pure resistance, it will be readily apparent that introducing a frequency-dependent reactive component to the load, will change the degree of the above effects and even their nature, depending on the kind and amount of reactance present. However, the above simple argument demonstrates the possibility of negative as well as positive damping occurring on a power system and suggests the desirability of further study of possible effects resulting therefrom. This is so particularly on power systems with long high voltage lines for which series capacitor compensation of inductive reactance is often employed, and for systems in which shunt compensation is carried out by capacitors and reactors.

In general, when a synchronous machine accelerates, the voltages of those load buses which, as a consequence, have high transfer admittances, are increased by the increase in the machine e.m.f. and are reduced by the increase of instantaneous system reactances, thereby changing the load on the system. Thus, inductive reactances and series compensating capacitors reduce, while shunt capacitors increase the load voltage. Consequently, increase in machine e.m.f. and the effects of shunt compensation reduce the accelerating forces, while line inductances and series compensation by capacitors increase the accelerating forces, that is, the former promote positive damping, while the latter produce negative damping.

4.1.1 Calculation of Power System Network Damping Effects

In order to handle the situation arising due to the influence of network damping effects, an appropriate phasor diagram on a plane X-Y is selected to move in an anticlockwise direction with an angular velocity ω_o, as explained in Section (2.2.2).

4.1.1.1 System Representation

It is aimed here to investigate and highlight the damping effects of power system transmission and distribution networks consequent on the introduction into the calculations, of instantaneous frequency variations during transient disturbances. Accordingly, all loads will be considered as constant impedances, and all synchronous machines will be represented as in Section (3.2.1) (that is, a comprehensive representation, including the influence of rotor angular velocity variations for each machine and taking account of voltage regulator, saturation and flux decay effects). In this way, assessed changes in instantaneous frequency on the system, although subject to the approximation that the loads remain fixed, will be reasonably adequately represented to demonstrate the damping effects intended.

Representation of the transmission and distribution network will need to be consistent with the nature of the network and the accuracy required, with the network being changed on the basis of instantaneous frequency by calculating the instantaneous values of inductive reactances and capacitive susceptances depending on the instantaneous frequency existing on the particular part of the system involved, for each particular time interval, "Δt". It will be noted that in the process of calculation, the various network reduction theorems employed are valid for fixed frequency operations. In these studies consequently, network reductions with the aid of Thevenin's theorem are carried out at particular "frozen" instants of time using the corresponding values of the appropriate parameters at those instants.

4.1.1.2 Procedure for Swing Curve Calculations

Damping effects for any given condition of operation may be readily illustrated and observed from the corresponding swing curves which may be obtained as follows:-

(a) Position the various phasors on the X-Y plane, initially for predisturbance conditions, as in Section (2.2.2), and subsequently for each change in operating condition by the method outlined in Section (2.2.2) (c - f).

Then for each particular operating condition (application of fault, removal of fault and so on) the appropriate section of swing curve may be calculated in the following way:-

(b) Form the admittance matrix for the entire system when the inductive reactances and capacitive susceptances are calculated for the current values of instantaneous frequency in the various parts of the system.

(c) Determine the driving point and transfer admittances of the various machines.

(d) Determine the new angular positions of the various machine e.m.f's by solving the transient stability equations by the Kutta-Runge method[162], employing the inertia factors and current values of e.m.f's as outlined in Section (3.2.1) (that is, including the instantaneous rotor angular velocity variations, and voltage regulator, saturation and flux decay effects in the synchronous machine representations).

(e) Resolve the machine e.m.f's into real and imaginary components as,

$$\underline{V}_m = E_m \cos \delta_m^i + jE_m \sin \delta_m^i$$

by using the latest available values of δ_m^i.

(f) Calculate the new node voltages, line currents, and phase angles, as outlined in the Appendix (10. 1).

(g) Determine the instantaneous frequency of the voltage at each node k, as outlined in Section (2. 2. 2) as,

$$f_k^i = \frac{\theta_k^i - \theta_{ok}^i}{2\pi \cdot \Delta t} + f_o$$

and for each branch current,

$$f_{k\ell}^i = \frac{\theta_{k\ell}^i - \theta_{ok\ell}^i}{2\pi \cdot \Delta t} + f_o$$

(h) Modify the instantaneous frequency by using an accelerating factor as,

$$f_k^i = f_k^{i-1} + (f_k^i - f_k^{i-1}) \text{ x accelerating factor}$$

and $f_{k\ell}^i = f_{k\ell}^{i-1} + (f_{k\ell}^i - f_{k\ell}^{i-1}) \text{ x accelerating factor}$

(i) Test if the difference between the instantaneous frequencies of the various respective node voltages and branch currents for two consecutive iterations, is within a predetermined index, say 10^{-4}. If this condition is not satisfied, return to step (b) and recycle.

(j) Write the various quantities.

In step (h) above, an accelerating factor greater than unity is chosen to produce convergence in a minimum number of iterations. A value for this factor of 1. 35 has been found to be a satisfactory compromise between excessive iterations resulting from smaller values, and instability of the solution produced by over-correction when larger values are chosen. With the above value, convergence to within the requirements of step (i) usually requires five to seven iterations.

4.1.2 Illustrative Problem Including Transmission Damping Effects

Figure 4.2 is the line diagram of a 4-machine power system (based on an example from Reference 195)*, which is presented to illustrate the behaviour of a power system when representation of the transmission and distribution network takes account of instantaneous frequency deviations. Further relevant information is given in Tables I, IV(a) and IV(b).

Calculation follows the procedure of Section (4.1.1.2), with synchronous machines represented as in Section (3.2.1). Loads are here considered as fixed impedances at system nominal frequency, and the transmission lines are represented by their equivalent pi's, with inductive reactances and capacitive susceptances modified in accordance with instantaneous frequency changes. For purposes of comparison, calculation has been carried out with and without the inclusion of effects of instantaneous frequency on the transmission network, and in each case representation of the synchronous machines and loads has been the same in order to isolate the actual effects produced on the system by the transmission network. In this study, a 3-phase to ground fault occurs on line 16 close to bus 15; the latter is isolated from the fault by breaker B_1 within a certain time, and after a further period, breaker B_2 disconnects line 16, thereby clearing the fault.

Figure (4.3a) shows the relative swing curves with respect to machine 4 when breaker B_1 operates in 129 milliseconds and breaker B_2

* With lines 5, 6, 7, & 8 (Fig. 4.2) added to increase the size of the transmission network and thereby illustrating damping more effectively.

TABLE IV(a)* Transmission Line Impedances (at 50 c/s) for Fig. 4.2 on 100 MVA Base

Branch no.	Impedance in P. U.	Branch no.	Impedance in P. U.
1	0 + j 0.13	9	0.131 + j 0.798
2	0 + j 0.28	10	0.0172 + j 0.164
3	0 + j 0.259	11	0.1016 + j 0.379
4	0 + j 0.15	12	0.0552 + j 0.205
5	0.05 + j 0.43	13	0.069 + j 0.144
6	0.0414 + j 0.58	14	0.268 + j 1.27
7	0.07 + j 0.679	15	0.0129 + j 0.0688
8	0.08 + j 0.65	16	0.0129 + j 0.0688

TABLE IV(b)* Load Impedances on 100 MVA Base (at 50 c/s), for Fig. 4.2.

Load	Impedance in P. U.	Load	Impedance in P. U.
L_1	2.04 + j 0.08	L_4	5.33 + j 4.83
L_2	0.94 + j 0.636	L_5	12.55 + j 4.82
L_3	2.93 + j 2.74	L_6	0.838 + j 0.623

* Network constants are expressed at system nominal frequency.

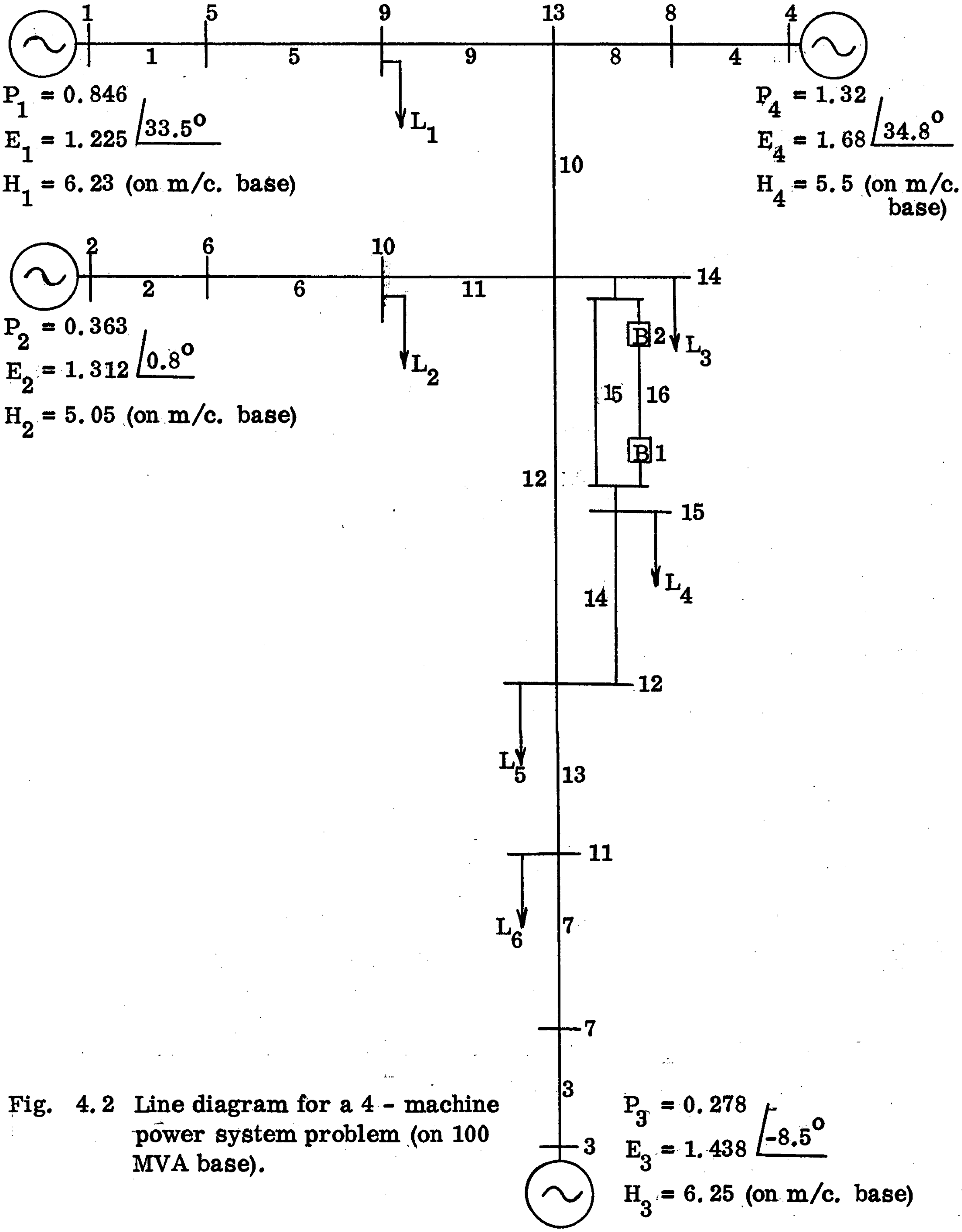

Fig. 4.2 Line diagram for a 4 - machine power system problem (on 100 MVA base).

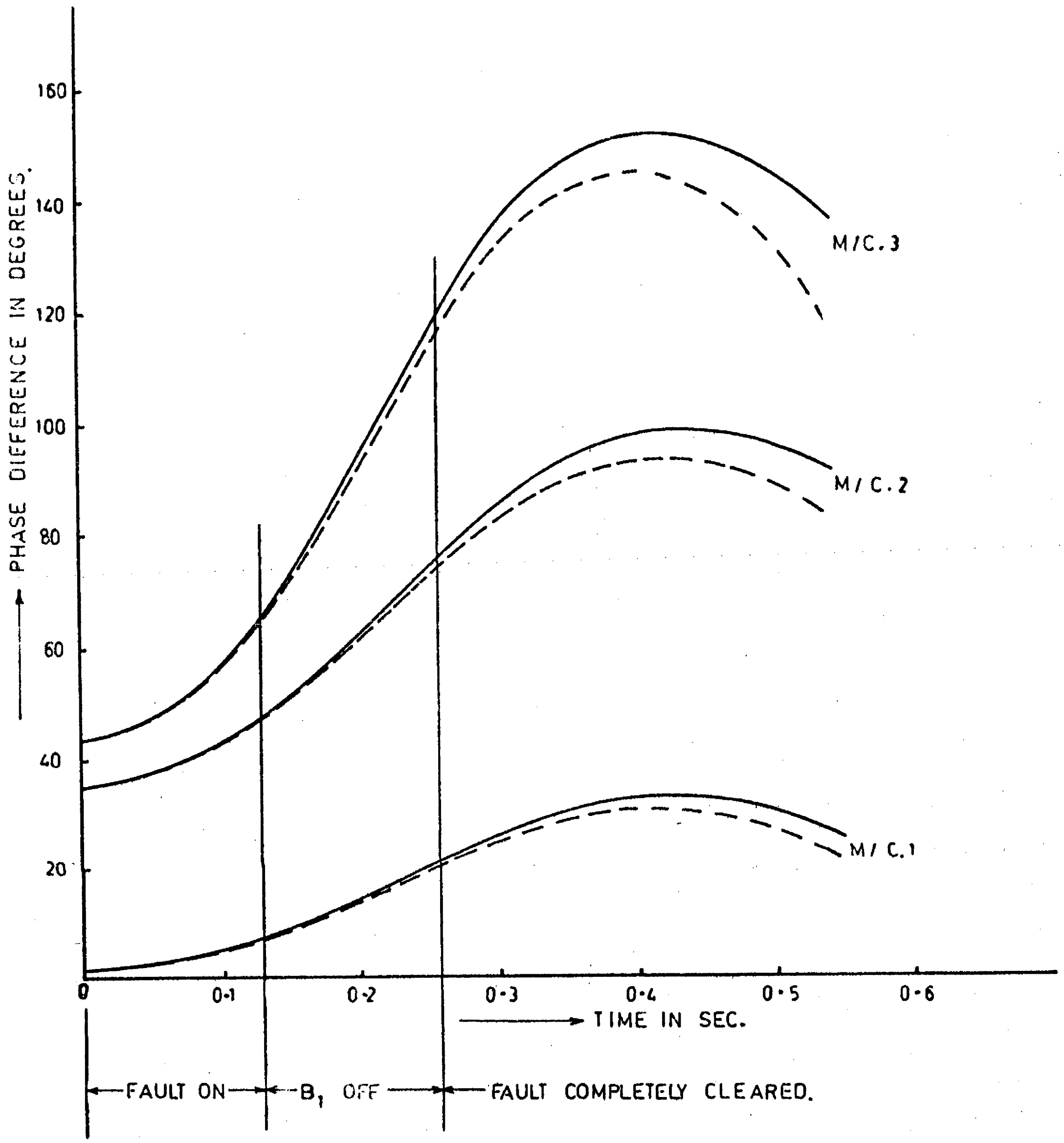

Fig. 4.3 (a) Relative swing curves for Fig.4.2 W.R.T. M/C. 4. (Total fault clearance time = 258 m sec.).

——————— With transmission damping.
– – – – – –Without " "

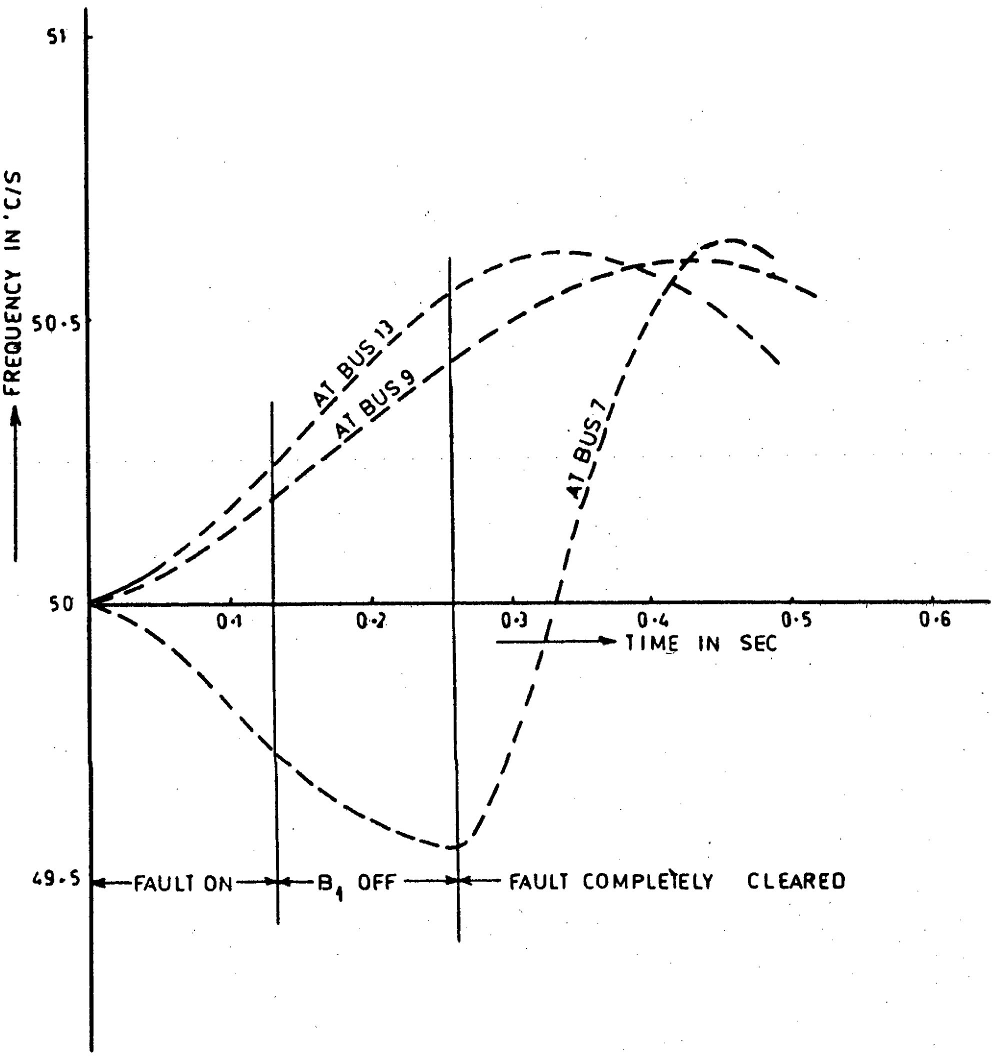

Fig. 4.3 (b) Instantaneous frequency variations at key buses when transmission damping is neglected. (Total fault clearance time = 258 m sec.).

clears line 16 in a total time from fault inception of 258 milliseconds. Figure (4.3b) shows the instantaneous frequency variations of various buses under the conditions of Figure (4.3a).

If the operation of breaker B_1 is delayed to take 138 milliseconds, and breaker B_2 is delayed to clear the fault in a total time from inception of 276 milliseconds, the curves of Figure (4.4a) result. Corresponding voltages at the major load buses 9, 10, 11, are shown respectively in Figures (4.4 b, c, d) and Figure (4.4e) indicates the instantaneous current variations through the important line no. 11.

It may be observed that taking account of the effects of instantaneous frequency changes in the network, the existence of negative damping is indicated and, in the case of Figure 4.4, produced a significantly different calculated behaviour from that obtained by neglecting instantaneous frequency changes. In the former case, the system is assessed as unstable, whereas in the latter, there is apparent stability. The margin of difference between the two methods of calculation may be expressed quantitatively by noting that for the conditions of Figure (4.4), when calculating without including instantaneous frequency variation effects in the network, either

(i) anextra 10 MW of load must be added at bus no. 11, or

(ii) total fault clearance time must be increased by 9 milliseconds,

in order to make the resulting swing curves coincide with those obtained for the original system with the inclusion of instantaneous frequency effects.

4.2 Discussion

The example od Section (4.1.2) suggests that it may be unsafe to assume that damping effects in power system networks can be neglected. Figure (4.4e) indicates that the current variations in key branch no. 11 are

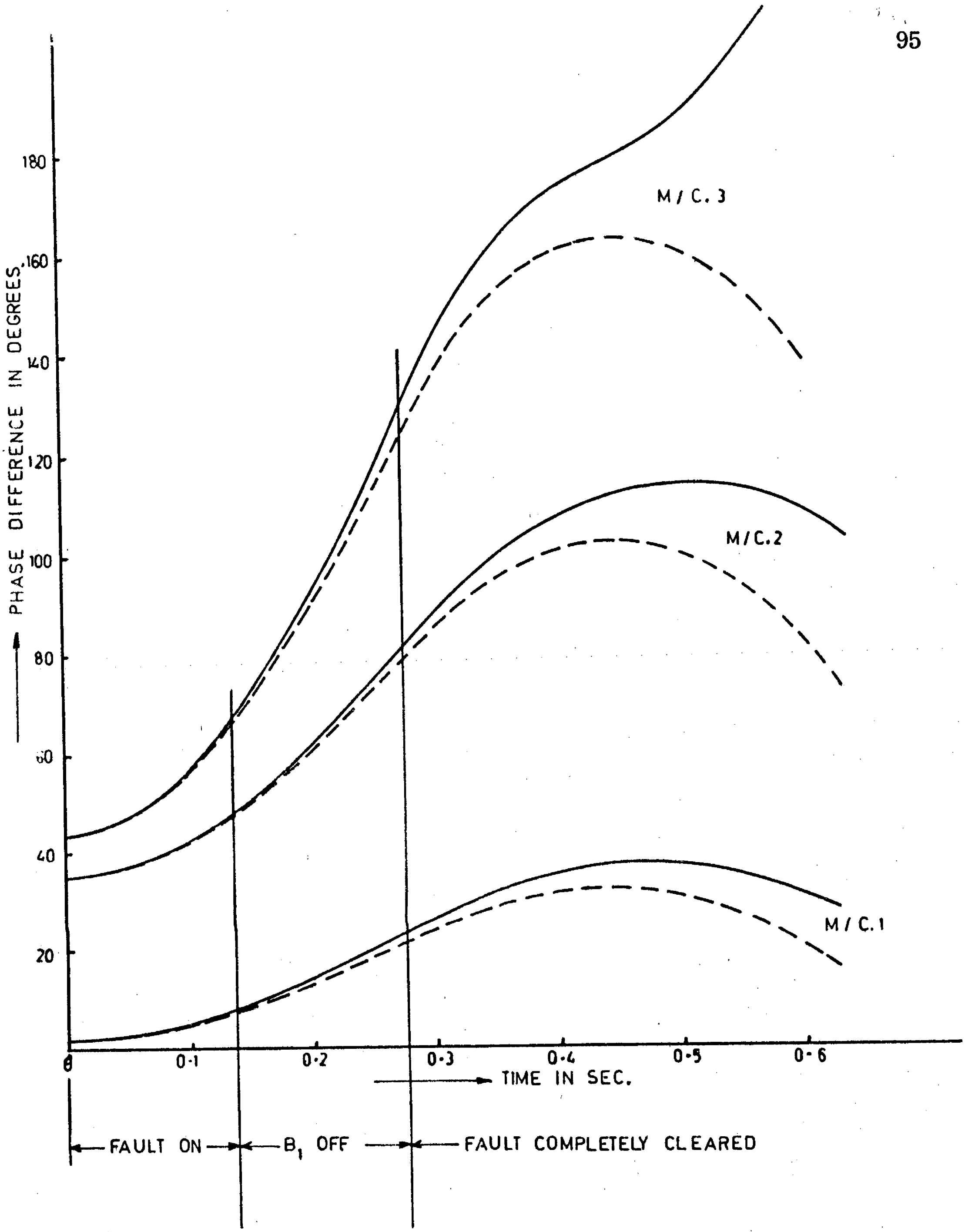

Fig. 4.4(a) Relative swing curves for Fig. 4.2 W.R.T. M/C 4
(Total fault clearance time = 276 m sec.).

——— With transmission damping.
– – – – Without " "

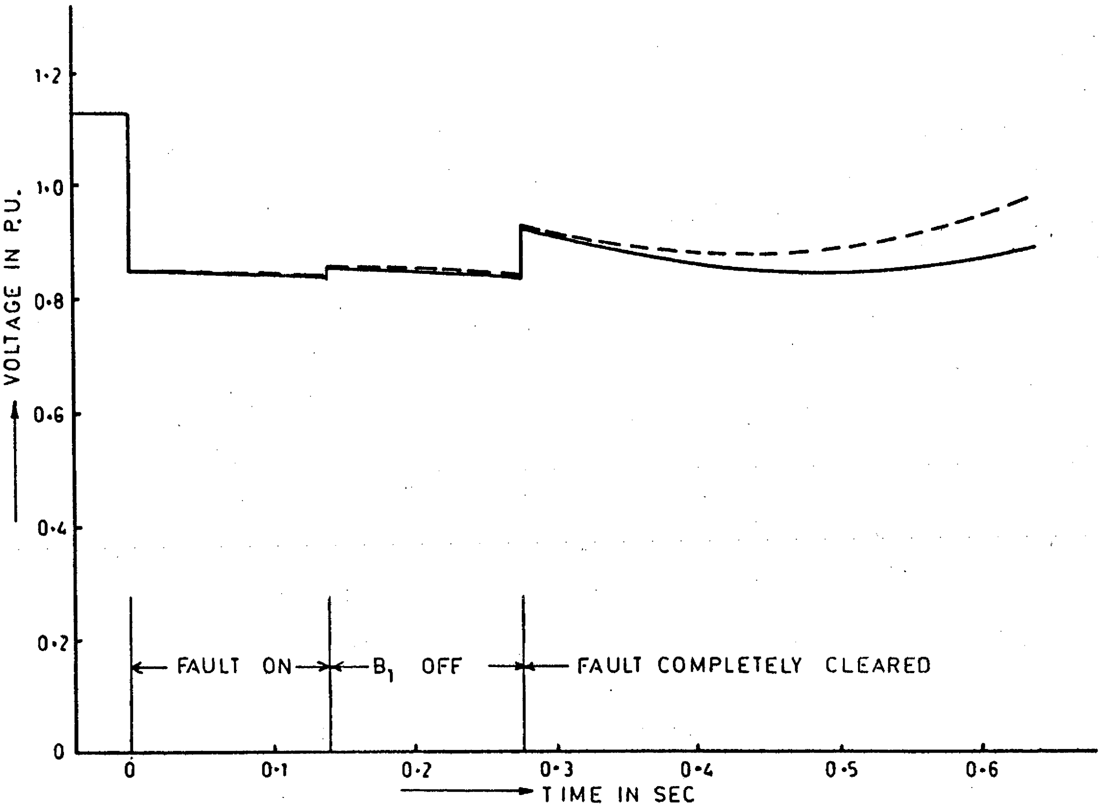

Fig. 4.4 (b) Voltage variations at bus no. 9.
(Total fault clearance time = 276 m sec.).

——— With transmission damping.
– – – – Without " "

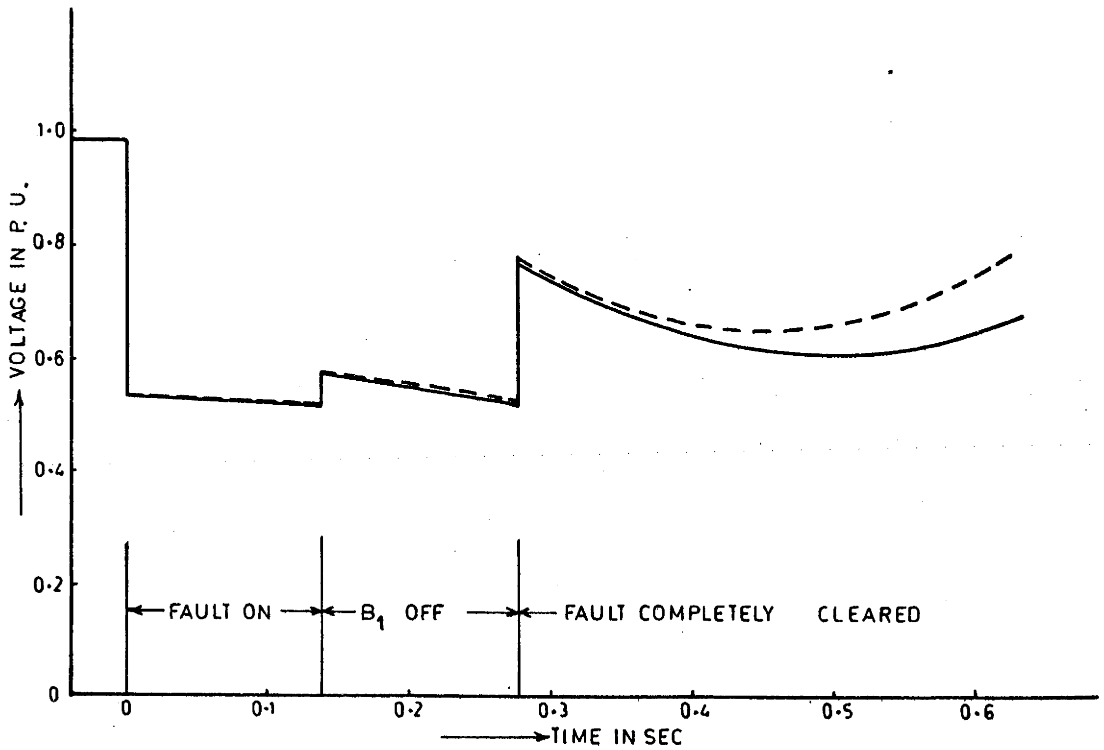

Fig. 4.4 (c) Voltage variations at bus no. 10.
(Total fault clearance time = 276 m sec.).

——————— With transmission damping.
– – – – – Without " "

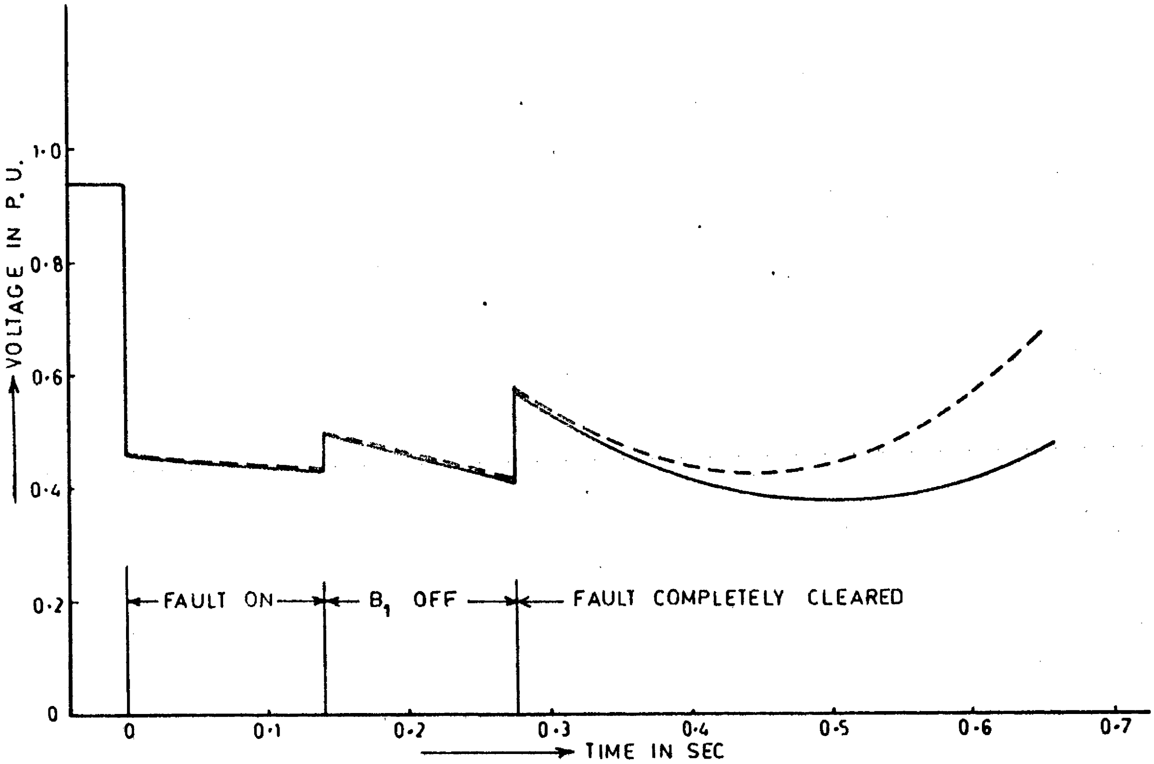

Fig. 4.4 (d) Voltage variations at bus no. 11.
(Total fault clearance time = 276 m sec.).

——————— With transmission damping.
– – – – – Without " "

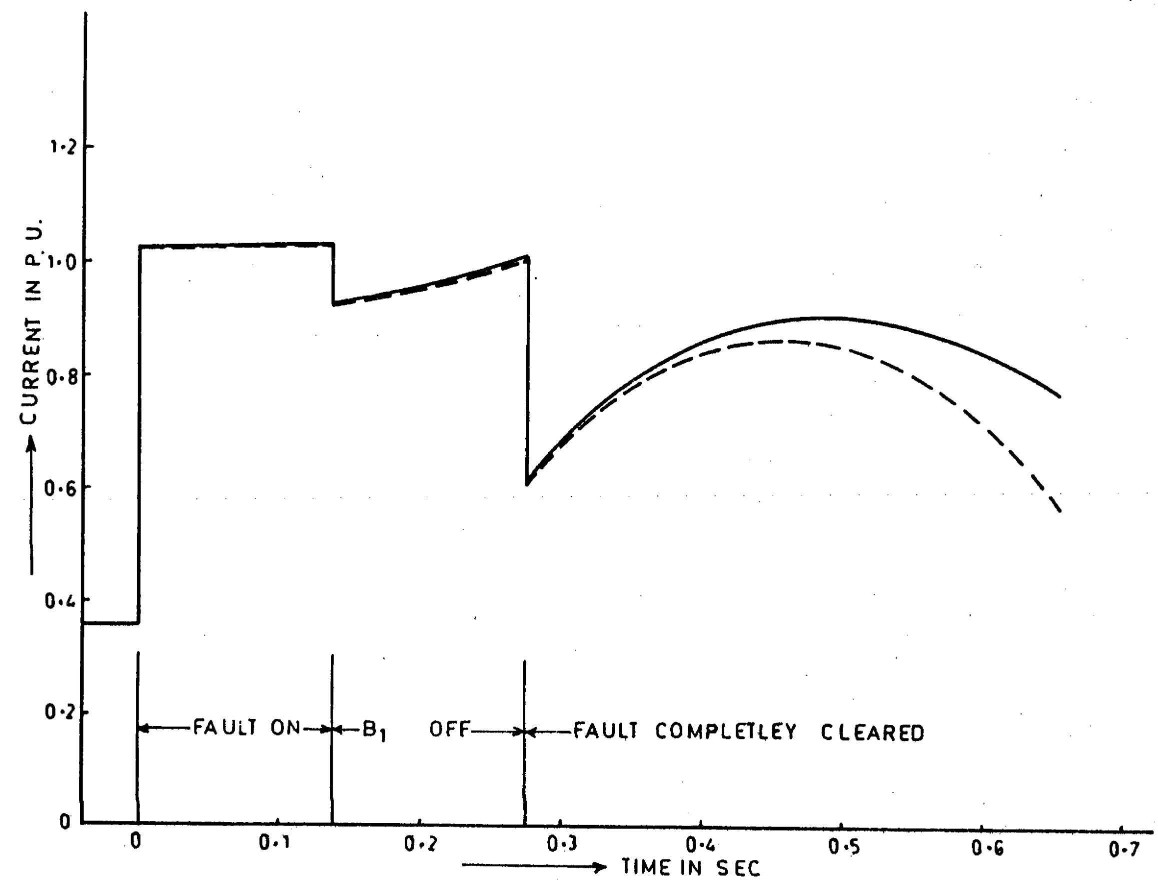

Fig. 4.4.(e) Current variations through branch no. 11.
(Total fault clearance time = 276 m sec.).

——————— With transmission damping.
— — — — — Without " "

significantly larger when instantaneous frequency variations are introduced in the calculations, so that protective relay settings based on calculations in which damping is not considered, may be unsound. For example, machine 2 might be inappropriately isolated by the opening of a breaker close to bus no. 10. Figures (4.4 b, c, d), show that the voltages at the respective major load buses 9, 10, 11 are lower when transmission damping is included than otherwise: this reduced voltage leads generally to a reduced overall load on the system and is a factor in the negative damping behaviour. Further, the lower voltages indicated by the calculations imply that particular loads may be influenced markedly; for example, induction motors would draw more current (than appears from calculations which neglect damping), and this may further upset the current and voltage distributions as calculated.

It is apparent from Figure (4.4) that the question of whether or not a system is in fact stable may be differently assessed by including or not including transmission network damping. In the example given, this difference in deduced behaviour by the two approaches seems sufficiently marked to warrant inclusion of instantaneous frequency variation in the transmission network for transient stability studies.

Power systems will exist in which network damping has values in the range from significantly negative, through zero, to significantly positive. In general, negative damping will tend to occur in systems with long lines, particularly if series compensation by capacitors is present, while positive damping will tend to exist on systems with shunt compensation by capacitors and/or transmission lines of short length only.

Because of the need to calculate new transfer and driving point admittances at each iteration when including the effect of instantaneous frequency variation in the power system network, necessary computing time will be longer in this case than when network damping is neglected. With the calculation procedures presented in Section (4. 1. 1. 2), for the example of Section (4. 1. 2), computing time (using an IBM 360/50 digital computer) was respectively 7. 8 minutes (damping included) and 0. 7 minutes (damping not included). The extra calculating time may often be acceptable.

Attention is redrawn to the representation of loads by fixed impedances in this study in order to simplify isolation of the instantaneous frequency variation effects in the transmission and distribution networks. In the process, although the resulting instantaneous frequency changes in the system and the voltage, current and load deviations may be consequently only approximate, the nature of the effects and their influence and significance have been demonstrated.

5. LOAD CONSIDERATIONS

Whatever the characteristics of the loads, a power system has to meet their demands under normal and abnormal situations; consequently a knowledge of load characteristics has been emphasized in the literature. Voltage-dependent behaviour has attracted much attention in the past, but frequency-dependent behaviour of loads has received little attention due to lack of suitable analytical treatment and required information.

The more usual loads met in practice include:-

(a) Induction motors.
(b) Mercury arc rectifiers.
(c) Discharge lamps.
(d) Arc-furnaces.
(e) Electric welders.
(f) Filament lamps.
(g) Element heaters.

Due to lack of adequate information and convenient methods of representation in stability studies, all the above loads have been represented in various ways, for example by:-

(i) Constant shunt impedances at system nominal frequency, giving active and reactive powers directly proportional to the square of the terminal voltage.

(ii) Constant current sinks, giving active and reactive powers directly proportional to the terminal voltage.

(iii) Non-linear loads.

All the above representations treat the loads as being static and independent of operating frequency, but they are in fact dynamic and frequency-dependent, and it has usually been considered that the results obtained in this way are safe[195]; however, the examples included in Section 5.1.2.2 suggest that this belief may be erroneous.

For purposes of the present work, the loads have been grouped into three categories:-

(i) Frequency-dependent dynamic; such as induction motors.

(ii) Frequency-dependent static; such as loads from (b) to (e) in the above list.

(iii) Fixed impedance loads independent of operating frequency.

The detailed load composition may be obtained from a load survey in the first instance and convenient sub-division may be made as above in order to assess stability under transient conditions, for which the transient frequency variation in the various parts of the system will affect the input power to all loads in categories (i) and (ii).

5.1 Frequency-Dependent Dynamic Loads - Induction Motors

The most usual dynamic loads met in practice are induction motors, with comparatively few synchronous motors and even less synchronous converters. Induction motors contribute significantly to power system loads, and have consequently attracted much attention in the past, their importance being emphasized in the literature from various aspects. For example, References (214 and 215) consider power station auxiliaries, and References (216, 229 and 237) consider other important applications of induction motors in power systems. Their input active and reactive powers depend upon the instantaneous magnitudes of the terminal voltage (to a small extent) and operating frequency (to a large extent).

5.1.1 Dynamic and Frequency-Dependent Representation

Consider the situation regarding large induction motors (such as pump motors in power stations) : they have been represented in detail in the comprehensive computer programs developed for power system stability studies[214, 215, 219], because a great deal of information is available; their representation has ranged from steady-state equivalent circuits, through approximate equations to exact equations in 2-axis form derived from the circuit analysis of the machines, and has taken account of varying terminal voltage and operating frequency[225].

On the other hand, the bulk of the induction motor loads which consists of small size general purpose motors has not been given attention due to lack of appropriate information. Groups of such induction motors have sometimes been represented by fixed impedances at system nominal frequency. However, it has been pointed out[195], that damping can arise from the change of load due to instantaneous frequency variations under disturbed conditions, but this factor has been neglected. Here the aim is to develop suitable methods to represent induction motor loads as frequency-dependent and dynamic, when the only information available is the number of motors and their ratings.

5.1.1.1 Frequency Range

In order to study the dynamic and frequency-dependent behaviour of induction motors, a frequency range of 50 $\pm$ 2.5 c/s has been selected. The 2.5 cycles change has been distributed over 18 intervals, each of 0.05 secs.; the law of variation, as shown in Figure (5.1), closely corresponds to the swing curves of synchronous machines under disturbed conditions. In practice, frequency variations are less (as discussed in Section 2) but the above excursions will serve to compare the proposed

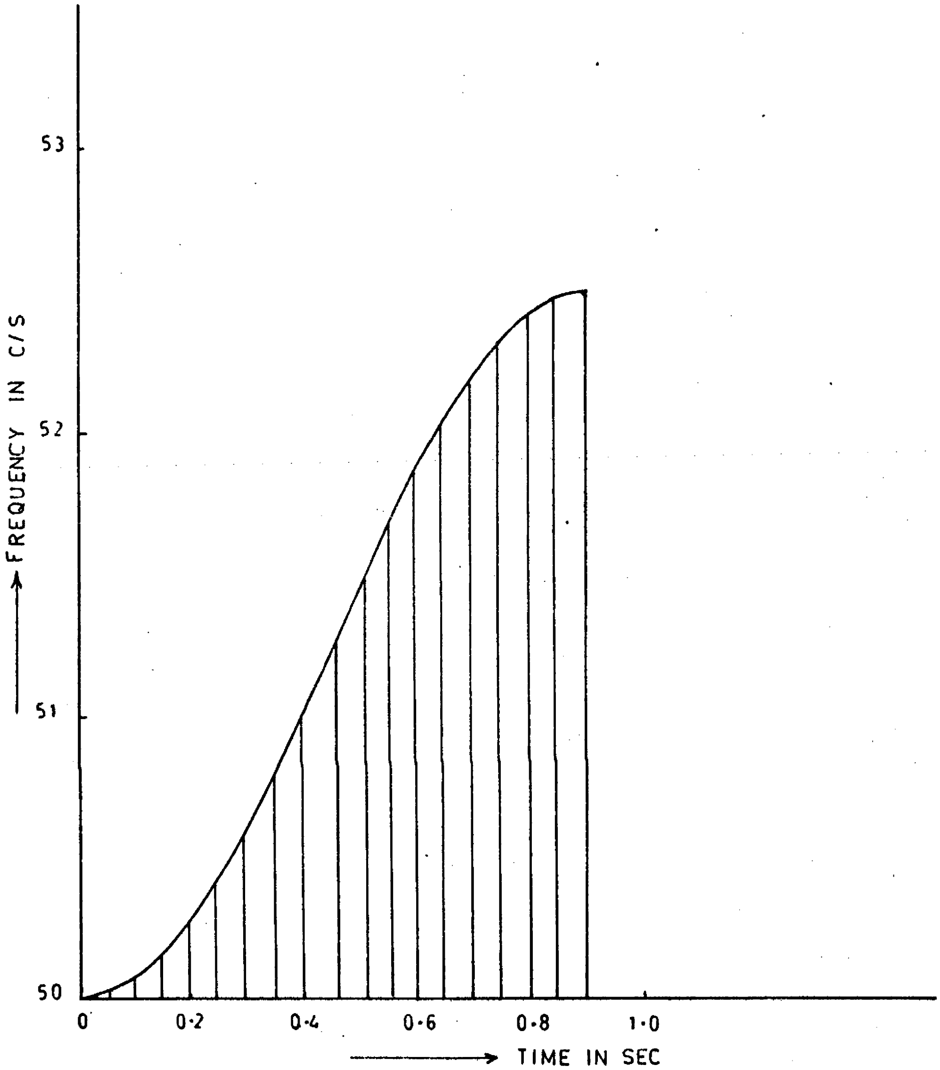

Fig. 5.1 Operating frequency vs. time at the motor terminals.

approximate method with more precise calculations carried out using equivalent circuits (Figure (5.2)).

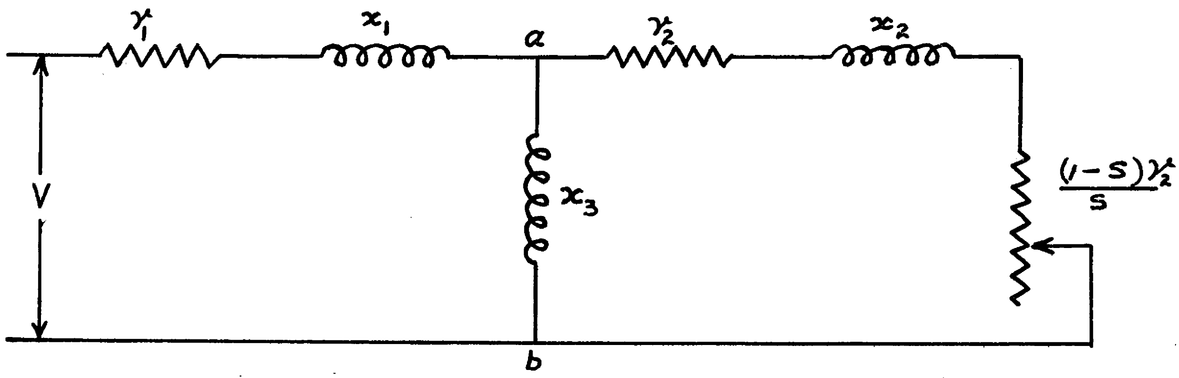

Fig. 5.2 Induction motor equivalent circuit.

5.1.1.2 Characteristics of Induction Motors

Consider the characteristics shown in Figure (5.3) : it is observed that the three characteristics namely, (a) Torque-slip, (b) Stator current-slip, and (c) Power factor-slip, are linear during the workable range of slip. Accordingly, by utilizing the linearity of the above characteristics, a new approach has been developed which can enable us to treat a small induction motor on a frequency-dependent and dynamic basis. The linear property of the torque-slip characteristics has previously been employed for studying the natural oscillations of induction motors[123].

It may be noted that equation (10.6) of appendix 10.2, indicates that the slope of the torque-slip characteristics is inversely proportional to the operating frequency at s = 0.

5.1.1.3 Core Losses

Core losses depend upon the instantaneous magnitude of frequency and flux density. For a constant terminal voltage, increased frequency reduces the flux density. As the eddy current losses are directly

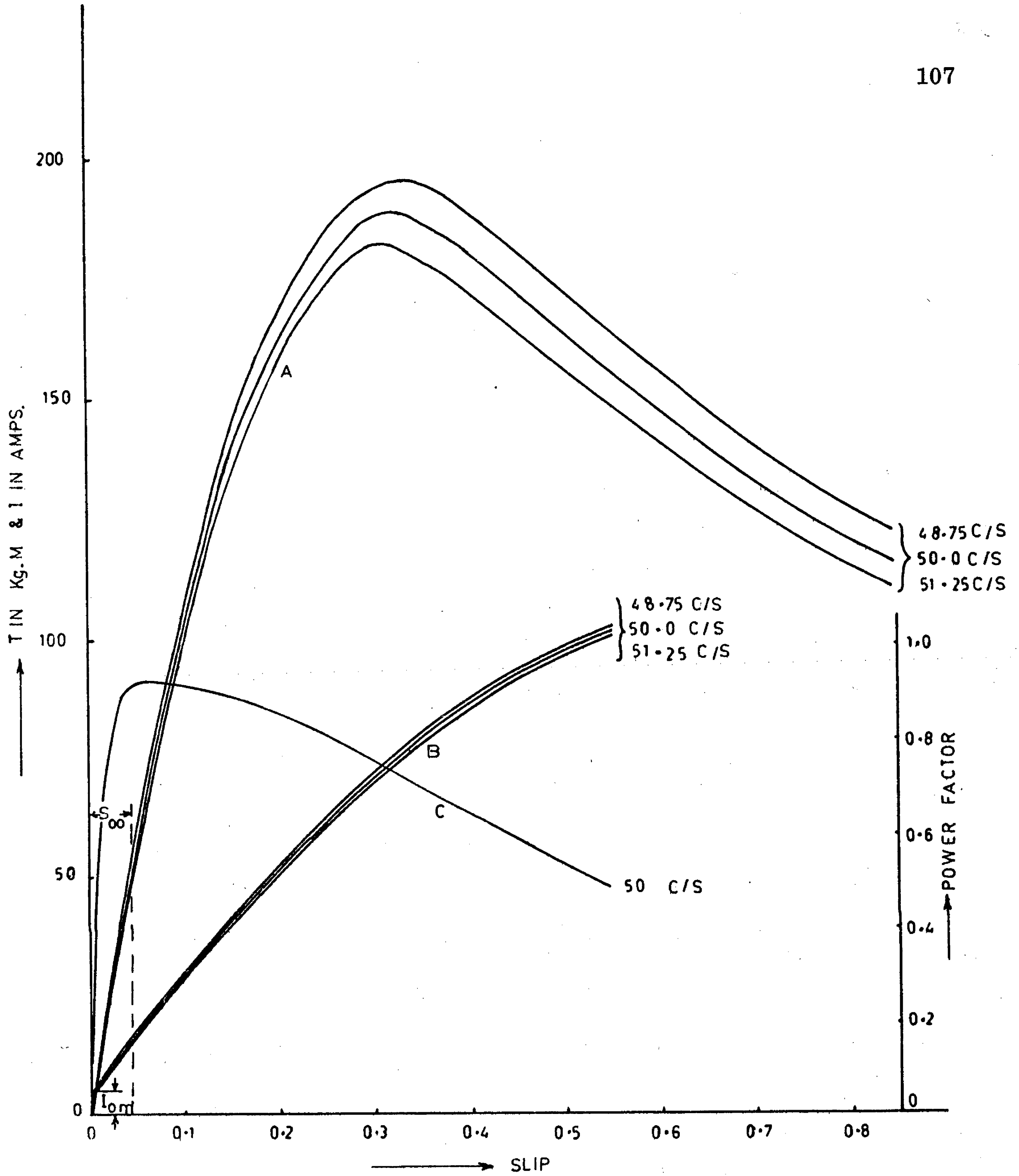

Fig. 5.3 characteristics of 15 h.p. squirrel cage induction motor for various operating frequencies.

A Torque-slip
B Stator current-slip
C Power factor-slip

proportional to $B^2 f^2$, these losses remain constant, whereas the hysteresis losses, which are proportional to $B^{1.6}f$, will be slightly reduced, giving only a slight overall reduction in core losses. Iron losses can therefore be treated as substantially constant when the terminal voltage is held constant.

5.1.1.4 Representation with Equivalent Circuits

Figure 5.4 shows the torque-speed characteristics at various frequencies for a 15 h.p. induction motor, when the terminal voltage is held constant. The characteristics are substantially linear over the working range; moreover, the part of the characteristic F'K' is small.

Consider the behaviour of the motor when the operating frequency is changed from f_o to f : immediately the operating characteristic changes, that is for frequency f_o, the motor operates on characteristic no. 1 (at point F), under steady-state conditions. The time interval for this change in frequency has been taken as "Δt" sec. On changing the frequency from f_o to f, the torque developed by the motor corresponds to the point F'. The motor accelerates and follows the path on the characteristic no. 2, as shown. The final speed at the end of the time interval "Δt" depends on the inertia factor of the machine. For higher values of inertia factor, the speed will change from n_o to n' whereas for lower values it will change from n_o to n". Assuming the F'K' part of the torque-speed characteristic linear, the equation of motion for the motor can be derived as in appendix 10.6.

The slope of the torque-speed characteristic may be determined by changing the speed slightly, for example by 0.01% and determining the corresponding torque for the given instantaneous operating frequency.

In Figure (5.5) the variations of torque developed by the

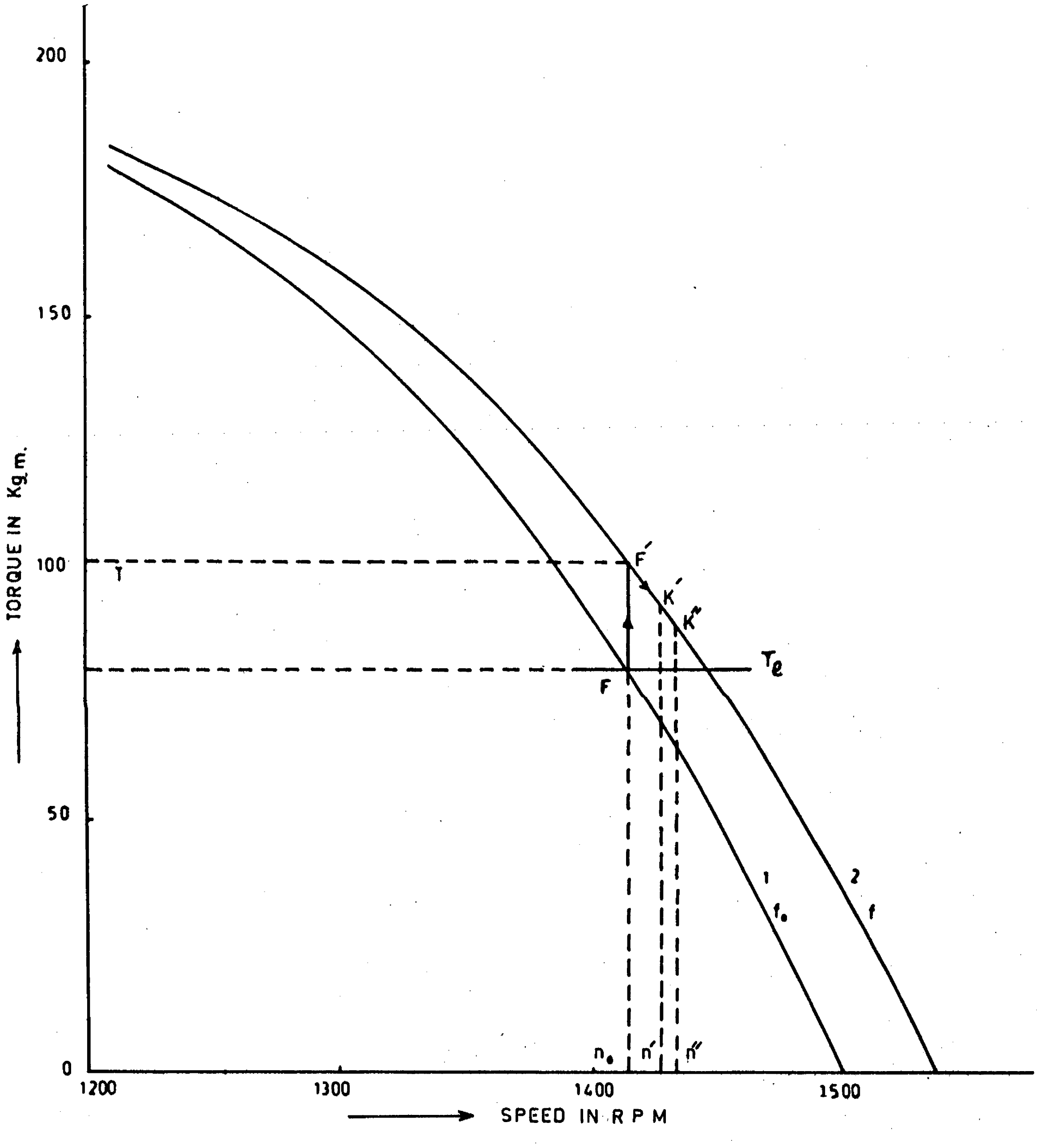

Fig. 5.4 Torque speed characteristics of 15 h.p. squirrel cage induction motor illustrating the effect of change in operating frequency.

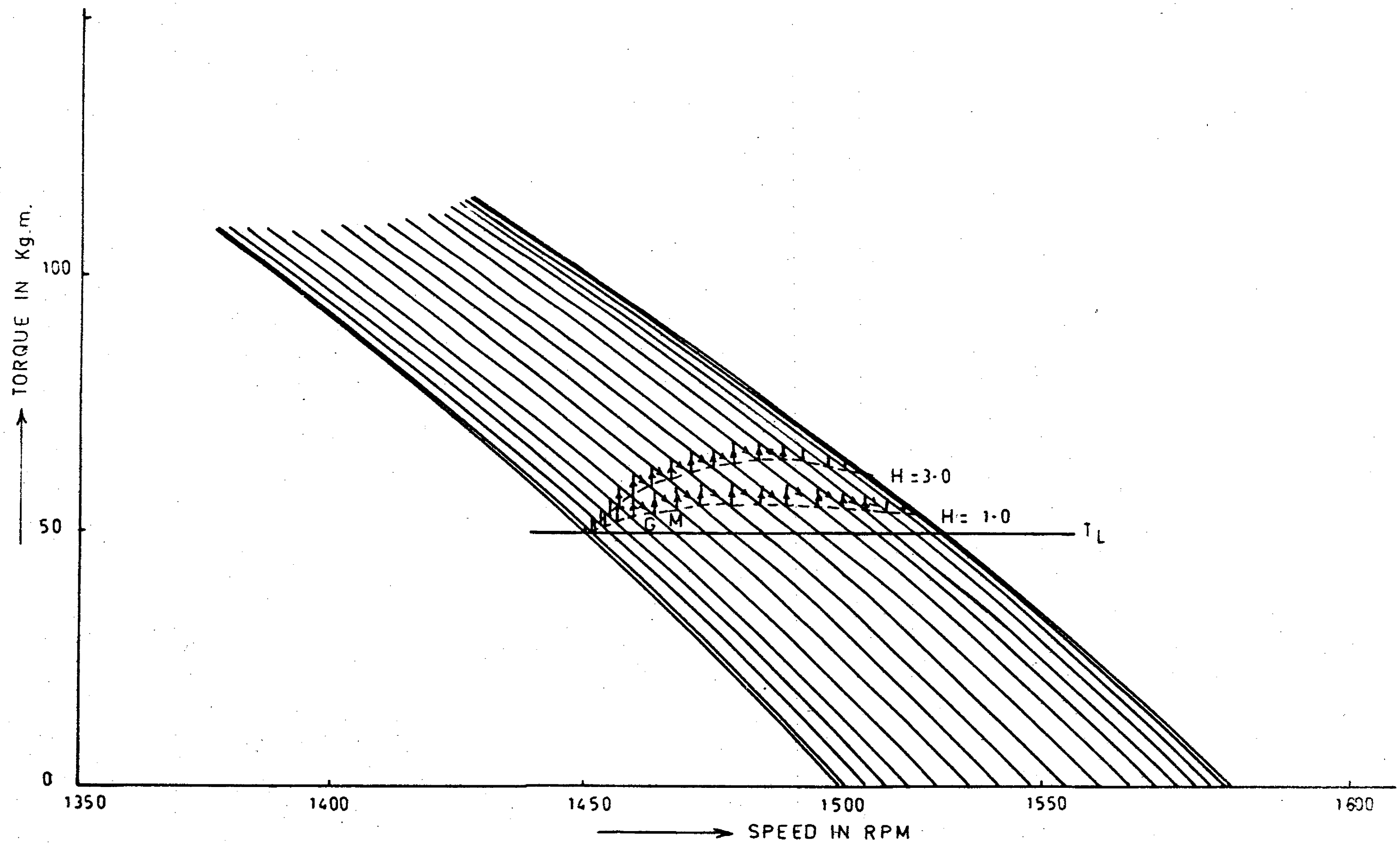

Fig. 5.5 Torque-speed characteristics of 15 h.p. squirrel cage induction motor indicating the dynamic and frequency-dependent behaviour with different inertia factors when the load torque is constant and frequency varies from 50.0 to 52.5 c/s in 0.9 sec. as shown in Fig. 5.1.

motor at the end of each time interval are shown for various values of inertia factor. The instantaneous value of the active power input may be determined by the torque corresponding to points M, G, etc. from the following steps:-

(a) Calculate the load torque for a given or assessed full load slip as:-

$$T = \frac{m V_a^2 \frac{r_2}{s_{oo}} p}{2\pi f_o \left\{ (R_1' + \frac{r_2}{s_{oo}})^2 + (X_1' + x_2)^2 \right\}}$$

(b) Calculate the actual full load speed for slip s_{oo} as:-

$$n_{oo} = n_1 (1 - s_{oo})$$

(c) Change the instantaneous frequency by one step as in conformity with the relation of variations of frequency chosen in Section 5.1.1.1 for the time interval of "Δt" secs. (arbitrarily chosen here as 0.05 sec.).

(d) Modify the equivalent circuit reactances for the instantaneous frequency.

(e) Calculate the new synchronous speed.

(f) Calculate the instantaneous slip at the beginning of the time interval as:-

$$s = \frac{n_1 - n_o}{n_1}$$

(g) Determine the instantaneous torque developed by the motor corresponding to slip s as:-

$$T = \frac{m V_a^2 \frac{r_2}{s} p}{2 \pi f \left\{ (R_1' + \frac{r_2}{s})^2 + (X_1' + x_2)^2 \right\}}$$

(h) Determine the instantaneous slope of the torque-speed characteristic.

(i) Determine the value of the coefficient A from the initial conditions at the beginning of the time interval "Δt" from equation (10.32) or (10.35).

(j) Calculate the new instantaneous speed of the motor at the end of the time interval "Δt" from equation (10.33) or (10.36).

(k) Calculate the instantaneous slip at the end of "Δt" as:-

$$s_o = \frac{n_1 - n_o}{n_1}$$

(ℓ) Calculate the active and reactive power input to the equivalent circuit for slip s_o.

(m) Calculate the active power input to the motor by adding iron losses to the active power obtained for step (ℓ).

In the foregoing procedure, the friction and windage losses have been considered as an integral part of the load supplied by the induction motor.

The above steps from (c) to (m) are repeated for each step change in frequency, and in this way the dynamic and frequency-dependent behaviour of an induction motor can be studied for various values of inertia factor. The curves in Figures (5.8, 5.9 (a and b)) have been obtained in this way.

5.1.1.5 Induction Motor Parameters

Full load slip normally varies from 5.5% to 1%, inertia factor from 0.1 to 0.3 and magnetising current from 50% to 20% of the full load current for general purpose induction motors, over a range of 1 to 1000 horsepower as shown in Table V and Figures (5.6 (a to e)) which have been assembled from information provided by several manufacturers*. It has been verified in practice that the inertia factor contribution of loads such as drilling, grinding, milling and spinning machines, fans, lathes, pumps, compressors, etc. is quite significant, and at least equal to that of the driving motor. The tests quoted previously from Reference (137) can give some idea of load torque variation with speed, otherwise the safest case is to treat the load torque as being constant. Installations with exceptionally high inertia factor, such as Ward-Leonard Illgner speed control, and large motors fall under the category of important induction motors and should be considered separately.

Considering induction motor installations under steady-state conditions, inertia has no effect : if the load falls by 1% with 1% reduction in frequency, then the load torque is approximately independent of speed; whereas if the load falls by 2% with 1% reduction in frequency, then the load torque is approximately directly proportional to the speed. The load reductions assumed in Reference (219) indicate $T_{\ell} \propto \omega^{n}$, where $n > 1$.

5.1.1.6 Approximate Methods of Calculation

(A) Assessment of Active Power

It is somewhat unlikely that comprehensive parameters on induction machines connected to a power system will be normally readily available; this raises the need to predict the various key parameters of induction motors. In an attempt to discover typical trends in parameters versus motor ratings, Figures (5.6 (a to e)) have been assembled from information supplied by various manufacturers*. Although individual motors of a given rating have parameters extending over relatively broad limits, an attempt has been made to draw mean curves as shown. It will be seen later that these curves are useful, particularly when it is realised that a power system will normally supply thousands of different motors, and statistical factors will consequently apply.

Appendix 10.4 shows that inertia factor is approximately independent of the number of poles, and Appendix 10.5 indicates how equivalent parameters can be determined for a mixed group of induction motors, using information on parameters of individual machines, if known, or employing the curves of Figures (5.6 (a to e)) (as being representative) in the more usual case in which all that is known about individual machines is horsepower rating and number of units.

---

* Information kindly supplied by the following manufacturers is gratefully acknowledged:-

(i) The English Electric Company Pty. Ltd.
(ii) Hawker Siddeley Brush Pty. Ltd.
(iii) Westate Electrical Industries Ltd.
(iv) Warburton Franki Industries (Melb.) Pty. Ltd.
(v) Siemens Holske Siemens Schuckert (A/asia) Pty. Ltd.
(vi) Australian Electrical Industries Pty. Ltd.

TABLE V

Showing various typical induction motor parameters - full load slip, inertia factors, and overall changes in active and reactive powers at 51.25* c/s, as shown in Figure 5.1 and expressed as % change/2.5% change in frequency, when the load torque is constant.

No.	h. p.	H in (KW-sec. / KVa rating)	Full load slip in %	% overall change at 51.25 c/s		Full load line current in amps.	Magnetising line current in amps.
				Active Power	Reactive Power		
1	5 SR	0.18	2.0	5.59	-1.62	7.5	3.97
2	7.5SC	0.113	5.3	4.44	-0.79	10.0	4.6
3	10 SC	0.1	4.66	3.21	-0.76	13.5	6.1
4	10 SC	0.12	2.3	2.93	1.38	13.5	4.6
5	10 SR	0.284	1.67	10.61	1.35	14.5	5.8
6	15 SC	0.106	2.32	2.74	1.76	20.5	6.1
7	15 SR	0.172	3.0	4.77	0.27	21.5	10.15
8	20 SC	0.12	3.33	3.65	0.047	26.5	9.7
9	20 SC	0.14	1.86	2.88	1.08	26.5	9.36
10	20 SR	0.2	3.7	6.26	4.01	27.5	10.0
11	25 SC	0.134	4.0	4.38	2.30	32.0	9.5
12	30 SC	0.18	2.38	3.12	8.85	40.5	10.5
13	40 SC	0.175	1.5	2.80	1.73	54.0	15.4
14	40 SC	0.24	2.66	3.55	1.04	52.5	18.5
15	40 SR	0.38	1.28	7.28	2.75	55.0	19.71
16	50 SC	0.144	1.51	2.58	1.12	71.0	26.5
17	50 SC	0.2	2.66	5.26	1.95	64.0	19.5
18	50 SC	0.217	1.33	3.33	1.13	64.5	21.5
19	60 SR	0.157	2.8	4.32	2.26	80.0	28.4
20	75 SR	0.137	2.3	3.37	0.68	102.5	42.7
21	75 SC	0.218	1.35	3.36	2.96	103.0	29.5

..../Ctd.

22	100 SR	0.153	2.4	3.82	2.21	147.0	45.8
23	100 SC	0.22	2.13	4.65	2.62	125.0	23.5
24	200 SC	0.25	1.46	5.64	6.25	136.0	32.5
25	200 SC	0.3	1.87	7.62	11.25	250.0	51.8
26	250 SC	0.25	1.33	4.11	6.08	40.0	8.07
27	450 SC	0.28	1.48	5.36	8.66	71.0	12.1

SC - Squirrel cage induction motor

SR - Slipring induction motor

* Because there is maximum acceleration at this frequency during the whole change as shown in Figure (5.1).

Figure (5.7) shows the torque-slip characteristics of an induction motor operating at the point F with slip s_o. When the operating frequency is changed from f_o to f, the motor operates on a characteristic corresponding to f (it has been assumed that $f > f_o$). As already mentioned, the slope of the characteristic at $s = 0$ varies inversely with the operating frequency (as shown by equation (10.6), and the operating point F shifts to F', having the instantaneous slip s. The motor accelerates, and its slip falls, following the curve F'O in Figure (5.7). The equation of motion can be derived as in appendix (10.7).

In assessing the instantaneous active power input by the approximate method, the following steps are involved:-

(a) Calculate the synchronous speed of the induction motor for the specified number of poles as:-

$$n_1 = \frac{60 \cdot f_o}{p}$$

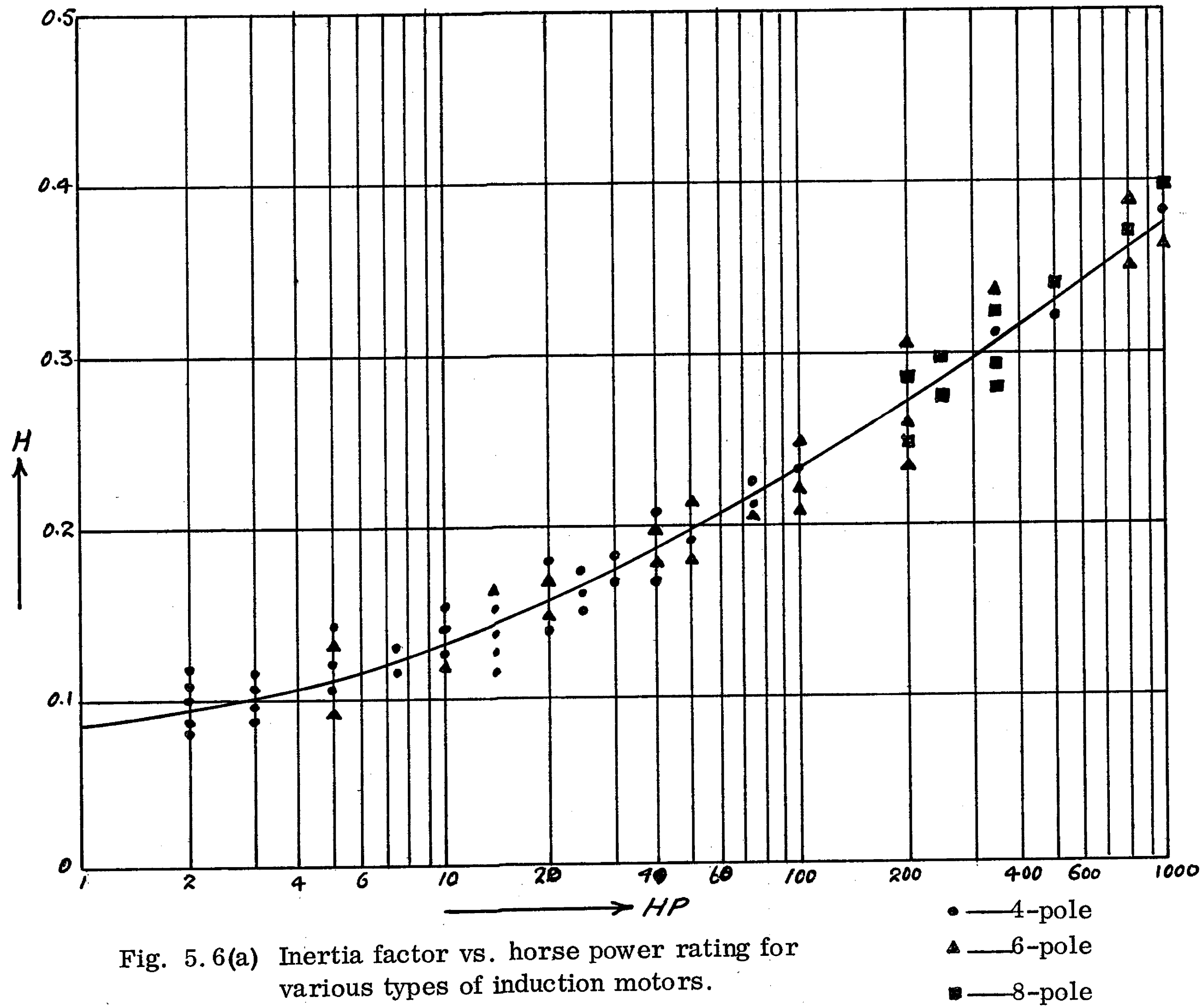

Fig. 5.6(a) Inertia factor vs. horse power rating for various types of induction motors.

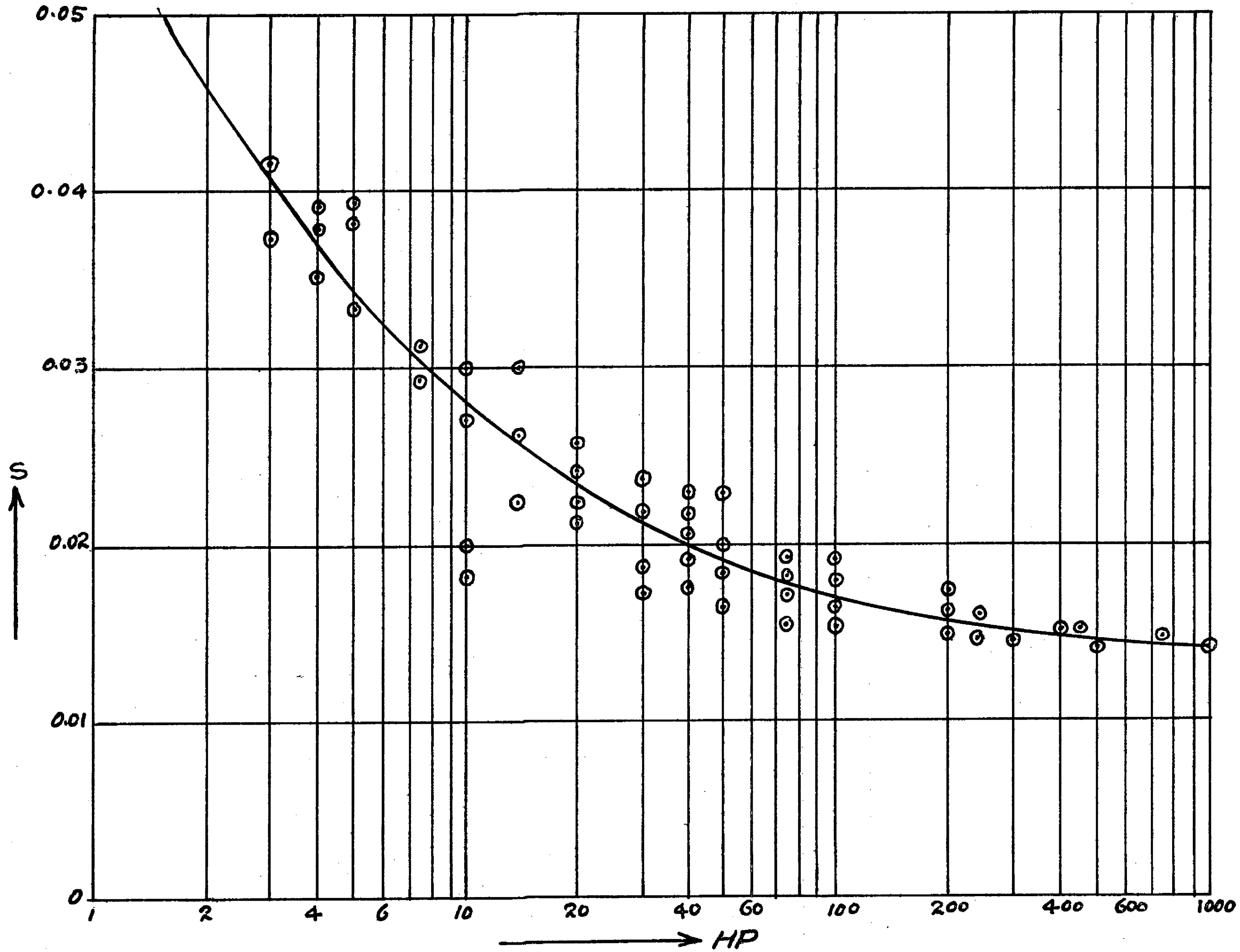

Fig. 5.6(b) Full load slip vs. horse power rating for various induction motors.

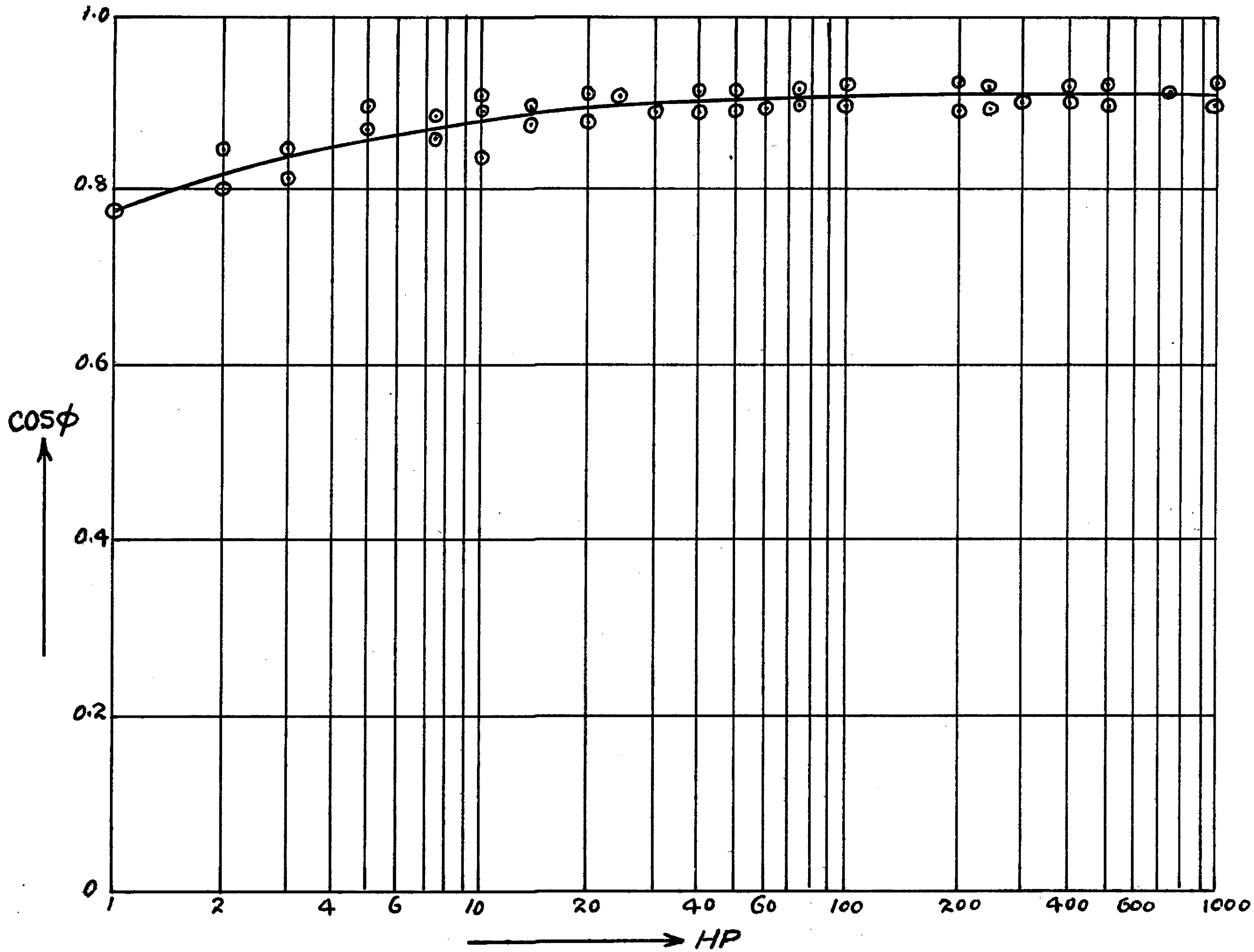

Fig. 5.6(c) Power factor vs. horse power rating for various induction motors.

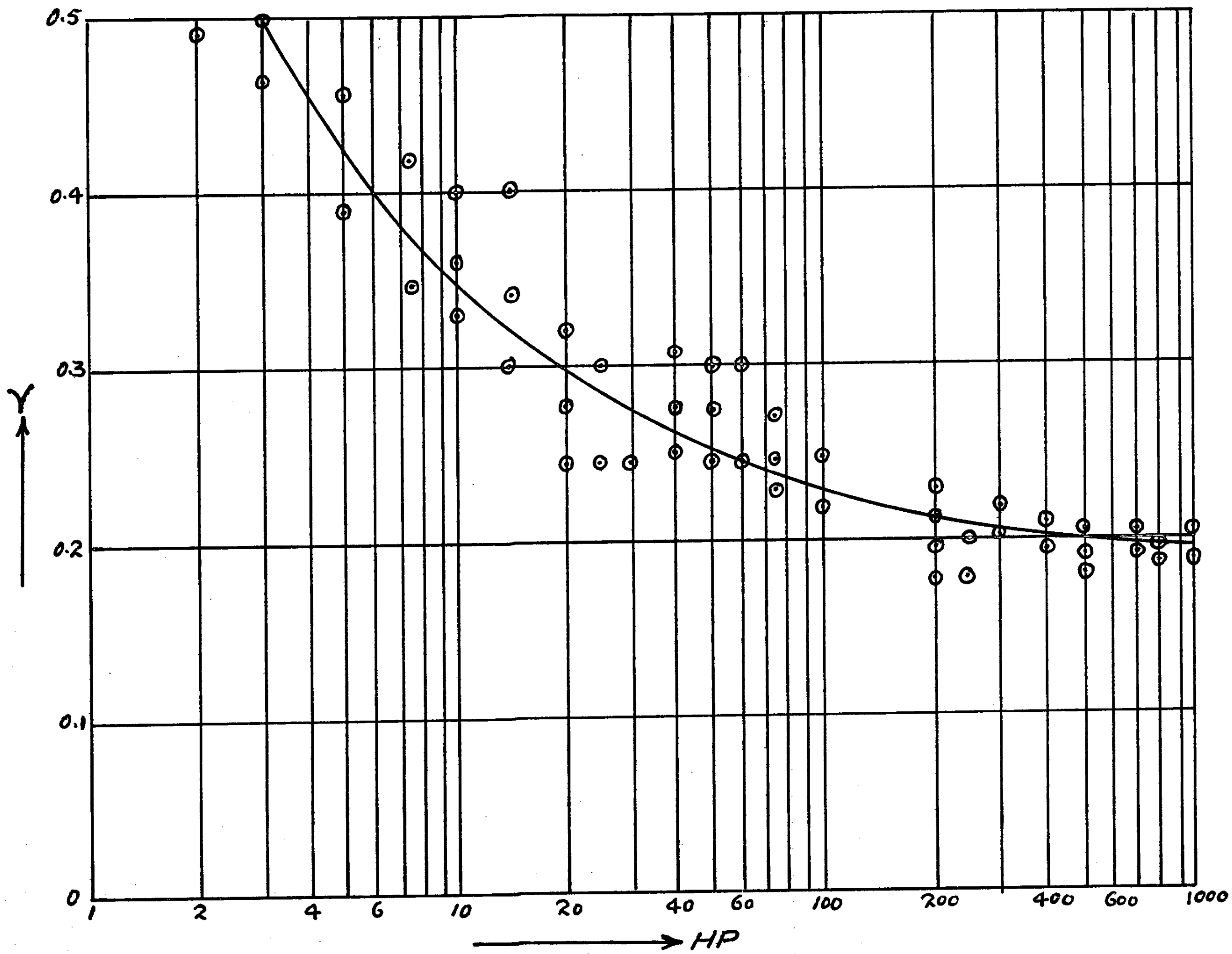

Fig. 5.6(d) Magnetising current vs. horse power rating for various induction motors.

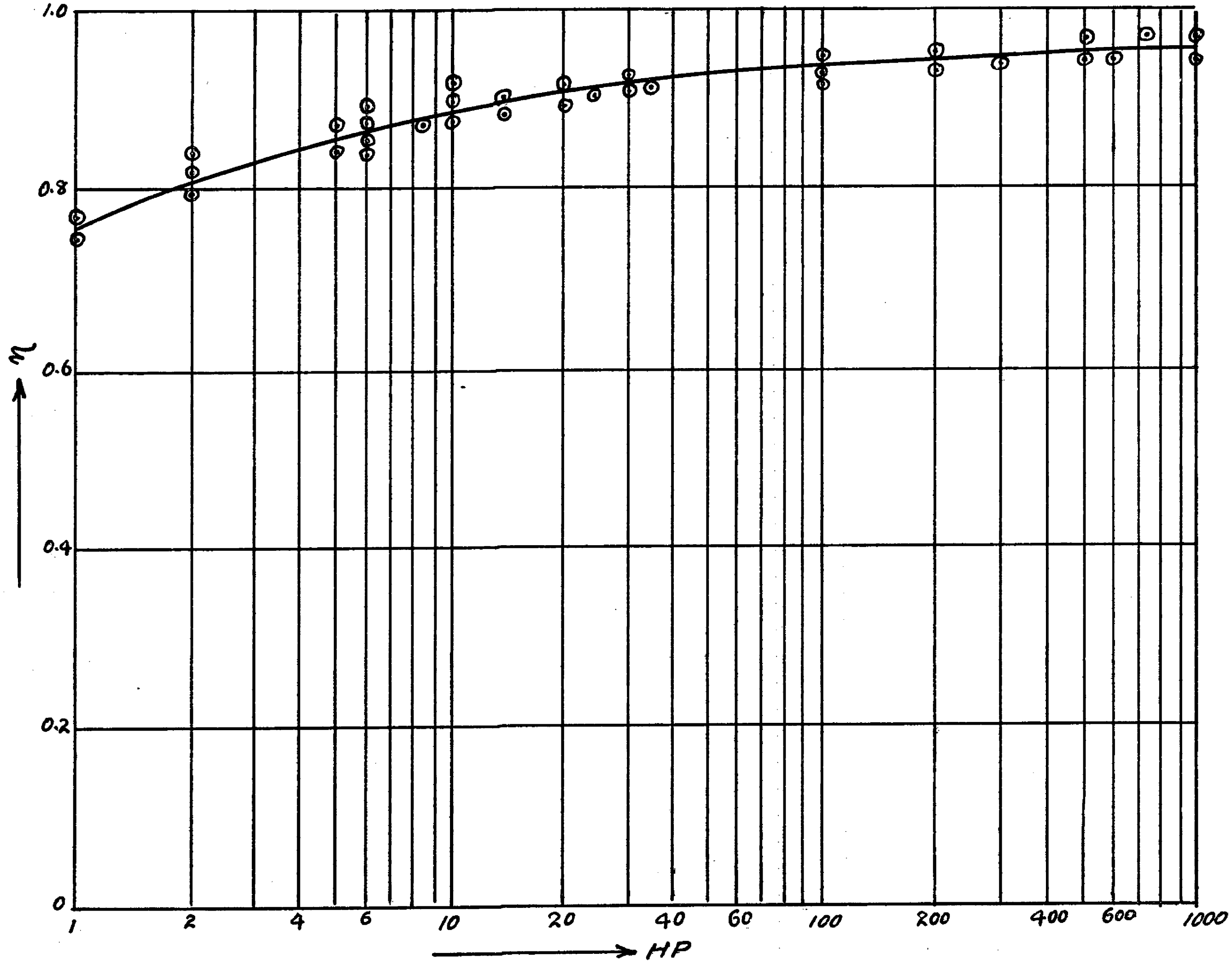

Fig. 5.6(e) Efficiency vs. horse power rating for various induction motors.

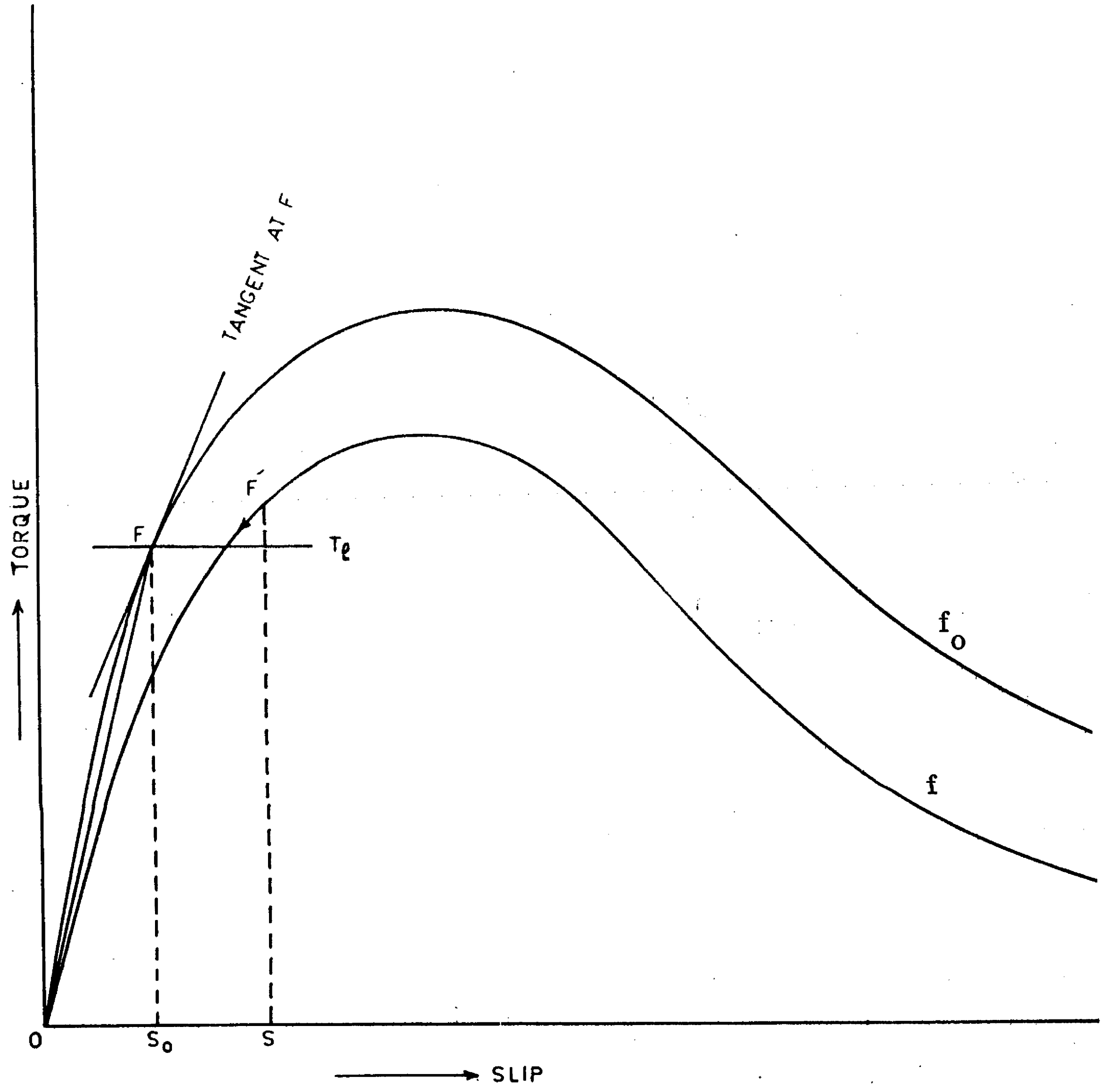

Fig. 5.7 Torque slip characteristics indicating the slope used by the suggested approximate method.

(b) Calculate the actual speed of the motor for a given or assumed full load slip, as:-

$$n_{oo} = n_1 \ (1 - s_{oo})$$

(c) Calculate the load torque, as:-

$$T_\ell = \frac{hp \times 746 \times 60 \times \eta}{2 \pi \ n_{oo}}$$

(d) Calculate the slope of the torque-slip characteristic, as:-

$$\alpha = \frac{T_\ell}{s_{oo}}$$

(e) Change the operating frequency by one step as in (c), Section 5.1.1.4.

(f) Modify α by equation (10.6) for the instantaneous frequency.

(g) Calculate the coefficient A' from the initial conditions at the beginning of the time interval "Δt" from equations (10.40) or (10.44).

(h) Calculate the new instantaneous slip at the end of the time interval "Δt" from equations (10.41) or (10.45).

(i) Calculate the instantaneous torque developed by the motor at the end of the time interval "Δt", as:-

$$T_o = s_o \cdot \alpha$$

(j) Calculate the instantaneous speed of the motor at the end of the time interval "Δ t", as:-

$$n_o = n_1 (1 - s_o) \cdot \frac{f}{f_o}$$

(k) Calculate the active power input to the motor as:-

$$P = \frac{T_o \times 2\pi n_o}{60 \times \eta}$$

In the above procedure, the windage and friction losses have been considered as an integral part of the load supplied by the motor, whereas the iron losses are indirectly included in the efficiency of the motor, which has been assumed constant because its change is negligible.

The steps (e) to (k) are repeated for each step change in instantaneous frequency, and in this way the dynamic and frequency-dependent behaviour of an induction motor can be studied conveniently without the knowledge of equivalent circuit constants. By following the above method, the appropriate curves in Figure (5.8) have been obtained.

Examination of Figure (5.7) reveals that the slope of the torque-slip characteristic used is greater than the actual, and from Figure (5.8), it is observed that only 90% of the overall change in active power has been taken into account because of this fact. Two alternatives for improvement are,

(i) Reduction of slope of the torque-slip characteristic

(ii) Increase of working slip

The first alternative depends upon the overall swing of the slip, which is determined by the inertia factor, whereas the second alternative changes the slope of the torque-slip curve and shifts the operating point to the right. Various values of working slips for different motors have been tried, and the results have indicated that a notional increase of 40% in overall

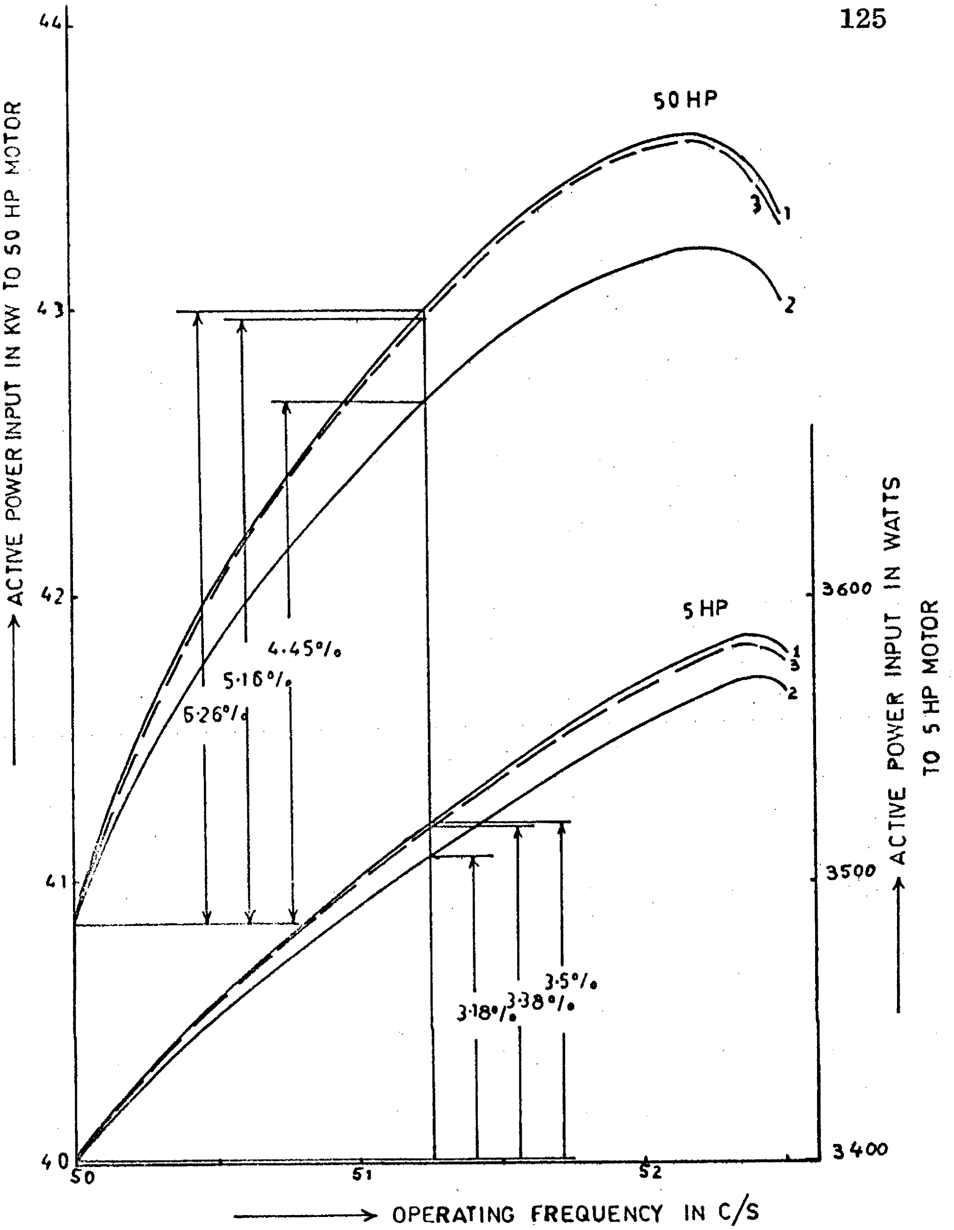

Fig. 5.8 Active power input to 5 h.p. and 50 h.p. squirrel cage induction motors vs. frequency for normal full load slip and 40% increased slip.

% values indicate overall change in active power input when treated frequency-dependent dynamically.

1 - Active power input by equivalent circuit.
2 - " " " " suggested method with normal s.
3 - " " " " " " " increased s.

working slip, improves the assessment to within $\pm$ 2% of the overall change in active power as shown in Figure (5.8). Consequently, in step (b) above, s_{oo} = 1.4 x full load slip.

Figures (5.9 (a and b)) and Table VI illustrate the magnitude of errors associated with the above method of viewing groups of machines under variable frequency conditions (as shown in Figure 5.1). Using this approach, an equivalent motor of the total group rating can be obtained (as shown in Appendix 10.5) and equivalent induction machine parameters are then available for comprehensive assessment of the power system, even when the only details available are the number of induction motors and their horsepower rating. It is clear from Figures (5.9 (a and b)) and Table VI that acting on meagre information and employing the approximate method proposed, performance can be assessed within reasonable agreement of that possible using more detailed information and more exact methods.

The above method has been used successfully by the writer in the study of frequency-dependent dynamic behaviour of groups of induction motors, calculations such as in the example of Section (5.1.2) indicating that the method retains good accuracy.

(B) Assessment of Reactive Power

The total input reactive power is absorbed in the magnetising and leakage reactances. Considering the no-load approximate representation as shown in Figure (5.10(a)), the part of the reactive power absorbed by this section is inversely proportional to the operating frequency. Figure (5.10(b)) indicates the equivalent circuit for the induction motor with the no-load section omitted. The total resistance component of the circuit depends upon the instantaneous slip of the induction motor, and falls when the slip increases. If the operating frequency goes up, then the instantaneous working slip rises and results in a reduction of overall resistance of the branch. The reactance

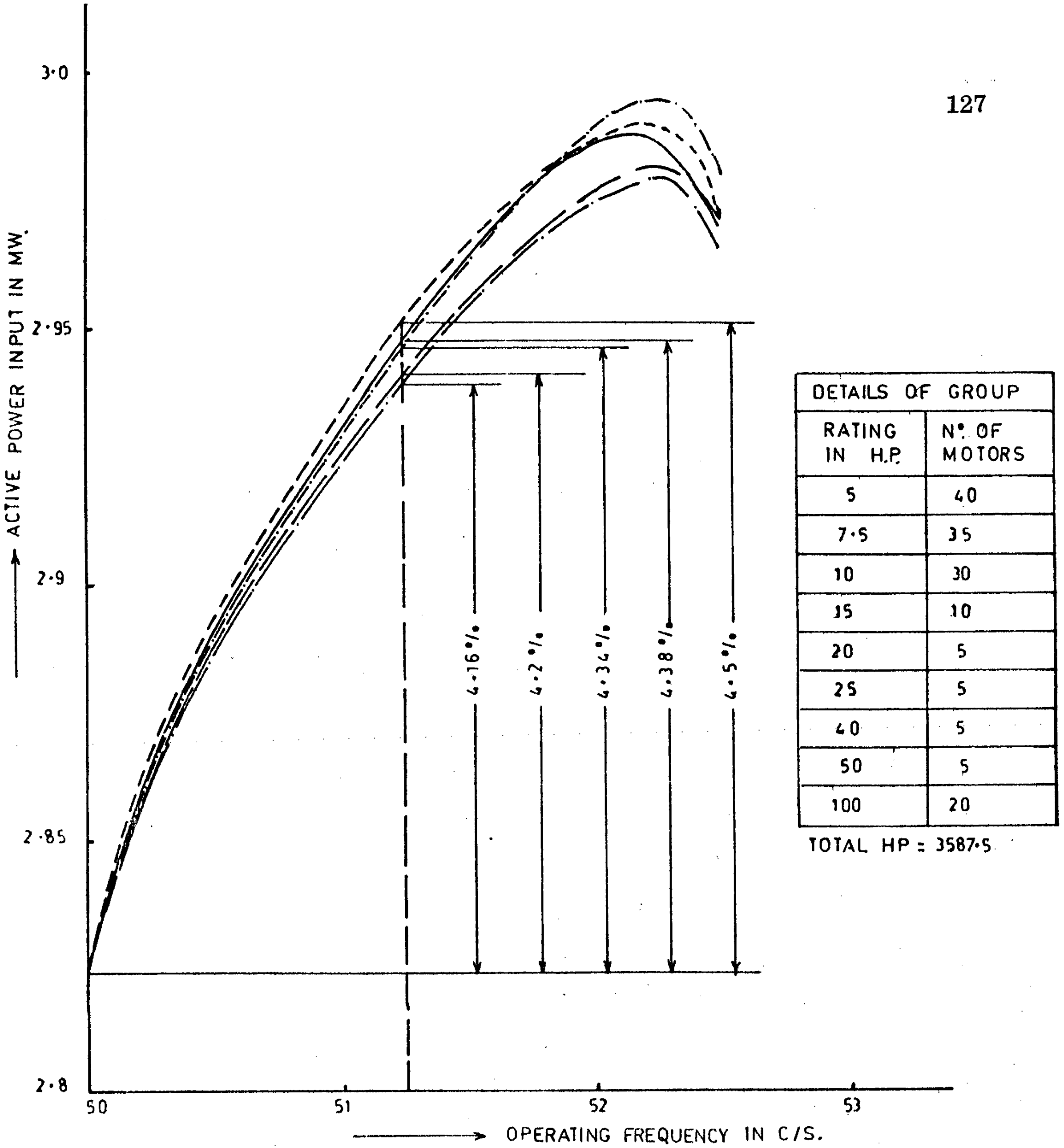

DETAILS OF GROUP	
RATING IN H.P.	N°. OF MOTORS
5	40
7·5	35
10	30
15	10
20	5
25	5
40	5
50	5
100	20

TOTAL HP = 3587·5

Fig. 5.9(a) Active power input to a group of 3587.5 h.p. induction motors vs. instantaneous frequency.

% values indicate overall change in active power under different conditions when treated frequency-dependent and dynamically. (Equivalent parameters have been ascertained from Figs. 5.6(a) to (e) by equations outlined in Appendix 10.5).

—·—·—·— By equivalent circuit.
— — — — — App. method with known parameters.
———————— " " " assumed "
——— ——— " " " 5% increase in power factor.
———·——— " " " 10% decrease in H.

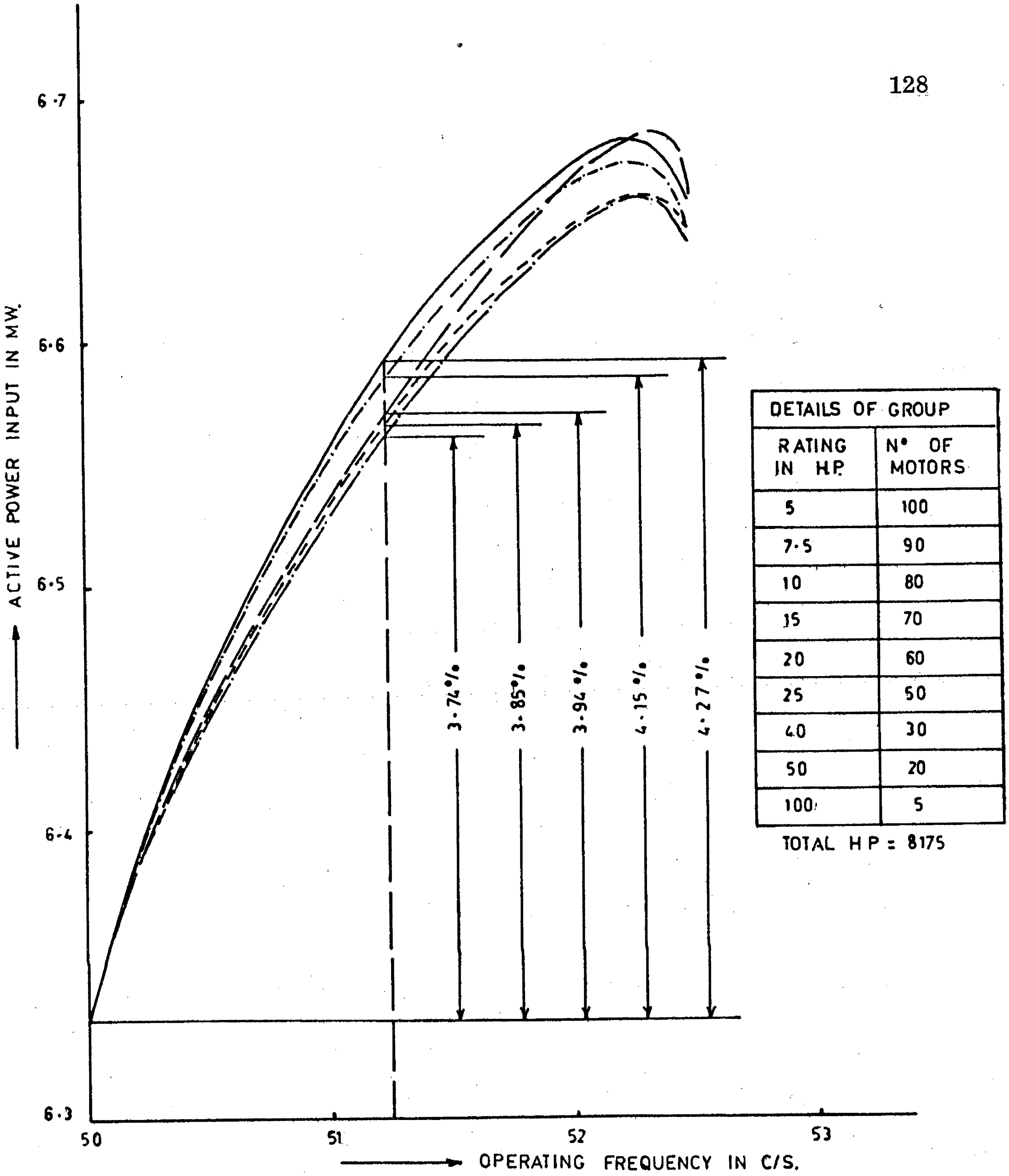

Fig. 5.9(b) Active power input to a group of 8175 h.p. induction motors vs. instantaneous frequency.

% values indicate overall change in active power under different conditions when treated frequency-dependent dynamically. (Equivalent parameters have been ascertained from Figs. 5.6(a) to (e) by equations outlined in Appendix 10.5).

By equivalent circuit.
App. method with 20% increase in slip and 10% increase in H.
" " " assumed parameters.
" " " known parameters.
" " " 20% decrease in slip and 10% decrease in H.

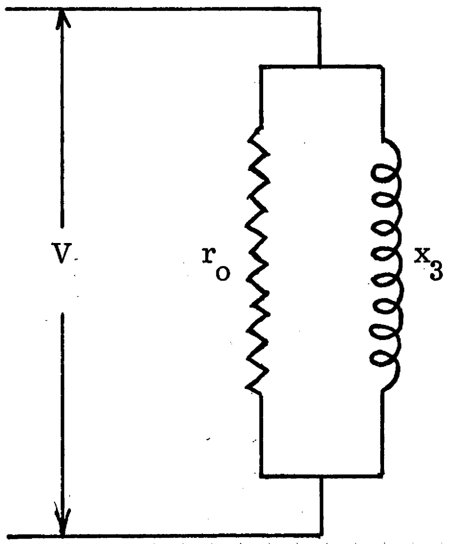

Fig. 5.10(a) No-load section of induction motor equivalent circuit.

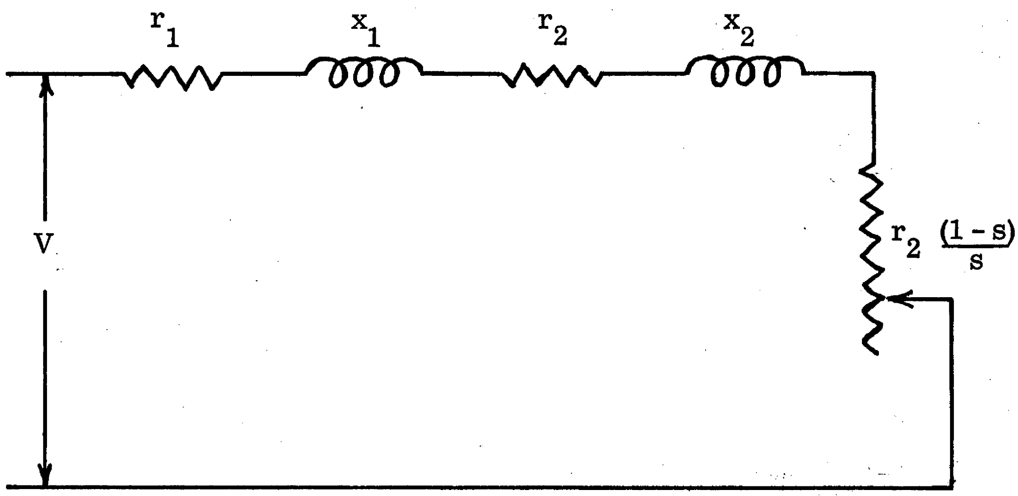

Fig. 5.10(b) Induction motor equivalent circuit (with no-load section omitted).

being frequency-dependent, the reactive power will go up under the above conditions.

In the case of small motors, such as 1, 2, 5 h.p. etc., the magnetising reactive power is usually predominant and results in a nett reduction of overall reactive power input under the above conditions. On the other hand, the reactive power absorbed by the leakage reactance is predominant for large size motors, such as 25, 50, 100 horsepower, etc. and results in a nett increase of overall reactive power. However, it is very difficult to put a firm dividing line between small size and large size motors; for example, two 50 h.p. squirrel cage induction motors supplied by the same manufacturer can behave differently with regard to reactive power input, as shown in Figure (5.11) where one machine clearly has more leakage reactance than the other.

The reactive power input to an induction motor under disturbed conditions depends upon the following factors:-

Output
Power factor
Slip
Ratio of stator leakage reactance to magnetising reactance
Ratio of rotor resistance to stator resistance

Figure (5.11) indicates the behaviour of reactive power input to various types of motors versus operating frequency.

Two alternative methods for considering reactive power are:-

(1) Treat the reactive power as constant for a group of induction motors, because

(i) Such loads have a power factor ranging from 0.75 to 0.93; that is, the ratio between active

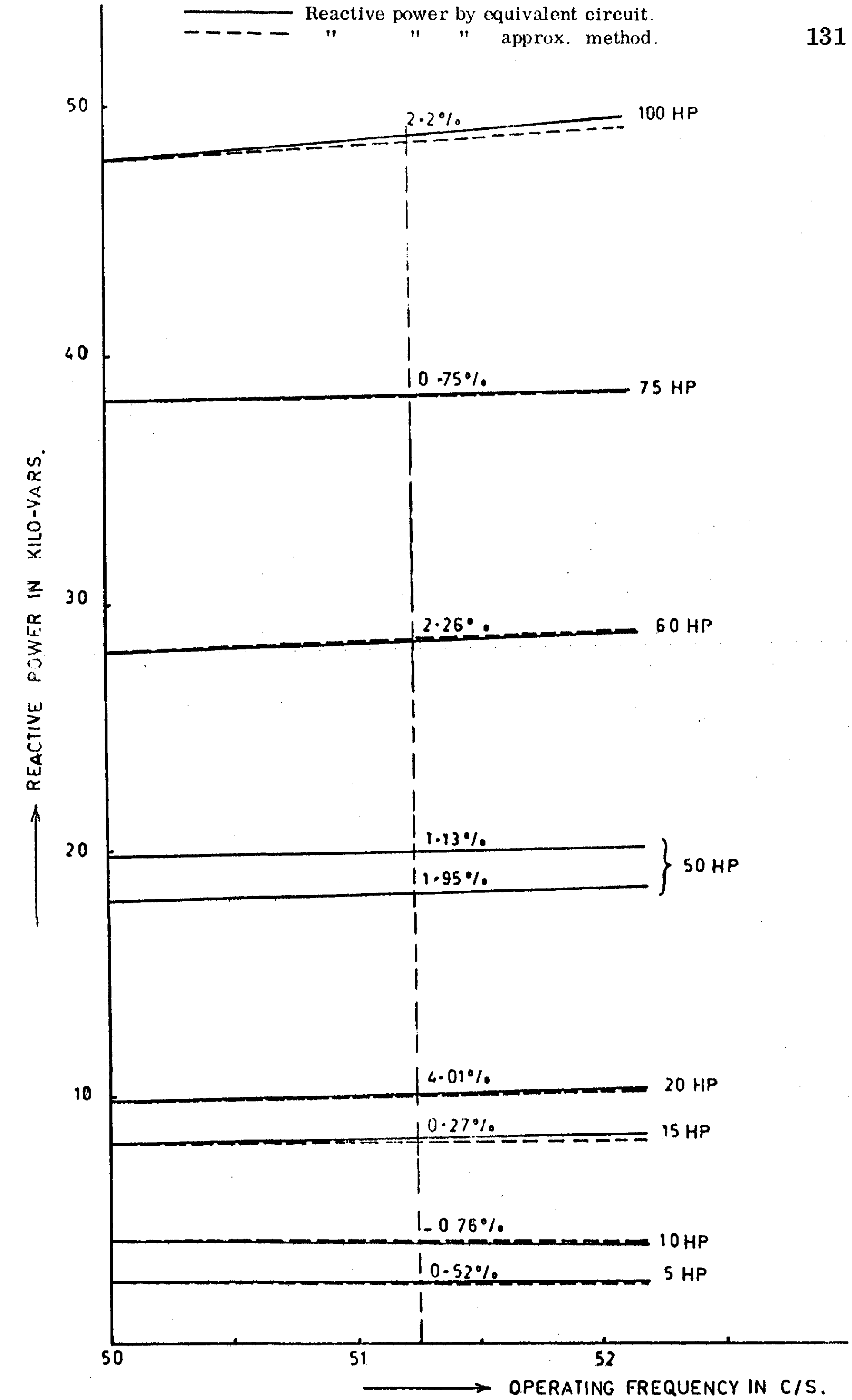

Fig. 5.11 Reactive power input vs. operating frequency for various induction motors.

(% values indicate overall change in reactive power by equivalent circuit) and reactive power varies from 1.1 to 2.5 and the change in reactive power has very little effect on the active power demand as shown in Appendix 10.8.

(ii) The overall change in reactive power is quite significantly less than that of active power as shown in Figure (5.11) and Table V (for most of the motors).

(2) Treat the reactive power as variable.

With respect to (2), there are a further two alternatives. The first one is the use of the power factor characteristic shown in Figure (5.3), but the power factor variations do not follow a regular pattern as shown in Figure (5.12), due to the fact that the maximum torque and maximum power factor do not occur at the same slip. The peak of the power factor curve falls within the working range of the torque-slip characteristics as shown in Figure (5.3), and moreover, its position varies from machine to machine. Consequently, some motors will have rising characteristics of $\frac{\Delta(\text{power factor})}{\Delta(\text{slip})}$ vs. frequency and some falling, as shown in Figure (5.12), but differing in magnitudes as well. As a result of this irregular pattern followed by different induction motors, the power factor vs. slip characteristics cannot be employed without greater errors than employing the stator current vs. slip characteristics in the assessment of reactive powers for the induction motors during disturbances.

The second alternative is to use the stator current characteristics shown in Figure (5.3) for various frequencies vs. slip. From equation (10.8), $\frac{\partial I}{\partial s}$ at $s = 0$ is independent of frequency and the characteristics are linear within the full load range as shown. The intercept on the vertical axis represents the magnetising current, which varies inversely with frequency as discussed previously.

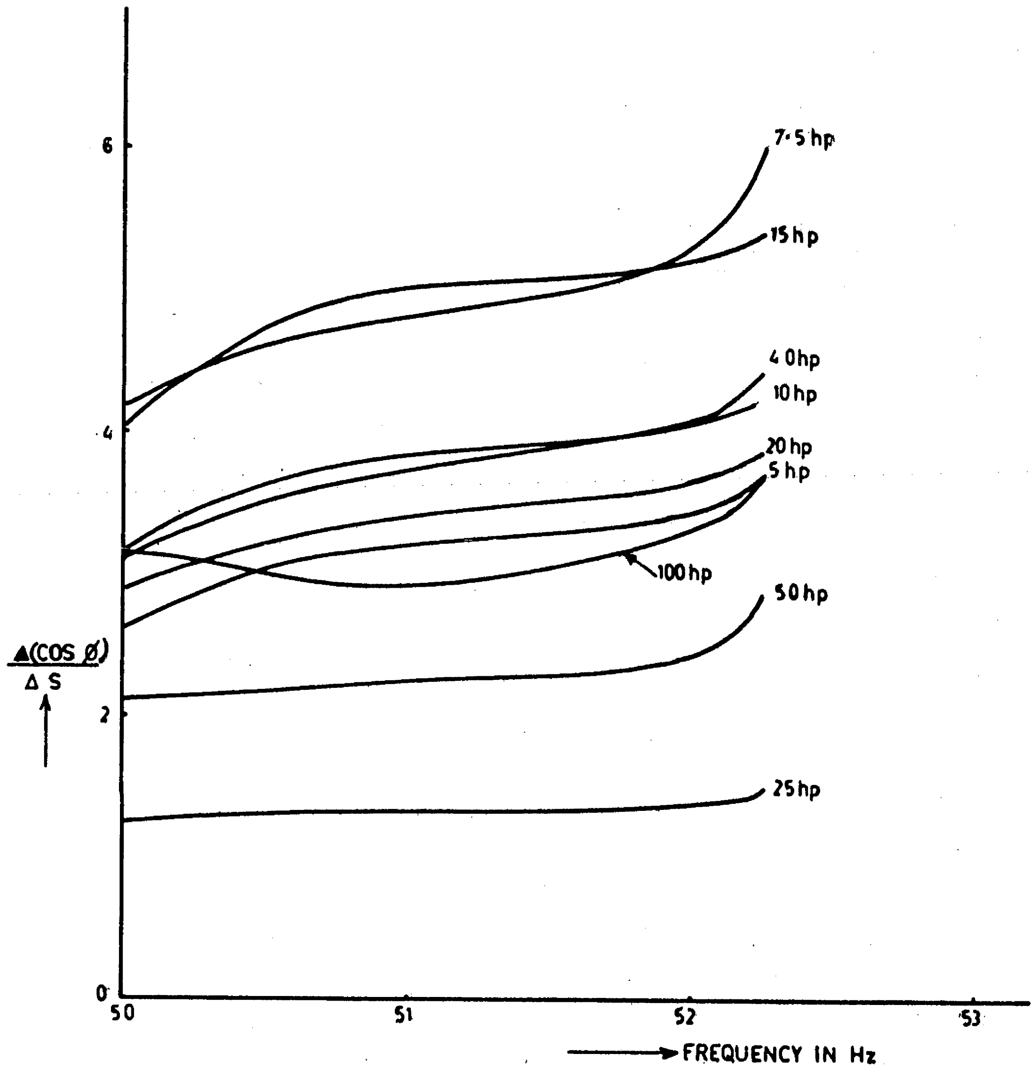

Fig. 5.12 $\frac{\Delta (\cos \phi)}{\Delta s}$ for various motors.

Using the linearity property of the characteristics,

that is, $I \propto s$,

or $I = I_{om} + C's$, where C' is the slope which depends upon the instantaneous operating frequency and is used as shown in appendix 10.2. In this way about 80% of the overall change in reactive power can be taken into account in the assessment, as indicated in Figure (5.11).

(C) Limitations of the Approximate Method

(i) The method is not valid when the voltage collapses to an extent such that the motors will no longer be working in the stable regions of their torque-slip characteristics.

(ii) In the presence of rapid-acting modern fault clearing equipment, for which the clearance time varies from 2-5 cycles [237], the motors will normally be operating during the fault period in the stable regions of their torque-slip characteristics if the available terminal voltage is not below a certain minimum value as shown by the following examples:-

10 horsepower induction motor,

Full load slip = 2.9%

Full load power factor = 0.86

Full load efficiency = 87%

Inertia factor = 0.13

Assuming the contribution of load moment of inertia equal to that of the motor,

the effective inertia factor $= 0.26$

Full load input volt amperes $= \dfrac{10 \times 746}{0.86 \times 0.87}$

$= 10,000$

Kinetic energy stored in the rotating parts at synchronous speed $= 0.26 \times 10,000$

$= 2,600$ joules

Assuming $\dfrac{T_{max}}{T} = 2.5$ for the motor, $\dfrac{s}{s_{max\,T}}$ from Figure 10.2, is equal to 0.22 for $A = \infty$

Therefore the slip for maximum torque $= \dfrac{2.9}{0.22}$

$= 13.2\%.$

For the approximate method, the instantaneous operating slip should be well below 13.2%, otherwise the motor will not be working on the linear part of the torque-slip characteristics.

Let the maximum permissible slip be 10%, after which the motor needs normal voltage at its terminals.

Kinetic energy released by the rotating parts when the slip increases to 10%,

$= 2600\ (0.971^2 - 0.9^2)$

$= 2600 \times 0.13284$

$= 346$ joules.

Load torque $= \frac{7460}{0.971}$

$= 7700$ watts.

Load power at 10% slip speed (assuming T_ℓ = Constant),

$= 7700 \times 0.9$

$= 6930$ watts.

Average load power demand during the fault,

$= (\frac{6930 + 7460}{2})$

$= 7195$ watts.

Let the fault clearance time be 0.25 sec., i.e. 12.5 cycles on 50 cycle system.

The energy requirements for the load during fault time $= 7195 \times 0.25$

$= 1799$ joules.

Let the voltage available to the motor fall to x per unit during the fault.

Motor electrical torque developed just after the fault

$= 7700\ x^2$.

Motor torque just before the fault clearance,

$= \frac{7700}{0.029} (0.1)\ x^2$ (assuming the torque-slip characteristic to be linear)

$= 26,500\ x^2$.

Mechanical power output of the motor just after the fault,

$= 7460\ x^2$ watts.

Power output just before the fault is cleared $= 23,850\ x^2$ watts.

Average mechanical power output of the motor during the fault,

$$= \frac{(7700 + 23,850)}{2}\ x^2 = 15,775\ x^2 \text{ watts.}$$

Total energy provided by the motor during the fault,

$$= (15,775\ x^2)\ 0.25 + 346 = 346 + 3944\ x^2 \text{ joules.}$$

Then equating the energy requirements,

$$346 + 3944\ x^2 = 1799$$

$$\text{or } x^2 = \frac{1453}{3944} = 0.37$$

$$\text{or } x = 0.608.$$

i.e. If the fault clearance time is 0.25 secs., the minimum voltage should not be less than 60.8% of its initial value, and if the fault clearance time is reduced to 0.2 sec., then the minimum voltage should be 58.5%.

In the case of a 1000 horse power induction motor, the minimum voltage for 0.25 sec. fault clearance time should be 51% when $\frac{T_{max}}{T} = 3$ and $A = \infty$, whereas if the fault clearance time falls to 0.2 secs., the minimum voltage should be 48%.

The approximate method presented herein for the treatment of induction motors in transient stability studies is clearly limited by the assumption that the normally provided induction motor protective devices (such as protection against phase failure, under-voltage and over-current) do not operate during the fault periods employed. This assumption, although restrictive to a degree, nevertheless enables a large proportion of the practical operating situations to be represented and is an assumption which is normally used in stability studies even when considering single induction motors[224].

5.1.2 Application to Stability Problems

The suggested representations of induction motor loads may be employed in transient and dynamic stability studies as discussed below: -

5.1.2.1 Procedure for Transient Stability Studies

(a) Obtain an overall power balance under steady-state conditions, in conventional form.

(b) Calculate the synchronous speed for the equivalent induction motors as:-

$$n_{1j} = \frac{60\, f_o}{p_j}$$

(c) Calculate the actual speed of the various motors as:-

$$n_{ooj} = n_{1j}\,(1 - s_{ooj})$$

Where $s_{ooj} = 1.4 \times (\text{equivalent slip})_j$ section (5.1.1.6A).

(d) Calculate the various load torques as: -

$$T_{\ell j} = \frac{60\ (\text{motor load})_j\ \eta_j}{2\,\pi\, n_{ooj}}$$

(e) Calculate the slopes of torque-slip characteristics as: -

$$\alpha_j = \frac{T_{\ell j}}{s_{ooj}}$$

(f) Determine the induction motor currents for the induction motor loads as: -

$$I_j = \frac{(\text{Induction motor MVA in per unit})_j}{(\text{Load bus voltage})_j}$$

(g) Determine the slopes of the current-slip characteristics as: -

$$C'_j = \frac{I_j - I_{omj}}{s_{ooj}}$$

(h) Determine the equivalent shunt impedance for all the induction motor loads on the basis of terminal voltage.

(i) Apply the disturbance.

(j) Modify the slopes of torque-slip characteristics for all the load buses by equation (10.6) for the currently existing value of load bus frequencies and voltages.

(k) Modify the slopes of current slip characteristics for all the induction motor loads by equation (10.9), for the currently appropriate value of load bus frequencies.

(l) Calculate the coefficient A'_j from the initial conditions at the beginning of the time interval "Δt" from equations (10.40) or (10.44).

(m) Calculate the new instantaneous slips at the end of the time interval "Δt" by equations (10.41) or (10.45).

(n) Calculate the instantaneous torques developed by the equivalent induction motors at the end of the time interval "Δt", as: -

$$T_{oj} = s_{oj} \cdot \alpha_j$$

(o) Calculate the instantaneous speed of the motors as,

$$n_{oj} = n_{ij} \, (1 - s_{oj}) \, \frac{f_j}{f_o}$$

(p) Calculate the active power input to the various equivalent motors as,

$$P_j = \frac{T_{oj} \cdot 2\pi \cdot n_{oj}}{60 \, \eta_j}$$

(q) Calculate the input current to the various equivalent motors at end of the time interval "Δt", as,

$$I_j = \left(I_{omj} \cdot \frac{f_o}{f_j} + C'' \cdot s_{oj} \right) \times \left(\frac{\text{instantaneous bus voltage}}{\text{initial bus voltage}} \right)_j$$

(r) Calculate the reactive power input from a knowledge of current, voltage and active power.

(s) Represent each equivalent motor by its shunt impedance for the currently existing value of load bus voltages for the active and reactive powers obtained in steps (p) and (r).

(t) Calculate the driving point and transfer admittances for the various synchronous machines.

(u) Calculate the instantaneous angular position of the synchronous machines by solving their differential equations, for the time interval "Δt" (which is usually 0.05 sec.)

(v) Calculate the instantaneous load bus voltages and phase angles.

(w) Calculate the instantaneous frequency at each load bus and modify it with accelerating factor as,

$$f_j^{i} = f_j^{i-1} + (f_j^{i} - f_j^{i-1}) \times \text{accelerating factor}$$

(x) Test for convergence of power angles of various synchronous machines to be within, say, 10^{-3} of a degree, and instantaneous load bus voltage and frequency to be within, say, 10^{-6} P.U. If the test is not satisfied, go to step (j) and repeat.

(y) Write the final angular positions of the various synchronous machines.

The method outlined above proceeds towards a solution iteratively. For the purposes of highlighting the effects of frequency-dependent and dynamic representations of induction motor loads, the system has been represented at system nominal frequency.

5.1.2.2 Illustrative Problem Including Dynamic Loads

A four-machine problem[195] whose line diagram and circuit parameters are given in Figure (5.13a) is offered as illustrating the effects being considered*. In this problem an induction motor load is included at bus no. 7 as a part of the existing 84 MW total load. Figure (5.13b) shows the swing curves for all the four synchronous machines assessed by conventional digital computer programs (for example, as in Ref. 162), modified as indicated above to take account of dynamic frequency-dependent effects for the induction machines. The following cases have been plotted in Figures (5.13b&c):-

(i) Considering the 84 MW load as passive.

---

* This problem is almost identical with an example in reference 195, except that the part of the load on bus 7 is not removed on occurrence of the fault. The original H factors are retained for the synchronous machines because, in spite of the reduced amplitude of oscillations which occur relative to those which would exist if more modern (and smaller) H factors are employed, the effects of frequency-dependence of induction motor loads are still adequately demonstrated.

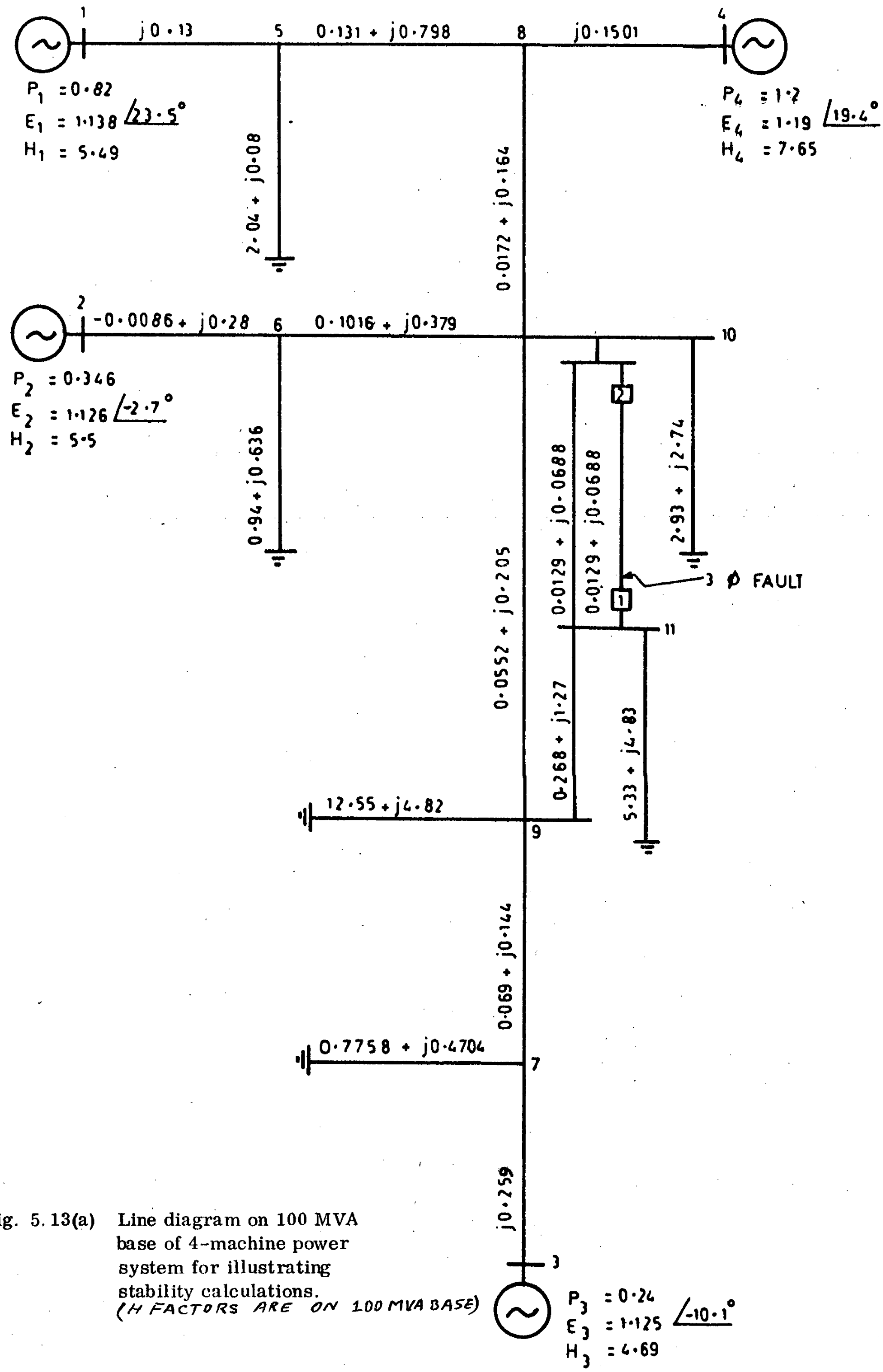

Fig. 5.13(a) Line diagram on 100 MVA base of 4-machine power system for illustrating stability calculations.
(H FACTORS ARE ON 100 MVA BASE)

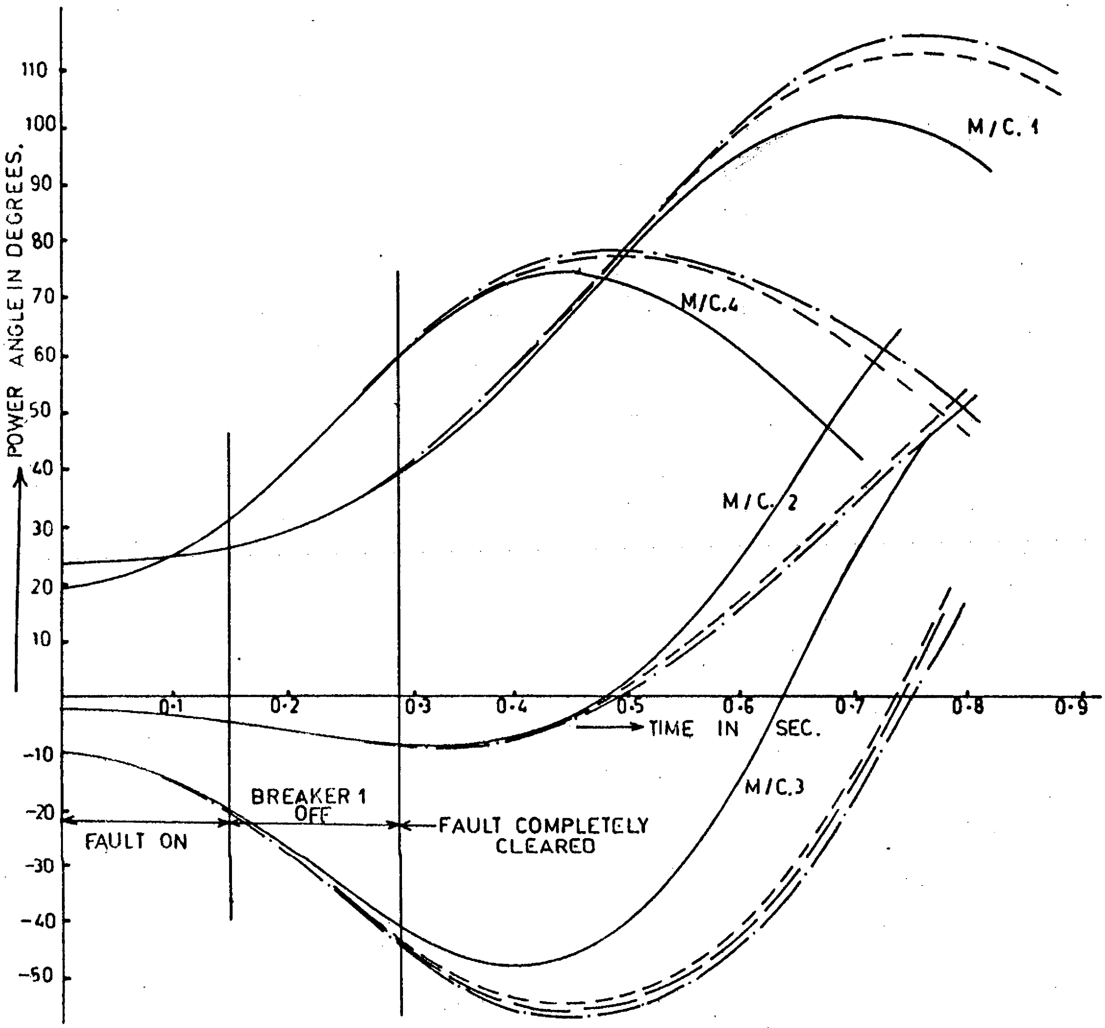

Fig. 5.13(b) Swing curves for 4-machines when 14.3% of 84 MW load at bus no. 7 is represented as frequency-dependent and dynamic.

——————— With passive loads.
———·——— " equivalent circuits.
——— ——— Approx. method with assumed parameters.
— — — — — " " " known "

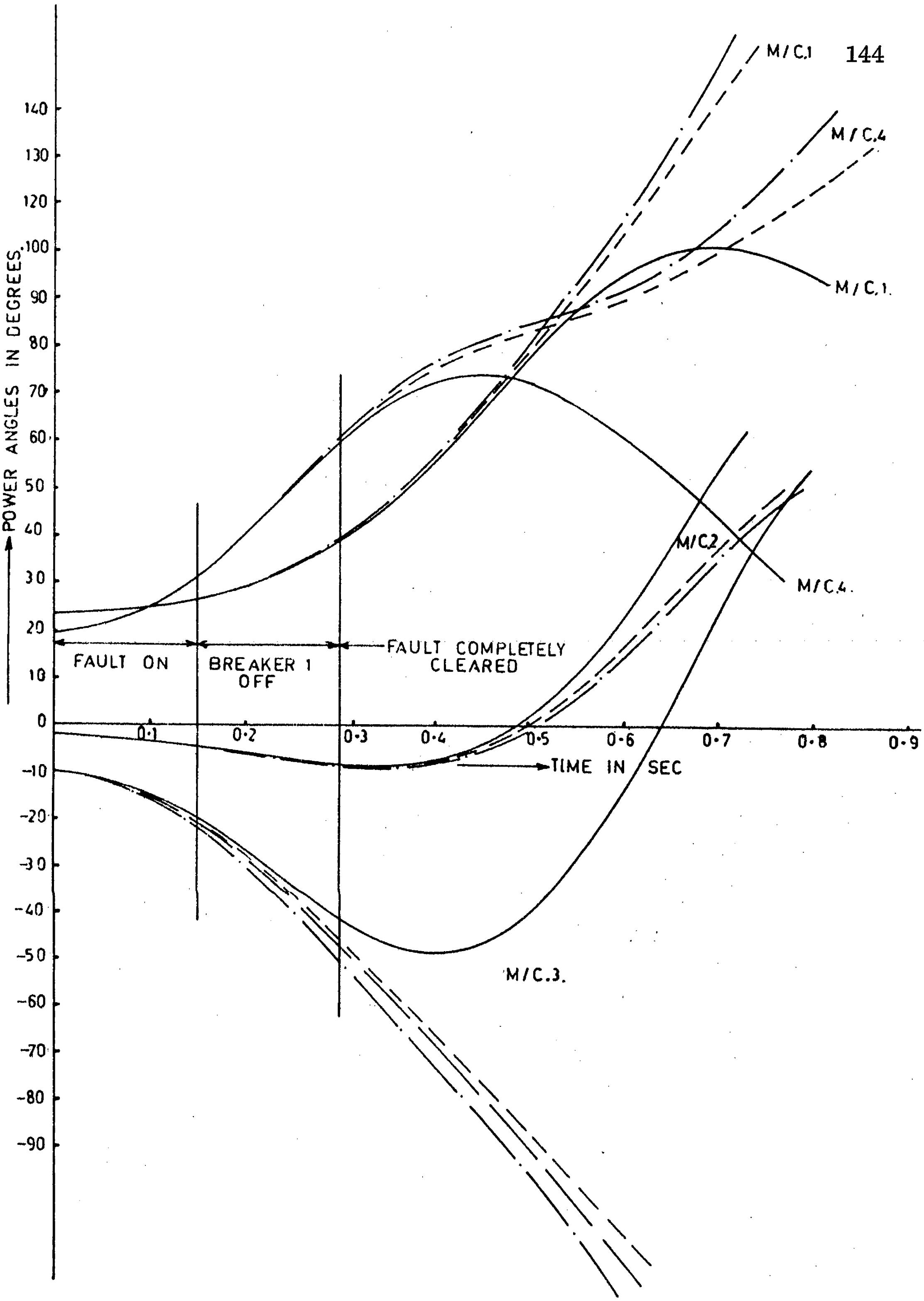

Fig. 5.13(c) Swing curves for 4-machines when 40% 84 MW load at bus no. 7 is represented as frequency-dependent and dynamic.

——— With passive loads.
—·— " equivalent circuits.
— — Approx. method with assumed parameters.
- - - " " " known "

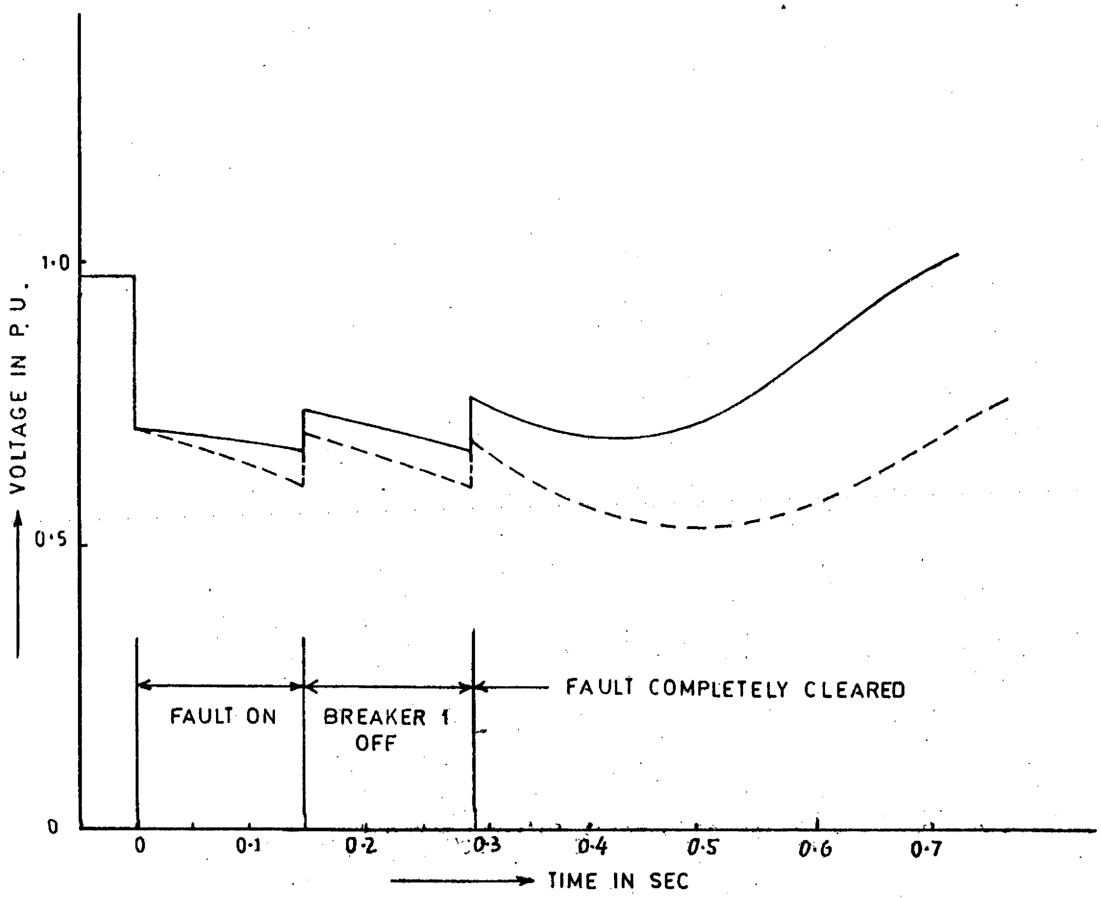

Fig. 5.13(d) Terminal voltage at bus no. 7 when loads represented passively and 14.3% of 84 MW load at bus no. 7 is treated as frequency-dependent and dynamic.

———— With passive load.
– – – – – " dynamic "

(ii) With 14.3% of the 84 MW (that is 12 MW) treated as dynamic and frequency-dependent induction motor load, being composed of small induction motors.

(iii) With 40% of the 84 MW (that is 33.6 MW) treated as in (ii).

It will be noticed that whereas in case (ii) the system has been assessed as stable, but with less margin of stability than case (i), case (iii) is unstable. Indeed, with about 35% of the 84 MW load being treated as dynamic frequency-dependent induction motor load, composed of small induction machines, the system just tends to instability.

(In obtaining the results presented in Figures (5.13b and c), adequate convergence occurred in 10 iterations when an accelerating factor of 1.35 was used for instantaneous frequency convergence (no effort has been made to optimise the time interval chosen in the example as the aim has been merely to compare the various calculations)).

5.1.2.3 <u>Accuracy of the Approximate Methods</u>

An object of Section (5.1) has been to be able to allocate induction motor parameters (relying on conformity to type) so that this information may be useful to power system planners to whom normally only number of units and horse power ratings are known. By employing information from manufacturers and considerations as outlined in the Appendices, the curves of Figures (5.6a-e) have been found useful in allocating appropriate parameters. To test the order of accuracy implied by these methods, single machines and groups of machines have been studied with respect to their behaviour over assumed realistic power system frequency excursions (as might be expected to be met during power system electromechanical oscillations) by employing, on the one hand, accurate information and accurate methods of computation; and on the other, assuming typical parameters and employing approximate methods of computation. In spite of the fact that many assumptions have been made in the latter case, agreement between the two assessments (as shown in Figures (5.8, 5.9a and b) appears reasonable.

Because motor efficiencies follow a well defined pattern, active power changes during transient conditions can be predicted considerably better than reactive power changes, which depend on more diverse factors. Introduction of deliberate errors in appropriate parameters for the conditions of Figures (5.9a and b) and Table VI gives results such that active power changes are assessed by the approximate method of calculation to within $\pm$ 5% of the true changes when the following factors have their stated limiting conditions:-

(a) Power factor within $\pm$ 5% of true value.

(b) Inertia factor within $\pm$ 10% of true value.

(c) Full load slip within $\pm$ 20% of true value.

Statistically, it is extremely unlikely that errors in assumed values for induction motor parameters would be outside the abovementioned tolerances, particularly on a system supplying large numbers of induction motors; results confirm this view.

Reactive power is influenced by many factors (Section (5.1.1.6). It is subject to greater errors in calculation, but changes in reactive power can normally be computed to within $\pm$ 20% of the true value (Figure (5.11)) and further, as shown in Appendix 10.8, change of reactive power has only a small effect on input active power, when the voltage is held constant.

A feature of the approximate method is the greatly reduced time for computations in relation to that required in the accurate method,

TABLE VI

Showing the effect of error in equivalent parameters on active power input to groups of induction motors at 51.25 c/s instantaneous frequency, when treated dynamically and frequency-dependent, for the frequency variations shown in Figure (5.1).

Active power input to 8175 hp group	Assessed change as % of true change	Active power input to 3787.5 hp group	Assessed change as % of true change	Remarks
6.3410 MW	-	2.8240 MW	-	At 50 c/s under steady-state conditions.
6.5908 "	100%	2.9466 "	100%	Calculations by actual equivalent circuit parameters.
6.5859 "	98.43%	2.9510 "	103.5%	Calculations by app. method with known parameters.
6.5870 "	98.87%	2.9470 "	100.32%	Calculations by app. method with assumed parameters.
6.5746 "	93.89%	2.9389 "	93.71%	Calculations by app. method with 5% reduction in true equivalent power factor and 20% reduction in true equivalent slip.
6.5986 "	103.53%	2.9522 "	104.56%	Calculations by app. method with 10% increase in true equivalent inertia factor.
6.5818 "	96.78%	2.9410 "	95.43%	Calculations by app. method with 5% increase in true equivalent power factor.
6.5940 "	101.68%	2.9485 "	101.55%	Calculations by app. method with 10% increase in true equivalent inertia factor 20% increase in true equivalent slip and 5% reduction in true equivalent power factor.

as in this latter case, each induction motor must be treated individually. In view of the reasonable degree of agreement between the two, the former method seems preferable in most cases.

To demonstrate the utility of dynamic frequency-dependent considerations of induction motors on power systems and the degree of accuracy attainable with the proposed approximate method of calculation with machine parameters assumed from typical values (in the absence of actual figures), the example of Section (5.1.2.2) has been presented. This shows clearly that the proposed approximate methods are sufficiently accurate in relation to what can be achieved by employing true induction motor parameter values.

5.2 Frequency-Dependent Static Loads

These loads have been mentioned previously on page 102, but little information is available on their frequency-dependent behaviour. Ref. 119, for example, gives some results on overall reduction in active power when frequency is reduced, but the information presented, being applicable to the particular system, and presenting an overall picture of load behaviour, does not separate out individual loads.

Static loads, except filament lamps and element heaters, are normally associated with additional static equipment - for example, discharge lamps employ shunt capacitors for power factor correction, arc furnaces employ series reactors to overcome lamp flicker in the system, and electric welders use series capacitors for power factor correction and to overcome the violent fluctuations in their power demands. It is clear that the frequency-dependent characteristics of static loads as regards active and reactive power demands, are influenced by compensating capacitors and reactors.

The composition of static-loads, obtained from load surveys, can be used conveniently in ascertaining the composite static-load characteristics with the aid of individual load characteristics, for use in stability studies.

5.2.1 Influence of Static-Load Characteristics in Stability Studies

Figure (5.14a) indicates in general the active and reactive power inputs to a passive inductive circuit versus instantaneous frequency. It will be noted that the active power falls linearly, whereas the reactive power has a saddle point at an operating frequency represented by the point D, which gives the limiting value of operating power factor at which $\frac{dQ}{df}$ changes its sign. In the case where synchronous machines in a power system accelerate under disturbed conditions, the system frequency increases, and the behaviour of the load characteristics shown in Figures (5.14a-d) will then be as follows:-

If the system is operating normally at B in Figure (5.14a), the active power falls continuously, whereas the reactive power rises; this causes an additional voltage drop in the transmission network, and as a result of this, the active power is further reduced, resulting in a nett increase in out-of-balance active powers for the synchronous machines. In this way the acceleration of the synchronous machines is promoted, thus causing negative damping. In the case where the operating frequency is at the point E, both active power and reactive power fall. Reduction of reactive power under these circumstances raises the system busbar voltages, thus reducing the nett change in active power, thereby causing positive damping.

In the presence of shunt compensation by capacitors, the nett reactive power characteristic is derived by subtracting capacitive Vars from inductive Vars over the frequency range, as shown in Figure (5.14b). The effect of such compensation is to shift the saddle point of the reactive power

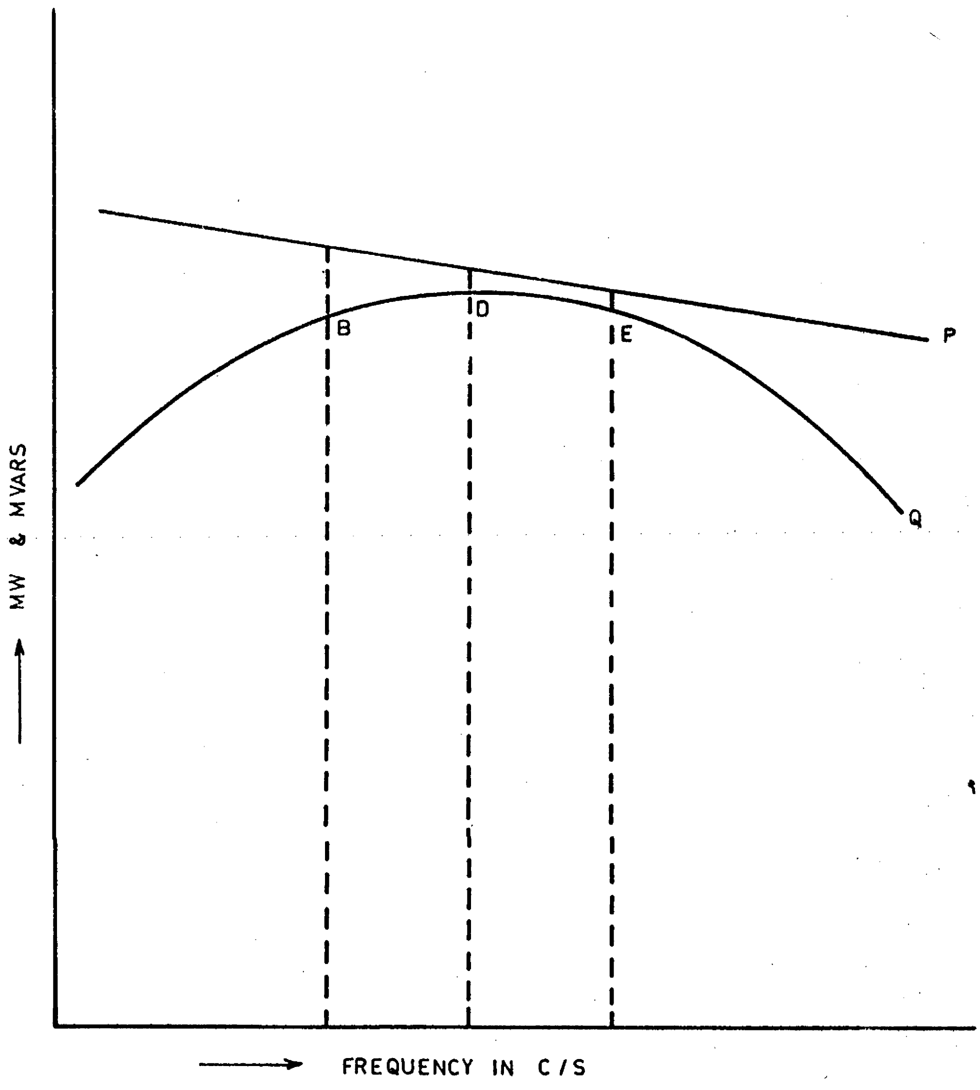

Fig. 5.14(a) General variations of active and reactive powers for passive loads as a function of frequency.

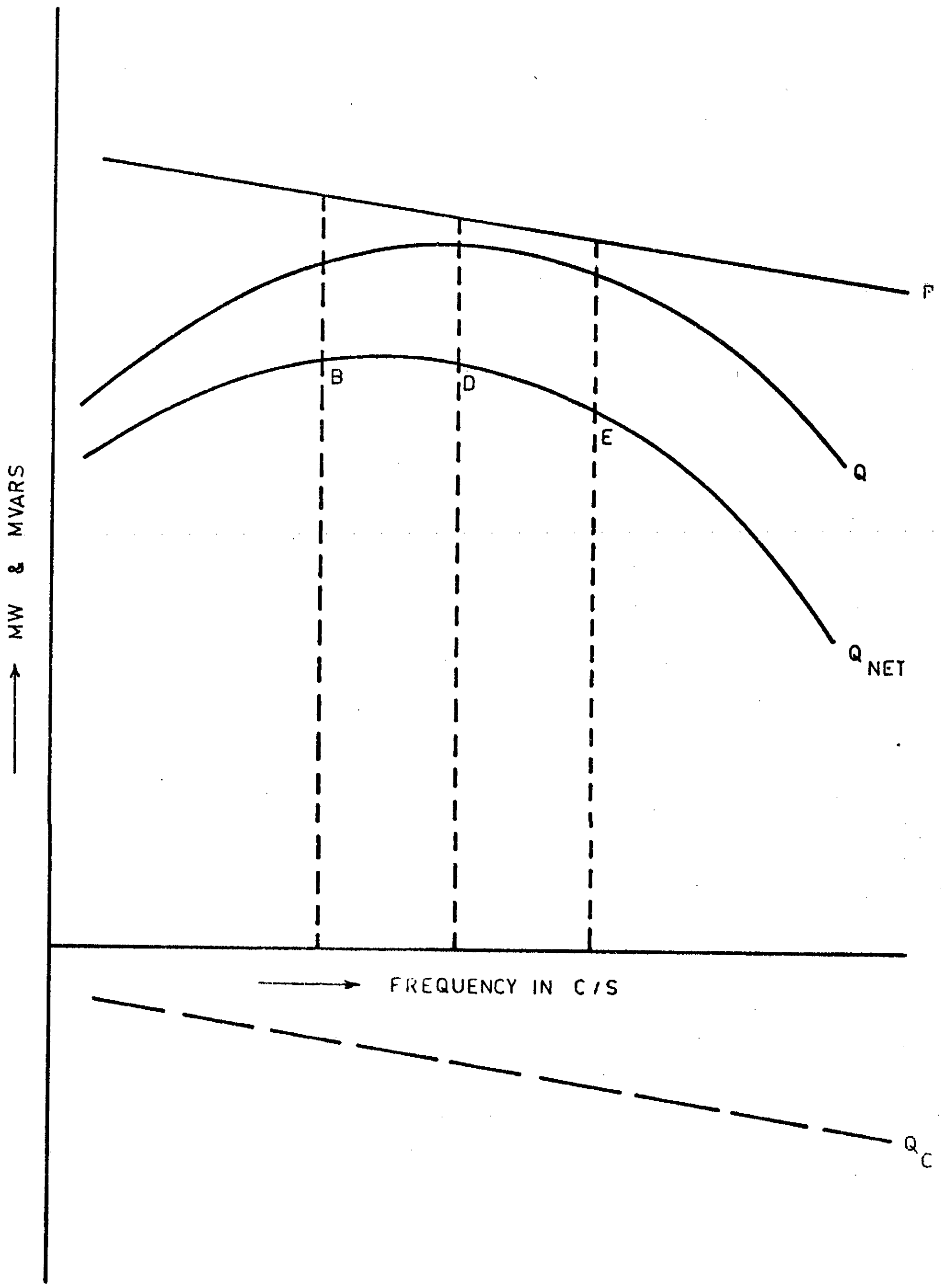

Fig. 5.14(b) Effect of shunt compensation by capacitors for Fig. 5.14(a).

characteristic to lower frequencies. Under these circumstances, the reactive power falls at a greater rate than without compensation, thereby boosting up the busbar voltages, and causing an increase in active power in the system. In this way, the reduction in active power in the original characteristic (without compensation), may be off-set, and may possibly make the change even positive, thus introducing positive damping.

Arc furnaces and electric welders cause violent fluctuations in active and reactive power inputs, and are a root cause of lamp flicker. To counteract such fluctuations, series capacitors are sometimes used[169, 202]. Under these circumstances the nett reactive power characteristic is derived by subtracting capacitive Vars from inductive Vars over a frequency range, as shown in Figure (5.14c). Such compensation affects both active and reactive power characteristics, producing a saddle point in the active power input characteristic at the series resonant frequency, which may occur at the normal system operating frequency (for 100% compensation), or below this, but not above the normal, because the latter would involve over-compensation, which is not usually provided. Active power behaves in almost the same way as before, but its rate of fall is enhanced, whereas the reactive power may change the nature of its behaviour. For example, if the system is operating at A, as shown in Figure (5.14c), the circuit is operating at above its resonant frequency, the active power falls (as the frequency rises due to the synchronous machine acceleration assumed in this discussion), and $\frac{dQ}{df}$ is positive. This causes reduction in system voltages as discussed earlier and introduces negative damping. This situation requires particular attention, because it changes $\frac{dQ}{df}$ from negative (with no compensation) to positive (with compensation), depending on the degree of compensation. Comparing series compensation with shunt compensation, the saddle point of the reactive power characteristic is

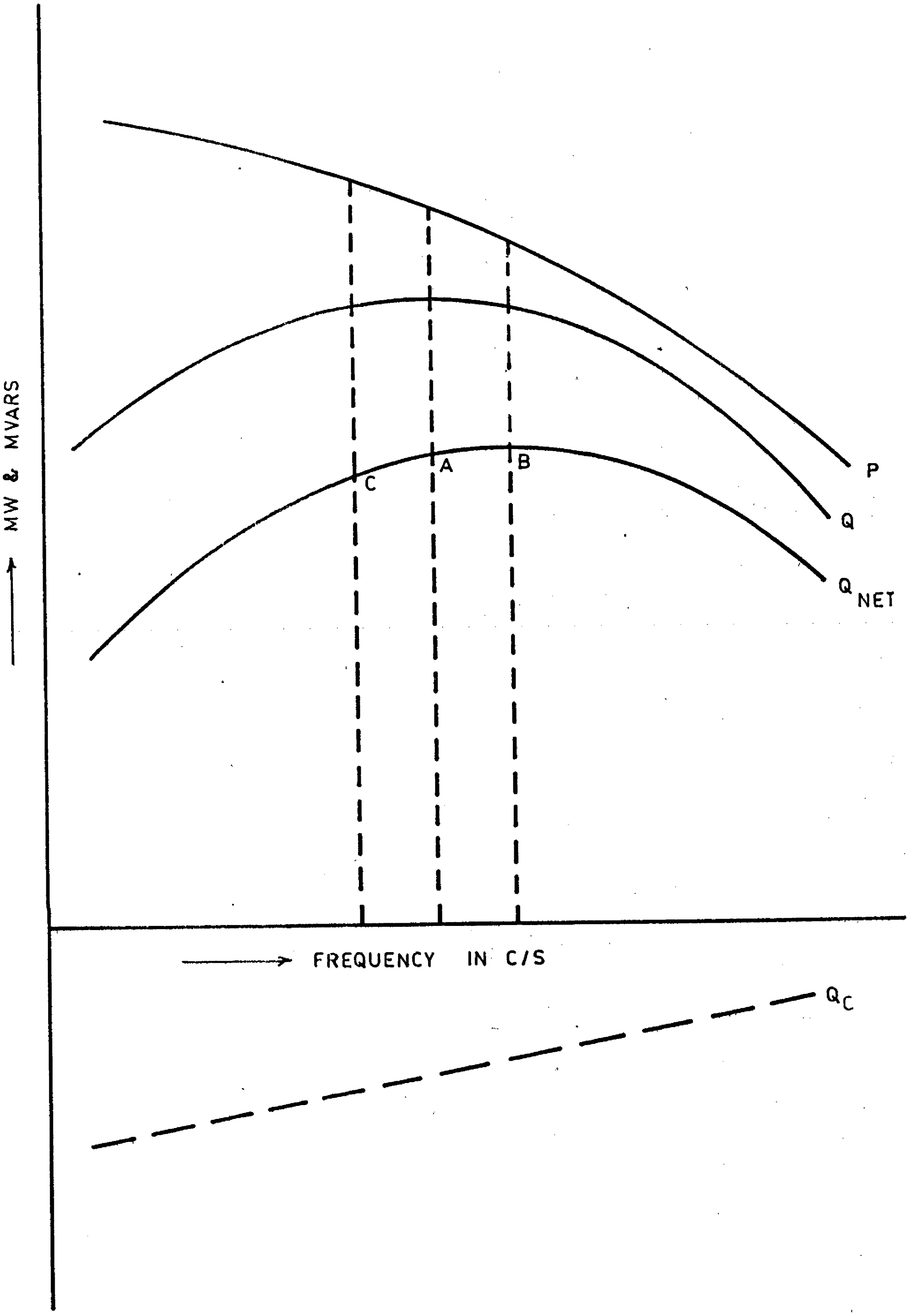

Fig. 5.14(c) Effect of series compensation by capacitors for Fig. 5.14(a).

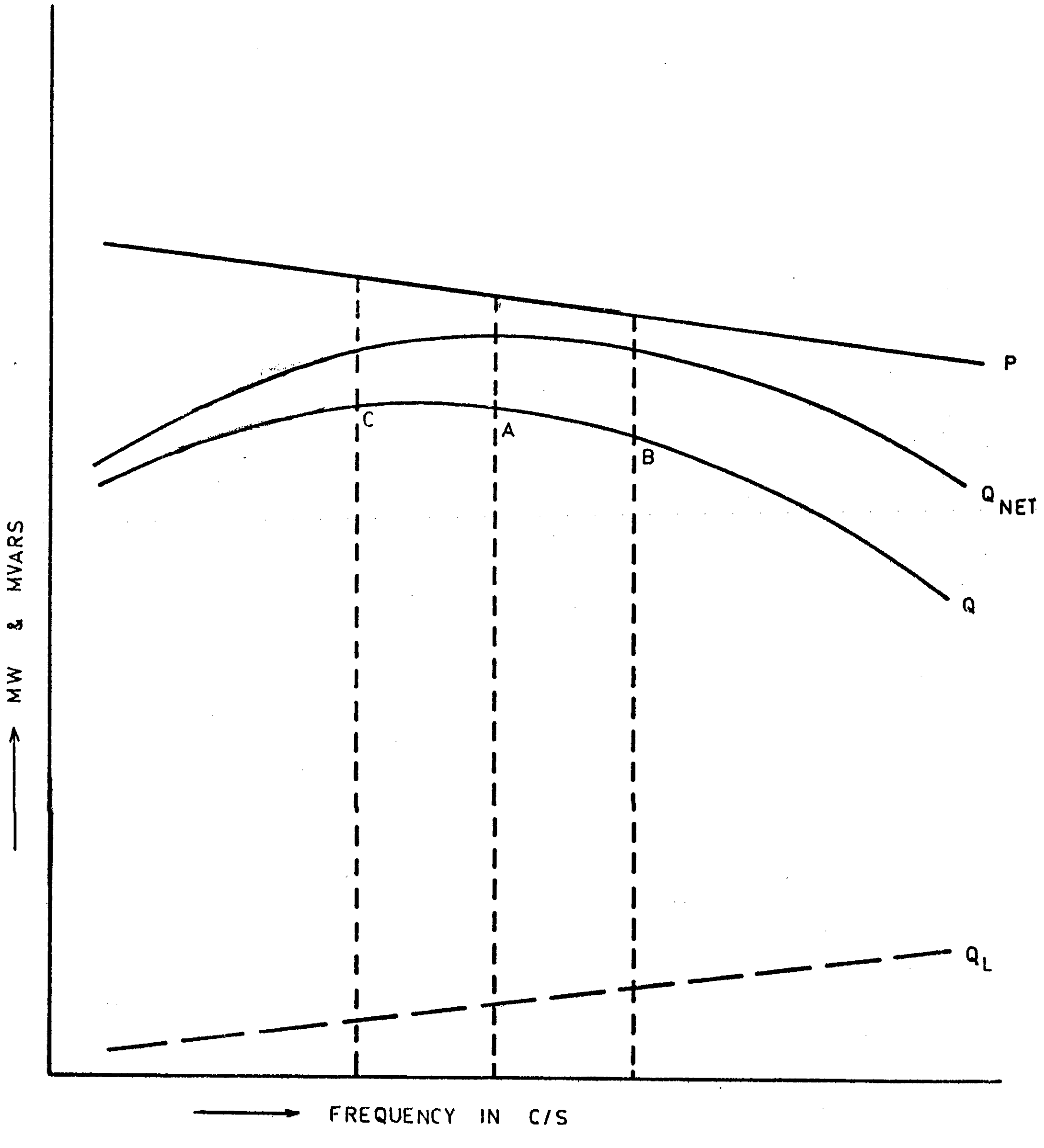

Fig. 5.14(d) Effect of shunt compensation by reactors for Fig. 5.14(a).

shifted towards a higher frequency by the former, and towards a lower frequency by the latter.

In order to maintain good voltage regulation from no-load to full load conditions, the high capacitive reactance effect of long high-voltage transmission lines is overcome by the shunt reactors installed at various points along the length of line. Under these circumstances the nett reactive power load characteristic is derived by adding the inductive Vars consumed by the shunt reactor to the bus load reactive power characteristic, as shown in Figure (5.14d). The saddle point of the reactive power characteristic is shifted towards a higher value of instantaneous frequency and behaves in the same way as in the case of series compensation by capacitors.

In the case where synchronous machines in a power system decelerate under disturbed conditions, that is, the instantaneous operating frequency at the load bus falls; the load characteristics shown in Figures (5.14a-d) will influence the behaviour of the power system synchronous machines as follows:-

In Figure (5.14a), the active power demand rises continuously, whereas the reactive variations depend upon the operating point; for example, if the system is operating at the point B, the reactive power demand falls, thereby improving the system voltages and enhancing the active power demands, producing negative damping; whereas if the system is operating at the point E, the reactive power demand rises, which reduces the system voltages, the active power demand falls and in this way positive damping results.

In Figure (5.14b), the reactive power variations depend upon the degree of shunt compensation and the position of the saddle point. The rapid rate of rise in reactive power introduces positive damping because the active power demand is reduced by reduced available system voltages.

In Figure (5.14c), the active power demand rises with an enhanced rate, which is responsible for negative damping, whereas the reactive power demand depends on the instantaneous operating point. If the system is operating at the point A, there exists negative damping because $\frac{dQ}{df}$ is positive, as explained earlier. The presence of shunt reactors shown in Figure (5.14d) will influence the behaviour of the system in the same manner as discussed with series capacitors in Figure (5.14c).

5.2.2 Frequency-Dependent Treatment of System Static Loads

5.2.2.1 Filament Lamps and Element Heaters

The power input to these loads is substantially independent of operating frequency, but depends upon terminal voltage. Representation by a fixed shunt resistance corresponds to variation of active power as dependent on the square of the instantaneous busbar voltage, which is a sufficiently adequate approximation for practical purposes.

5.2.2.2 Discharge Lamps

Discharge lamps have higher colour temperature, higher luminous flux per watt, and longer life than have filament lamps [172], and accordingly have become increasingly popular [154, 223]. All discharge lamps require a stabilising ballast which may be a resistance, inductance or capacitance, but the most common is the inductive ballast. The ballasts have iron losses which depend upon the instantaneous frequency and flux density. When the voltage is held constant, an increase in instantaneous frequency gives a reduction in magnetic flux density in the iron core; in this way the increase in iron losses due to frequency changes alone is approximately off-set by reduction in iron losses due to flux density changes as in the case of induction motors discussed in Section (5.1.1.3).

Figure (5.15a) shows an equivalent circuit for a discharge lamp.

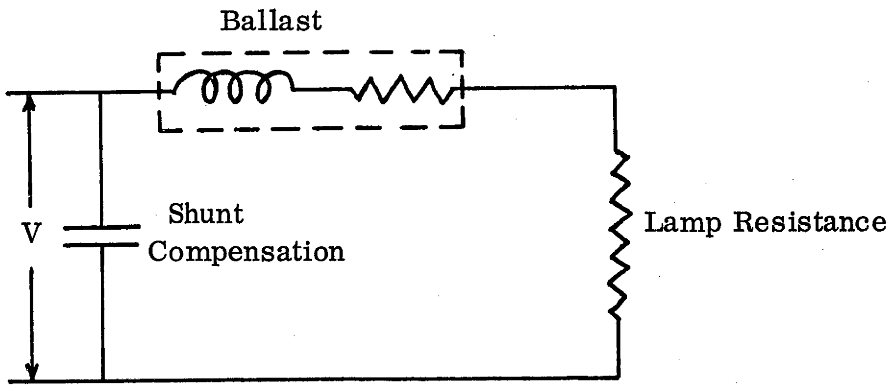

Fig. 5.15(a) Equivalent circuit for a discharge lamp.

The effective resistance of the lamp depends upon the instantaneous current, as explained in Section (5.2.2.4). Figure (5.15b) indicates the active and reactive power inputs versus operating frequency to a typical combination of discharge lamps; the results indicate 1.02% reduction in active power and 1.15% reduction in reactive power when the operating frequency rises by 1% in the absence of shunt compensation. Operating power factor varies from 0.5 to 0.55, consequently shunt capacitors are usually employed to improve these values to between 0.8 to 0.9, either individually or in groups. In the presence of shunt capacitors, the active power remains unaffected, but the rate of fall of reactive power with frequency is increased, as shown in Figure (5.15c).

5.2.2.3 Mercury Arc Rectifiers

In the last decade the mercury arc rectifier has been used

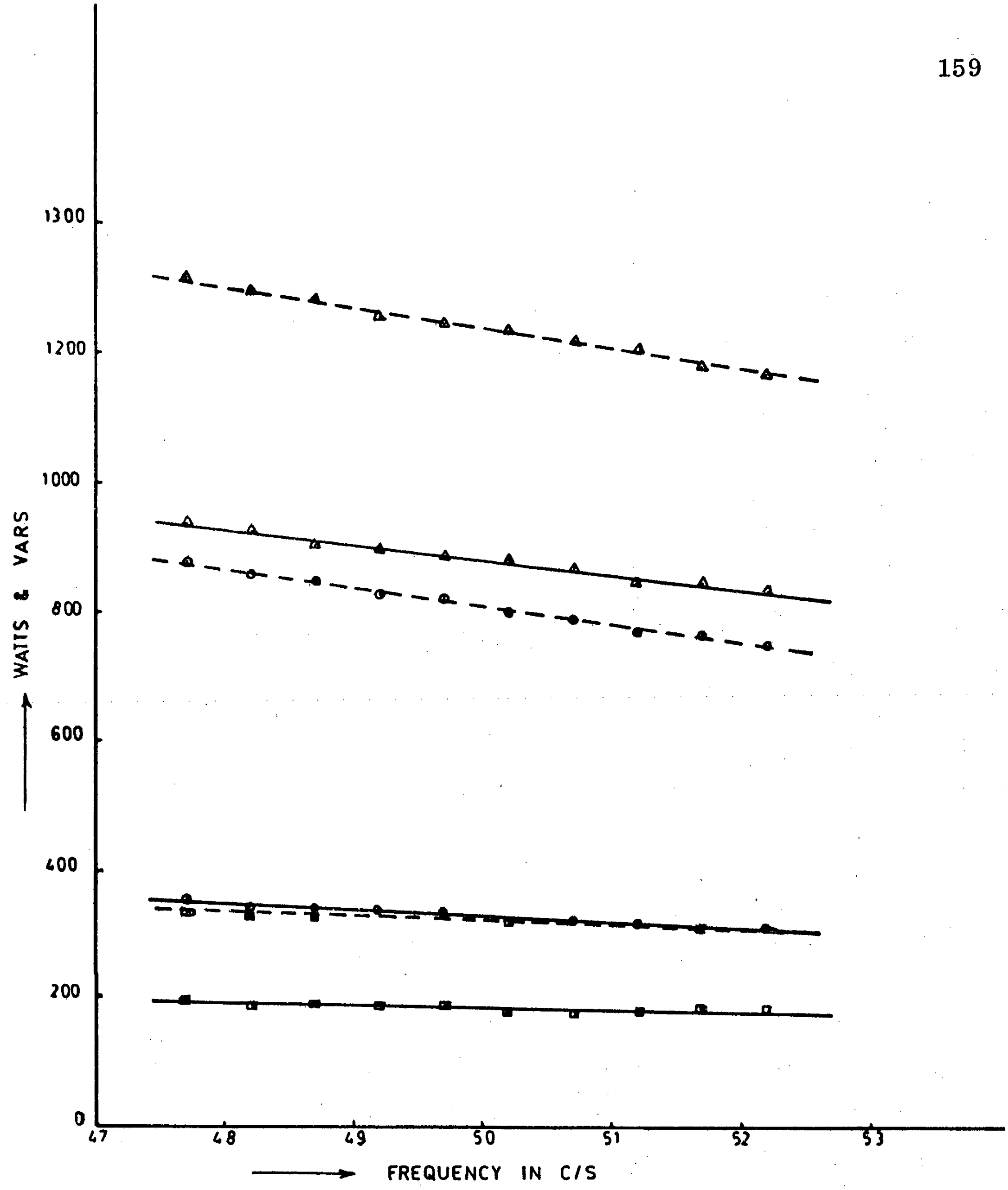

Fig. 5.15(b) Active and reactive power inputs to various discharge lamps as a function of frequency.

——— Active power.
– – – Reactive power.
⊡—Fluorescent lamps (4 - each 40 watts).
⊙—Sodium vapour " (2 - " 125 ").
△—Mercury " " (2 - " 400 ").

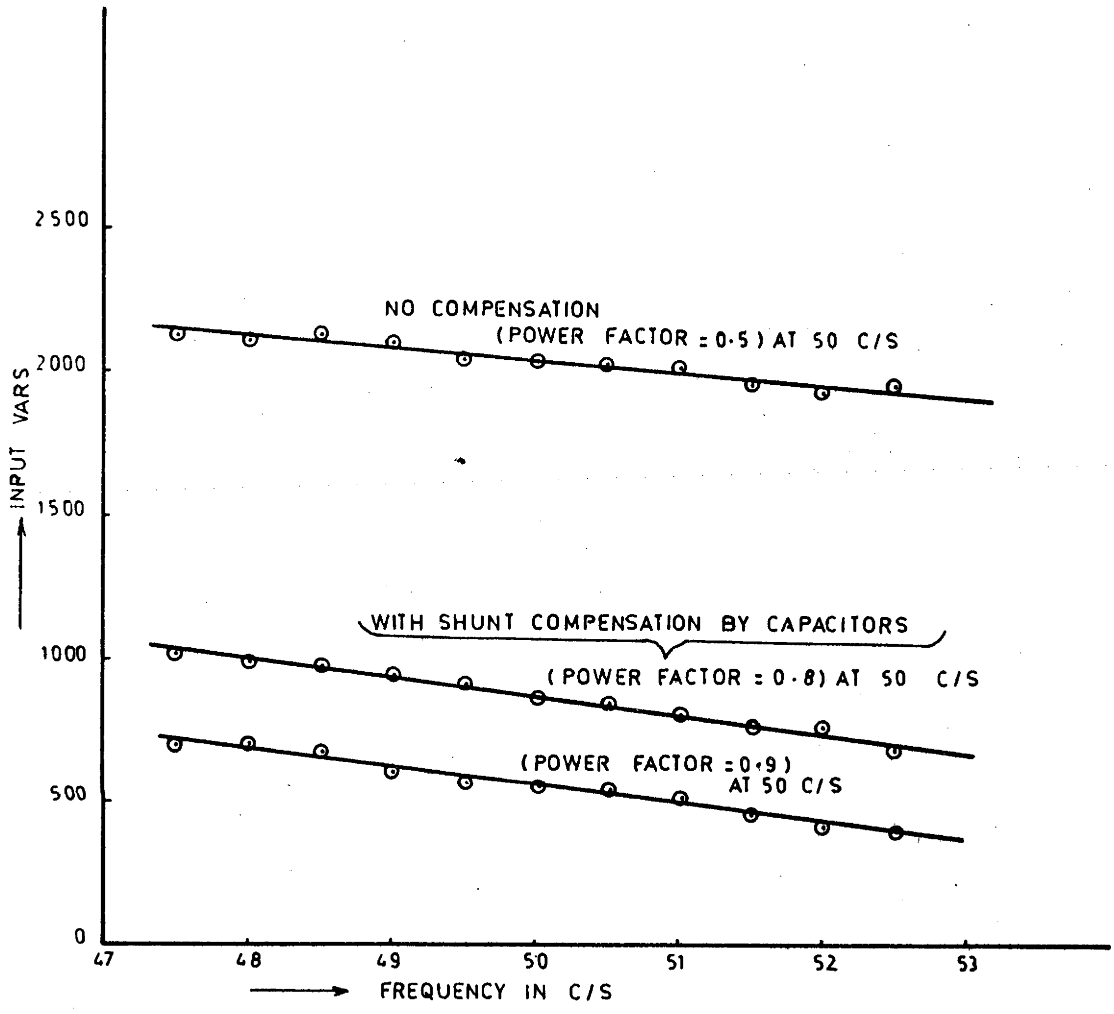

Fig. 5.15(c) Effect of shunt compensation by capacitors for specified power factors for discharge lamps as a function of frequency.

extensively for d.c. transmission links, and in investigating these systems for stability under disturbed conditions, it has been represented in detail[233]. In studies on industrial applications, however, mercury arc rectifiers have been represented simply by shunt impedances independent of frequency : it is necessary here to consider frequency-dependent representation*

Figure (5.16a) indicates an equivalent circuit of a mercury arc rectifier, in which the plasma resistance is a very small part of the total resistance of the circuit, and can be treated as constant. The

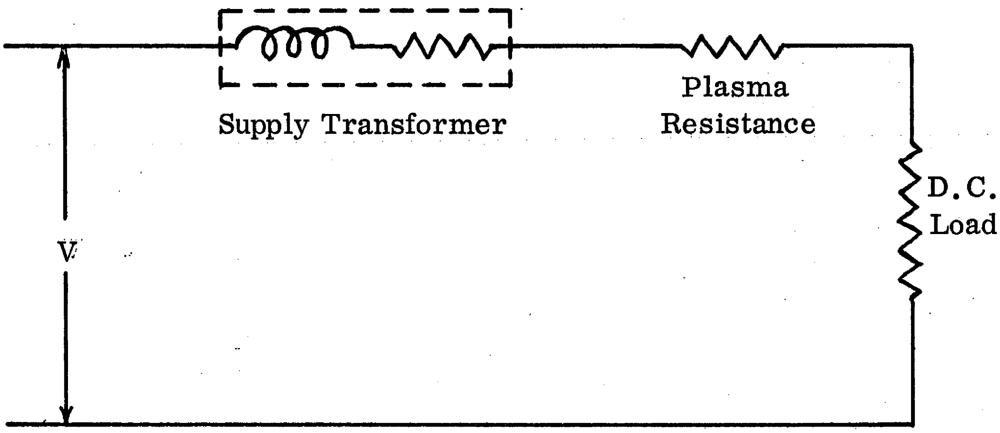

Fig. 5.16(a) Equivalent circuit for a mercury arc rectifier.

inductive reactance is frequency-dependent and its variation with instantaneous frequency will affect the active and reactive power inputs. By controlling the firing angle, the mercury arc rectifier can be operated either for constant voltage output[157] or for constant current output (as in electrochemical processes[109]). Figure (5.16b) indicates active and reactive power inputs to a mercury arc rectifier when supplying a constant d.c. load current. The active power reduction with rise in frequency is small for this constant resistance inductive load, and is of the order of 0.5% for 1% increase in

* Mercury arc rectifier applications are assuming less importance (except for high voltage D. C. transmission links), because of increasing use of semiconductor devices.

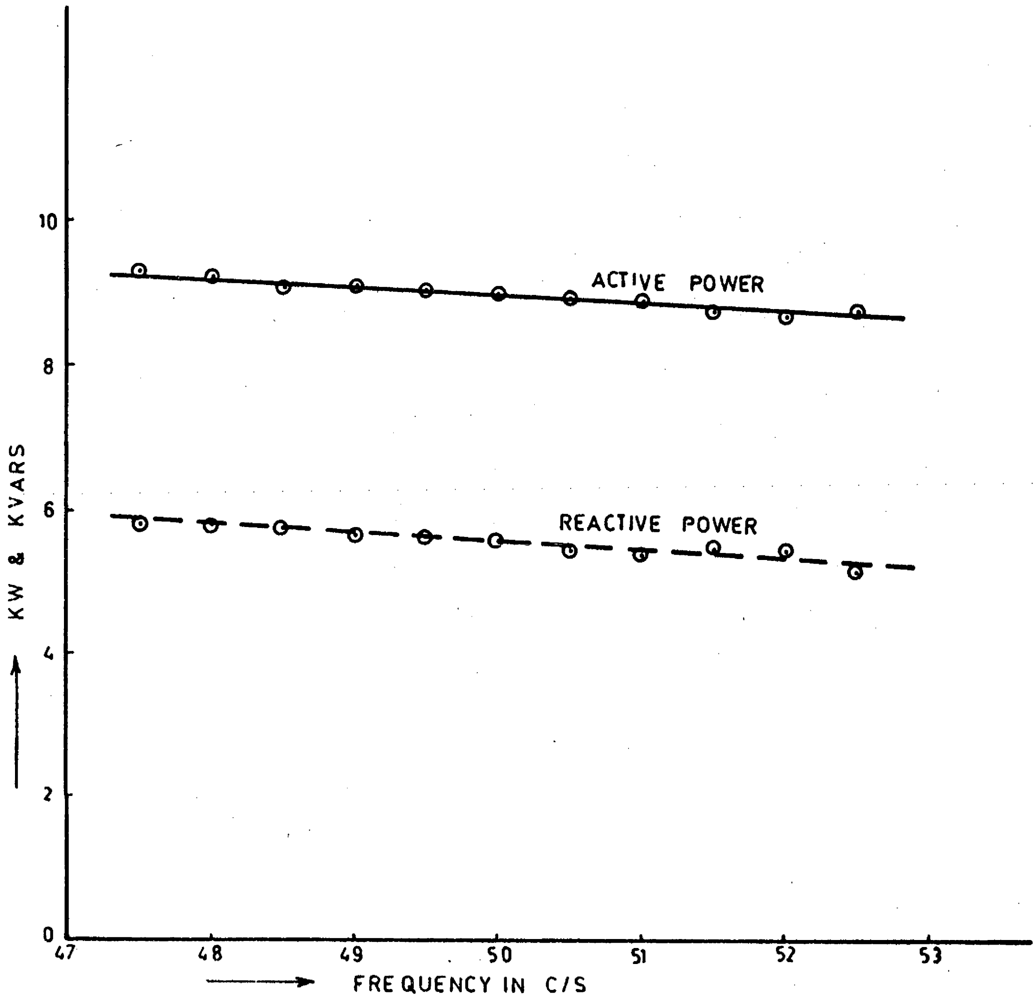

Fig. 5. 16(b) Active and reactive inputs to a 10 KW mercury arc rectifier (when supplying 20 amps. d.c.) as a function of frequency.

frequency, as shown in equation (10.54) of Appendix (10.10); reactive power reduction is 1% for 1% increase in frequency.

5.2.2.4 Arc Furnaces

The arc has a falling volt-ampere characteristic as shown in Figure (5.17a) and is consequently unsuitable for a constant voltage supply. For satisfactory operation, a stabilising series resistance or reactance is essential, and in general, transformers with high leakage reactance, usually supplemented by series reactors, are employed[172]. Long electric arcs in air have also been observed with slightly rising volt-ampere characteristic[152], but usually the characteristic is falling[172]. The total reactance in the circuit depends upon the instantaneous frequency.

Figure (5.17b) indicates an equivalent circuit for an arc furnace. The arc resistance is current-dependent and falls when the current rises, resulting in a reduced arc voltage, as shown in Figure (5.17a). Considering the voltage drop across the total effective resistance of the circuit (A to B), the fall in arc voltage is approximately compensated by the voltage drops due to the impedances of the main transformer, buffer reactor, furnace transformer, leads and electrodes.

In this way the voltage drop across the effective resistance of the circuit becomes approximately constant, indicating $R \propto \frac{1}{I}$, and the input active power is directly proportional to the furnace current. From the characteristics of arc furnaces plotted in Reference 109 (page 227), and in Reference 182, it is observed that the total input active power to an arc furnace is directly proportional to the arc current over the working range.

An arc furnace load varies violently during the whole of its operation except during refining. The violent change in active and reactive power drawn from a power system causes violent voltage fluctuations and

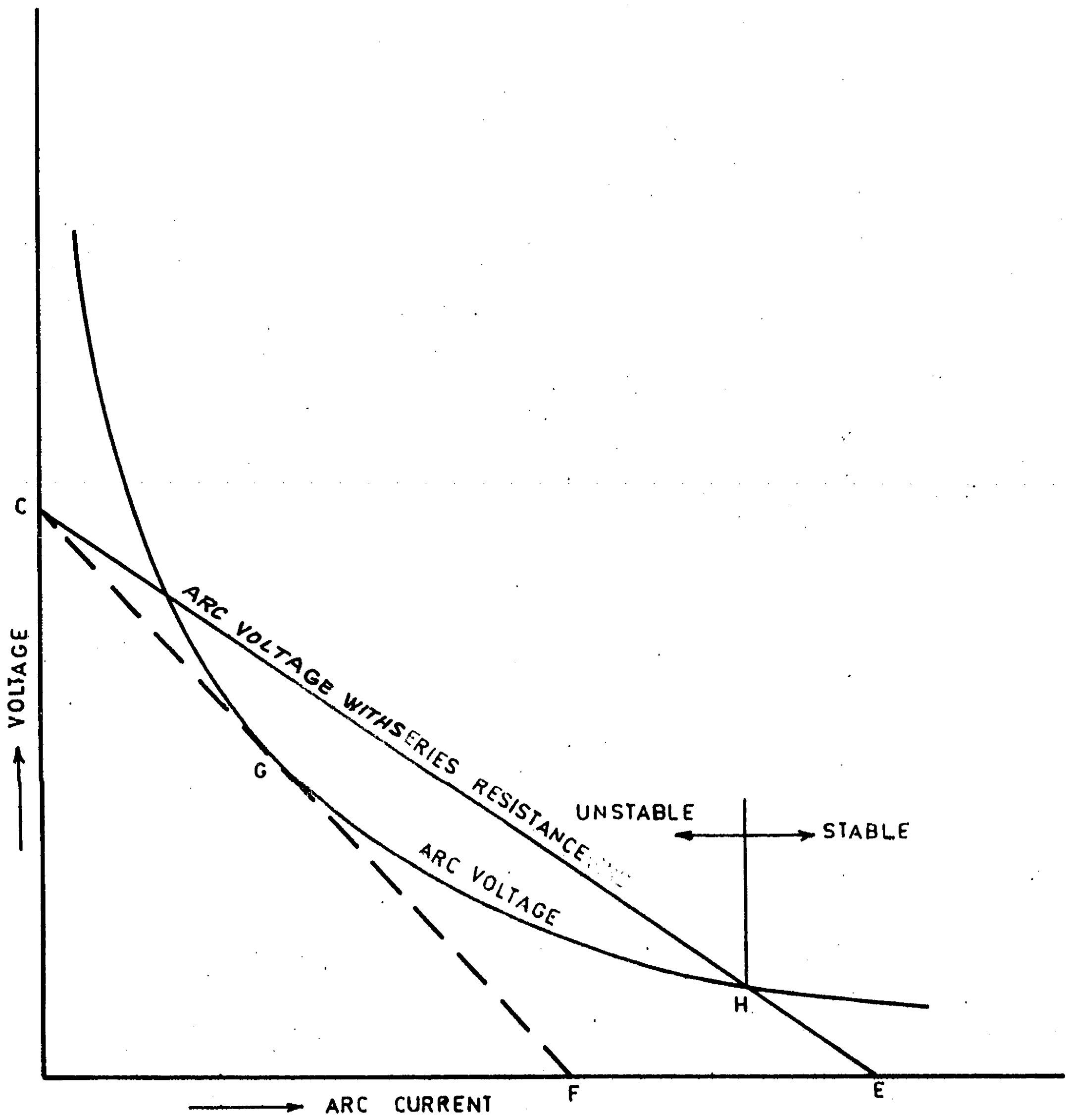

Fig. 5.17(a) Volt-amp. characteristic of an arc in air.

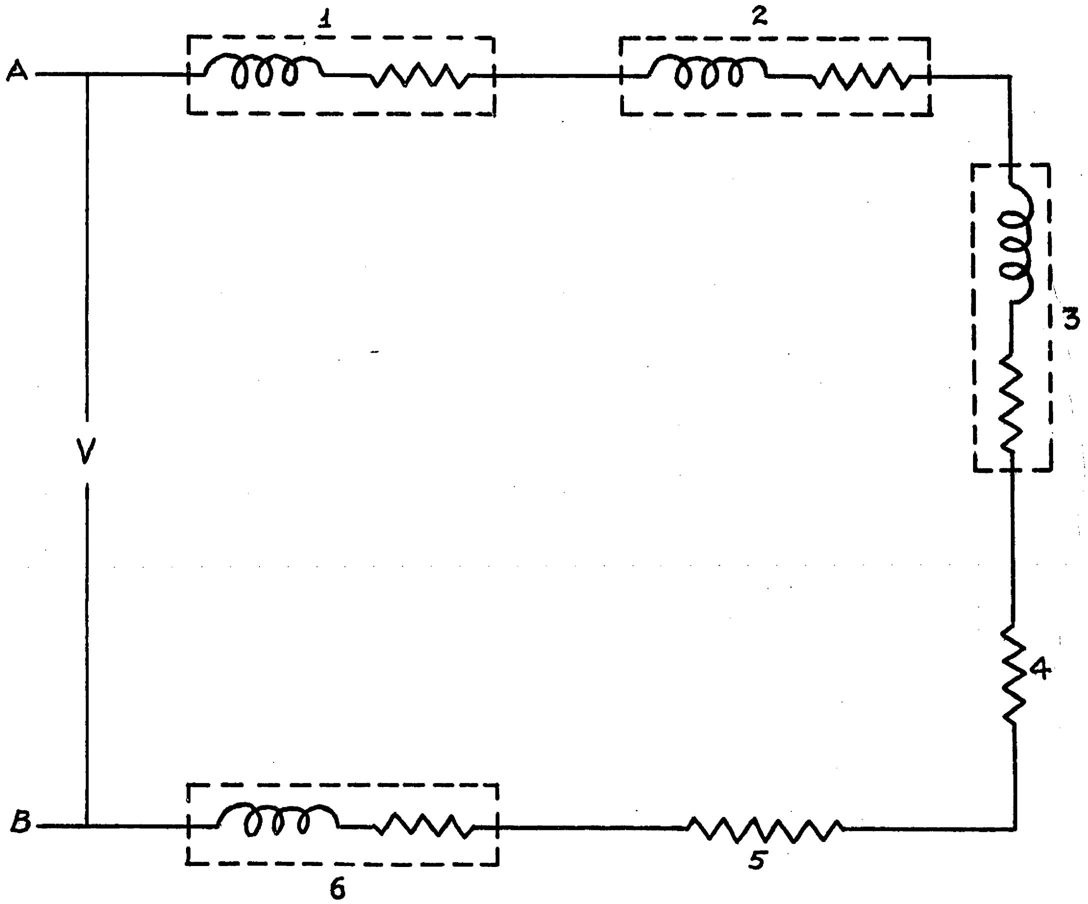

Fig. 5.17(b) Equivalent circuit for an Arc Furnace

1— Main transformer
2— Buffer reactor
3— Furnace transformer
4— Electrode resistance
5— Arc resistance
6— Furnace leads

results in lamp flicker. In order to investigate the effects of arc furnaces in a power system, a comprehensive survey of arc furnace installations was carried out by an AIEE sub-committee[169] with the object of reducing objectionable lamp flicker. The corrective equipment suggested was the use of buffer reactors[167] and synchronous condensers[168], and later, series capacitors (for reduction of synchronous condenser size[202]). The inclusion of buffer reactors is simple and cheap[167, 168], but affects the overall power factors. Due to the inductive reactance being frequency-dependent, the input active and reactive power is inversely proportional to the instantaneous frequency as shown by equations (10.51) and (10.53) of Appendix (10.9). Figure (5.17c) indicates active and reactive power inputs to a 45-ton arc furnace with and without buffer reactor. The synchronous condenser, if installed[168], will provide the entire reactive power for the arc furnace at full load and roughly 50% of that absorbed in the buffer reactor. In this situation, the synchronous condensers should be treated dynamically for stability studies of the power system as a whole.

5.2.2.5 Electric Welders

For both arc welding and resistance welding, the electrodes are supplied by special high leakage reactance transformers, and usually operate at 0.2 to 0.3 power factor[109]. In this case, the power drawn by a welder will be either full on or full off, and this causes violent fluctuations in active and reactive power inputs and causes lamp flicker; for this purpose, series capacitors are used, due to their instantaneous response[202]. The presence of series capacitors in welder circuits aggravates the variations in active and reactive power inputs when the instantaneous operating frequency changes. Figure (5.18) indicates the active and reactive power inputs to a 200 KVA welder with series capacitors.

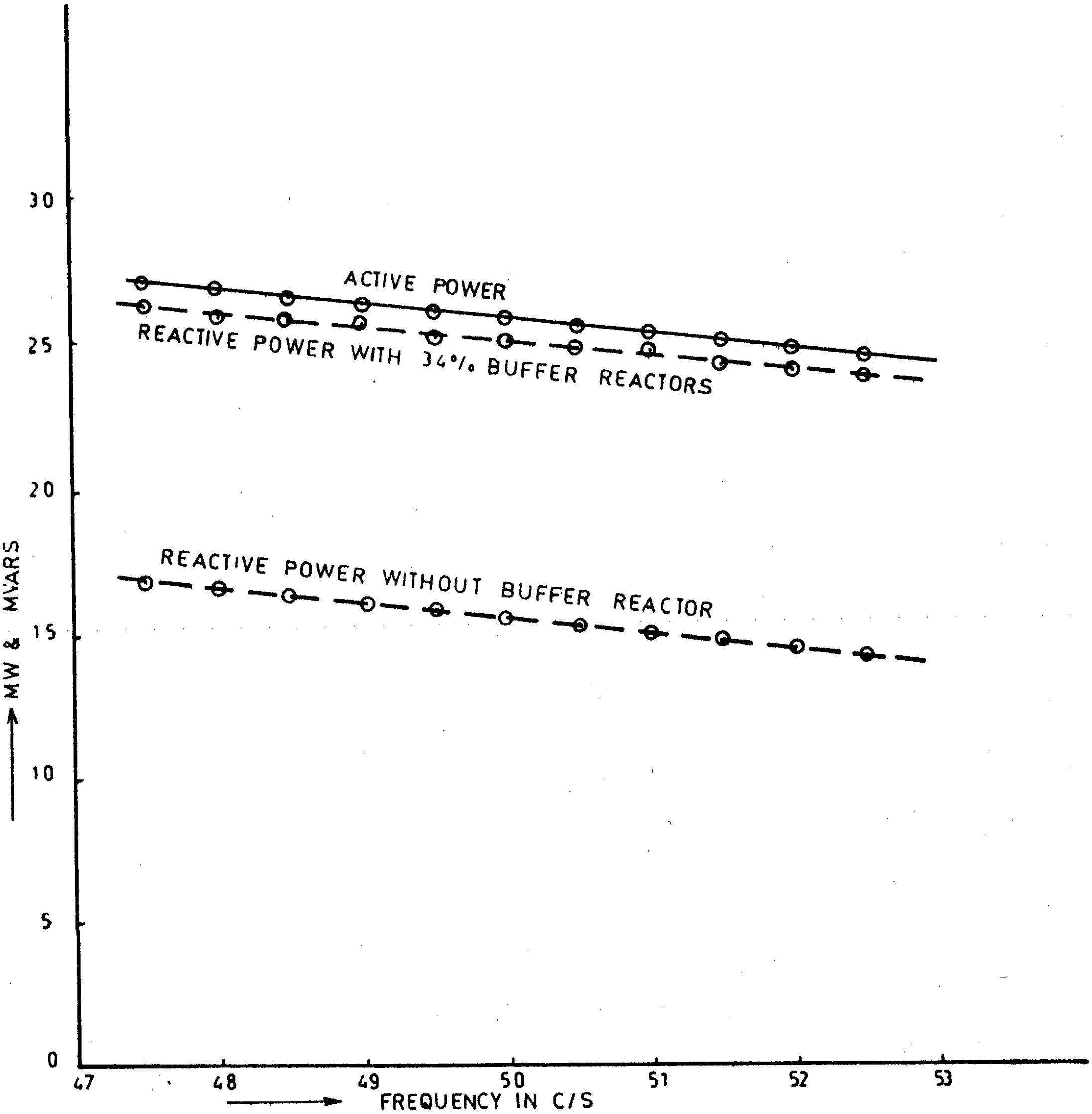

Fig. 5.17(c) Active and reactive power inputs to an arc furnace as a function of frequency.

Furnace transformer rating= 30MVA

$X_{furnace}$ = 50% at 50 c/s.

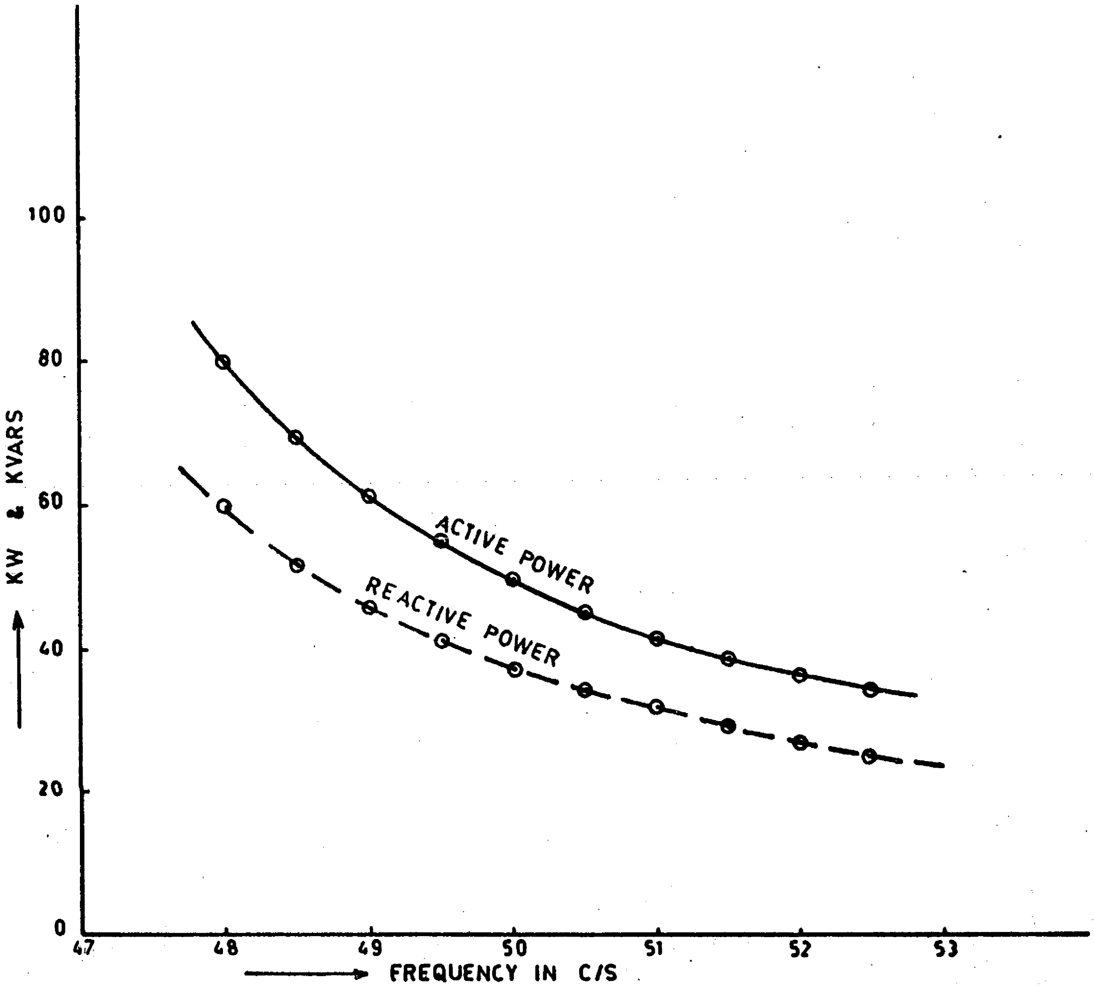

Fig. 5.18 Active and reactive power inputs to a 200 KVA electric welder with series compensation (for 0.8 power factor lagging) as a function of frequency.

5.2.3 Representation of Frequency-Dependent Static Loads

Static loads met in practice can be represented by an equivalent circuit, such as by resistance and inductance in series; inductive reactance varies directly with instantaneous frequency, and the effective resistance of the equivalent circuit may be current-dependent, or independent. As shown in the Appendices (10. 9) and (10. 10), equations (10. 51) and (10. 54), the active power input to an inductive circuit in which the effective resistance is current-dependent or constant, falls when the instantaneous frequency rises, and the reactive power input varies inversely with frequency when the effective resistance is current-dependent, equation (10. 53). Also from Appendix (10.10), the reactive power characteristic of an inductive circuit in which the effective resistance is constant, has a saddle point when the operating power factor is 0.707 lagging : that is, the reactive power is maximum at this power factor. At power factors above 0.707, $\frac{dQ}{df}$ is positive, and below this, $\frac{dQ}{df}$ is negative.

5.2.4 Application to Stability Problems

The factors discussed above may be important in assessing power system stability. Necessarily, information is required on the composition and type of power system loads, and this will normally be available in each case. For stability studies, each system load can be divided with the aid of a load survey into four components:-

(a) Mercury arc rectifiers.

(b) Resistance loads.

(c) Induction motor loads.

(d) Lighting loads, arc furnaces and electric welders.

Mercury arc rectifiers used for electrochemical purposes can be adequately represented by constant current sinks as far as the bus voltage is concerned, and by constant resistance inductive circuits for frequency-dependent considerations, otherwise they can be treated in more detail[233].

The resistance load can be represented by fixed shunt conductance, whereas the induction motor loads can be handled dynamically and frequency-dependently as presented in Section (5.1)* or by lumped impedances.

From Sections (5.2.2.2) and (5.2.2.4) it is observed that the effective instantaneous resistance of discharge lamp loads and arc furnace loads varies inversely with the instantaneous value of current. Such loads are predominantly affected by voltage, in particular for reactive power demands as shown in Figure (5.19).

The usual operating power factor for discharge lamp loads is 0.5 to 0.55 lagging. In the case where the bus voltage falls to 50% or below under disturbed conditions, the inductive part of the load will disappear, leaving only the capacitive part (the usual shunt compensation). Similarly, arc furnace loads, which normally operate at 0.707 to 0.9 power factor, will turn off if the bus voltage falls to 75% or below, due to inadequate voltage available to maintain the arc.

Lighting loads consist mainly of discharge lamps, as pointed out earlier in Section (5.2.2.2). The discharge lamp loads and arc furnace loads need special attention in stability studies because of possible inadequate voltage becoming available to them during the disturbance. They can be represented by an inductive circuit having current-dependent resistance and instantaneous frequency-dependent reactance.

---

* The underlying assumptions regarding the tripping by protective relays of induction motor loads, have been explained on pages 137 & 244.

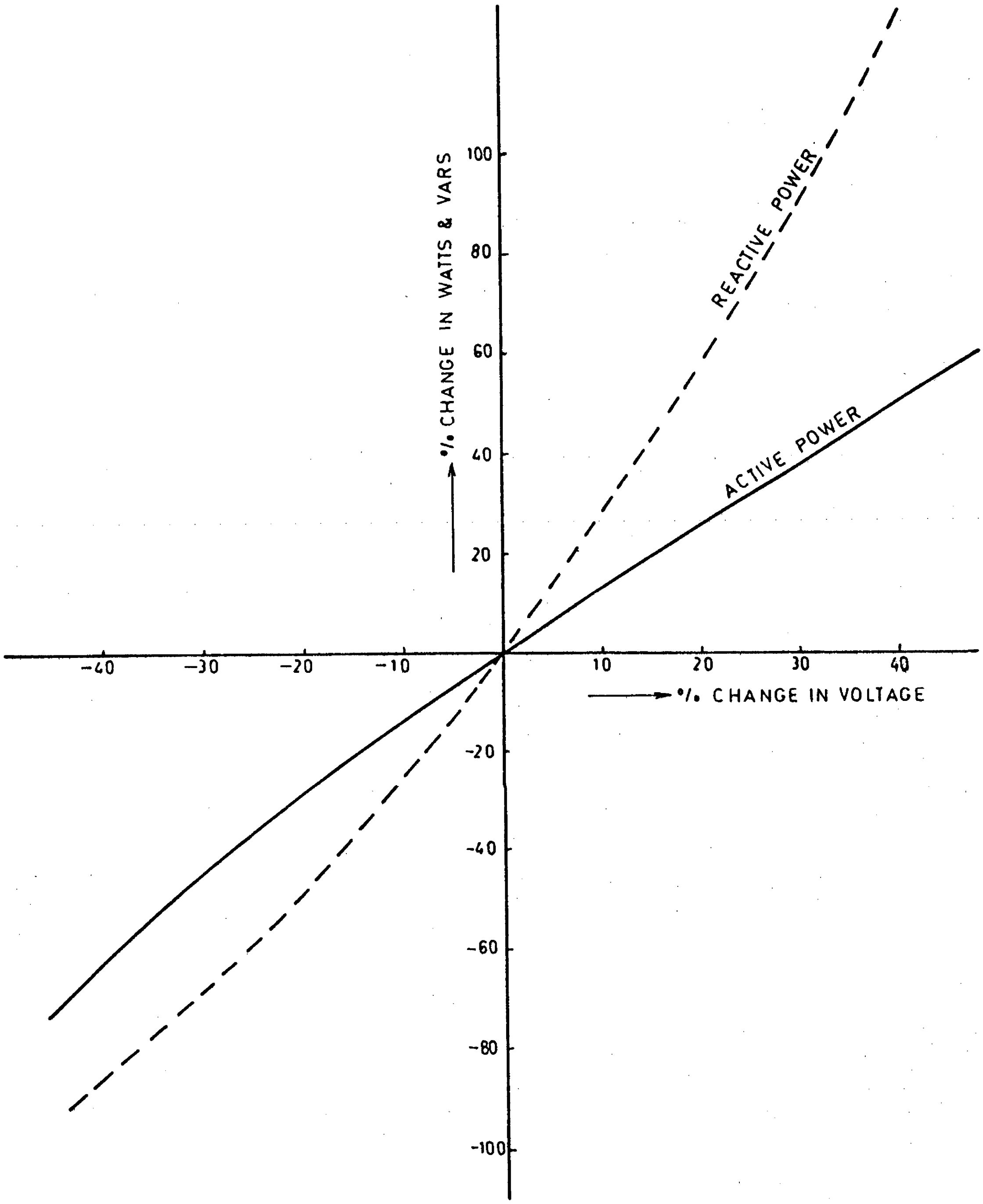

Fig. 5.19 Active and reactive power inputs to a circuit with current-dependent effective resistance as a function of terminal voltage.

5.2.4.1 Procedure for Stability Studies

Using a digital computer, the following approach may be used:-

(a) Obtain an overall load balance under steady state conditions, in conventional form[195].

(b) Calculate the effective resistance, inductive reactance and the current for current-dependent resistance loads.

(c) Apply the disturbance.

(d) Calculate the various bus voltages of interest.

(e) Modify the inductive reactance of the network for the bus voltage instantaneous frequencies.

(f) Determine the instantaneous current for the current-dependent resistance loads.

(g) Modify the instantaneous effective resistance of each static load circuit as,

$$R = R_{initial} \times \frac{\text{Initial current}}{\text{Instantaneous current}}$$

(h) Test for convergence, that is, the difference in resistance R for two successive iterations, should be within a predetermined index, say 1 part in 10^6; if the test is not satisfied return to step (f) and repeat.

(i) Determine the instantaneous active and reactive power and corresponding shunt admittance on the basis of instantaneous bus voltage.

(j) Determine the driving point and transfer admittances for the various synchronous machines.

(k) Calculate the instantaneous angular position of the synchronous machines by solving their differential equations, for the time interval "Δt" (which is usually 0.05 sec.).

(ℓ) Calculate the instantaneous load bus voltages and phase angles.

(m) Calculate the instantaneous frequency at each load bus and modify it by an accelerating factor as,

$$f_j^i = f_j^{i-1} + (f_j^i - f_j^{i-1}) \text{ x accelerating factor}$$

(If an accelerating factor of 1.35 is used, convergence normally occurs within 10 iterations).

(n) Test for convergence for the power angles of the various synchronous machines to be such that the difference in their values in two successive iterations is within, say 10^{-3} degrees, and the instantaneous load bus voltage and frequency differences for successive values is within say 1 part in 10^6. If the test is not satisfied, return to step (e) and repeat.

(o) Write the final angular positions of the various synchronous machines.

The method outlined above proceeds towards a solution iteratively.

5.2.4.2 Illustrative Problem Including Static Loads

In order to highlight the influence of such passive frequency-dependent and voltage-dependent loads, a four-machine problem[195], the line diagram and circuit parameters* of which are given in Figure (5.20a) and Table I, is worked out. In this problem, a passive frequency-dependent load is included at bus no. 7 as a part of the existing 68 MW total load, while representing the remaining system at system nominal frequency. Figure (5.20b) shows the swing curves for all four synchronous machines assessed by conventional digital computer programs (used for example in Ref. 162), modified as indicated above to take account of the frequency effects. The following cases have been plotted in Figures (5.20b and c):-

(i) Considering the 68 MW load as constant shunt impedance independent of instantaneous frequency.

(ii) With 15% of the 68 MW (that is 10.2 MW), treated as current-dependent and frequency-dependent load.

(iii) With 40% of 68 MW (that is 27.2 MW) treated as in (ii).

It will be observed from Figures (5.20b and c) that the system is assessed as stable in case (ii), but with less margin of stability than case (i); case (iii) is unstable.

The reason for a reduced margin of stability is due to reduced bus voltage available for the load at bus no. 7 under fault conditions, and after the fault, as shown in Figure (5.20d). It is noteworthy that a system which can appear to be stable when neglecting the frequency-dependence of loads in the assessment, may be unstable when frequency-dependence is taken into account. In the above instance when the total "passive" load is 25% of the total at bus no. 7, the system verges to instability when frequency-dependence is taken into account, but will tolerate an additional load of approximately 10 MW (at bus no. 7) before instability is apparently reached when frequency-dependence is neglected.

* The configuration and parameters are identical with a problem as taken from Ref. 195, as these illustrate the effects required adequately.

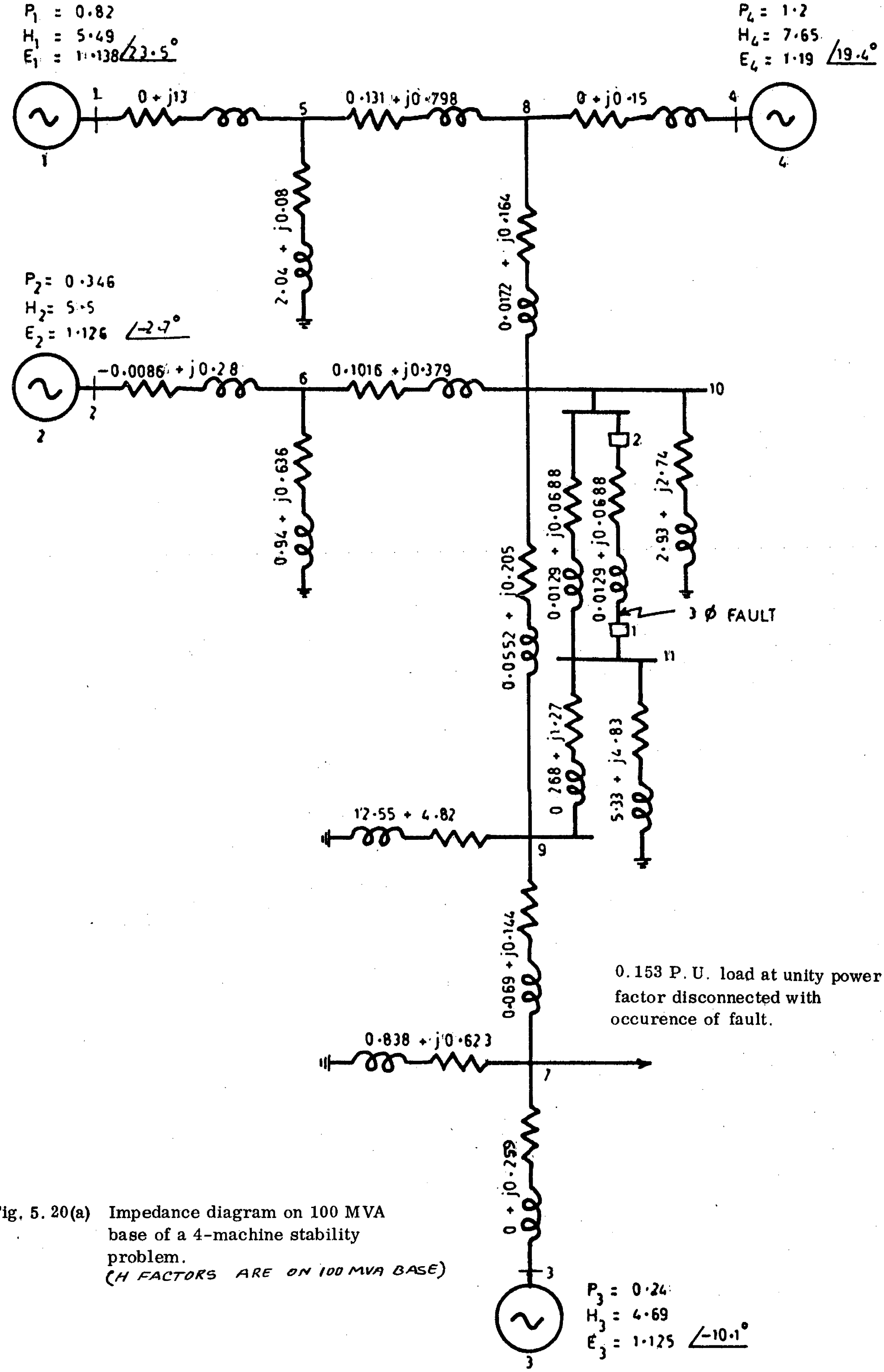

Fig. 5. 20(a) Impedance diagram on 100 MVA base of a 4-machine stability problem.
(H FACTORS ARE ON 100 MVA BASE)

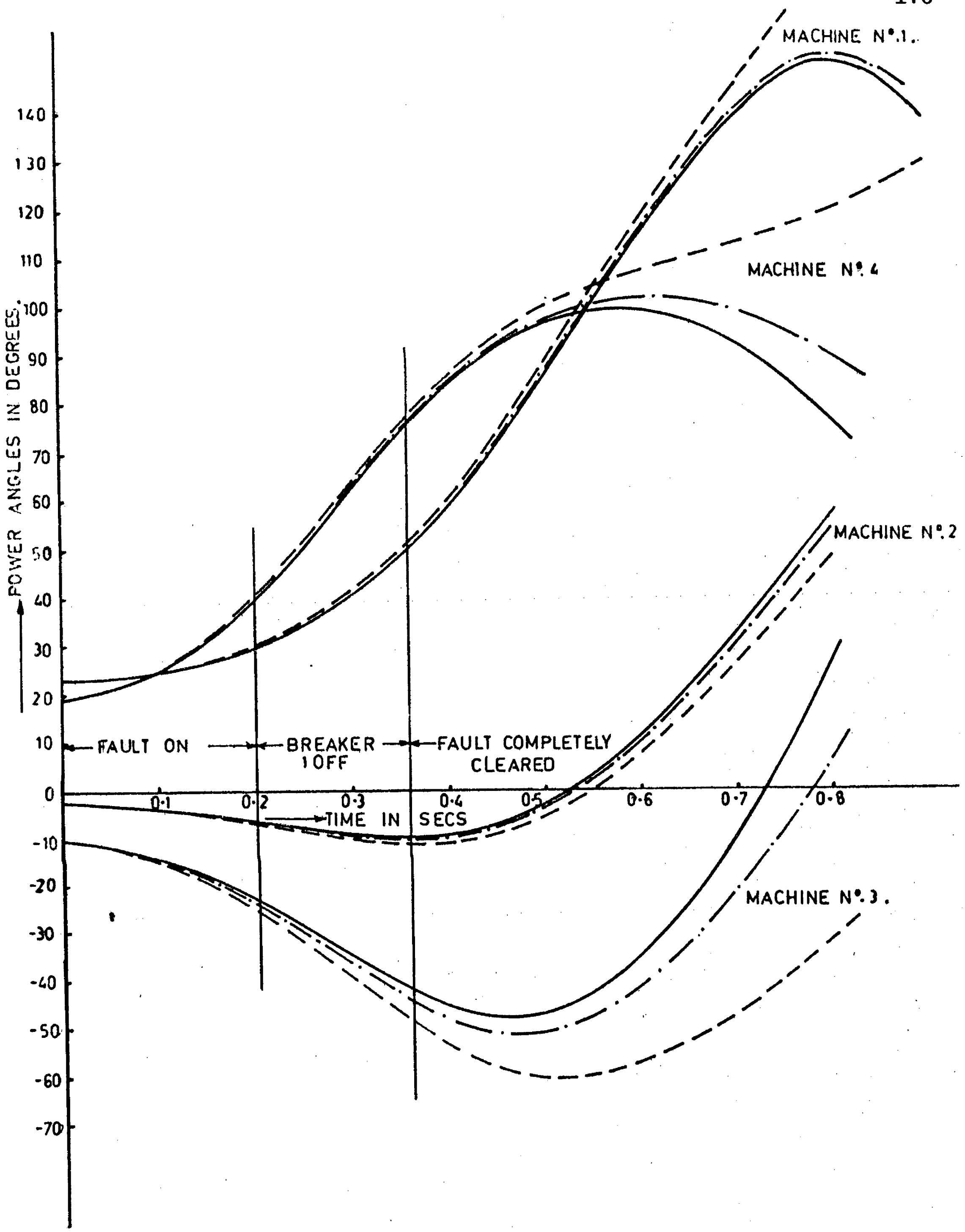

Fig. 5.20(b) Swing curves for Fig. 5.20(a).

——————— With loads independent of frequency.
—·—·— " 15% at bus no. 7 frequency-dependent load.
— — — — " 40% " " " " " "

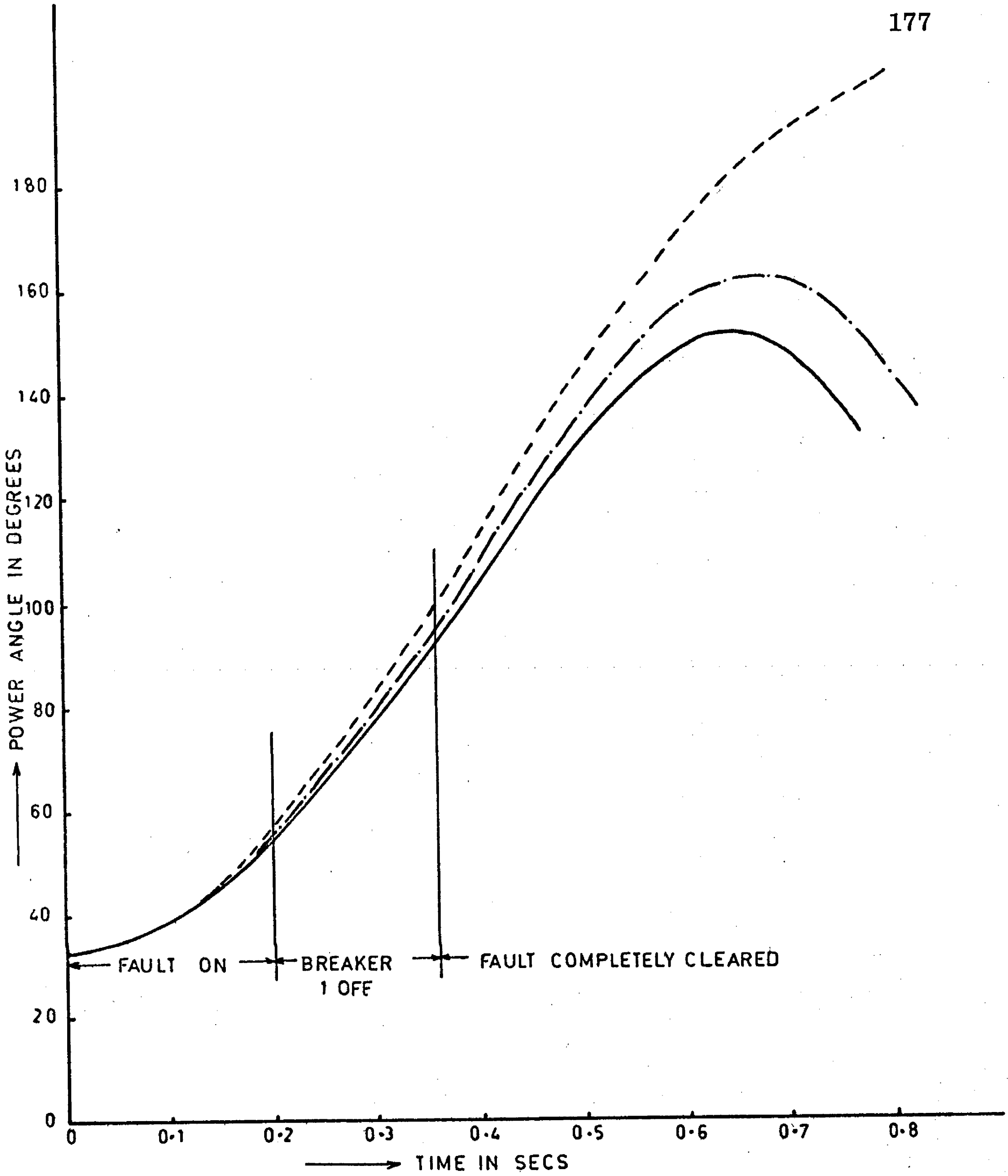

Fig. 5.20(c) Relative swing curve for machine no. 1 with respect to machine no. 3.

———————	With loads independent of frequency.
—·—·—	" 15% at bus no. 7 frequency-dependent load.
— — — —	" 40% " " " " " "

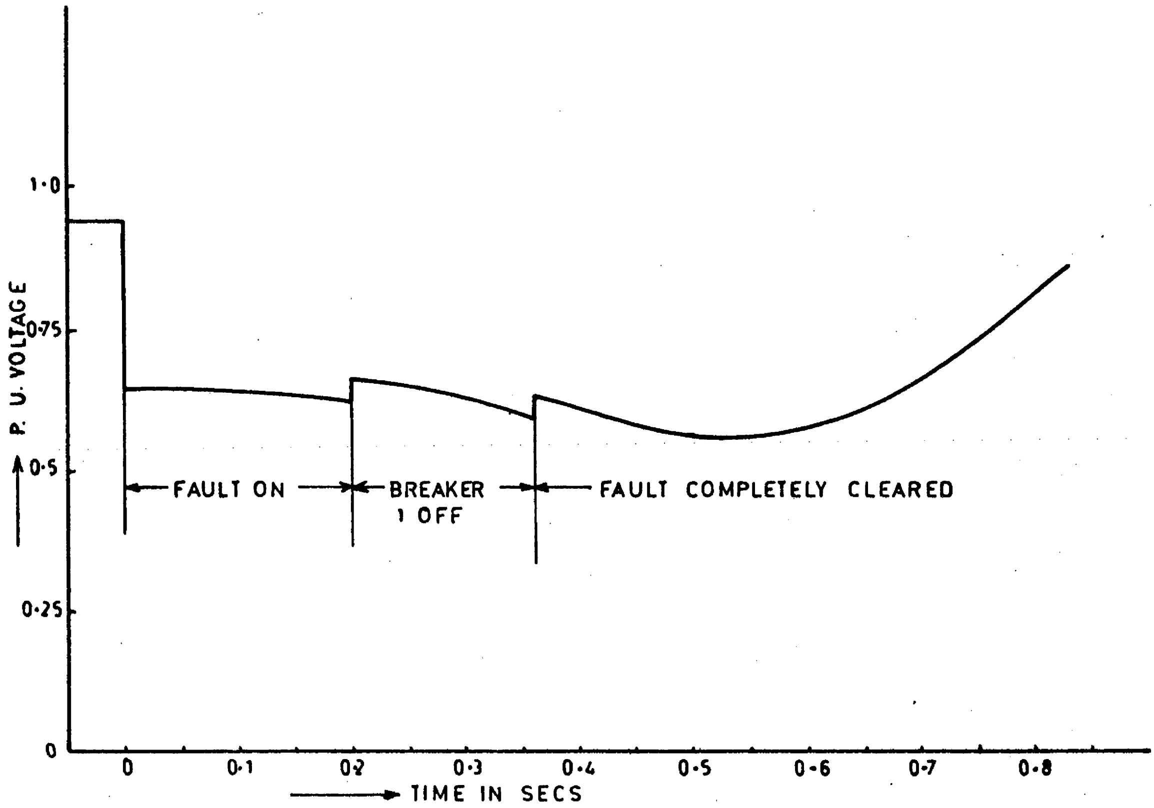

Fig. 5.20(d) Terminal voltage at bus no. 7.

5.3 Discussion

5.3.1 Influence of Dynamic Loads

Induction motor loads are affected more by instantaneous operating frequency than by operating voltage[119, 156], for their active power demands, because they adjust their working slips according to the available voltage and the mechanical load characteristics, thus drawing approximately the same active power for a constant mechanical output power. The four-machine problem worked out in Section (5.1.2.2) to illustrate the influence of system dynamic loads, indicates negative damping due to such loads, and there is a reduction in the transient stability margin. The main reason for the reduced margin of stability is the presence of reduced voltage soon after the fault and after its clearance. This reduction in voltage is aggravated by the induction motor load at bus no. 7, as shown in Figure (5.13d), because due to reduced terminal voltage, the induction motor load (at bus 7) exerts extra load *, so promoting deceleration of machine no. 3, and reducing the margin of stability. In a case where machine no. 3 accelerates, the induction motor load will exert positive damping, thereby increasing the stability margin or the permitted fault clearance time.

5.3.2. Effect of Static Loads

Static loads have previously been reported to be more influenced by terminal voltage than by the operating frequency[129], but in fact these loads are frequency-dependent as well as voltage-dependent as shown in Section (5.2.2), by the experimental results. The representation

---

* The term "extra load" signifies the difference in active power demand of the load at bus no. 7 with passive representation and when represented dynamically and frequency-dependently.

of arc-furnaces and discharge lamps by current-dependent effective resistances, reveals that the active power demand will be directly proportional to the circuit current, which is confirmed from the operating characteristics of such loads in References (172 and 182). During disturbances, such static loads offer extra load* due to the reduced available voltage. For example, in Section (5.2.4.2), in the transient stability study problem, the static load at bus no. 7 offers extra load due to reduced available voltage during the fault, and after the clearance of the fault : this has resulted in reduction in stability margin.

In the example, the extra load applied by the static loads has promoted deceleration of machine no. 3. However, if machine no. 3 happened to be accelerating, then these loads would exert positive damping, resulting in increase in stability margin.

Certain static loads require special attention. For example, arc loads may extinguish suddenly due to insufficient voltage to maintain the arcs, thereby relieving the system of load. This may create further problems in the system as apart from the active load components being suddenly removed, the transformer remaining in the circuit will present a mainly reactive power demand (although this will be only relatively small).

---

* The term "extra load" signifies the difference in active power demand with passive representation (in which case, the active power is directly proportional to the square of the voltage), and with current-dependent resistance and frequency-dependent inductive reactance (in which the active power demand is directly proportional to the terminal voltage).

6. COMPREHENSIVE TRANSIENT STABILITY STUDIES

As pointed out in Section (1.2), changes in instantaneous operating frequency under disturbed conditions have been neglected in the past, on the basis that the effects are not only negligible, but that any damping which arises is positive and results in a system which is safer in fact than is shown by calculations which neglect damping[195].

The magnitude and nature of transient frequency variations occurring on a power system have already been discussed in Section (2), and the effects of such transient frequency variations on individual power system components (synchronous machines, transmission network, loads) have been studied separately in Sections (3, 4 and 5). Each of these separate studies has been necessarily incomplete because of the tight inter-dependence between the various parts of the system characteristics and the actual magnitudes of the frequency excursions. However, it has been considered worthwhile to conduct the separate studies in order to isolate and highlight the frequency deviation effects in each power system component.

It is the aim of the present section to integrate all of the effects previously considered, and to obtain a comprehensive and realistic assessment of power system transient stability behaviour when frequency deviation effects are properly included. At the same time, all other refinements in representation of power system components hitherto available can also be introduced. This will enable a comparison of the assessment of a practical power system with and without the inclusion of instantaneous frequency effects, thus allowing a judgment to be made on the necessity or otherwise of including such additional refinements. It will be seen below that the implication from the separate studies, that is, that neglect of instantaneous frequency effects can sometimes lead to erroneous and unsafe predictions, is reinforced, and two realistic power system examples confirm this.

Including the effects of instantaneous frequency deviations in transient stability calculations will tend to produce a more accurate assessment of actual system behaviour and should allow systems to be designed and operated closer to their stability limits.

6.1 System Representation

It is considered that as comprehensive a representation as is possible should be employed in order to give a detailed treatment of power system behaviour when introducing instantaneous frequency variations. Accordingly, the various components of a power system are represented as below, and it may be noted that the calculation procedure of Section (6.2) can be adapted readily to take account of any existing refinements in calculations. It is stressed however, that in practice on existing power systems, comprehensive information for a detailed study is not readily available and the accuracy of data is often uncertain, thereby introducing substantial difficulties in attempts at precise system studies.

6.1.1 Synchronous Machines

Apart from introducing instantaneous frequency effects on the e.m.f., inertia factor and reactance (Section (3.2.1)), transient damping torques have been incorporated (Section (3.2.2)), as well as representation by the 2-axis theory, and the inclusion of voltage regulator, saturation and flux decay[214, 216]. Although in this study governor effects were neglected due to interest being centred on the transient period only, these may readily be incorporated[229].

6.1.2 Transmission Network

Consideration of transmission network damping has been taken into account by modifying the network parameters (inductive reactances and capacitive susceptances of series and shunt branches) in accordance with instantaneous frequency variations of bus voltages and branch currents (Section 4.1).

6.1.3 System Loads

Loads have been divided into three categories and represented accordingly:-

(a) Frequency-dependent dynamic loads: synchronous motors are represented in a manner completely analogous to the representation of synchronous generators, while induction motors are represented either singly or in groups by the aid of appropriate torque-slip characteristics (Section (5.1.1)) or in 2-axis form in the case of important induction motors[214].

(b) Frequency-dependent static loads: arc furnaces, electric welders, mercury arc rectifiers and discharge lamps and others, are represented with due regard being taken of their frequency-dependent characteristics (Section (5.2.2)).

(c) Frequency-independent loads: represented by fixed impedances.

In treating all loads, account is taken of the instantaneous voltages existing at the load buses and their influence on the respective loads.

6.2 Stability Calculation Procedure

In order to integrate all of the effects introduced in Sections (3, 4 and 5), the following steps allow calculations of power system transient stability, including frequency-dependence as well as the more usual refinements.

(a) Obtain an initial power balance by the conventional methods of load flow study[185].

(b) Calculate synchronous machine excitation voltage, e.m.f. behind quadrature axis synchronous reactance, and direct and quadrature components of the machine current with respect to the reference bus.

(c) Calculate the equivalent induction motor parameters, for single machines or groups, wherever they occur in the system (Section (5.1.2.1)).

(d) Calculate the currents drawn and the load torques of the various equivalent induction motors in (c), as well as the appropriate slopes of their torque-slip and stator current-slip characteristics (Section (5.1.2.1)).

(e) Calculate the initial currents, resistances and equivalent reactances of the frequency-dependent and frequency-independent static loads (Section (5.2.4.1)),

(f) Apply the disturbance.

(g) Form the admittance matrix for the whole system.

(h) Locate the system on an X-Y plane rotating with synchronous angular velocity at system nominal frequency (Section (2.2.2)), in order to allow handling of frequency deviation effects. That is, for conditions corresponding in the first instance to zero time after the disturbance, and subsequently corresponding to the conditions applying to each new iteration, determine bus voltages, branch currents, resultant air gap fluxes and their phases (Section (4.1.1)).

(i) Determine the driving point and transfer impedances with all loads represented by their instantaneous equivalent impedances (Section (5.1.2)).

(j) Determine synchronous machine instantaneous angular positions by solving their differential equations. This gives the magnitude and location of the synchronous machine e.m.f. phasors at the end of a chosen step time interval, Δt.

(k) For the new angular positions of the synchronous machine phasors, determine the various bus voltages, branch currents, their phase angles on the X-Y plane, their mean instantaneous frequencies, and the slip of rotors w.r.t. resultant air gap fluxes (Section (3.2.2)).

(ℓ) Up to this point, the system has been treated at the instantaneous frequencies corresponding to those existing at the previous step, and must now be changed to correspond to the new instantaneous frequencies. In order to do this, the mean instantaneous frequency at each point in the system is modified by an accelerating factor to ensure effective convergence during the subsequent iterations necessary to achieve solution for the particular time interval, Δt.

Steps (m) to (q) then employ the modified mean instantaneous frequency.

(m) Determine the new induction motor power inputs and static frequency-dependent load inputs (Sections (5.1.2.1 and 5.2.4.1)). Represent all loads, including frequency-independent loads, by their equivalent circuits on the currently existing values of bus voltages.

(n) Calculate synchronous machine damping (Section (3.2.2.1)) and braking powers[229], and modify the accelerating power available to each synchronous machine.

(o) Modify synchronous machine e.m.f's, stored energies, reactances, and the parameters of the transmission network.

(p) Test for convergence of the angular positions of the synchronous machines, successive values of which should be within a predetermined index, say, within 10^{-3} of a degree. If the test is not satisfied, return to step (g) and recycle, employing a step time interval, Δt.

(q) Write the various quantities.

For each step time interval, Δt, operation of the above schedule proceeds to a solution usually within 5 to 7 iterations if an accelerating factor of 1.35 (which has been found optimum) is used for step (ℓ). Δt may be chosen = 0.05 seconds, as is usual in stability calculations.

The above procedure provides swing curves applicable to each operating condition of the network, that is, each time the condition of operation is changed (fault on, fault cleared and so on), it is necessary to perform iterations within the steps (f) to (q).

6.3 Representative Power System Studies

Two representative power system problems are discussed below, with the object of indicating,

(a) The varied nature in system behaviour possible;

(b) The relative influence and significance of the complexity with which the power systems are represented;

so that the degree of complexity of representation may be related to the value and effort involved in securing the appropriate results and to determine which assumptions may or may not be neglected.

For both problems, the cases given in Table VII have been calculated and plotted:-

TABLE VII - Methods for Representing Power Systems for Calculation Purposes, and the Corresponding Computing Times*

Method of Representation	4-Machine Problem (Section 6.3.1)	Large Inter-connected System (Section 6.3.2)
(i) As in conventional studies with synchronous machines represented in 2-axis form, account being taken of voltage regulator, saturation, transient saliency and flux decay effects, but no frequency-dependent representation of any part of the system.	0.7 minutes	7.0 minutes
(ia) As in conventional studies, but with synchronous machines represented by an e.m.f. behind direct axis transient reactance.	0.4 "	6.5 "
(ii) With representation as in (i), plus the effect of change in machine e.m.f., and stored energy in the moving parts.	1.1 "	9.5 "
(iii) With representation as in (ii), plus synchronous machine damping.	1.5 "	12.5 "
(iv) With representation as in (iii), plus the effect of change in transmission network parameters.	4.4 "	51 "
(v) With representation as in (i), plus the effect of dynamic and static frequency-dependent loads.	4.6 "	54 "
(vi) With representation as in (iv), plus the effect of dynamic and static frequency-dependent loads.	5.2 "	62 "

* Using an IBM 360/50 digital computer.

6.3.1 4-Machine Problem

Figure 3.6(a) gives the line diagram of a 4-machine problem based on an example from Reference 195. Each of the major loads at buses 5, 6 and 7, has been taken to have the following composition:-

50% induction motor load

20% static frequency-dependent load

30% frequency-independent load

(The above composition conforms to common experience[119, 127*]).
It may be noted that this system includes a configuration in which a major load is supplied by distant generators, that is, the greater portion of the loads at buses 6 and 7 must be supplied by machines 1 and 4.

A 3-phase to ground fault is applied close to bus 11 on the transmission line shown in Figure (3.6a). Breaker B_1 opens in 78 m sec., isolating bus 11 from the faulted line, and subsequently after 156 m sec. from the time of fault inception, breaker B_2 disconnects the faulty transmission line, thus clearing the fault.

Figures (6.1a - d) show the swing curves for the above transient disturbance when the system is represented by the methods of Table VII. Figure (6.1e) gives the voltage variations at bus 7 while Figure (6.1f) shows current variations in the branch between nodes 8 and 10.

The calculations and plotted results show clearly that the system is subject to negative damping when instantaneous frequency effects

---

* Although these references are 20 years old, the above load composition can still be approximately valid at present - for example, it corresponds substantially to the load on the N.S.W. System.

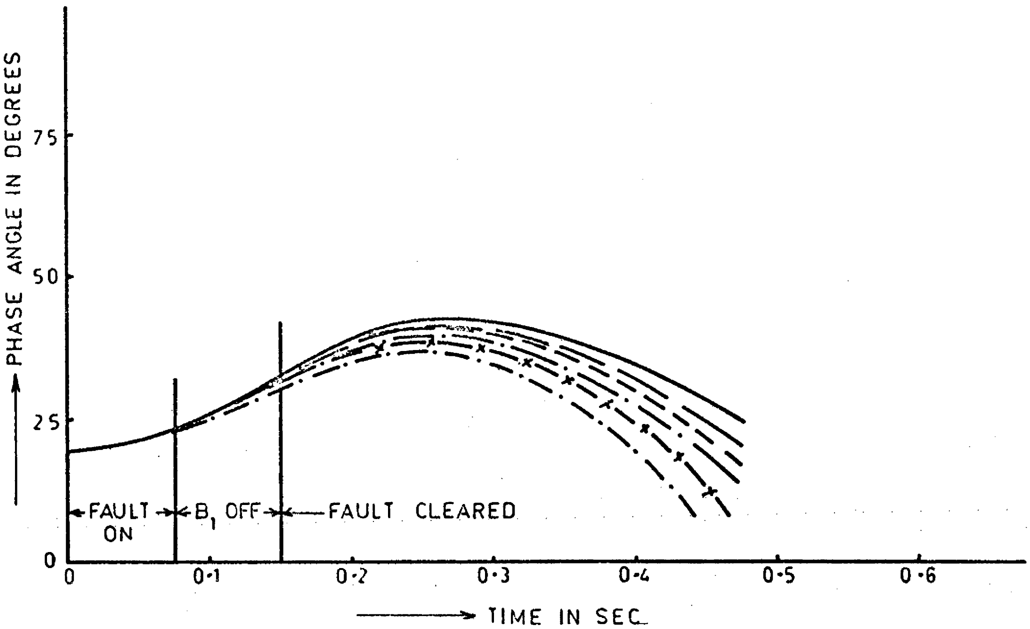

Fig. 6.1(a) Swing curves for machine No. 1 of Fig. 3.6(a).

(i)	————	With VOLT. REG., SATN, TRANS. SAL. AND FLUX DECAY.
(ii)	—— ——	(i) + instantaneous effects on machine e.m.f. and M.
(iii)	——·——	(ii) + machine damping.
(iv)	– – – – – –	(iii) + transmission network damping.
(v)	—·—· —	(iv) + system load variations.
(vi)	—x—x—	(i) + " " "

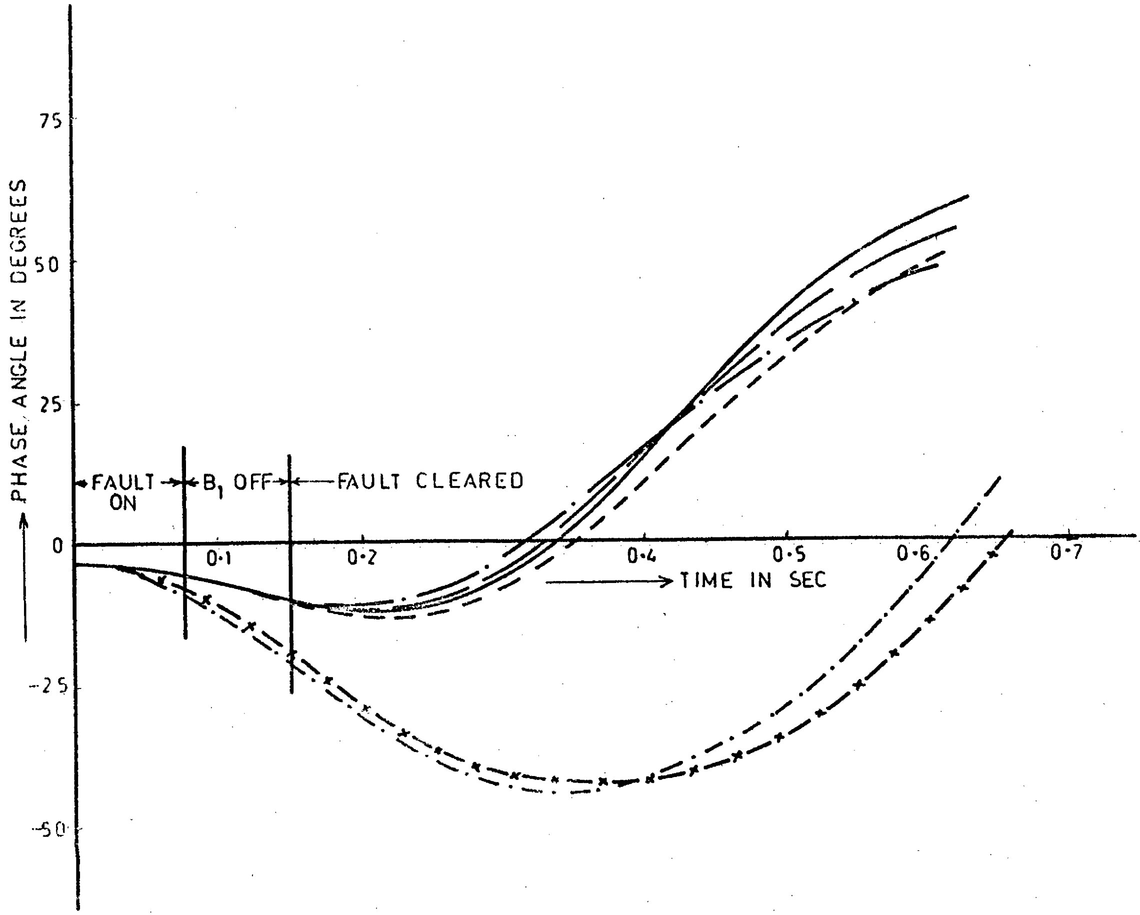

Fig. 6.1(b) Swing curves for machine no. 2 of Fig. 3.6(a).

(i) ——————— With VOLT. REG., SATN., TRANS. SAL. AND FLUX DECAY.
(ii) ——— ——— (i) + instantaneous effects on machine e.m.f. and M.
(iii) ———·——— (ii) + machine damping.
(iv) — — — — — (iii) + transmission network damping.
(v) —·—·— (iv) + system load variations.
(vi) —x——x— (i) + " " "

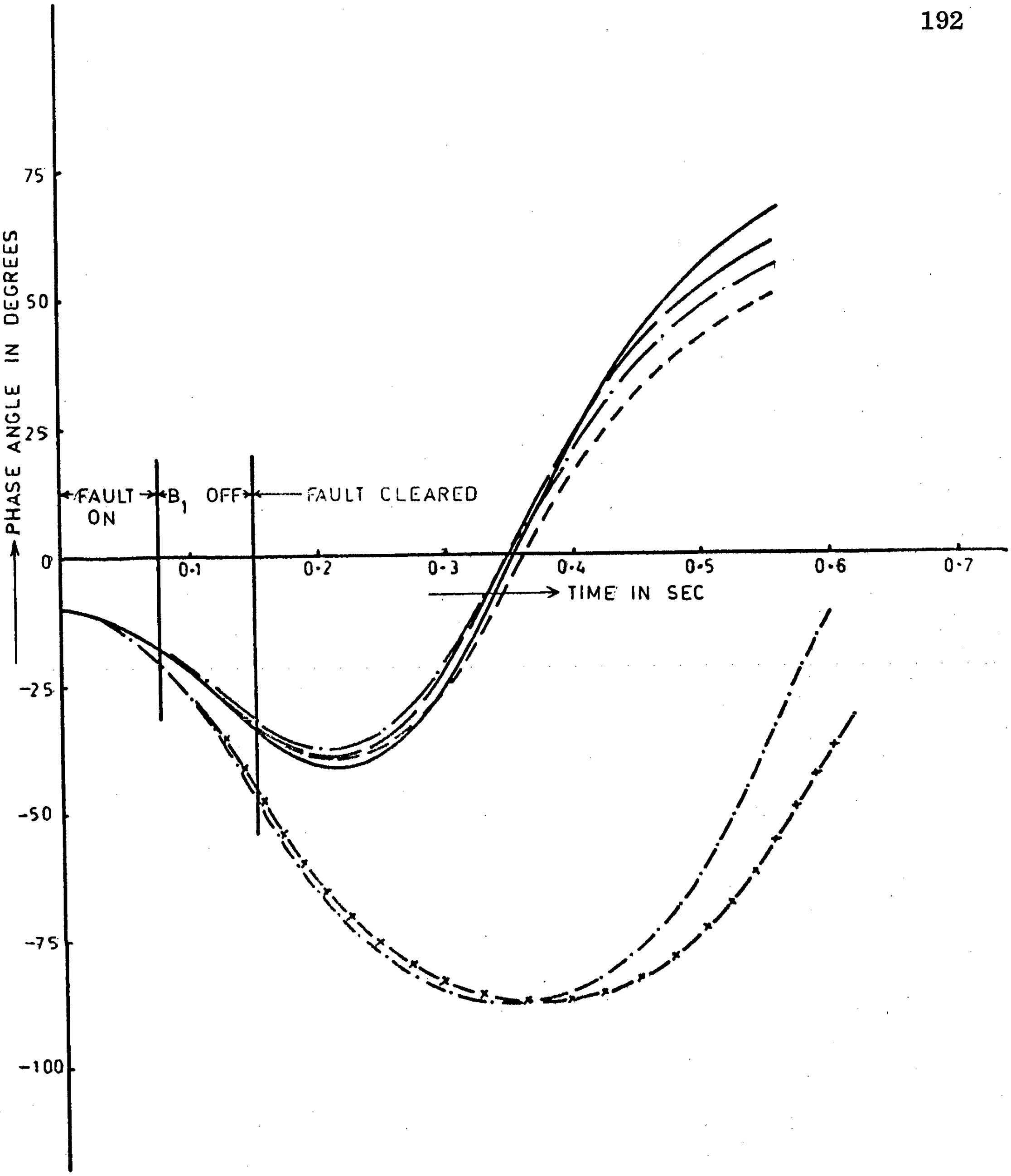

Fig. 6.1(c) Swing curves for machine no. 3 of Fig. 3.6(a).

(i) ———— With VOLT. REG., SATN., TRANS. SAL. AND FLUX DECAY.
(ii) — — (i) + instantaneous effects on machine e.m.f. and M.
(iii) —·— (ii) + machine damping.
(iv) - - - - (iii) + transmission network damping.
(v) —·—·— (iv) + system load variations.
(vi) —x—x— (i) + " " "

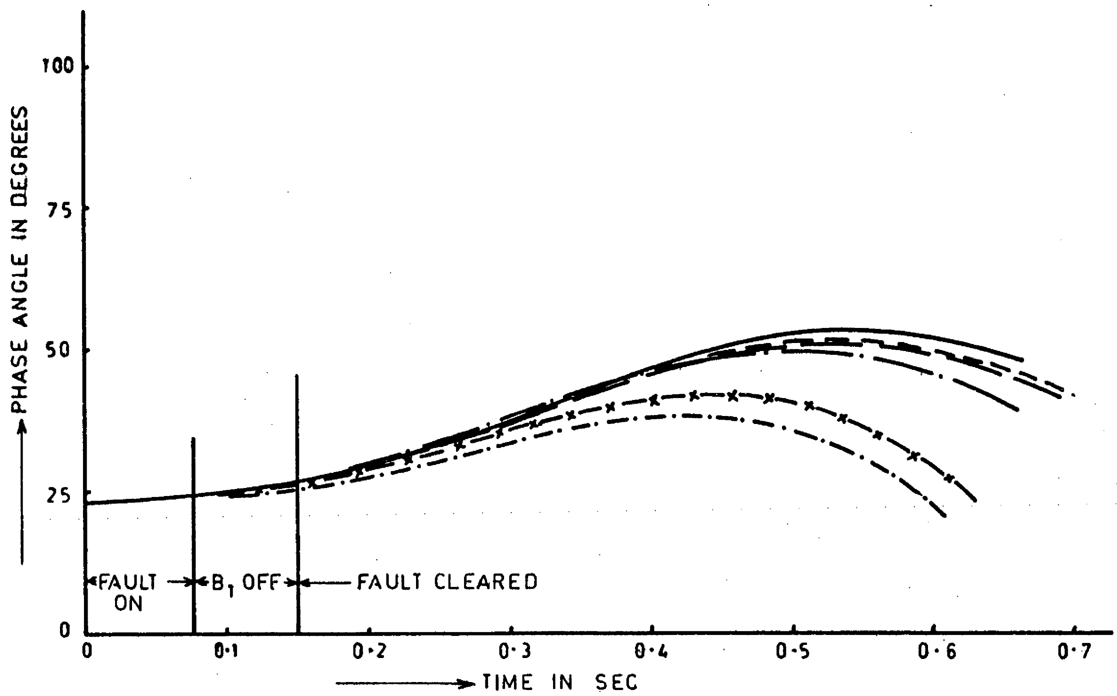

Fig. 6.1(d) Swing curves for machine no. 4 of Fig. 3.6(a).

(i) ———— With VOLT. REG., SATN., TRANS. SAL. AND FLUX DECAY.
(ii) —— —— (i) + instantaneous effects on machine e.m.f. and M.
(iii) ——·—— (ii) + machine damping.
(iv) – – – – – (iii) + transmission network damping.
(v) —·—·— (iv) + system load variations.
(vi) —×—×— (i) + " " "

are considered. Although overall negative damping is contributed to by the synchronous machines themselves and by the transmission network, the major effect results from the dynamic loads which apply extra load on decelerating machines due to the reduced voltage when instantaneous frequency considerations are included, as shown in Figure (6.1e). The increased load supplied at bus no. 7 resulting from the above behaviour is also demonstrated by the increased current flowing between nodes 8 and 10, shown in Figure (6.1f).

As a comparison between the results achieved by the various calculation procedures of Table VII, the fault clearance time, which causes the system to be just on the point of instability was ascertained and is shown in Table VIII:-

TABLE VIII - Comparison of Critical Fault Clearance Time by Various Methods of Representation

Method of Representation	Critical fault clearance time for the system to be just on the point of instability. 4-Machine Problem (Section 6.3.1)	Large Inter-connected System (Section 6.3.2)
(i) As in conventional studies with synchronous machines represented in 2-axis form, account being taken of voltage regulator, saturation, transient saliency and flux decay effects, but no frequency-dependent representation of any part of the system.	266 m sec.	498 m sec.
(ia) As in conventional studies, but with synchronous machines represented by an e.m.f. behind direct axis transient reactance.	261 "	488 "
(ii) With representation as in (i), plus the effect of change in machine e.m.f., and stored energy in the moving parts.	272 "	510 "
(iii) With representation as in (ii), plus synchronous machine damping.	278 "	516 "
(iv) With representation as in (iii), plus the effect of change in transmission network parameters.	270 "	503 "
(v) With representation as in (i), plus the effect of dynamic and static frequency-dependent loads.	162 "	553 "
(vi) With representation as in (iv), plus the effect of dynamic and static frequency-dependent loads.	170 "	563 "

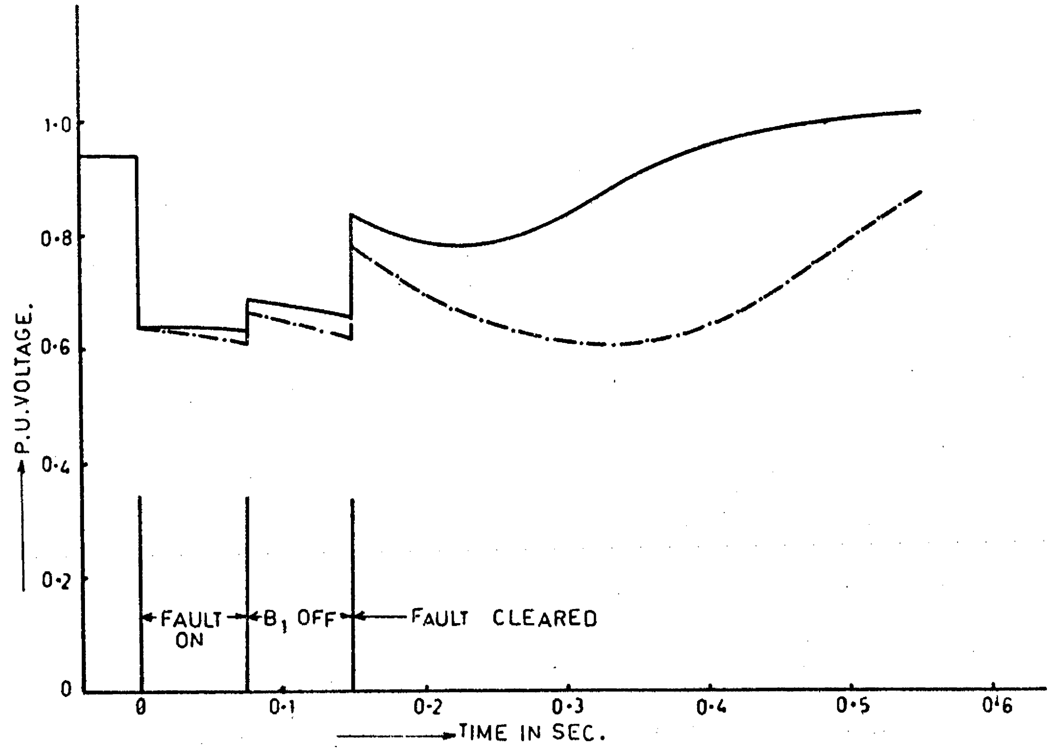

Fig. 6.1(e) Voltage variations at bus no. 7 of Fig. 3.6(a).

——————— With VOLT. REG., SATN., TRANS. SAL. AND FLUX DECAY.
—·—·— Including all the instantaneous frequency variation effects.

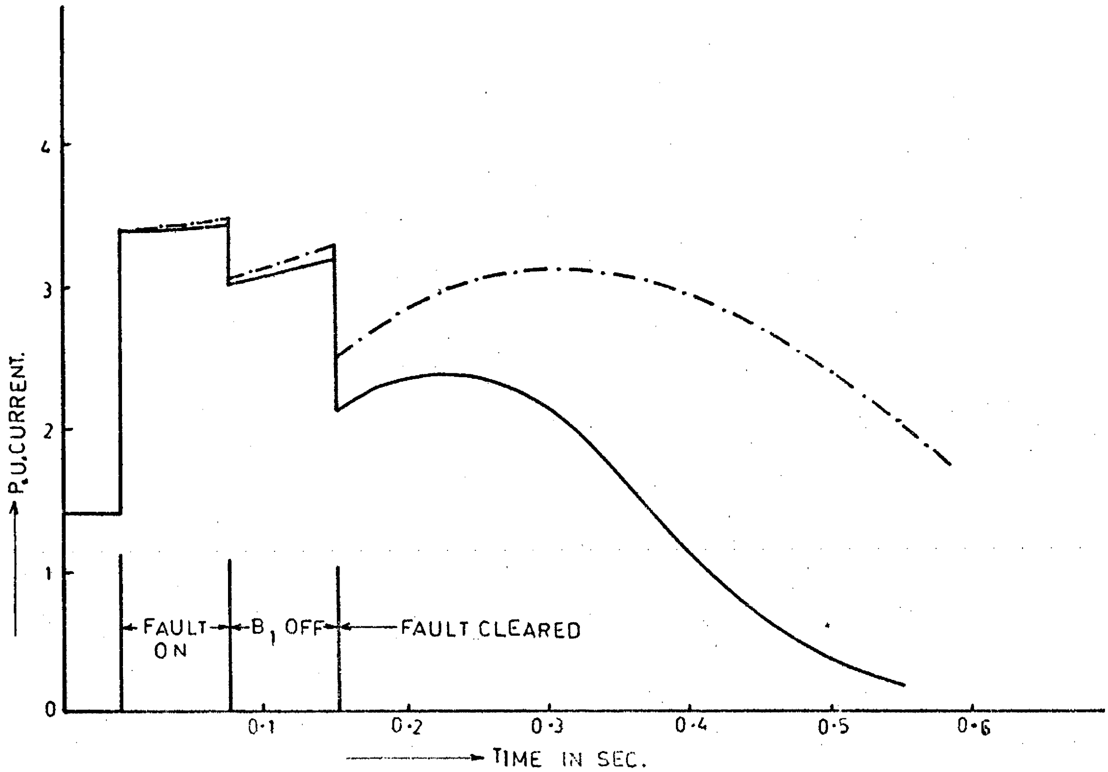

Fig. 6.1(f) Current variations through branch between nodes 8 and 10.

——— With VOLT. REG., SATN., TRANS. SAL. AND FLUX DECAY.
—·—·— Including all the instantaneous frequency variation effects.

The major effect produced by the system loads, particularly at bus 7, is demonstrated in the above results.

Comparing especially the calculations based on the conventional methods ((i) of Table VII), with those which include complete instantaneous frequency representation in the system, a major difference in assessment is obvious. In view of the nature of this system, which is possibly a somewhat extreme case, this difference is not surprising. However, the occurrence of features similar to the above is not unusual on major power systems, and deserves careful attention.

6.3.2 Large Interconnected System

Figure (6.2) presents the line diagram for a large interconnected power system similar to one projected for South Eastern Australia. Branch 24 is a proposed 330-kV tie-line on which 50% series capacitive compensation is suggested, and forms an important link. Although machine no. 1 has a large system of 10,000 MW behind it, finite inertia is still used in the calculations (no infinite bus). In the present study, a 3-phase to ground fault is applied close to bus 24 on the tie link (branch 24), followed by a dead time and subsequent reclosure. As in the problem of Section (6.3.1), the various methods of representation of Table VII (i) - (vi) have been employed in assessing transient behaviour of the system.

Tables IX to XIII inclusive provide further information on the system parameters.

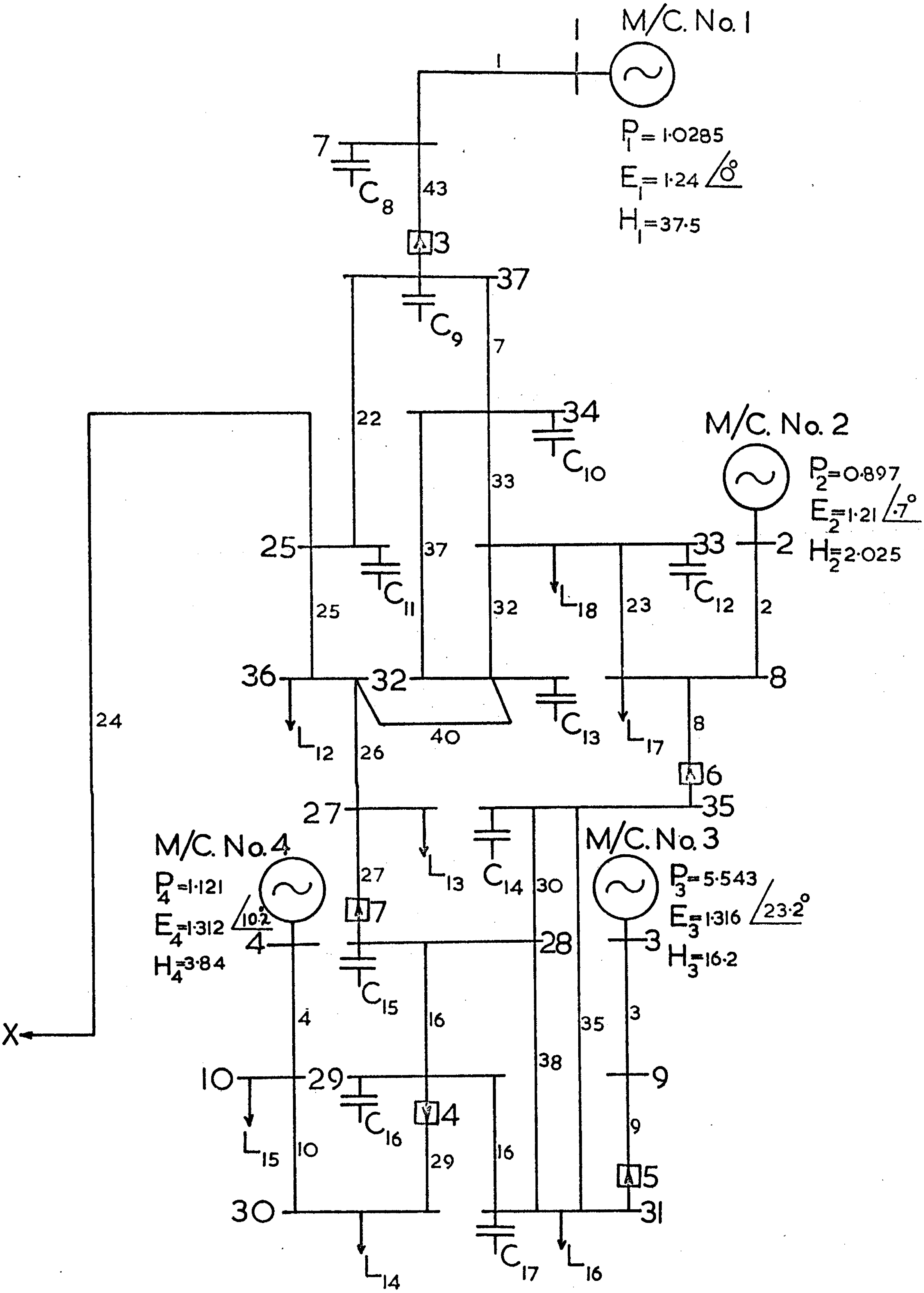
M/C. No. 1
P1 = 1·0285
E1 = 1·24 ∠0°
H1 = 37·5
M/C. No. 2
P2 = 0·897
E2 = 1·21 ∠·7°
H2 = 2·025
M/C. No. 3
P3 = 5·543
E3 = 1·316 ∠23·2°
H3 = 16·2
M/C. No. 4
P4 = 1·121
E4 = 1·312 ∠10·2°
H4 = 3·84
C8
C9
C10
C11
C12
C13
C14
C15
C16
C17
L12
L13
L14
L15
L16
L17
L18
X

TABLE IX - Transmission Line Impedances for Figure (6.2) on 1000 MVA Base

Branch No.	Impedance in P.U.	Branch No.	Impedance in P.U.
1	0 + j0.001	23	0.31 + j1.69
2	0 + j0.307	24	0.235 + j1.816
3	0 + j0.06	25	0 + j0.105
4	0 + j0.274	26	0.016 + j0.086
5	0.014 + j1.199	27	0 + j0.133
6	0 + j0.16451	28	0.002 + j0.022
7	0 + j0.147	29	0 + j0.067
8	0 + j0.0675	30	0.003 + j0.043
9	0 + j0.0257	31	0.009 + j0.278
10	0.024 + j0.157	32	0.133 + j0.708
11	0.043 + j0.478	33	0.439 + j2.407
12	0.0055 + j0.042	34	0.0613 + j0.427
13	0.33 + j1.08	35	0.014 + j0.187
14	0.265 + j0.788	36	0.002 + j0.021
15	0.7192 + j2.11	37	0.144 + j0.785
16	0.005 + j0.0705	38	0.011 + j0.152
17	0.0492 + j0.342	39	0 + j0.08
18	0.0095 + j0.066	40	0.081 + j0.443
19	0.0092 + j0.103	41	0.0178 + j0.1989
20	0.009 + j0.41	42	0.186 + j0.559
21	0.409 + j1.235	43	0.0154 + j0.118
22	0.0314 + j1.69	44	0.644 + j1.91

Series capacitive reactance for Branch No. 24 = 1.0885 P.U.

TABLE X - Load Admittances, on 1000 MVA Base, for Figure (6.2)

Load	Admittance in P.U.	Load	Admittance in P.U.
L_1	0.013 - j0.045	L_{10}	0.489 - j0.25
L_2	0.174 - j0.038	L_{11}	0.193 - j0.079
L_3	0.118 - j0.043	L_{12}	0.7 - j0.376
L_4	0.037 - j0.012	L_{13}	0.7 - j0.239
L_5	0.055 - j0.02	L_{14}	2.4 - j0.754
L_6	0.062 - j0.007	L_{15}	0.093 - j0.023
L_7	0.318 - j0.143	L_{16}	0.66 - j0.113
L_8	0.306 - j0.0954	L_{17}	2.2 - j0.665
L_9	0.791 - j0.397	L_{18}	0.6 - j0.0

TABLE XI - Shunt Susceptances on 1000 MVA Base, for Figure (6.2)

Capacitor	Susceptance in P.U.	Capacitor	Susceptance in P.U.
C_1	0.027	C_{10}	0.0389
C_2	0.0576	C_{11}	0.152
C_3	0.012	C_{12}	0.0256
C_4	0.008	C_{13}	0.0555
C_5	0.022	C_{14}	0.1234
C_6	0.02	C_{15}	0.1169
C_7	0.01171	C_{16}	0.1632
C_8	0.0655	C_{17}	0.3461
C_9	0.1975	C_{18}	0.124

TABLE XII - Tap Settings for On-Load Tap Changers, for Figure (6.2)

Tap Changer No.	Tap Settings
1	1.1
2	1.15
3	1.14
4	0.96
5	1.05
6	0.95
7	0.95

TABLE XIII - Synchronous Machine Parameters, for Figure (6.2), on 1000 MVA Base

M/c No.	Saturated Synchronous Reactance in P.U.		Potier Reactance = Direct axis Transient Reactance (X'_d)	Direct axis open circuit field time constant (seconds)	Voltage Regulator Characteristics * (Conventional, Continuously Acting)
	X_d	X_q			
1	0.008	0.001	0.0008	7.5	Exponential Response. Voltage Gain = 20. Total Excitation Time Constant = 0.5 seconds. (Exciter + Main Generator Field Winding).
2	1.5	0.307	0.22	7.5	
3	0.3	0.06	0.045	7.5	
4	1.4	0.274	0.21	7.5	
5	6.0	1.199	1.0	7.5	
6	0.75	0.1645	0.13	7.5	

* Voltage regulator gain for each machine has been adjusted so as to just overcome changes in e.m.f. due to flux decay, in conformity with reasonable practice (as, for example, suggested in Ref. 198).

Loads on each of the buses 8, 10, 12, 13, 14, 18, 20, 23, 26, 27, 30, 31 and 36 are composed of induction motors, 50%; static frequency-dependent loads, 20%; and static frequency-independent loads, 30%.

Relative swing curves for the above disturbance are plotted in Figures (6.3a - c); instantaneous frequencies at several machine terminals are given in Figure (6.4); Figure (6.5) shows various instantaneous frequencies of machine e.m.f. and resultant air-gap flux for machines 5 and 6; Figures (6.6a - d) give the voltage variations on several key buses; Figures (6.8a, b) give the current variations in branches 18 and 31 respectively.

The results show overall positive damping, a major reason for this being due to influence of the loads, through the action mainly of induction motors which present an enhanced load due to the drop in bus voltages, as shown in Figures (6.6a - d). This increase in load occurs at a time when the synchronous machines are accelerating and consequently the acceleration is opposed.

It may be noted that the tendency to positive damping is increased by the large amount of shunt capacitive compensation employed on the system and decreased by the series capacitive compensation on line 24. The overall effect of the transmission network itself as regards damping is, in fact, negative, as shown by the swing curves in Figures (6.3b and c), for the case when transmission network damping is introduced in the calculation procedure. Due to lack of sufficient shunt capacitive compensation, both machines (5 and 6) are adversely affected as is shown by their enhanced phase angle swings.

Of all synchronous machines on the system, nos. 5 and 6 show the greatest frequency deviations, and indicate the influence of overall positive

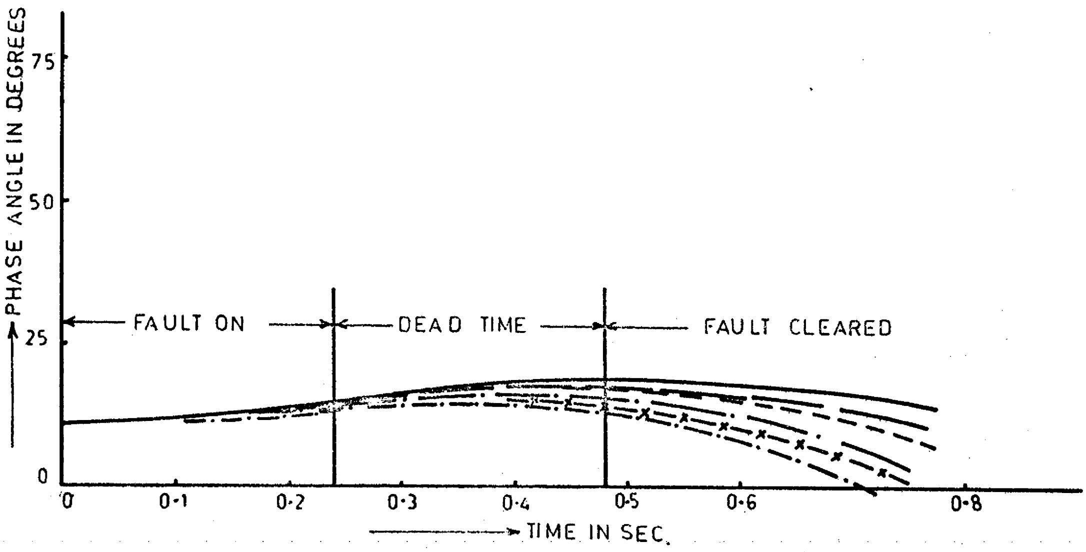

Fig. 6.3(a) Relative swing curves of m/c no. 3 with respect to m/c no. 1 of Fig. 6.2.

(i) ———— With VOLT. REG., SATN., TRANS. SAL. AND FLUX DECAY.
(ii) —— —— (i) + effect of instantaneous frequency on m/c e.m.f. and M.
(iii) ——·—— (ii) + machine damping.
(iv) – – – – – (iii) + transmission network damping.
(v) —·—·— (iv) + system load variations.
(vi) —x—x— (i) + " " "

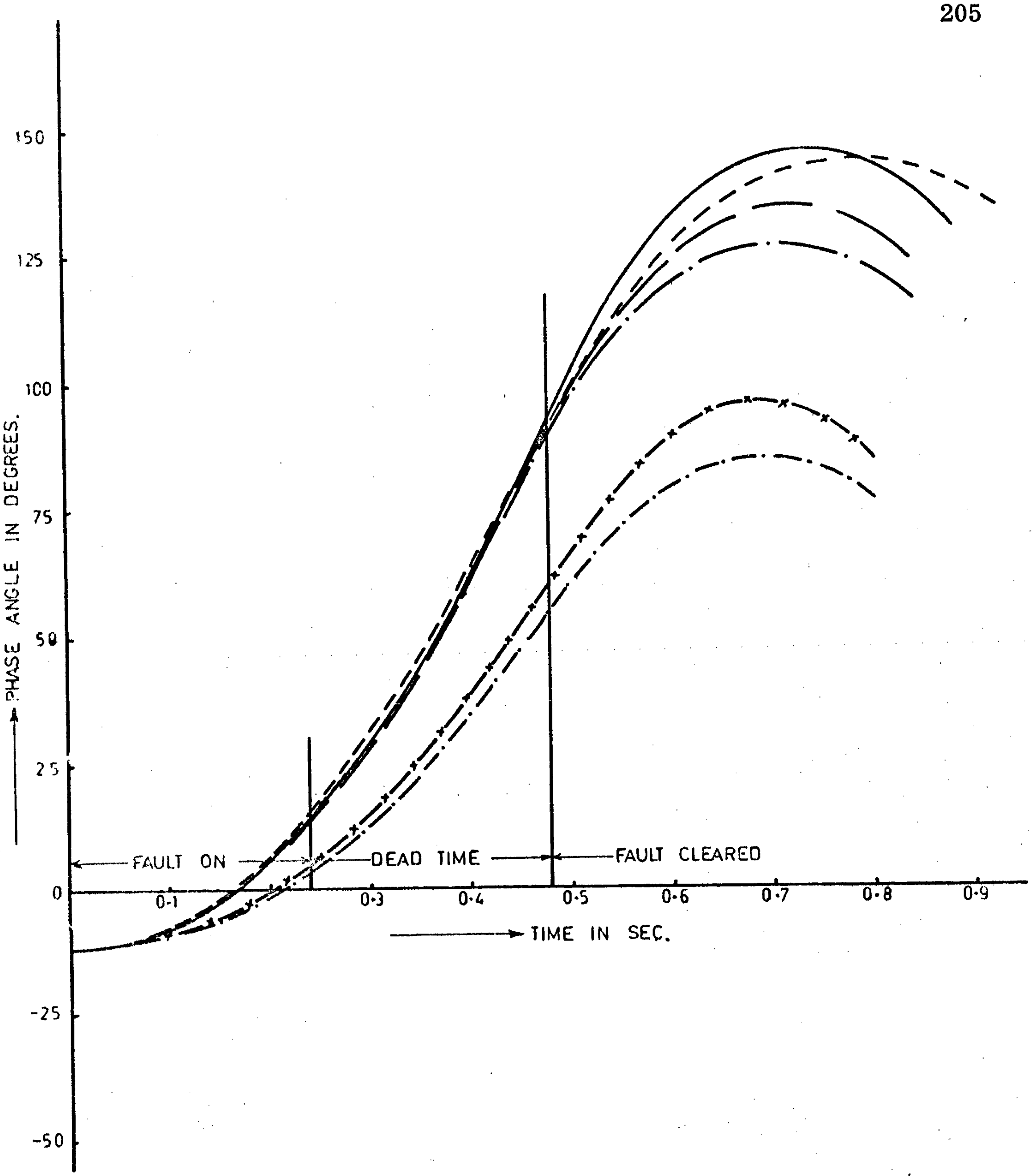

Fig. 6.3(b) Relative swing curves of m/c no. 5 with respect to m/c no. 1 of Fig. 6.2.

(i) ———— With VOLT. REG., SATN., TRANS. SAL. AND FLUX DECAY.
(ii) —— —— (i) + effect of instantaneous frequency on m/c e. m. f. and M.
(iii) ——·—— (ii) + machine damping.
(iv) – – – – (iii) + transmission network damping.
(v) —·—·— (iv) + system load variations.
(vi) —x—x— (i) + " " "

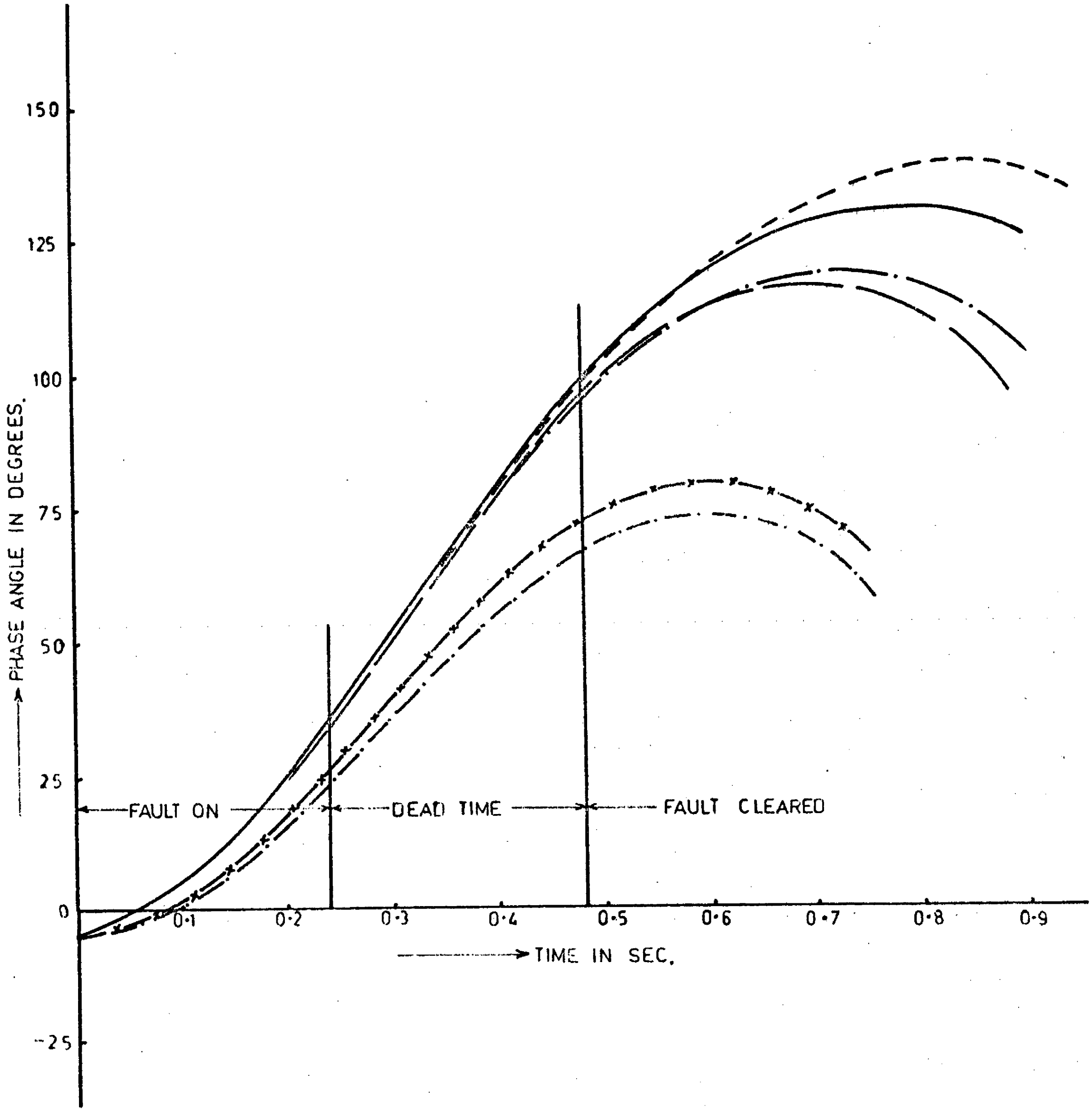

Fig. 6.3(c) Relative swing curves of m/c no. 6 with respect to m/c no. 1 of Fig. 6.2.

(i) ———— With VOLT. REG., SATN., TRANS. SAL. AND FLUX DECAY.
(ii) —— —— (i) + effect of instantaneous frequency on m/c e.m.f. and M.
(iii) ——·—— (ii) + machine damping.
(iv) – – – – – (iii) + transmission network damping.
(v) —·—·— (iv) + system load variations.
(vi) —x—x— (i) + " " "

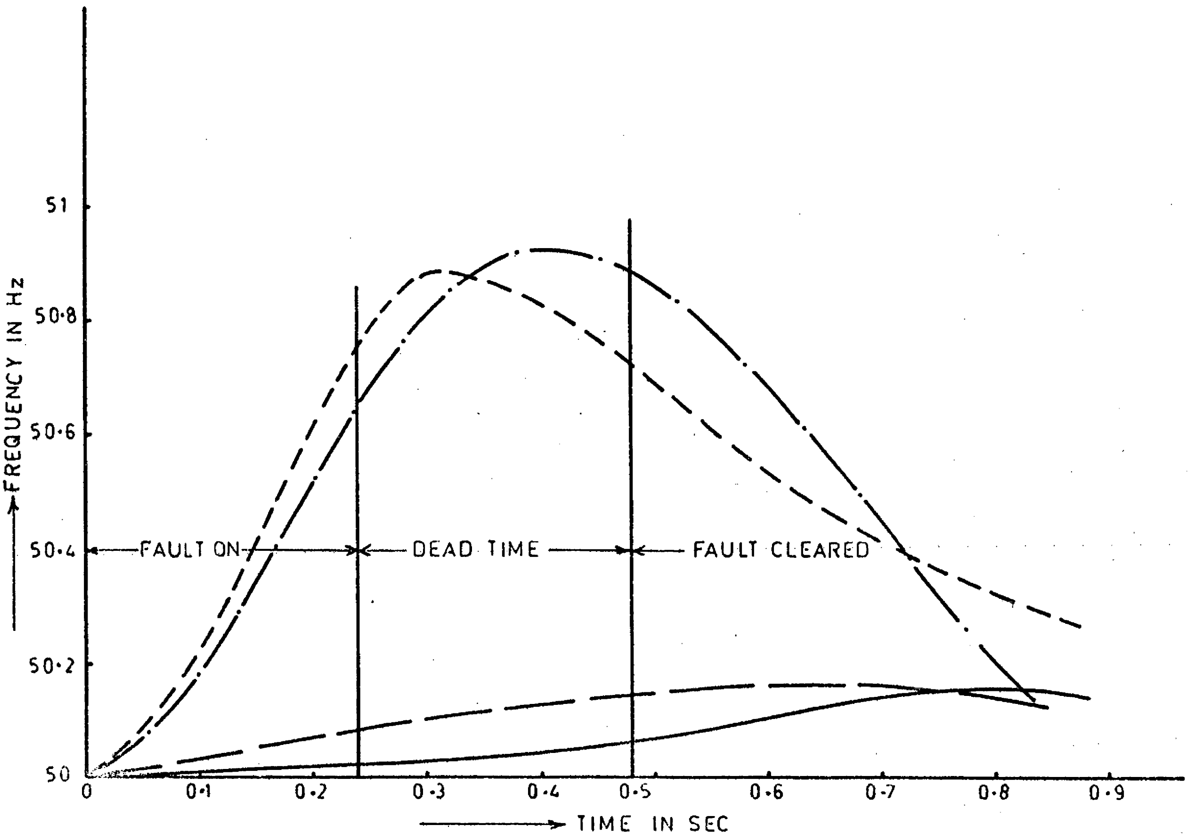

Fig. 6.4 Instantaneous frequency at machine terminals.

———————	For m/c no. 1.
—— ——	" " " 3.
——·——	" " " 5.
– – – – –	" " " 6.

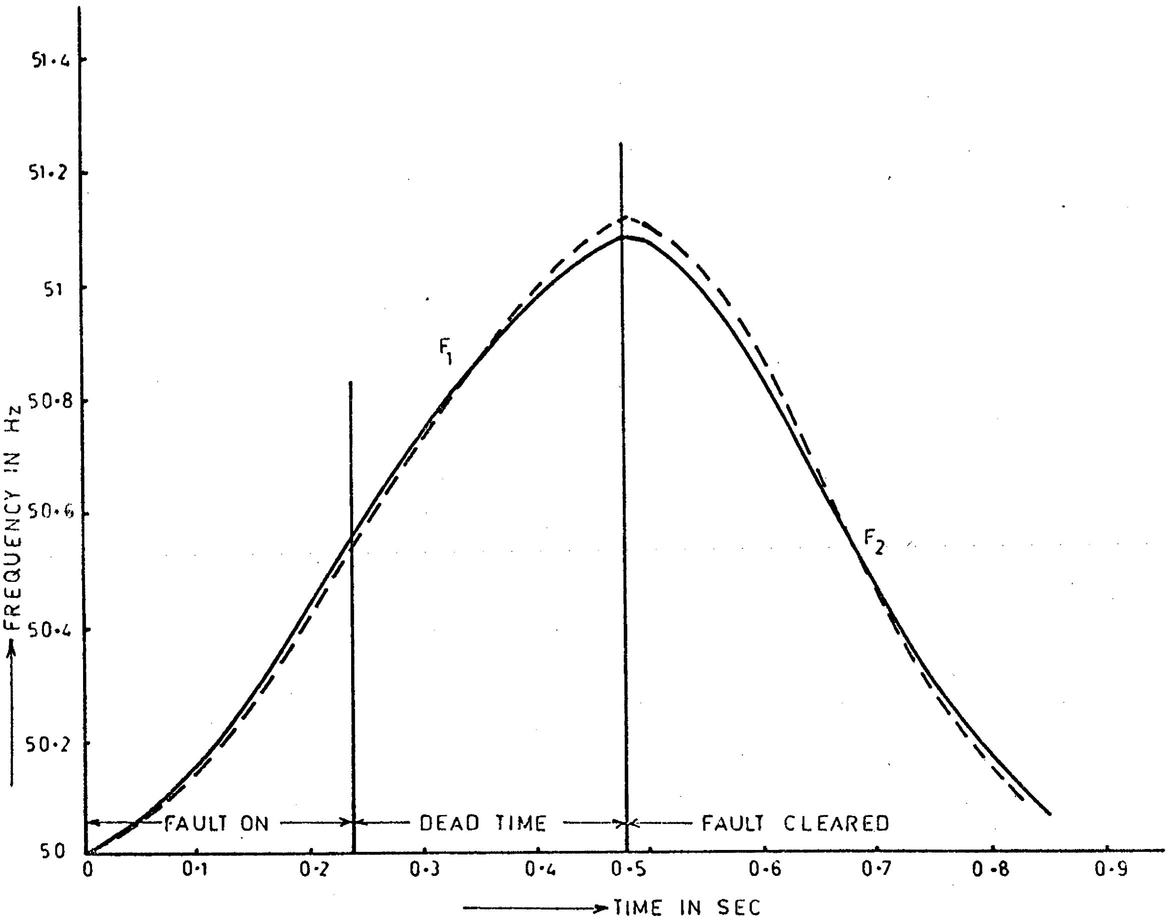

Fig. 6.5(a) Instantaneous frequency variations for m/c no. 5 of Fig. 6.2.

– – – – – For E_Q

——— " Φ

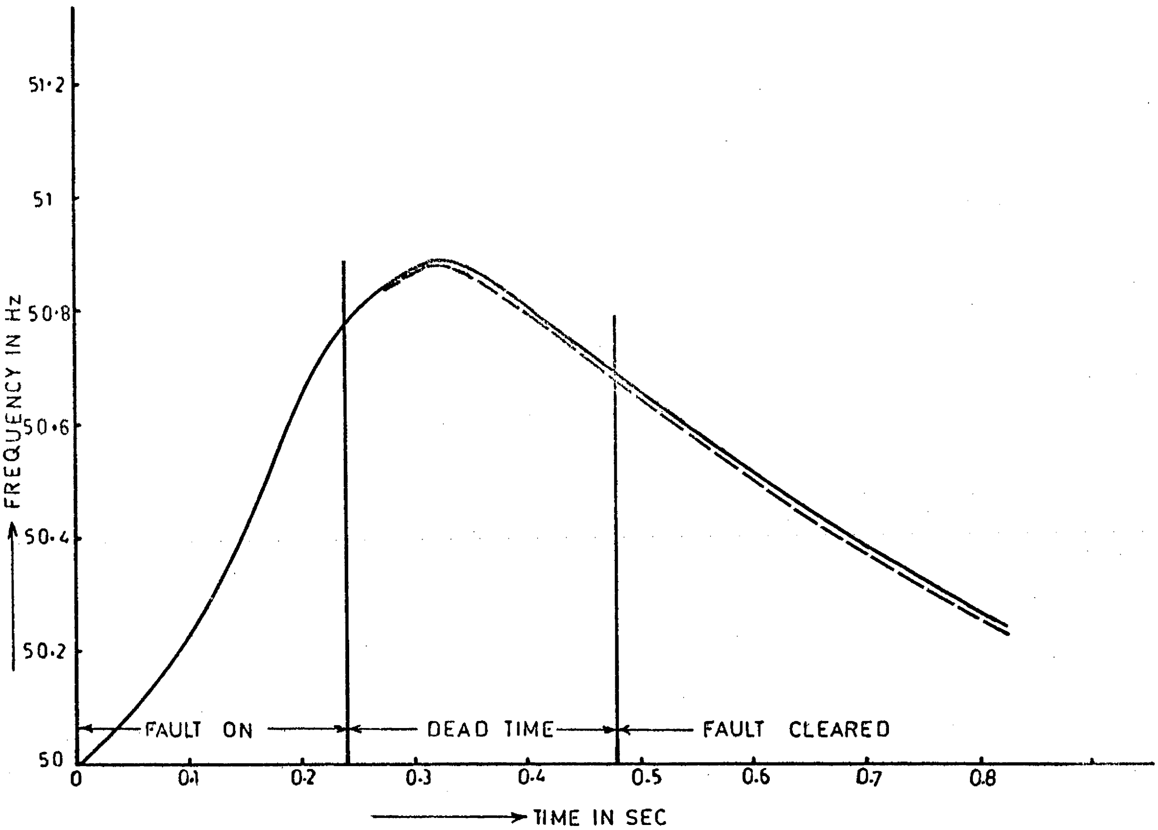

Fig. 6.5(b) Instantaneous frequency variations for m/c no. 6 of Fig. 6.2.

------ For E_Q

——— " Φ

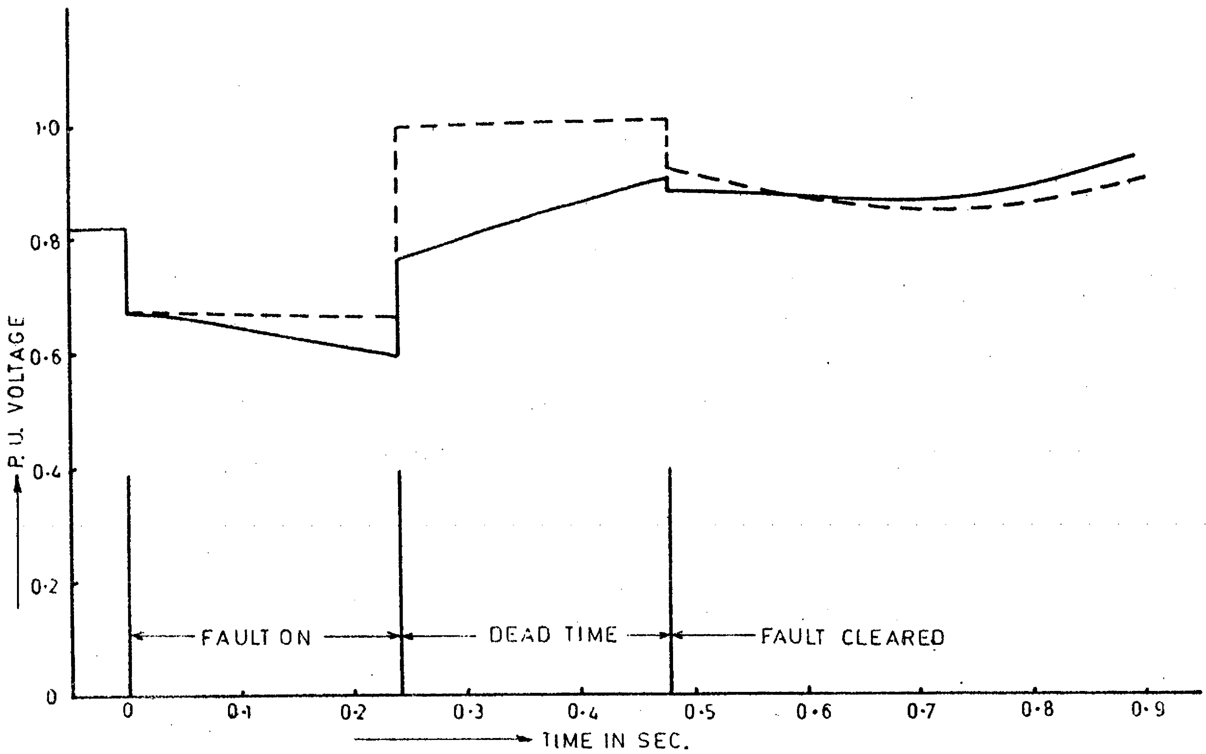

Fig. 6.6(a) Voltage variations at bus no. 22.

– – – – – With VOLT. REG., SATN., TRANS. SAL. AND FLUX DECAY.

———— " complete instantaneous frequency representation.

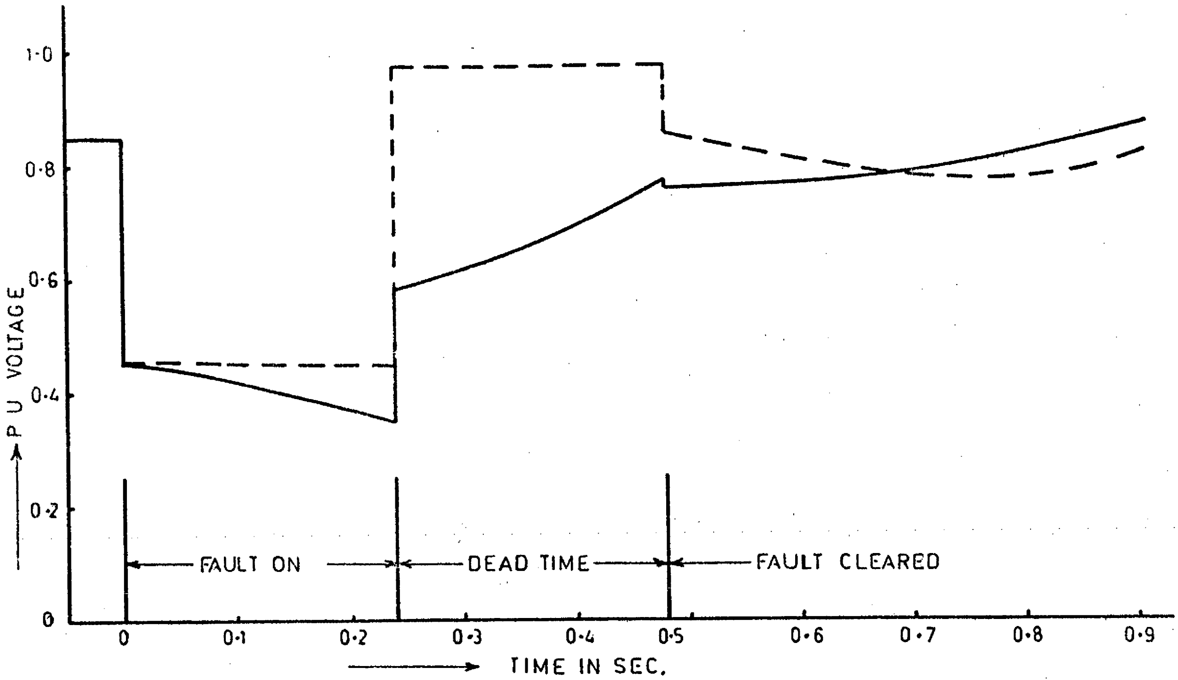

Fig. 6.6(b) Voltage variations at bus no. 23.

- - - - - - With VOLT. REG., SATN., TRANS. SAL. AND FLUX DECAY.
———— " complete instantaneous frequency representation.

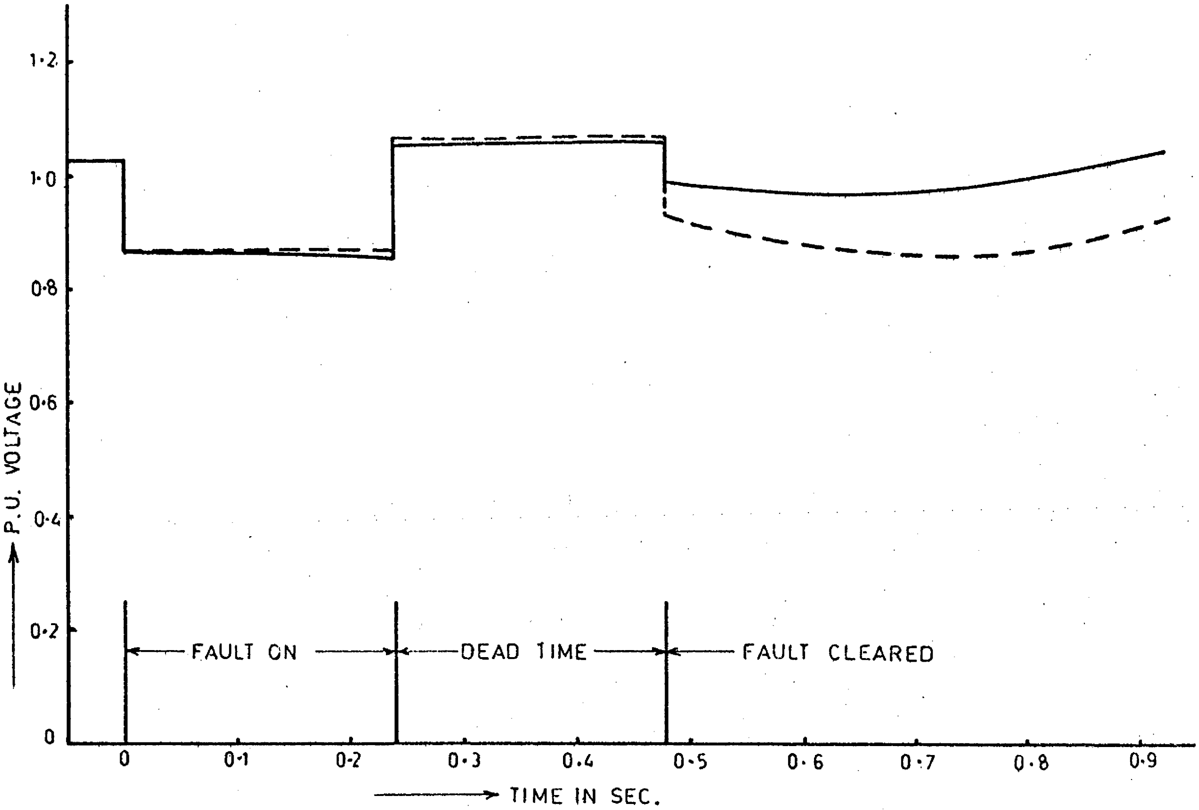

Fig. 6.6(c) Voltage variations at bus no. 25.

- - - - - - With VOLT. REG., SATN., TRANS. SAL. AND FLUX DECAY.
———— " complete instantaneous frequency representation.

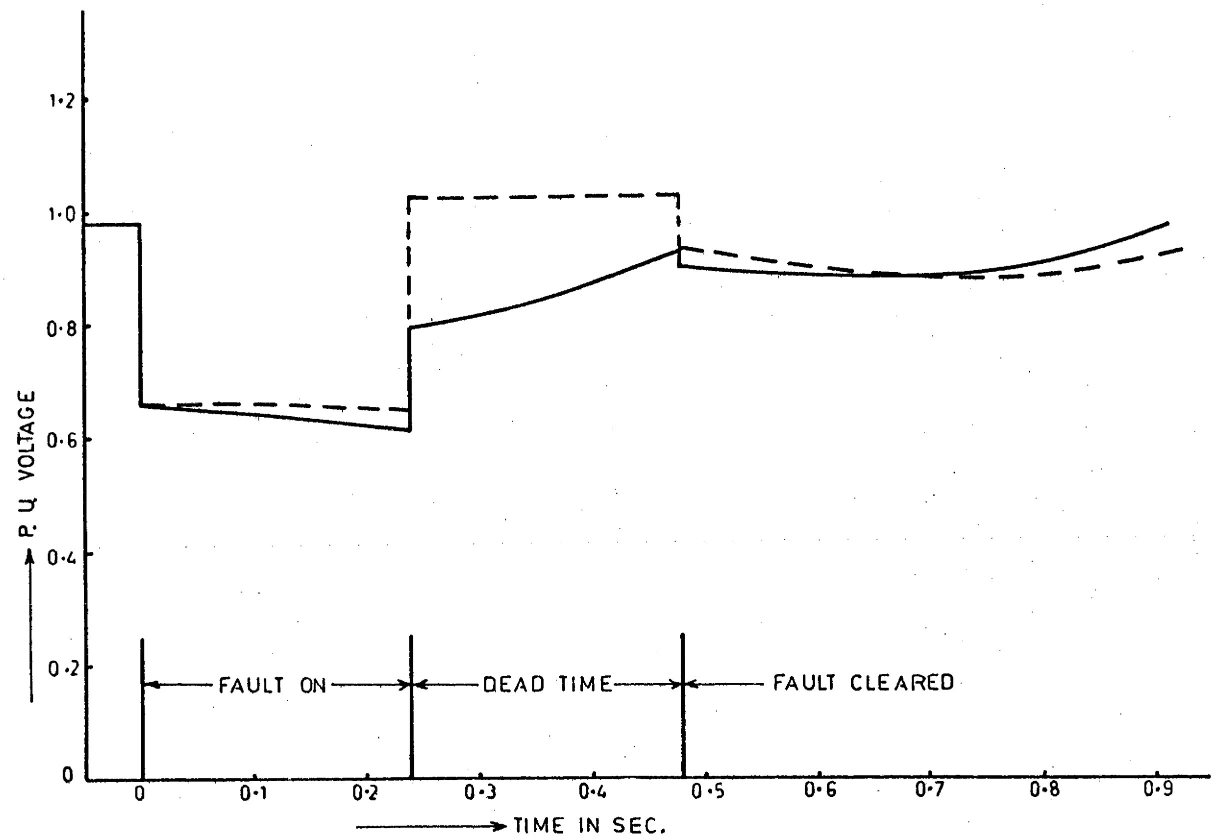

Fig. 6.6(d) Voltage variations at bus no. 26.

– – – – – With VOLT. REG., SATN., TRANS. SAL. AND FLUX DECAY.

———— " complete instantaneous frequency representation.

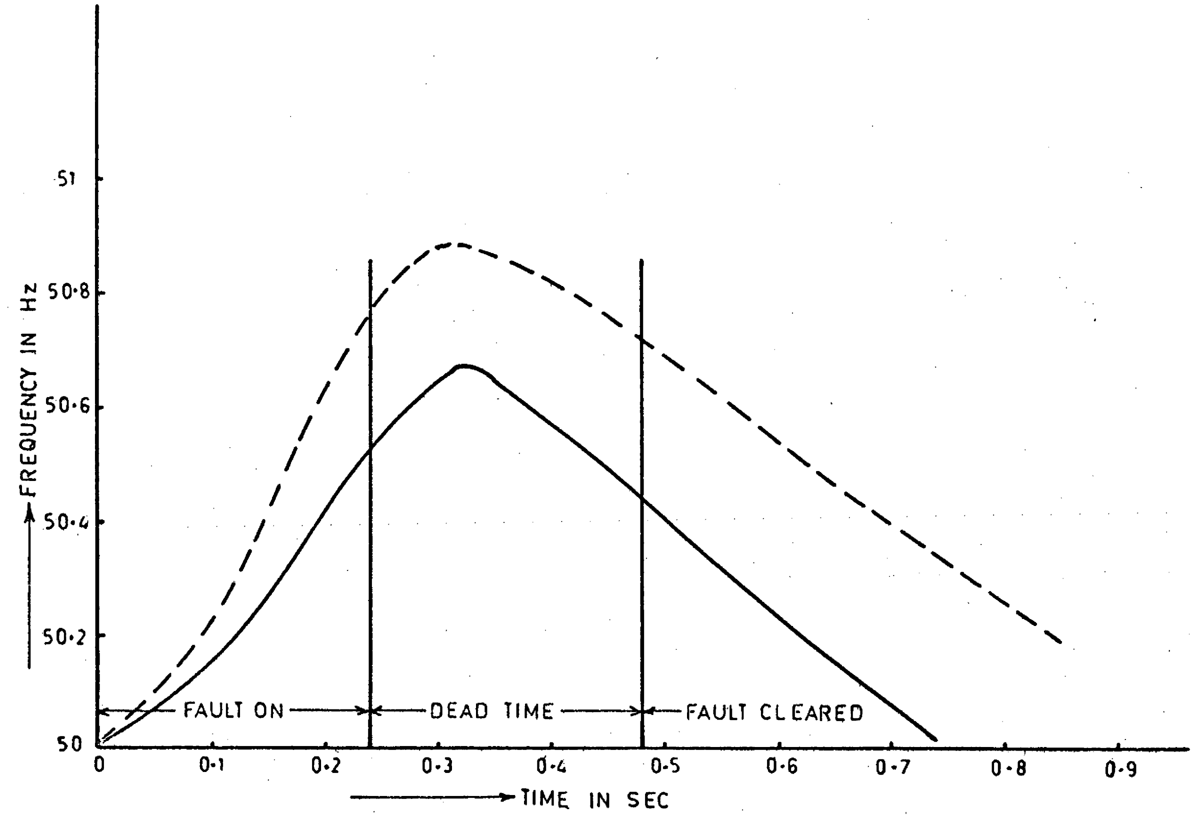

Fig. 6.7(a) Instantaneous frequency variations at bus no. 22.

– – – – – – With VOLT. REG., SATN., TRANS. SAL. AND FLUX DECAY.
———————— " complete instantaneous frequency representation.

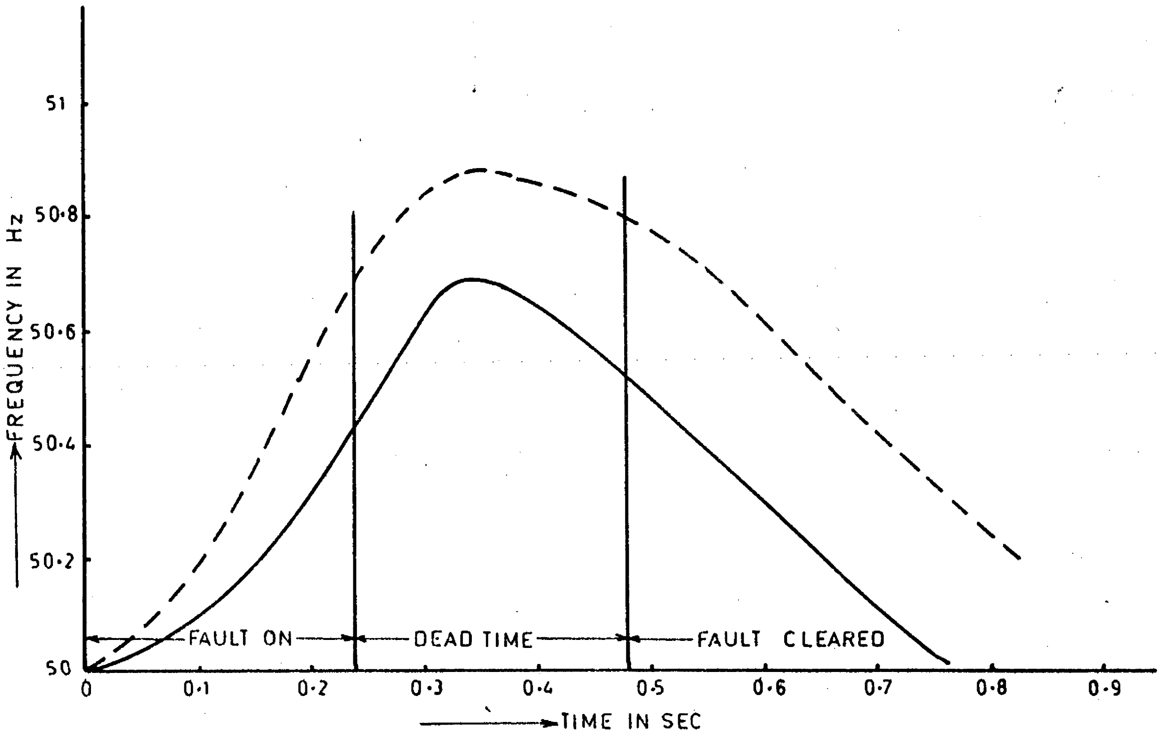

Fig. 6.7(b) Instantaneous frequency variations at bus no. 26.

- - - - - - With VOLT. REG., SATN., TRANS. SAL. AND FLUX DECAY.

———— " complete instantaneous frequency representation.

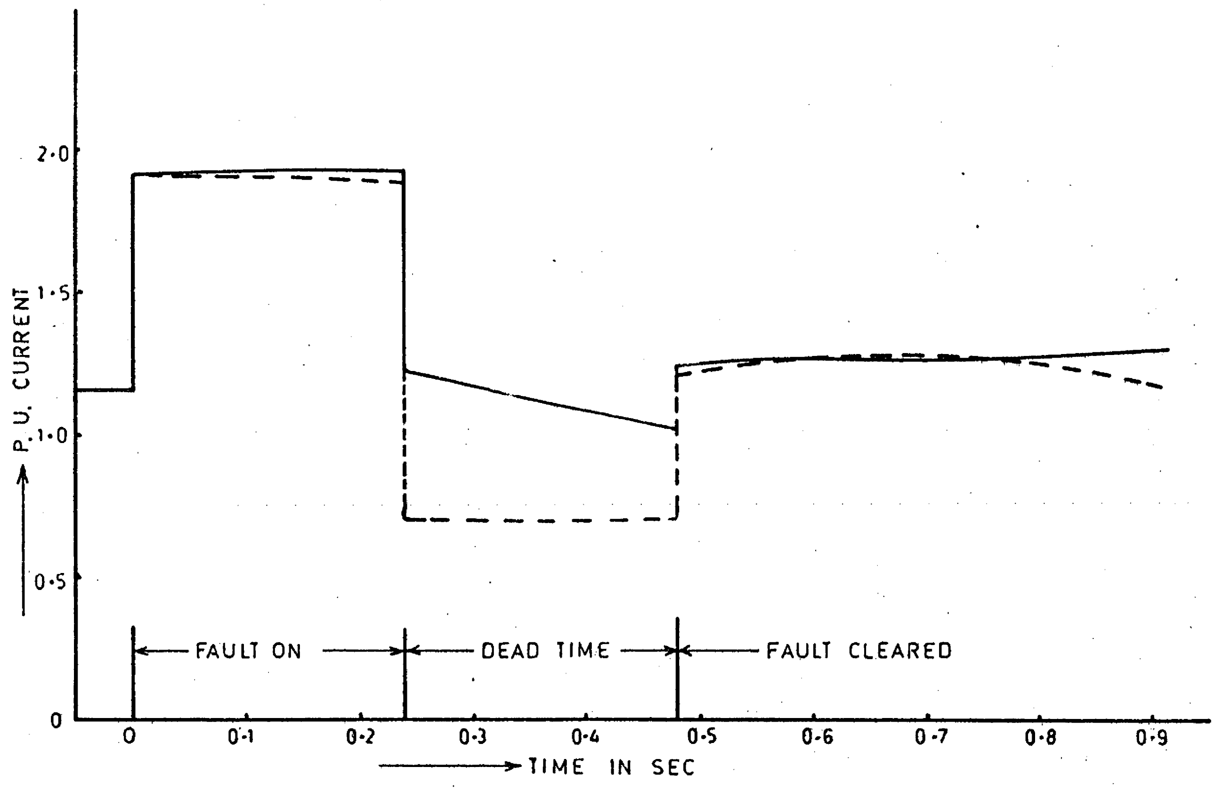

Fig. 6.8(a) Current variations for branch no. 18.

- - - - - - With VOLT. REG., SATN., TRANS. SAL. AND FLUX DECAY.
———— " complete instantaneous frequency representation.

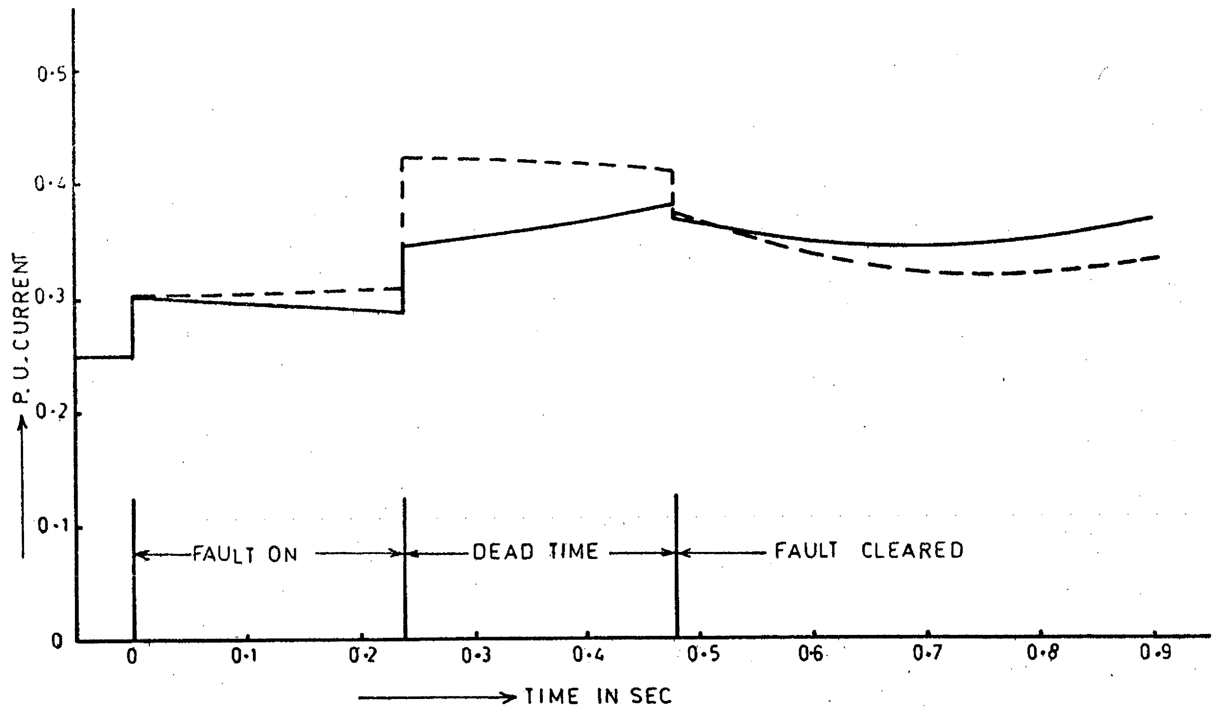

Fig. 6.8(b) Current variations for branch no. 31.

------ With VOLT. REG., SATN., TRANS. SAL. AND FLUX DECAY.
———— " complete instantaneous frequency representation.

damping due to instantaneous frequency effects on the various power system elements. Machine no. 5 starts with negative damping as shown in Figure (6.5a) due to induction motor torque and continues up to the point F_1, then the damping becomes positive until the machine starts decelerating after reclosure; it continues to have negative damping due to induction generator torque up to the point F_2, then again the damping becomes positive. Machine no. 6 begins with positive damping of very small magnitude, due to induction generator torque, and again positive during the decelerating time due to induction motor torque.

Table VIII gives a comparison, based on fault clearance times to cause the system to be just on the verge of instability, between the methods of system assessment. It may be noted that the calculations including the regulating devices only ((i) of Table VII) appear to give safe results, because of the overall positive damping existing on the system. The results confirm the importance of the system load frequency-dependence.

6.4 Discussion

The examples presented in Sections (6.3.1) and (6.3.2) are realistic, in spite of the fact that the first might be considered an extreme case. The results of the studies are significant in that the systems show quite different behaviour in most respects, apart from the fact that frequency-dependence of loads appears to have a very large influence in both cases. With the load composition employed in the calculations, the induction motors clearly have a pronounced effect. In the first example, load behaviour contributes to negative damping, while in the second, it results in positive damping.

The first example illustrates very graphically that the usual practice of neglecting damping in power systems can lead to erroneous and unsafe conclusions. Even though the system may be viewed as somewhat unusual, its essential features are not necessarily so, and the conclusion that the incorporation of instantaneous frequency effects in transient stability studies is necessary, seems warranted. Even in the case where damping is positive and it may appear that it can be neglected, (for example, in the system of Section (6.3.2)), the voltage and current distributions in the network as assessed by conventional means are more favourable than when assessed on the basis of instantaneous frequency considerations, and consequently the neglect of the latter consideration can still give results which are erroneous, as they may lead to unsafe protective relay settings.

Table VII shows the different amounts of computing time required to perform calculations for both problems by the various methods of representation. It is evident that if instantaneous frequency effects are to be incorporated in a study, there is no significant advantage in approximation, and a completely comprehensive assessment should be made. When this is done, a very rich source of information regarding the whole power system is available.

Aspects of including transient frequency deviation effects in power system studies are discussed in Section 7.

7. DISCUSSION

An objective of the work reported herein has been to bring calculated assessment of a power system into closer correspondence with the behaviour of the actual system. Major obstacles to attaining this objective are the relative inaccuracy with which power system parameters are known, and the shortage of information on actual system behaviour when subjected to the conditions postulated in the calculated studies. Notwithstanding the above difficulties, however, various (relatively small effective-magnitude) refinements have been introduced in the past two decades, taking advantage of the power of digital computers. Although the meagre amount of confirmatory evidence from actual power system tests tends in general to support the validity of the computational refinements being introduced, there seems little cause for complacency in this regard.

As already mentioned in section 1.2, a simplification employed in all power system transient stability calculations has hitherto been the treatment of components at system nominal frequency, in spite of the awareness that transient frequency deviations occur during disturbances. This attitude has been apparently taken as a consequence of the viewpoint that such deviations have negligible effect, or at least that their neglect produces safe results. The approach in the present work has been to question and assess whether in fact existing procedures are adequate, and if not, then to ascertain the nature and magnitude of any discrepancy. Because of the aforementioned lack of accuracy in system parameters, and shortage of information on actual power system behaviour, what may be expected to be achieved in the addition of a further refinement to calculations, is a check on the accuracy and relevance of the existing models or representations employed in relation to existing knowledge about power systems, and the capability to ascertain whether or not the proposed refinements are significant.

In introducing transient frequency deviation considerations into power system calculations, the overall viewpoint has been adopted that computational methods introduced should rely only on parameters and other information which might reasonably be expected to be available to power system investigators and planners. It is considered that the methods of study proposed herein substantially fulfil the objective. The information required additional to that normally used in conventional studies (including, for synchronous machines - asynchronous characteristics, governor constants, voltage regulator constants, damping characteristic of the prime mover; for transmission networks - line length, conductor size and spacing; for dynamic loads - number of induction motors and their ratings; for static frequency-dependent loads - details regarding arc furnaces, discharge lamps, mercury arc rectifiers and electric welders), although not readily available to the writer, may reasonably be expected to be available to power system personnel.

Consistent with the above, sections 3, 4 and 5 have aimed to isolate the instantaneous frequency variation effects in specific power system components, while section 6 has been concerned with the study of complete power systems when taking account of transient frequency deviations. Methods have been developed to handle each part of a power system (in addition to the overall system): the various aspects of these methods have already been discussed in sections 3.3, 4.2 and 5.3 respectively for synchronous machines, transmission networks and static and dynamic loads. Accordingly, the discussion in the present section will be limited substantially to considerations involving overall power systems and general computational procedures.

7.1 Remarks on the Developed Computational Procedures

It is relevant to mention that the calculation methods developed to take account of transient frequency deviations have been based largely on the operating characteristics of the various power system components. Thus, induction motors have been handled from knowledge of the torque-slip and stator current-slip characteristics; arc loads have been treated from the viewpoint of the volt-ampere characteristic of the arc; synchronous machine damping has been based on the appropriate asynchronous characteristics of the synchronous machines.

7.1.1 On the Calculation of Time-Varying Processes by Steady-State Techniques

The concept of instantaneous frequency (instantaneous rate of change of time phase divided by 2π) has been introduced in Section 2.2 and employed in Sections 3 to 6 in order to ascertain the effect of transient frequency deviations. In the process of calculations, various network reduction theorems and computational procedures normally valid for fixed frequency operation, are employed - the problem of extension to take account of transient frequency deviations is handled by carrying out computations iteratively at particular "frozen" instants of time, using the corresponding values of appropriate parameters at these instants (as indicated in Section (4.1.1.1)).

7.1.2 Limitation of the Studies to the Transient Stability Interval

The present study and approach to the problem of instantaneous frequency variations on power systems has been limited to the transient stability interval (consequently governor effects have not been included), but the calculation models and procedures are not restricted to this interval and can easily be applied to the dynamic region, i.e. to multi-swing studies. Furthermore, the methods of sections 2 to 6 can readily be incorporated in the latest digital computer programs already developed for power system stability studies.

Reasons for not going beyond the transient stability interval in the studies actually conducted in this project are essentially due to:-

(i) The non-availability to the writer of information regarding:-

(a) Synchronous machines - governor and voltage regulator constants, asynchronous characteristics, and prime-mover damping characteristics.

(b) Induction motors - protective relay characteristics.

(c) Static loads - protective circuit characteristics.

(ii) The fact that comparison over the transient stability interval between studies including, and those not including transient frequency deviations, has in any case highlighted the magnitude and nature of the differences in the two methods of approach. Moreover, stability studies are not often extended past the transient stability interval, except in some large sophisticated system assessments, for example Ref. 237.

7.1.3 Integration Errors

As has been apparent, exclusive use has been made in this project of the Runge-Kutta method of integration, which is being employed increasingly in transient stability studies, owing to its inherent accuracy. Because the error in this method is of the order of $(\Delta t)^5$, (Reference 161), the absolute error in the integration itself is considerably less than 1%, which, for engineering purposes, may be regarded as exact[224].

The integration step interval, Δt, has been selected as 0.05 sec. throughout the previous calculations, but this factor is discussed further in the next section (7.1.4).

7.1.4 Choice of Step Size "Δt"

The main aim of sections 3, 4 and 5 was to highlight the influence of transient frequency deviations on the predicted performance of the various power system elements when considered individually. In the above studies, a step size of 0.05 secs. was chosen as being adequate to compute the appropriate equations in view of the fact that in any case the treatment of only sections of the power system as being transient frequency-dependent (the rest of the system being considered at system nominal frequency), produces an approximate solution only. However, such an approximate solution does underline the various effects of interest and, because it employs a similar step size to that used in standard calculations, it serves as a reasonable basis for comparison between solutions obtained by the methods proposed herein and the conventional procedures.

In the studies of section 6, a step size interval of 0.05 secs. has also been employed in the overall system assessment, but in this case, because the whole system has been treated as frequency-dependent (with consequent enhanced accuracy over that of studies which consider only part frequency-dependence), the question naturally arises as to the influence of the step size on overall accuracy - this is now considered.

In order to ascertain the sensitivity of the solutions of the problems in section 6 to the magnitude of Δt, calculations have been performed employing different step intervals, with the following outcome:-

Table XIV records the peak swings for each of the four machines of the problem in section 6.3.1 for case (iv) of Table VII, when $\Delta t = 0.05$ and 0.025 secs. It will be noted that the calculated peak swing values agree to within 0.1% to 0.5% of the actual peak swing values (within the accuracy possible from the calculation). The corresponding computed critical fault clearance times agree to within much better than $\frac{1}{2}$ millisecond. It will be noted however, that as the frequency-dependence of the system loads has been neglected in case (iv), a large discrepancy between the two step intervals is not to be expected.

TABLE XIV - Comparison Between Peak Swings for Different Step Time Intervals for Case (iv) of Table VII (section 6.3.1)

	First Peak Swings in Degrees	
Δt in sec.	0.05^{o}	0.025^{o}
Machine 1	42.78^{o}	42.57^{o}
Machine 2	-16.08^{o}	-16.06^{o}
Machine 3	-42.53^{o}	-42.48^{o}
Machine 4	36.87^{o}	36.82^{o}
Computing Time *	4.4 minutes	8.0 minutes
Critical Fault Clearance Time	270 m sec.	270 m sec.

* Using IBM 360/50 digital computer.

Table XV shows the peak swings for the same problem of section 6.3.1 when all power system components are considered frequency-dependent (case (vi) of Table VII), when Δt varies over a range from 0.05 to 0.002 secs. It will be apparent that little variation in computed values is to be expected for $\Delta t \leq 0.005$ sec., and that choice of $\Delta t = 0.05$ sec. produces errors of between 0.03% and 4.6% in peak values of the swings. This latter error seems too large, and it would appear to be more appropriate to select $\Delta t = 0.025$ secs. or even 0.01 secs. (if computing time is not at a premium). The respective computed critical fault clearance time changes from 170 m secs. for $\Delta t = 0.05$ sec. to 171 m secs. for the smaller values of Δt (i.e. 0.6% difference in clearance time when Δt changes from 0.05 to 0.025 secs.); this places the discrepancy into better perspective.

TABLE XV - Comparison Between Peak Swings for Different Step Time Interval for Case (vi) of Table VII (section 6.3.1)

	First Peak Swings in Degrees				
Δt in sec.	0.05	0.025	0.01	0.005	0.002
Machine 1	34.28	33.72	33.52	33.45	33.44
Machine 2	-45.00	-44.29	-44.26	-44.25	-44.25
Machine 3	-89.79	-87.13	-86.07	-85.65	-85.64
Machine 4	35.11	35.06	35.14	35.13	35.12
Computing Time *	5.2 min.	9.8 min.	24 min.	48 min.	117 min.
Critical Fault Clearance Time	170 m sec.	171 m sec.	171 m sec	171 m sec.	171 m sec.

* Using IBM 360/50 digital computer.

When step size Δt is changed in the case of the large interconnected system in section 6.3.2, peak swing behaviour for all machines is as shown in Table XVI. It will be seen that the solution may be considered substantially accurate for $\Delta t \leq 0.012$ secs. and that the error in taking $\Delta t = 0.05$ sec. varies between 0.2% to 1.5%. If a step time interval $\Delta t = 0.025$ secs. is chosen, the maximum error becomes 0.3%, which is more than satisfactory. The critical fault clearance time will be seen to decrease by 2 m secs. as Δt is reduced from 0.05 secs. to 0.025 secs. or smaller (0.4%).

TABLE XVI - Comparison Between Peak Swings for Different Step Size Interval, Case (vi) of Table VII (section 6.3.2)

	First Peak Swings in Degrees			
Δt in sec.	0.05	0.025	0.012	0.005
Machine 1	20.45	20.59	20.62	20.63
Machine 2	23.97	24.23	24.29	24.30
Machine 3	46.53	46.59	46.63	46.63
Machine 4	33.37	33.26	33.25	33.25
Machine 5	96.32	97.50	97.79	97.81
Machine 6	84.43	85.25	85.38	85.40
Computing Time *	60 min.	117 min.	230 min.	560 min.
Critical Fault Clearance Time	563 m secs.	561 m secs.	561 m secs.	561 m secs.

* Using IBM 360/50 digital computer.

The above computations indicate that a choice of $\Delta t = 0.05$ secs., which is desirable when comparing the results of the present work with conventional calculating procedures, is probably adequate also for practical purposes. In this case computing errors of the order of up to $\pm$ 5% or so may be expected for individual synchronous machine phase angle peaks which occur at different times but, as the corresponding error in critical fault clearance time may be expected to be less than $\pm$ 1%, these results are probably acceptable. On the other hand, there is no doubt that if the extra computing time is available, choosing $\Delta t = 0.025$ secs. may be advantageous, particularly where various refinements, differing but little from each other, are being investigated. Moreover, because the approximate peak values (due to an insufficiently small Δt) may be larger or smaller than the true values (by 'exact' computation), due to the dependence of the accelerating or retarding forces on relative machine rotor positions during the transient period, it cannot be said that any particular computation is optimistic or pessimistic unless the true value is known.

In the event of electrical transients (for example, for induction motor studies) or sub-transient periods being introduced into the power system stability programs, it is clear that Δt will need to be chosen less than 0.005 sec. ($\frac{1}{4}$ cycle on a 50 cycle/sec. system), depending on the relevant time constants involved.

7.2 Computing Requirements

Table XVII shows various factors relating to computations for the problems of section 6. All programs were written in FORTRAN IV E Language and executed on an IBM 360/50 digital computer (core storage available = 220,000 bytes (1 byte = 8 bits)).

TABLE XVII - Comparison of Computing Requirements for the Problems of Section 6 for Case (vi) of Table VII

Problem	4-Machine Problem Section 6.3.1	6-Machine Problem Section 6.3.2
No. of buses	11	44
No. of lines	12	44
No. of shunt capacitors	-	18
No. of loads	6	18
Program compile time	1.8 minutes	2.9 minutes
Execution time	2.8 "	57.1 "
Printout time	0.6 "	2.0 "
Storage	42,000 bytes	120,000 bytes

The computing time required for a study depends on the following factors:-

(a) System size, i.e. number of buses, lines, series branches with capacitive compensation, shunt capacitors and reactors and frequency-dependent loads.

(b) Number of equivalent synchronous machines.

(c) Fault location.

(d) Time length of the study.

Computing time is affected by (c) in a manner dependent on circumstances, for example, in the large interconnected system of section

6.3.2, the fault on line 24 close to bus no. 24, isolates the two smaller systems - one involving a 2 x 2 admittance matrix for the machines and a 16 x 16 admittance matrix for the system, the other involving a 4 x 4 admittance matrix for the machines, with a 28 x 28 admittance matrix for the system. This situation occurs during the fault application time and continues during the dead time (with the systems separated) - during these times, system size is reduced with consequent reduction in computing time. After the fault is cleared, the system size returns to its original form, i.e. a 6 x 6 matrix for the machines, and a 44 x 44 matrix for the network. As a consequence of the above operation, the execution time listed in Table XVII may be separated into three parts, corresponding respectively to conditions during the fault application, dead time, and after fault clearance.

Execution time for the computer programs will depend approximately on size of admittance matrix involved, which in turn depends on factors (a & b) above, modified by (c). Very approximately, it might be expected that the execution time will depend on the square of the number of buses; the time will be reduced however by the reduction in system size during the fault period and dead time. In Table XVII, execution times for the two problems will not follow the law depending on the square of the number of bus bars, because of the different types of fault applied and the length of time for each study.

Although some trouble has been taken in writing the programs to reduce computing time as far as possible, program optimisation in the limited project time available has not been practicable; moreover, the prime objective of the work has been to study the effects of transient frequency deviations on power systems, rather than to produce a completely refined set of optimum computer programs. In principle however, program optimisation involves no fundamental difficulties.

By giving attention to the following factors, computing time may be reduced to a certain extent:-

(a) Forming the admittance matrix through a connection matrix.

(b) Modifying the statements involving arithmetical operations.

(c) Modifying step size adaptively, such that the changes in the various quantities involved in the computations determine the step time interval chosen at each step.

(d) Employing a display system rather than a printer for output of swing curves.

For a significant reduction in computing time, however, it appears necessary to tackle, from a new viewpoint, the whole problem of the determination of driving point and transfer admittances for the various synchronous machines, because this is the most time-consuming part of the procedures.

With respect to reduction in computing time by possible reduction in complexity of refinements introduced in the frequency-dependence, it is evident from Table VII, that if system loads are to be represented as being frequency-dependent (these have the greatest influence, as discussed further in section 7.3), little extra computing time is necessary to include all of the frequency-dependent refinements (approximately 15% increase). Consequently, there seems only slight profit from simplifying the refinements as a means to reduce computing time.

7.3 Relative Importance of the Various Factors Represented

Figures 6.1 (a-d), 6.3 (a-c) and Table VIII allow comparison to be made between the effects of each factor on critical fault clearance time from the information derived and shown in Table XVIII.

TABLE XVIII - Comparison of Various Factors for Their Influence on Critical Fault Clearance Time

Factor	Circumstance	Contribution of the factor to critical fault clearance time.			
		4-machine problem Section 6.3.1		Large Interconnected System Section 6.3.2	
		in m secs.	percentage*	in m secs.	percentage*
All factors represented.	Case v Table VIII	-96	-36.1	+65	+13.1
System loads	Case vi Table VIII	-100	-37.5	+60	+12.0
Transmission network damping.	Case iv Table VIII	-8	-3.0	-13	-2.6
Machine e.m.f. and angular momentum	Case ii Table VIII	+6	+2.25	+12	+2.4
Machine damping	Case iii Table VIII	+6	+2.25	+6	+1.2
Regulating devices and other synchronous machine refinements.	Case i Table VIII	+5	+1.8 #	+10	+2 #

* % calculations are based on the fault clearance time of case (i) Table VIII.

\# % calculations are based on the fault clearance time of case (ia) Table VIII.

Inspection of the results of studies of the two problems shows the following order of importance, as far as influence on critical fault clearance time is concerned, of the various factors which have been included in the power system representation as being frequency dependent: -

(a) System loads.

(b) Transmission network damping.

(c) Machine e. m. f. and angular momentum.

(d) Machine damping.

(e) Voltage regulator, flux decay, transient saliency and saturation.

It will be noted that in the problems studied, by far the major effect occurs as a result of the frequency-dependence of the system loads, while the factors: transmission network damping; machine e. m. f. and angular momentum; machine damping; and the group;- voltage regulator, flux decay, transient saliency and saturation, have a much smaller effect - all being approximately of the same order.

Machine reactance of itself has a quite negligible influence when considered frequency-dependently, as already indicated in section 3. 3. 1, and is consequently not considered separately in Table XVIII. Its effect on critical fault clearance time is of the order of 0. 1% or so. However in calculations involving frequency-dependent considerations of all power system components (as in the problems of section 6) machine reactance frequency-dependence has been taken into account because it can be considered as part of the power system network and consequently imposes an insignificantly extra demand on computing time.

It will be appreciated that the relative influence of each of the factors included will depend on system parameters and configurations; consequently, the above results are not proposed as indicating hard and fast rules, but show merely the influence of each factor in the specific instances taken.

The contributions of the various factors (system loads, transmission network damping, machine e. m. f. and angular momentum, and machine damping) to the critical fault clearance time, depend of course on the circumstances under which the particular factor has been represented (i.e. on whether all factors are represented simultaneously as being frequency-dependent or only some factors are so represented). However, the orders of the various effects, in the examples considered, are given adequately in Table XVIII.

A further point (already noted previously - for example, in Table XIII) involves the degree of influence on power system behaviour exerted by factor (e) above. In the studies actually computed, lack of adequate information has caused the voltage regulators to be adjusted such that flux decay is just overcome - a perfectly reasonable method of operation and consistent with reported practice[198]. However, this manner of voltage regulator adjustment is not always valid; recent tendencies being in the direction of allowing the voltage regulators to more than overcome the flux decay effects. Consequently, situations may be expected in which effect (e) above does not retain its same relationship to factors (b, c & d) as in the two problems considered here.

Table XIX indicates the order of effect produced in critical switching time by the factors: transient saliency, machine damping and air-gap flux decrement. (The figures cited appear to be representative of those to be found in the literature, although wide variations in these values have been reported). Referring to Table XVIII, shows that even the relatively minor effects introduced in the present report have a magnitude comparable to those in Table XIX which it is already considered worthwhile to include in power system studies. Frequency-dependence of the factors (a-d) above, therefore, has clearly a non-negligible significance in power system transient stability studies.

TABLE XIX - Showing the Effect of Various Factors (Normally Included in Present-Day Studies) on Critical Fault Clearance Time[224].

Factor neglected	Error in critical fault clearance time	
	Typical figure	Maximum value
Saliency	Under-estimation by 3.5%	Under-estimation by 14%
Synchronous machine damping. *	Under-estimation by 1%	Under-estimation by 3%
Induced current effects.	Over-estimation by 3.5%	Over-estimation by 17%

* Reference 195 reports a figure less than 2% in the presence of flux decay. Note that the extreme errors cannot be added as they occur under different conditions .

Finally, it is worth pointing out that not only is frequency-dependence of system components in stability studies of importance in present-day power system studies, but there is a clear trend for this dependence to assume increasing importance in the future, due to various factors, including the following:-

(i) The tendency for large synchronous machines to have low inertia and high internal reactance.

(ii) With the developments of (i), synchronous machine damping assumes greater importance.

(iii) The extension of power system studies into asynchronous modes of behaviour in which transient frequency deviations of up to $\pm$ 5% or so may occur.

(iv) The consideration of employing braking resistors and series capacitors requires a more refined indication as to whether their use is warranted. This can be achieved only through inclusion of frequency-dependent effects which have been shown to have significant influence on power system assessment.

(v) From the viewpoint of economy, a system should be designed to operate as close as possible to its transient stability limits.

(vi) The increasing awareness of the influence of frequency-dependence of system loads.

In summary, it is apparent that frequency-dependence of power system loads has the greatest influence on power system behaviour in relation to the other frequency-dependent factors considered in this study; even so, the relatively minor factors (transmission network damping, machine e. m. f. and angular momentum, and machine damping) have sufficient significance to warrant inclusion in stability studies, particularly as the extra computing time required to include these latter factors is relatively small (section 7. 2).

7.4 Reliability of Data and Accuracy of Prediction

As already suggested in the introduction to sections 1 and 7, a severe restriction on attempts to produce more precise power system calculations is presented by the fundamental difficulty involving the unavailability and accuracy of data. Many studies are normally undertaken before the components for the system or parts of the system in question have been manufactured, in which case, the information used must be design data (rather than test data), which, according to Hore[224] involves an uncertainty as to reliability of the order of $\pm$ 15% or so. Even in studies on an existing system, although it is theoretically possible to obtain test data from the apparatus, Hore considers that errors of between ± 5% and ± 10% may be expected. (He does, however, note that closer tolerance agreement between design and actual parameters may be achieved by manufacturers in equipment at an extra cost).

Not all power system Engineers are as pessimistic as Hore in relation to accuracy of data, but this factor is nevertheless of major significance and may hamper further developments in refining system behaviour until more reliable data appear.

As to the appropriateness of attempts to introduce effects (into power system calculations) whose magnitude is apparently smaller than the errors to be expected in the data on power system components, this important matter must be considered further, especially in relation to the overall prediction accuracy for the system.

Tests carried out on the British 132 KV grid system in 1956 established the effective degree of reliability of the data available and computational methods employed, with the critical fault clearance time actually occurring being predicted to within 5%[173] (the predicted values being on the unsafe side). As has been noted previously, very little information on realistic power system tests is available - a later study[198] did not express a useful quantitative relationship between calculated and measured values, except to mention, in the discussion, that the predicted value of the initial rotor swing for the generator nearest to the fault was, on average, approximately 5% greater than the measured value - with the difference between predicted and measured values being greater for generators remote from the fault. This reference concluded that "predictions from conventional-type multi-machine studies showed slightly pessimistic forecasting of the magnitude of the first rotor swing. The findings of previous investigations[173], which suggested that the conventional method ignored factors which aid stability, are thus confirmed". The author has been unable to discover information on accuracy of computations in relation to practical tests for more refined representations than used in the above two reports. However, by implication, more recent studies, such as that concerning Dynamic Stability of the Peace River Transmission System[237], {in which high voltage lines have been represented without using equivalents (other transmission circuits have been considered as constant impedance π sections) and synchronous machines have been represented in differing degree of complexity - the most detailed including: direct and quadrature axes, flux linkage decay in both axes, saturation in both axes, positive sequence damping, mechanical damping, and detailed excitation and governor systems. Inertia constants were used for all units without the assumption of an infinite bus. (The study recommended use of braking resistors as an aid to stability}, appear to consider that agreement between calculated and actual system performance is very close, otherwise many of the effects actually represented would, because of their small magnitude, appear to be unprofitably represented.

Kimbark, in the discussion of a paper by Lokay & Bolger[219], has commented that the stability limits calculated by conventional method (which has been used for many years) agree within 1 or 2% with limits calculated by a method which includes the following refinements: machine damping, excitation control and resulting change of field flux linkage, saturation, system damping, and speed governor action. Although some of the representations in the study concerned are suspect (particularly machine damping and system damping), it is indicative of the 'state of the art' that quantities as small as 1% to 2% in their overall influence, are considered as non-trivial.

In view of the above, although there is still a great deal of uncertainty about overall prediction accuracy which can be achieved with the data available, it might be considered reasonable to expect 5% (or better) agreement between theory and practice when adequate care is taken in obtaining the necessary data. In this situation, quantities which affect system performance by amounts even as low as .1% or so, may be considered to be of interest, particularly if the nature and direction of their effects are not obvious.

The apparent inconsistency between the achievement of 5% or better expected agreement between predicted and measured overall power system behaviour and the uncertainty of data on power system components of up to $\pm$ 15% or so (as indicated by Hore) may be explained at least in part, by the fact that a given error in a given parameter of a particular power system component does not affect the whole system of which it is part, to nearly the same extent. For example, a 10% error in a reactance in series with a larger reactance of nine times the nominal value of the first (reactance), influences the total nominal reactance by only 1%. Again, an error in inertia factor of a synchronous machine will have a reduced influence on critical fault clearance time, as this latter is affected by the square root of the inertia factor (reference 224, page 366).

In considering whether a factor should or should not be included in a representation, it may be noted that the error resulting from neglect of the factor is likely to be greater than that which follows from including it together with inaccuracies in its parameter values. (For example, in the case of a particular synchronous machine connected to an infinite bus through a reactor X_e, considered on page 315 of reference 224, it is shown that neglect of saliency introduces an (under estimation) error in critical fault clearance time of 5.3%. The author has recalculated this problem but with a 10% increase in X_e and X_q, combined with a 10% reduction in X_d, with the consequence that these changes in reactance cause only a 0.7% change in critical fault clearance time).

Further considerations on the problem of whether or not to include a particular factor depend on the magnitude and direction of the effects which the factor may be expected to produce on the predictions. Although certain factors may be relatively small in magnitude, (or may be subject to a large degree of uncertainty in the magnitude of their parameters), if there is confidence as to their nature and influence, there seem strong reasons for inclusion. Neglecting the contributions of machine e.m.f. and angular momentum, voltage regulator action, saturation and saliency, is possible as it produces an underestimation of critical fault clearance time (safe solution), whereas neglecting flux decay produces overestimation of fault clearance time (unsafe solution), and seems undesirable. Factors, on the other hand, such as synchronous machine damping, transmission network damping and system load damping, may each produce either reduced or enhanced critical fault clearance times, depending on circumstances, and should therefore not be neglected. Even though it is apparent that neglecting certain factors may be safe, it seems desirable to include all factors whose effect is known to be non-trivial, as this produces a prediction closer to the true value (in spite of uncertainties in the values of the parameters).

Finally, load demand is a determining factor in power system planning, and although forecasts of magnitude and composition of system loads are not precise, the <u>actual</u> load demands which must be met are factual entities which the system must supply, and which must be known as accurately as possible. Forecasts may be continually modified in the light of new information, but once a given peak load demand has been established, the system must be proved capable (through control and adjustment - for example, by tap-changing, excitation, compensation, load allocation) of meeting that demand. It is the task of a study to investigate each such situation and to produce predictions as close as possible to the true values - any factor which assists this process is of interest and utility.

In the light of the discussion of the present section, the magnitude of the effects introduced by transient frequency-deviation considerations (recorded in Table XVIII for two specific problems) are such that the respective effects have adequate significance for inclusion in power system transient stability studies. It is clear, however, that much must still be done in relating predicted with actual power system performance before full confidence can be established in any assessment procedures.

7.5 Recommendations Regarding Practical Power System Studies

The studies carried out in this project have indicated the importance of taking transient frequency deviation effects into account in power system stability studies. In two realistic problems investigated, the degree of influence exerted - with frequency-deviation effects included - when expressed in terms of critical fault clearance time, has amounted to 1%-3% for each of the factors: machine damping, machine e.m.f. and angular momentum, and transmission network damping. In the case of system loads, magnitude of influence amounted to 37.5% and 12% in the respective problems (Table XVIII). (With all of the above factors included simultaneously, the total influence produced by transient frequency deviation considerations on critical fault clearance time was respectively 36.1% and 13.1%). The above degree of influence of frequency-dependent factors in the problems concerned, compares with about 2% effect on critical fault clearance time produced by including voltage regulator action, flux decay, saturation and saliency.

In making recommendations regarding use of the work (reported herein) in practical power system studies, it seems clear that because of the major effect exerted by the loads, and as in any case loads are key factors in influencing overall system performance, their precise treatment cannot be neglected. The studies presented in Section 6.3 demonstrate the major influence of frequency-dependence of system loads on the stability of the system, all other frequency-dependent factors having relatively small effect. However, the above relative comparison between the various frequency-dependent factors will not necessarily apply for other power systems, and, because of the comparatively small increase in computer time required to include all refinements (approximately 15% increase as indicated in Section 7.2), it seems highly desirable that all factors should be included.

A further strong reason for considering all frequency-dependent factors, even though some of these have only minor effect on transient stability, exists because of the bearing which all frequency-dependent factors have on the voltage and current distribution in the system. For purposes of protective relay settings under disturbed conditions, it would seem to be unwise to ignore even the minor factors, because avoidable uncertainties find their way into the derived relay settings, which may prove disadvantageous under abnormal conditions.

The present studies have shown that the degree of significance of frequency-dependent effects is adequate to warrant their inclusion in power system transient stability investigations, and it is recommended that assessment of actual power systems should take these effects into account. In order to assure a reasonable accuracy of computation consistent with the nature and magnitude of the effects represented, section 7.1.4 has indicated that the Runge-Kutta integration method, employing normally a step time interval of 0.05 sec. is satisfactory, although cases may arise in which a shorter interval of 0.025 sec. may be necessary for enhanced accuracy.

8. FURTHER WORK

Report of the work in this thesis has covered the introduction of transient frequency deviation effects in power system stability studies. On a number of occasions, it has been clear that various aspects of the problem have not been completely solved and may, with advantage, be studied further. The following is noted in particular:-

8.1 Dynamic Region Studies

As has already been indicated in section 7.1.2, the procedures developed herein can be employed in studying the dynamic stability (multi-swing) region if the necessary information on system parameters is available. Further study is needed on:-

(a) The performance of induction motor protective devices - for example, providing protection against; phase failure, under voltage and overcurrent - for isolating operation of induction motors from the rest of the system under abnormal circumstances.

In the past, (and in the present studies), it has been assumed that induction motor protective relays are so sluggish that there is sufficient delay in their operation, during which time the fault can be cleared and normal system configuration restored. If their response is instantaneous, (which is not likely, as such response does not occur even for the more refined protective devices used for synchronous generators), the resulting isolation of the induction motors will pose serious problems because of sudden change in load demand, the degree of seriousness depending upon the system configuration. Because of the delayed operation of induction motor protective devices, this factor has been neglected even in the case of important induction motors, such as feed water pump motors in power stations.

Information on the actual protective system behaviour is relevant to studies in the dynamic region, and is suggested as a profitable line for further investigations. It may be useful to study the dynamic performance of the protective systems from the design parameters, taking account of the types of circuit breakers employed for isolating purposes. Experimental investigations are required to establish the response of the protective systems to terminal voltage variations.

(b) Characteristics of the protective systems of arc furnace loads - arc furnace loads normally operate at more than 80% power factor, and in cases where the arc furnace terminal voltage falls to 80% or below, the arc will extinguish due to insufficient voltage being available for its maintenance - active load will therefore be dropped from the system, leaving the furnace transformer operating at no load, drawing magnetising current at very low power factor, together with a capacitive current (which may probably overcompensate the inductive vars) if, as is common, shunt capacitors are used for power factor improvement and arc cessation. Investigations require to establish whether or not the arc will restrike if normal voltage is restored. The problem involves the dynamic behaviour of electrode moving equipment in conjunction with the protective relays and the types of circuit breakers employed. In the past, such loads have been represented by lumped impedances, but a more appropriate representation would be valuable.

(c) Asynchronous system operation - the present thesis presents refinements which can handle asynchronous operation if synchronous machine asynchronous characteristics are known. Asynchronous torques can possibly be assessed by employing the asynchronous characteristic of the machine and the rotor instantaneous slip with respect to the instantaneous resultant air gap flux, as has been used in evaluating synchronous machine damping in section 3. With the above information, asynchronous power system operation may be studied.

8.2 Validity of Induction Motor Model

The induction motor model used in the present studies is limited in the manner discussed in section 5.1.1.6, where it is seen that with too drastic a collapse of supply voltage, the motor will be operating in an unstable region of its torque-slip characteristic for which the representation is not valid. For studies which involve serious collapse of voltage, therefore, it is necessary to develop an improved model.

8.3 Considerations of Back Swings of Synchronous Machines

In the case of synchronous machines, impulsive forces come into play both when a fault occurs and when it is cleared. These forces have been demonstrated clearly by the back swings of synchronous generators on an actual system, as well as in micro-machine studies[198]. Such impulsive forces may be negative or positive.

To take account of the back swing in stability studies, a method has been suggested in reference 174, to delay the acceleration for a particular time (0.06 sec. (3 cycles) stated). This is not satisfactory however, as reference 198 indicates that the nature and magnitude of back swing may vary according to the circumstances. Even if the figure of 0.06 sec. were applicable to a given machine under all conditions, it might still change for different machines. An investigation is needed to clarify the factors which influence the back swing, following which a mathematical model may be formed for inclusion in the swing curve computations.

8.4 Considerations of Electrical Transients of Asynchronous Machines

In the case of asynchronous machines, electrical transients have been neglected in the present studies, but in the light of the above back swing considerations of synchronous machines (Section 8.3), and the rapid fault clearing achieved by modern equipment, electrical transients need to be considered. A possible approach is to represent the induction motor by two parallel circuits, one considering the dynamic and frequency-dependent behaviour as proposed in the present thesis, and the other considering the electrical transients. Mutual effects between the two circuits would need to be included.

8.5 Man-Machine and Computer Program Optimization

Some of the long computing times required in the present work indicate that major power systems may require very lengthy runs on computers to investigate thoroughly problems which incorporate a large number of calculating refinements. It is possible with present day input/output equipments and procedures to devise methods of handling problems in which obviously unprofitable computations can be eliminated or terminated at any stage by appropriate man-machine interaction during the course of a study. Graphical and cathode ray console terminals seem useful in this respect. Computer Program Optimization (Section 7.2) would also be helpful.

8.6 Reliability of Data

The need for more accurate power system data has been evident in the present work. More attention must be directed to this problem, otherwise the development of further refinements in power system calculations will be seriously hampered.

8.7 Comparison Between Predicted and Actual Power System Behaviour

There is little doubt that a comprehensive set of practical tests designed to assess in detail the accuracy and relevance of computational procedures and models would be of tremendous value to the electric power industry.

The studies suggested in Sections 8.6 and 8.7 above, seem capable of realisation only through major effort and co-operation between the manufacturers, electricity authorities and consumers.

9. CONCLUSIONS

It has been the aim of the work described in this report to investigate both separately and in an integrated manner, the effects of transient frequency deviations on power system components, with a view to ascertaining the degree of importance which these effects exert on power system behaviour. The general approach to the problem has involved the use of actual operating characteristics, thereby by-passing uncertainties on the various parameters involved. A further objective guiding the work has been the desire to develop procedures employing data which may be reasonably expected to be available to power system investigators.

To consider the frequency-dependence of the various power system elements in transient stability studies, the following procedures, along with their computer programs, have been developed: -

(a) Determination of the instantaneous frequency of a bus voltage or a branch current in any part of a power system subjected to a disturbance.

(b) Ascertaining the effect on stability of change in synchronous machine e. m. f., stored energy and machine reactance, due to change in instantaneous rotor angular velocities under abnormal situations.

(c) Developing methods for taking account of synchronous machine damping by employing the asynchronous characteristics (asynchronous output power vs. slip), and the rotor slip with respect to the resultant air gap flux.

(d) Considering the transmission network damping effects due to change in network parameters as a result of deviations in instantaneous frequencies.

(e) Representing the normal general purpose induction motor loads either for a single machine or for machine groups as frequency-dependent and dynamic.

(f) Representing the normally met passive loads - such as: mercury arc rectifiers, arc furnaces, discharge lamps and electric welders - as frequency-dependent.

The computing procedures for taking account of transient frequency deviations have been applied to two realistic power system problems, and the magnitude of influence exerted by each factor has been identified. The major influence has been contributed by the system loads, but even (frequency-dependent) factors such as transmission network damping, synchronous machine e. m. f., angular momentum and damping, have been found to produce a non-negligible effect, whose influence can be as large as that of other refinements already considered worthwhile for inclusion in transient stability studies, (for example, voltage regulator action, saliency, saturation and flux decay).

The procedures developed for including transient frequency deviation effects in power system stability studies are applicable not only to the transient period but, in the presence of adequate information regarding values of the necessary parameters, can be employed also for dynamic stability (multi-swing) studies.

In the course of this work, it has become evident that much remains to be done in improving the reliability of data and in investigating the degree of agreement between power system performance as predicted by the various procedures and models available, and that which applies in actual practice on a real system - this situation imposes severe restrictions on the evaluation of any refinements (including those introduced herein) to power system study procedures. It is suggested that these problems and other more specialized factors arising from the present studies, are worthy of further attention.

As a result of the work reported, it can be recommended that transient frequency deviations should be taken into account in power system transient stability studies which, if they are to take proper advantage of the refinements, should employ an accurate method of integration (such as the Runge-Kutta method) with possibly a step time interval of 0.025 sec. or less, although the normal step time interval of 0.05 sec. may normally be expected to be adequate. It is desirable to include all frequency-dependent factors in the representation of the system for, although the system load effects are the most predominant, neglect of the smaller factors allows only a small saving in computing time (less than 15%) and even if in this case stability is assessed with acceptable accuracy, current and voltage distributions in the system may be sufficiently in error to give erroneous relay settings.

The procedures and models introduced to take account of transient frequency deviation effects can be readily incorporated in digital computer conventional transient stability programmes.

10 APPENDIX

10.1 Solution of voltages under transient conditions

The bus where the e.m.f. of a machine acts will be referred to as the machine internal bus. Under transient disturbances, when the e.m.f's of the various machines swing, the voltage and current phasors for the whole system change their phase angles with respect to the X-axis of the reference plane (See Figure 2.2).

Voltage at the machine internal bus m, is

$$\underline{V}_m = E_m \cos \delta_m + jE_m \sin \delta_m \tag{10.1}$$

Replace all the loads by their equivalent admittances at the system nominal frequency Then, as a first approximation, the voltages for all other buses are taken as

$$\underline{V}_k = 1 + j0$$

By using the above approximate voltage values, node voltages are corrected one by one while assuming the others as constant. Let a voltage correction for the node k, that is,

$$\Delta\underline{V}_k = a_k + jb_k$$

be added to the voltage of node k, so that it gives the nett current to the node as zero.

Estimated voltage of node k,

$$\underline{V}_k = e_k + jg_k$$

Nett current to the node,

$$\underline{I}_k = c_k + jd_k$$

$$= \sum_{\ell=1}^{N} \left[(G_{k\ell} + jB_{k\ell}) \cdot (e_\ell + jg_\ell) \right]$$

Equating the real and imaginary components of $\underline{I}_k$, gives

$$c_k = \sum_{\ell=1}^{N} (G_{k\ell}\, e_\ell - B_{k\ell}\, g_\ell)$$

$$d_k = \sum_{\ell=1}^{N} (G_{k\ell}\, g_\ell + B_{k\ell}\, e_\ell)$$

In order to make the nett current input to the node k equal to zero,

$$(a_k + jb_k) \cdot (G_{kk} + jB_{kk}) + \underline{I}_k = 0 \qquad (10.2)$$

or $$a_k = \frac{-\underline{I}_k}{G_{kk} + jB_{kk}}$$

$$b_k = \frac{-\underline{I}_k}{G_{kk} + jB_{kk}}$$

or $$a_k = -(c_k\, G_{kk} + d_k\, B_{kk}) \,/\, (G_{kk}^2 + B_{kk}^2)$$

$$b_k = (c_k\, B_{kk} - d_k\, G_{kk}) \,/\, (G_{kk}^2 + B_{kk}^2)$$

In this way, voltages for all the other nodes are calculated in complex form and the process is repeated until the voltage correction falls within a predetermined index, for example 10^{-5} P.U. volts.

The corrected voltage for the node k is then

$$\underline{V}_k = (e_k + a_k) + j\,(g_k + b_k)$$

Branch Currents

$$\underline{I}_{k\ell} = (\underline{V}_k - \underline{V}_\ell) \cdot (-\underline{Y}_{k\ell}) = r_{k\ell} + j\,r'_{k\ell} \qquad (10.3)$$

$$= \left[(e_\ell - e_k) + j\,(g_\ell - g_k) \right] \cdot (G_{k\ell} + jB_{k\ell})$$

Equating the real and imaginary components,

$$r_{k\ell} = (e_\ell - e_k)\,G_{k\ell} - (g_\ell - g_k)\,B_{k\ell}$$

$$r'_{k\ell} = (e_\ell - e_k)\,B_{k\ell} + (g_\ell - g_k)\,G_{k\ell}$$

Phase angles

$$\theta_{k\ell} = \text{Arctan}\,\frac{r'_{k\ell}}{r_{k\ell}}$$

$$\theta_k = \text{Arctan}\,\frac{(g_k + b_k)}{(e_k + a_k)}$$

In operation, using an accelerating factor of 1.6, the above method converges in 15-20 iterations to give a solution correct to within the abovementioned index of 10^{-5} P. U. volts.

10.2 Torque-Slip and Current-Slip Characteristics versus Frequency

Figure (5.2) indicates the equivalent circuit of an induction motor. $R'_1 + jX'_1$ is the equivalent impedance of $r_1 + jx_1$ and jx_3, in parallel as shown in Figure (10.1). By applying Thevenin's theorem,

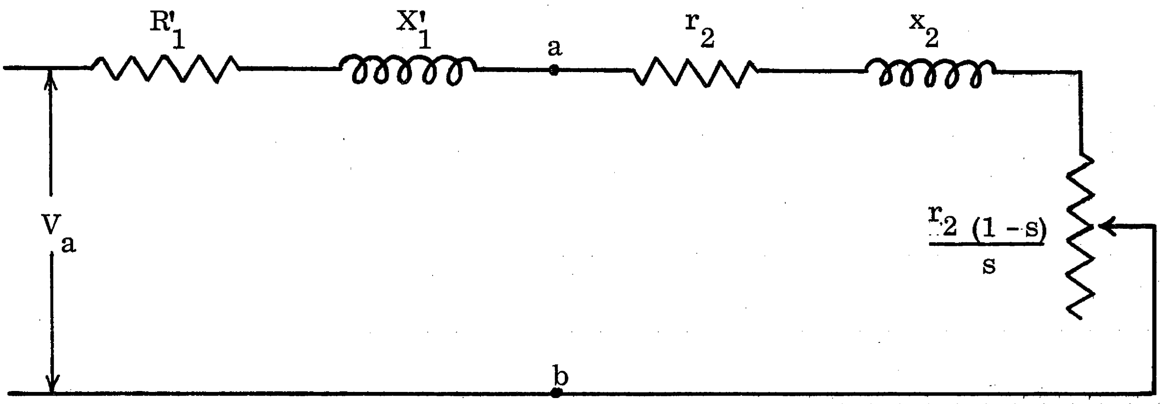

Fig. 10.1 Equivalent circuit for Fig. 5.2 by Thevenin's theorem.

$$x_{11} = x_1 + x_3$$

$$V_a = V \frac{jx_3}{r_1 + jx_{11}}$$

and
$$T = \frac{m V_a^2 \frac{r_2}{s} p}{2\pi f \left\{ (R'_1 + \frac{r_2}{s})^2 + (X'_1 + x_2)^2 (\frac{f}{f_o})^2 \right\}} \text{ newton-m} \qquad (10.5)$$

From equation (10.5), the slope of the torque-slip characteristic at $s = 0$,

$$\frac{\partial T}{\partial s} = \frac{m V_a^2 p}{2\pi f r_2} \qquad (10.6)$$

The current drawn by the motor,

$$I = \frac{V_a}{\sqrt{(R_1' + \frac{r_2}{s})^2 + (X_1' + x_2)^2 \cdot (\frac{f}{f_o})^2}} \tag{10.7}$$

From equation (10.7), the slope of the current-slip characteristic at s = 0,

$$\frac{\partial I}{\partial s} = \frac{V_a}{r_2} \tag{10.8}$$

Equation (10.8) indicates $\frac{\partial I}{\partial s}$ is independent of the instantaneous operating frequency, at s = 0.

From the current-slip characteristic, $I = I_{om} + C's$, where the coefficient C' is modified for instantaneous frequency as

$$C'' = C' \sqrt{\frac{R^2 + X^2}{R^2 + (\frac{f}{f_o})^2 X^2}} \tag{10.9}$$

and $$I = I_{om} \frac{f_o}{f} + C'' s \tag{10.10}$$

With the modified current and knowing the active power, the instantaneous reactive power can be calculated.

10.3 Normalized Torque-slip Curves for Induction Motors

From the equivalent circuit of an induction motor shown in figure (10.1),

$$T = \frac{m V_a^2 (\frac{r_2}{s})}{\omega_1 \left\{(R_1' + \frac{r_2}{s})^2 + (X_1' + x_2)^2\right\}} \tag{10.11}$$

The equation (10.11) can be normalized by writing it as a relation between the ratios ${}^{T}/_{T_{max}}$ and ${}^{s}/_{s_{max\,T}}$.

The torque developed by an induction motor is maximum when the power delivered to (${}^{r_2}/_{s}$) branch in figure (10.1) is a maximum. This requires the impedance matching principle in circuit theory, i.e. the power delivered to the branch (${}^{r_2}/_{s}$) will be a maximum when its magnitude is equal to the magnitude of the impedance of the remaining circuit.

i.e. $$\frac{r_2}{s_{max\,T}} = \sqrt{R_1'^2 + (X_1' + x_2)^2}$$

or $$s_{max\,T} = \frac{r_2}{\sqrt{R_1'^2 + (X_1' + x_2)^2}} \tag{10.12}$$

and $$T_{max} = \frac{0.5 \times m \quad V_a^2}{\omega_1 \left\{R_1' + \sqrt{R_1'^2 + (X_1' + x_2)^2}\right\}} \tag{10.13}$$

dividing equation (10.11) by (10.13),

$$\frac{T}{T_{max}} = \frac{2\left[R_1' + \sqrt{R_1'^2 + (X_1' + x_2)^2}\right] {}^{r_2}/_{s}}{(R_1' + {}^{r_2}/_{s})^2 + (X_1' + x_2)^2} \tag{10.14}$$

Substituting the value of r_2 in (10.14) from (10.12), and replacing $\left(\frac{X_1' + x_2}{R_1'}\right)$ by 'A', we get,

$$\frac{T}{T_{max}} = \frac{1 + \sqrt{A^2 + 1}}{1 + 0.5\sqrt{A^2 + 1}\left(\frac{s}{s_{max\,T}} + \frac{s_{max\,T}}{s}\right)} \tag{10.15}$$

Figure (10.2) indicates the effect of 'A' for normalized curves, for a general purpose induction motor within the range of 1 to 1000 horsepower for which the information such as inertia factor, power factor, efficiency, full load and magnetising current, has been assembled in section (5.1.1.5). The factor 'A' varies from 3 to 7 and the ratio T_{max}/T varies from 2 to 3.

If 'A' becomes infinitely large, there is very small influence on the normalized curves shown in figure 10.2, and the equation (10.15), becomes,

$$\frac{T}{T_{max}} = \frac{2}{\frac{s}{s_{max\,T}} + \frac{s_{max\,T}}{s}} \tag{10.16}$$

Equation (10.16) has been employed to study the starting performance of induction motors[186].

10.4 Effect of Number of Poles on Inertia Factor

From the design formula of an induction motor,[179]

$$\text{Input KVA} = \frac{1.11\, K_w\, \pi^2\, B\, ac\, d^2 \ell\, f_o}{\eta\, p \cos\phi}\, 10^{-3} \tag{10.17}$$

$$H = \frac{5.48 \times 10^{-6}\, J\, n_1^2}{\text{Rating in kVA}} \quad \text{KW-sec/KVA} \tag{10.18}$$

Assuming the rotor to be a solid cylinder,

$$J = \rho\, \frac{\pi d^2}{4}\, \ell\, \frac{d^2}{8} \quad \text{Kg - m}^2 \tag{10.19}$$

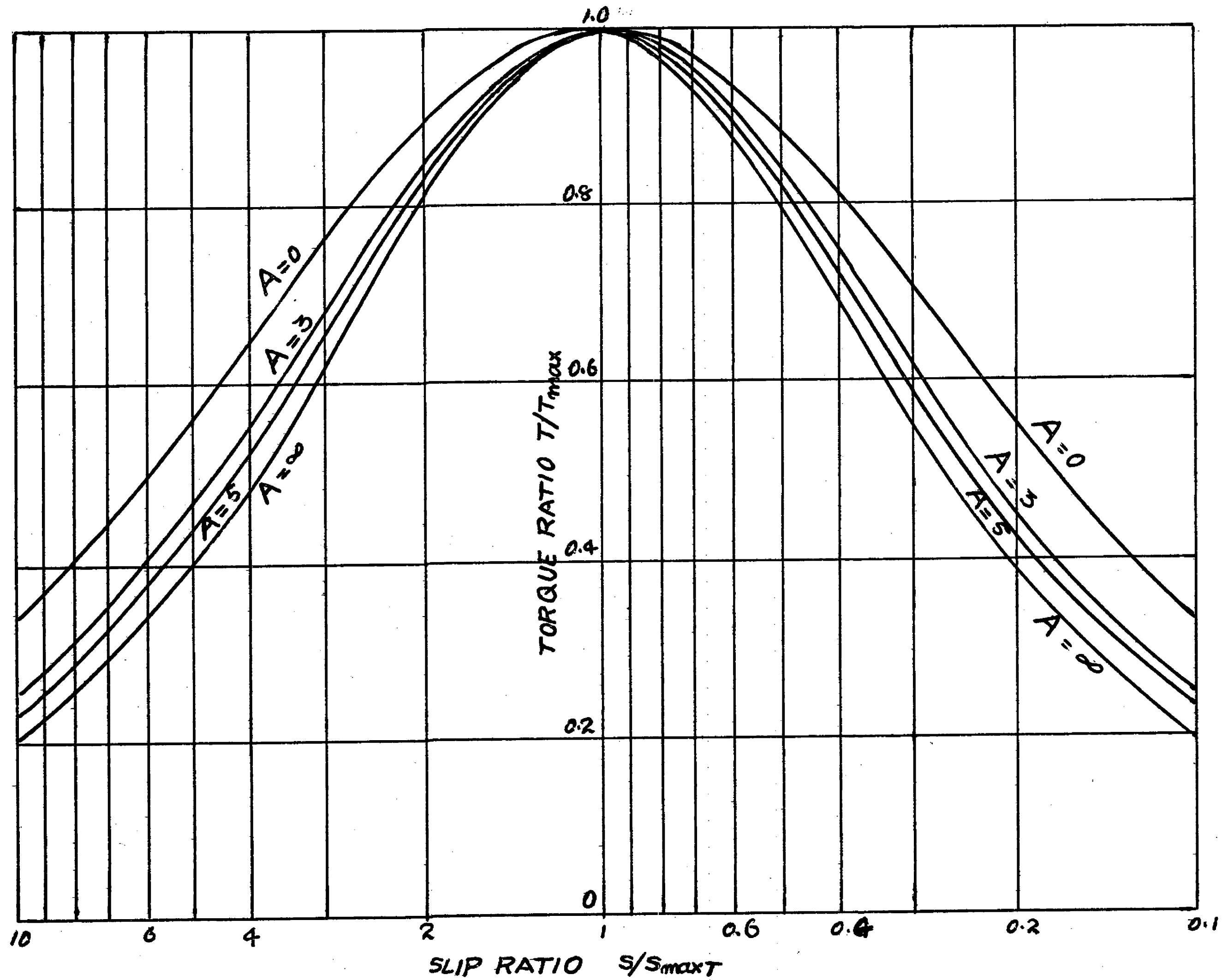

Fig. 10.2 Normalized torque-slip curves for polyphase induction motors.

or from equations (10.17, 10.18 and 10.19),

$$H = K \frac{d^2 f_o}{B\ ac\ p} \tag{10.20}$$

where $K = 17.7 \rho\ \eta \cos\phi$

The diameter of the rotor depends upon the number of poles and the shape of poles, such as square or rectangular. In order to study the effect of number of poles on the inertia factor, assume square poles, which is the usual practice.

That is, pole pitch = rotor length

or $$\ell = \frac{\pi d}{2p}$$

Substituting for ℓ in equation (10.17),

$$\text{Input KVA} \propto \frac{B\ ac\ d^3 f_o}{p^2}$$

For fixed values of Input KVA, B, ac and f_o,

$$\frac{d^3}{p^2} = \text{Constant}$$

or $$d \propto p^{2/3} \tag{10.21}$$

Substituting for d in equation (10.20),

$$H \propto \frac{p^{1/3}}{B\ ac} \tag{10.22}$$

Equation (10.22) indicates that the inertia factor will increase when the number of poles is increased for fixed values of specific magnetic and electric loading, which in practice depends on the $d : \ell$ ratio. However, because of the cube root, this increase is only a small one as the number of poles increases. From equation (10.22) there will be a reduction in inertia factor due to increased values of B and ac. Moreover, the inertia factor contribution by other moving parts of the motor, such as the overhangs of the rotor winding, sliprings, shaft, cooling fan, pulley and the rotor end rings, will fall due to reduced synchronous speed, which further reduces the overall inertia factor of the motor itself, and thus the inertia factor becomes approximately independent of number of poles. In practice, for economic reasons of manufacturing, it is not always possible to have square poles, because the standard frame sizes will restrict the choice of rotor diameter, and consequently the inertia factor does not follow a definite law. The inertia factor contribution of the load has been found at least equal to that of the driving motor as pointed out earlier.

10.5 Assessment of Equivalent Parameters (Full load slip, η, power factor, H and I_{om})

For an equivalent torque-slip characteristic, the overall slip for a group of induction motors is required.

In figure (10.3), the torque-slip characteristics of two induction motors are shown as nos. 1 and 2.

From the assumption of linearity,

$$T_1 = \alpha_1 s \text{ and } T_2 = \alpha_2 s$$

the resultant slip,

$$s = \frac{T_1 + T_2}{\alpha_1 + \alpha_2} \tag{10.23}$$

$$T_j = \frac{746 \times 60 \, hp_j}{2\pi \, n_{1j} \, (1 - s_j)} \quad \text{newton-m}$$

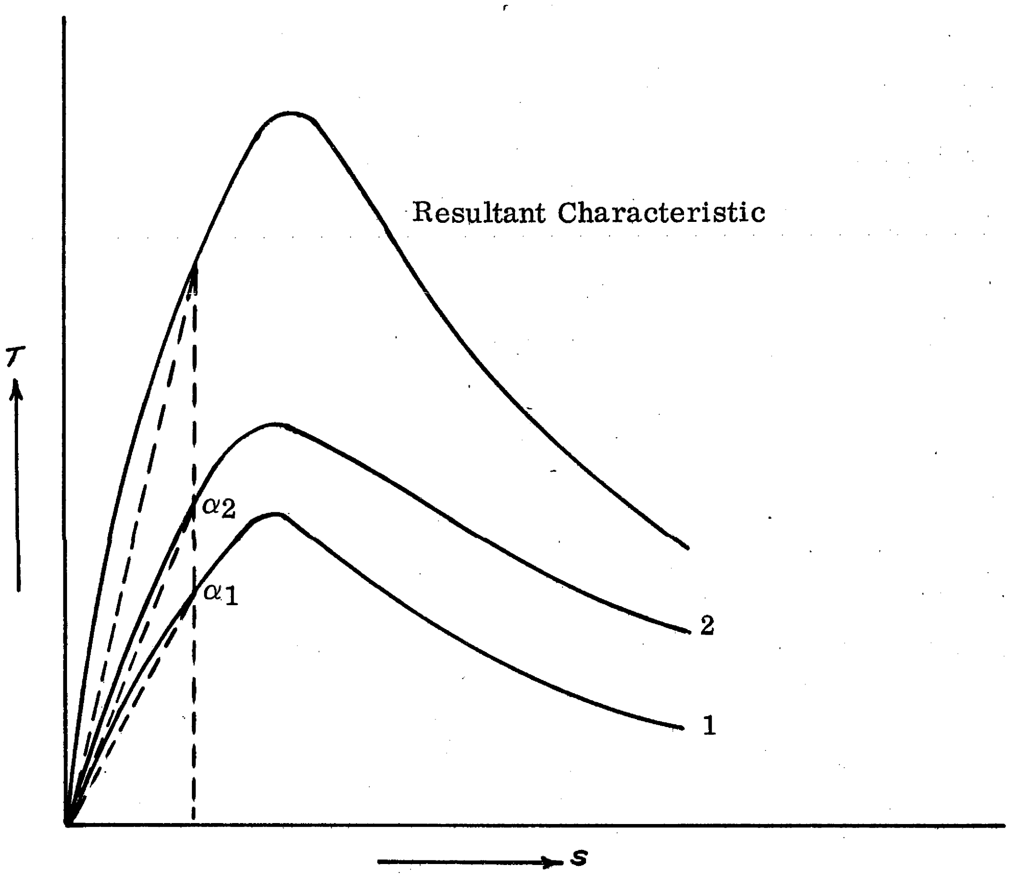

Fig. 10.3 Resultant of two torque-slip characteristics.

For an equivalent motor, substitute equation (10.24) in (10.23),

$$s = \frac{\dfrac{hp_1}{n_{11}(1-s_1)} + \dfrac{hp_2}{n_{12}(1-s_2)}}{\dfrac{hp_1}{n_{11}(1-s_1)s_1} + \dfrac{hp_2}{n_{12}(1-s_2)s_2}} \tag{10.25}$$

For j types of motors with K_j quantities,

Equivalent slip (in p.u.)

$$= \frac{\dfrac{K_1 \cdot hp_1}{n_{11}(1-s_1)} + \dfrac{K_2 \cdot hp_2}{n_{12}(1-s_2)} + \cdots \dfrac{K_j\, hp_j}{n_{1j}(1-s_j)}}{\dfrac{K_1 \cdot hp_1}{n_{11}(1-s_1)s_1} + \dfrac{K_2 \cdot hp_2}{n_{12}(1-s_2)s_2} + \cdots \dfrac{K_j\, hp_j}{n_{1j}(1-s_j)s_j}} \tag{10.26}$$

Equivalent efficiency

$$= \frac{\Sigma K_j \cdot hp_j}{\dfrac{\Sigma K_j\, hp_j}{\eta_j}} \tag{10.27}$$

Equivalent Inertia factor (in KW - sec/KVA)

$$= \frac{\Sigma \dfrac{K_j \cdot hp_j \cdot H_j}{\eta_j \quad \cos\phi_j}}{\Sigma \dfrac{K_j \cdot hp_j}{\eta_j \quad \cos\phi_j}} \tag{10.28}$$

Equivalent Power factor

$$= \frac{\Sigma \dfrac{K_j \cdot hp_j}{\eta_j}}{\Sigma \dfrac{K_j \cdot hp_j}{\eta_j \cos\phi_j}} \tag{10.29}$$

Equivalent magnetising current (as fraction of full load current)

$$= \frac{\sum \frac{K_j \cdot hp_j \cdot \gamma_j}{\cos \phi_j \quad \eta_j}}{\sum \frac{K_j \quad hp_j}{\cos \phi_j \quad \eta_j}} \tag{10.30}$$

10.6 Study with Equivalent Circuit

From the assumption of linearity, that is $T = \alpha\,\omega$

$$\text{then} \qquad J \cdot \frac{d\,\omega}{dt} = \alpha\,\omega - T_\ell \tag{10.31}$$

i. Assuming T_ℓ as constant,

$$\omega = \frac{T_\ell}{\alpha} + A' \cdot \exp\left(\frac{\alpha}{J}\right) t \tag{10.32}$$

$$\text{and} \qquad A' = \omega_o - \frac{T_\ell}{\alpha}$$

From equation (10.32) the instantaneous angular speed is given by,

$$\omega = \frac{T_\ell}{\alpha}\left(1 - \exp\left(\frac{\alpha}{J}\right) t\right) + \omega_o \exp\left(\frac{\alpha}{J}\right) t \tag{10.33}$$

ii. Assuming $T_\ell = a\,\omega$, where "a" is a constant, then the equation (10.31) becomes,

$$J \cdot \frac{d\,\omega}{dt} = \alpha\omega - a\omega \tag{10.34}$$

or $$\omega = A' \, . \, \exp \left(\frac{\alpha - a}{J}\right) t \tag{10.35}$$

and $$A' = \omega_o$$

From equation (10.35), the instantaneous angular velocity of the motor,

$$\omega = \omega_o \, . \, \exp \left(\frac{\alpha - a}{J}\right) t \tag{10.36}$$

10.7 Study with Proposed Approximate Method

From the assumption of linearity, $T = \alpha s$, under steady state conditions at the point F, $\alpha = \dfrac{T_\ell}{s_{oo}}$.

$$s = \frac{\omega_1 - \omega}{\omega_1}$$

or $$\frac{ds}{dt} = \frac{-1}{\omega_1} \cdot \frac{d\omega}{dt} \tag{10.37}$$

and $$J \, . \, \frac{d\omega}{dt} = \alpha s - T_\ell$$

or $$J(-\omega_1)\frac{ds}{dt} = \alpha s - T_\ell \tag{10.38}$$

i. Assuming T_ℓ as constant,

from equation (10.38), the instantaneous slip is obtained as,

$$s = \frac{T_\ell}{\alpha} + A' \, . \, \exp \left(\frac{-\alpha}{J\,\omega_1}\right) t \tag{10.39}$$

and $$A' = s_1 - \frac{T_\ell}{\alpha} \qquad (10.40)$$

The instantaneous slip in p. u. of the motor is given by,

$$s = \frac{T_\ell}{\alpha} \left(1 - \exp\left(-\frac{\alpha}{J\,\omega_1}\right) t\right) + s_1 \,.\, \exp\left(-\frac{\alpha}{J\omega_1}\right) t \qquad (10.41)$$

ii. Assuming $T_\ell = a\,\omega$, where "a" is a Constant, then equation (10.38) becomes,

$$J\,(-\,\omega_1)\,\frac{d\,s}{d\,t} = \alpha s - a\,\omega_1 + a\,\omega_1\,s \qquad (10.42)$$

or $$s = \frac{a\,\omega_1}{\alpha + a\omega_1} + A' \,.\, \exp - \left(\frac{\alpha + a\,\omega_1}{J\,\omega_1}\right) t \qquad (10.43)$$

From equation (10.43),

$$A' = s_1 - \frac{a\,\omega_1}{\alpha + a\,\omega_1} \qquad (10.44)$$

The instantaneous slip in P. U. of the motor is given by,

$$s = \frac{a\,\omega_1}{\alpha + a\,\omega_1} \left(1 - \exp - \left(\frac{\alpha + a\,\omega_1}{J\,\omega_1}\right) t\right) + s_1 \,.\, \exp - \left(\frac{\alpha + a\omega_1}{J\,\omega_1}\right) t$$

(10.45)

10.8 Effect of Reactive Power on Active Power

In order to see the effect of reactive power variations on the active power demand, an inductive load has been considered, as shown in figure (10.4), supplied through a transmission line of R' + j X' impedance.

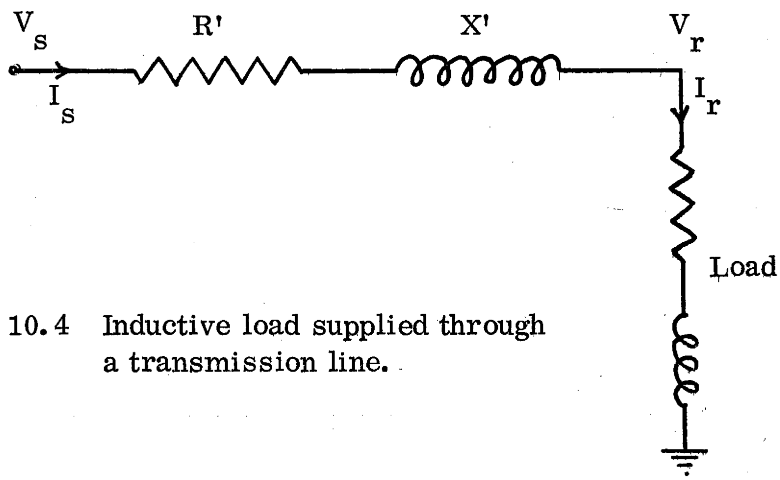

Fig. 10.4 Inductive load supplied through a transmission line.

By using the approximate formula for the sending end voltage,

$$V_s = V_r + I_r R' \text{Cos } \Psi + I_r X' \text{Sin } \Psi$$

Given I_r and V_r, the base current and voltage respectively,

$$\frac{V_s}{V_r} = 1 + \underbrace{\frac{I_r R'}{V_r} \cos \Psi}_{\text{I}} + \underbrace{\frac{I_r X'}{V_r} \sin \Psi}_{\text{II}} \qquad (10.46)$$

For a fixed value of V_r, the reactive power at the receiving end is proportional to $I_r \sin \Psi$. If this component falls, then the sending end voltage falls and results in a nett reduction in the active power demand at the sending end. For example, assuming that per unit resistance and reactance are 0.02 and 0.1 respectively,

For 0.8 lagging power factor load current of 1P.U. at 1 P.U. voltage,

$$V_s = 1 + \underbrace{0.02 \times 0.8}_{\mathrm{I}} + \underbrace{0.1 \times 0.6}_{\mathrm{II}}$$

$$= 1.076$$

For 1% change in reactive power at the receiving end, the term II in equation (10.46) is reduced by 1%, resulting in a 0.06% change in V_s, and the active power demand is reduced approximately by 0.12%; whereas for 0.9 lagging power factor load, 1% reduction in reactive power at the receiving end will result in a 0.0872% reduction in the sending end active power demand.

10.9 Variations of input power to an inductive circuit when the circuit resistance is inversely proportional to the current, that is, $R \propto \frac{1}{I}$

$$\text{or} \quad R = \frac{K}{I} \tag{10.47}$$

Current in an inductive circuit,

$$I = \frac{V}{\sqrt{R^2 + (2\pi fL)^2}} \tag{10.48}$$

Substituting for R in equation (10.48) and rearranging,

$$(K)^2 + 4\pi^2 f^2 L^2 I^2 = V^2$$

$$\text{or} \quad I^2 = \frac{V^2 - K^2}{4\pi^2 f^2 L^2} \tag{10.49}$$

Active power input,

$$P = I^2 . R$$

Substituting for I^2 and R from (10.47) and (10.49),

$$P = \frac{V^2 - K^2}{4\pi^2 f^2 L^2} \times \frac{K}{\sqrt{\dfrac{V^2 - K^2}{4\pi^2 f^2 L^2}}}$$

$$= \frac{K . \sqrt{V^2 - K^2}}{2\pi f L} \qquad (10.50)$$

or $$P \propto \frac{V \sin \phi}{f} \qquad (10.51)$$

Reactive power input,

$$Q = I^2 . 2\pi f L$$

Substituting for I^2 from (10.49),

$$Q = \frac{V^2 - K^2}{4\pi^2 f^2 L^2} \times 2\pi f L$$

$$= \frac{V^2 - K^2}{2\pi f L} \qquad (10.52)$$

or $$Q \propto \frac{V^2 \text{Sin}^2 \phi}{f} \qquad (10.53)$$

10.10 Variations of input power to an inductive circuit when the circuit resistance is independent of frequency

$$P = \frac{V^2 . R}{R^2 + 4\pi^2 f^2 L^2} \tag{10.54}$$

Equation (10.54) indicates that the active power falls when the instantaneous frequency rises.

$$Q = \frac{V^2 . 2\pi f L}{R^2 + 4\pi^2 f^2 L^2} \tag{10.55}$$

Differentiate equation (10.55) with respect to f,

$$\frac{dQ}{df} = \frac{2\pi L V^2 \left\{(R^2 + 4\pi^2 L^2 f^2) - 8\pi^2 L^2 f^2\right\}}{(R^2 + 4\pi^2 f^2 L^2)^2} \tag{10.56}$$

For a saddle point, $\frac{dQ}{df}$ should be zero.

From equation (10.56),

$$R^2 = 4\pi^2 f^2 L^2 \quad \text{or}$$

$$R = 2\pi f L \tag{10.57}$$

or Instantaneous Resistance = Instantaneous Reactance

or the operating power factor = 0.707

From equations (10.55 and 10.57), it is observed that Q is maximum when the operating power factor is 0.707, that is, Q will be maximum at a frequency which will operate the circuit at 0.707 power factor.

11. REFERENCES AND SELECTED BIBLIOGRAPHY

1. G. STERN,
"The Couplings of Alternating Current Dynamos in Parallel Circuit".
Electrical Review, March 16, 1888, pp.287-288.

2. NOTE,
"The Mordey Victoria Alternators".
Electrical Review, May 31, 1889, p.626.

3. C.P. STEINMETZ,
"Speed Regulation of Prime-Movers and Parallel Operation of Alternators".
AIEE, Trans., Vol. 18, 1901, p.741.

4. W.L.R. EMMET,
"Parallel Operation of Engine-Driven Alternators".
AIEE, Trans., Vol. 18, 1901, p.745.

5. E. HOSPITALIER,
"Notice of Exhibits in Class 23 in the Paris Exhibition - Production et Utilisation Mecaniques de l'electricite".
IEE Journal, Vol. 30, 1901, pp.26-28.

6. E.F. ALEXANDERSON,
"A Self-Exciting Alternator".
AIEE, Trans., Vol. 25, 1906, pp.61-80.

7. M. BROOKS,
"Interaction of Synchronous Machines - A Graphical Solution by Means of a New Circle Diagram".
AIEE, Trans., Vol. 26, Pt. II, 1907, pp.1027-1048.

8. W.B. JACKSON,
"Advantages of Unified Electric Systems Covering Large Territories".
AIEE, Trans., Vol. 30, Pt. I, 1911, pp.131-165.

9. R.A. PHILIP,
"Economic Limitations to Aggregation of Power Systems".
AIEE, Trans., Vol. 30, Pt. I, 1911, pp. 597-636.

10. R.F. SCHUCHARDT and E.O. SCHWEITZER,
"The Use of Power-Limiting Reactances with Large Turbo-Alternators".
AIEE, Trans., Vol. 30, Pt. II, 1911, pp. 1143-1194.

11. C.P. STEINMETZ,
"Development of the Modern Central Station".
AIEE, Trans., Vol. 30, Pt. II, 1911, pp. 1213-1249.

12. W.A. DURGIN and R.H. WHITEHEAD,
"The Transient Reactions of Alternators".
AIEE, Trans., Vol. 31, Pt. II, 1912, pp. 1657-1693.

13. D.B. RUSHMORE,
"Excitation of Alternating-Current Generators".
AIEE, Trans., Vol. 31, Pt. II, 1912, pp. 1841-1880,

14. M. LEBLANC,
"Electric Transmission of Energy by Alternating Currents at Very High Pressures".
IEE, Journal, Vol. 51, 1913, pp. 679-713.

15. E.P. HOLLIS,
"Reactance Coils in Power Circuits".
IEE, Journal, Vol. 52, 1914, pp. 254-261.

16. J. LYMAN, L.L. PERRY and A.M. ROSSMAN,
"Protective Reactors for Feeder Circuits of Large City Power Systems".
AIEE, Trans., Vol. 33, Pt. II, 1914, pp. 1509-1519.

17. K.M. FAYE-HANSEN and J.S. PECK,
"Current-limiting Reactances on Large Power Systems".
IEE, Journal, Vol. 52, 1914, pp. 511-529.

18. E.L.M. EMTAGE and A. ARNOLD,
"The Control of Electrical Generators by Automatic Pressure Regulators".
IEE, Journal, Vol. 52, 1914, pp. 769-773.

19. N.S. DIAMANT,
"Calculation of Sudden Short-Circuit Phenomena of Alternators".
AIEE, Trans., Vol. 34, 1915, pp.2237-2278.

20. N.L. POLLARD and J.T. LAWSON,
"Experience and Recent Developments in Central Station Protective Features".
AIEE, Trans., Vol. 35, Pt. I, 1916, pp.695-715.

21. J.A. JOHNSON,
"Reactors in Hydro-Electric Stations".
AIEE, Trans., Vol. 36, 1917, pp.105-124.

22. P.B. JUHNKE,
"Effect of Current Limiting Reactors on Turbo-Generator Systems Under Conditions of Short Circuit".
AIEE, Trans., Vol. 36, 1917, pp.125-152.

23. R.E. DOHERTY and O.E. SHIRLEY,
"Reactance of Synchronous Machines and its Applications".
AIEE, Trans., Vol. 37, Pt. II, 1918, pp.1209-1340.

24. R.F. SCHUCHARDT,
"The Use of Reactors on Large Central Station Systems".
AIEE, Trans., Vol. 39, Pt. 2, 1920, pp.1195-1214.

25. C.P. STEINMETZ,
"Power Control and Stability of Electric Generating Stations".
AIEE, Trans., Vol. 39, Pt. 2, 1920, pp.1215-1287.

26. J.T. BARRON and A.E. BAUHAN,
"Considerations Which Determine the Selection and General Design of an Exciter System".
AIEE, Trans., Vol. 39, Pt. 2, 1920, pp.1521-1561.

27. W. ROGOWSKI,
"Short-Circuit of an A-C Generator".
Arch. fur Elek., Vol. 11, 1922, pp.147-154.

28. L. ROMERO and J.B. PALMER,
"The Interconnection of Alternating Current Power Stations".
IEE, Journal, Vol. 60, 1922, pp.287-303.

29. N. L. POLLARD,
"Operating Experience With Current-Limiting Reactors".
AIEE, Trans., Vol. 42, 1923, pp. 546-551.

30. O. R. SCHURIG,
"A Miniature A.C. Transmission System - For the Practical Solution of Network and Transmission Problems".
AIEE, Trans., Vol. 42, 1923, pp. 831-840.

31. M.W. SMITH,
"Water Wheel Generators and Synchronous Condensers for Long Transmission Lines".
AIEE, Trans., Vol. 42, 1923, pp. 1043-1053.

32. R.D. EVANS and H.K. SELS,
"Power Limitations of Transmission Systems".
AIEE, Trans., Vol. 43, 1924, pp. 26-38.

33. R.D. EVANS and R.C. BERGVALL,
"Experimental Analysis of Stability and Power Limitations".
AIEE, Trans., Vol. 43, 1924, pp. 39-58.

34. C.M. LAFFOON,
"Short Circuits of Alternating-Current Generators".
AIEE, Trans., Vol. 43, 1924, pp. 356-373.

35. P.H. THOMAS,
"New Type of High-Tension Network - An Interconnecting System for the Supply of Electric Power Over Large Areas".
AIEE, Trans., Vol. 43, 1924, pp. 599-620.

36. F.H. KIERSTEAD and H.O. STEPHENS,
"Current-Limiting Reactors - Their Design, Installation and Operation".
AIEE, Trans., Vol. 43, 1924, pp. 902-913.

37. H.H. SPENCER and H.L. HAZEN,
"Artificial Representation of Power Systems".
AIEE, Trans., Vol. 44, 1925, pp. 72-79.

38. V. BUSH and R.D. BOOTH,
"Power System Transients".
AIEE, Trans., Vol. 44, 1925, pp. 80-103.

39. R. F. FRANKLIN,
"Short-Circuit Currents of Synchronous Machines".
AIEE, Trans., Vol. 44, 1925, pp.420-435.

40. C.A. NICKLE and F.L. LAWTON,
"An Investigation of Transmission-System Power Limits".
AIEE, Trans., Vol. 45, 1926, pp.1-21.

41. E. CLARKE,
"Steady-State Stability in Transmission Systems - Calculation by Means of Equivalent Circuits or Circle Diagrams".
AIEE, Trans., Vol. 45, 1926, pp.22-41.

42. R. WILKINS,
"Practical Aspects of System Stability".
AIEE, Trans., Vol. 45, 1926, pp.41-50.

43. R.D. EVANS and C.F. WAGNER,
"Studies of Transmission Stability".
AIEE, Trans., Vol. 45, 1926, pp.51-94.

44. R.E. DOHERTY and C.A. NICKLE,
"Synchronous Machines, I - Extension of Blondel's Two-Reaction Theory".
AIEE, Trans., Vol. 45, 1926, pp.912-947.

45. O.E. SHIRLEY,
"Stability Characteristics of Alternators".
AIEE, Trans., Vol. 45, 1926, pp.1108-1115.

46. R.E. DOHERTY and C.A. NICKLE,
"Synchronous Machines - Torque-Angle Characteristics Under Transient Conditions".
AIEE, Trans., Vol. 46, 1927, pp.1-8.

47. F.H. CLOUGH,
"Stability of Large Power Systems".
IEE, Journal, Vol. 65, No. 367, 1927, pp.653-673.

48. C.F. WAGNER and R.D. EVANS,
"Static Stability Limits and the Intermediate Condenser Station".
AIEE, Trans., Vol. 47, 1928, pp.94-123.

49. R.E. DOHERTY,
"Excitation Systems - Their Influence on Short Circuits and Maximum Power".
AIEE, Trans., Vol. 47, 1928, pp.944-956.

50. R.H. PARK and E.H. BANCKER,
"System Stability as a Design Problem".
AIEE, Trans., Vol. 48, 1929, pp.170-194.

51. S.M. JONES and R. TREAT,
"Power Limit Tests - On Southeastern Power and Light Company's System".
AIEE, Trans., Vol. 48, 1929, pp.268-282.

52. Y.K. KU,
"Transient Analysis of AC Machinery".
AIEE, Trans., Vol. 48, 1929, pp.707-715.

53. R.H. PARK,
"Two-Reaction Theory of Synchronous Machines - Generalized Method of Analysis".
AIEE, Trans., Vol. 48, 1929, pp.716-730.

54. E.J. BURNHAM, J.R. NORTH and I.R. DOHR,
"Quick-Response Generator Voltage Regulator - Field Tests Made with Oscillograph".
AIEE, Trans., Vol. 48, 1929, pp.903-911.

55. H.W. TAYLOR,
"Voltage Control of Large Alternator".
IEE, Journal, Vol. 68, No. 339, 1930, pp.317-338.

56. H.E. EDGERTON and F.J. ZAK,
"The Pulling Into Step of a Synchronous Induction Motor".
IEE, Journal, Vol. 68, 1930, pp.1205-1210.

57. I.H. SUMMERS and J.B. McCLURE,
"Progress in the Study of System Stability".
AIEE, Trans., Vol. 49, 1930, pp.132-161.

58. C.A. NICKLE and C.A. PIERCE,
"Stability of Synchronous Machines - Effect of Armature Circuit Resistance".
AIEE, Trans., Vol. 49, 1930, pp.338-351.

59. W.V. LYON and H.E. EDGERTON,
"Transient Torque-Angle Characteristics of Synchronous Machines".
AIEE, Vol. 49, 1930, pp.686-699.

60. H.L. HAZEN, O.R. SCHURIG and M.F. GARDNER,
"The M.I.T. Network Analyzer".
AIEE, Trans., Vol. 49, 1930, pp.1102-1114.

61. F.R. LONGLEY,
"The Calculation of Alternator Swing Curves - The Step by Step Method".
AIEE, Vol. 49, 1930, pp.1129-1151.

62. C.F. WAGNER,
"Damper Windings for Water-Wheel Generators".
AIEE, Trans., Vol. 50, 1931, pp.140-151.

63. R.C. BUELL, R.J. CAUGHEY, E.M. HUNTER and V.M. MARQUIS,
"Governor Performance During System Disturbances".
AIEE, Trans., Vol. 50, 1931, pp.354-369.

64. R.C. BERGAVALL,
"Series Resistance Method of Increasing Transient Stability Limit".
AIEE, Trans., Vol. 50, 1931, pp.490-497.

65. E. CLARKE,
"Simultaneous Faults on Three Phase Systems".
AIEE, Trans., Vol. 50, 1931, pp.919-941.

66. S.B. CRARY and M.L. WARING,
"Torque-Angle Characteristics of Synchronous Machines Following System Disturbances".
AIEE, Trans., Vol. 51, 1932, pp.764-774.

67. F.A. HAMILTON,
"Field Tests to Determine the Damping Characteristics of Synchronous Generators".
AIEE, Trans., Vol. 51, 1932, pp.775-779.

68. R.H. PARK,
"Two-Reaction Theory of Synchronous Machines - II".
AIEE, Trans., Vol. 52, 1933, pp.352-355.

69. H.L. BYRD and S.R. PRITCHARD,
"Solution of Two Machine Stability Problem".
Gen. Elec. Rev., Vol. 36, 1933, pp.81-93.

70. J.C. PRESCOTT and J.E. RICHARDSON,
"The Inherent Instability of Synchronous Machinery".
IEE, Journal, Vol. 75, (July-Dec.), 1934, pp.497-511.

71. S.B. CRARY, L.P. SHILDNECK and L.A. MARCH,
"Equivalent Reactance of Synchronous Machines".
AIEE, Trans., Vol. 53, 1934, pp.124-132.

72. H.B. DWIGHT,
"A Graphical Solution of Steady-State Stability".
AIEE, Trans., Vol. 53, 1934, pp.566-568.

73. F.H. GULLIKSEN,
"Electronic Regulator for AC Generators".
AIEE, Trans., Vol. 53, 1934, pp.877-881.

74. O.G.C. DAHL and A.E. FITZGERALD,
"Equivalent Circuits in Stability Studies".
AIEE, Trans., Vol. 53, 1934, pp.1272-1282.

75. W.D. HORSLEY,
"The Stability Characteristics of Alternators of Large Interconnected Systems".
IEE, Journal, Vol. 77, No. 467, 1935, pp.577-611.

76. O.G.C. DAHL,
"Stability of the General 2-Machine System",
AIEE, Trans., Vol. 54, 1935, pp.185-188.

77. C. KINGSLEY,
"Saturated Synchronous Reactance".
AIEE, Trans., Vol. 54, 1935, pp.300-305.

78. L.A. KILGORE,
"Effects of Saturation on Machine Reactances".
AIEE, Trans., Vol. 54, 1935, pp.545-550.

79. L.W. CLARK,
"Power Company - Service to Arc Furnaces".
AIEE, Trans., Vol. 50, 1935, pp.1173-1178.

80. B.B. PRENTICE,
"Fundamental Concepts of Synchronous Machine Reactance".
AIEE, Trans., Supplement to 1937 Transactions, pp.1-21.

81. S.B. CRARY,
"Two-Reaction Theory of Synchronous Machines".
AIEE, Trans., Vol. 56, 1937, pp.27-31.

82. A.S. LANGSDORF,
"Contributions to Synchronous-Machine Theory".
AIEE, Trans., Vol. 56, 1937, pp.41-48.

83. C. CONCORDIA and H. PORITSKY,
"Synchronous Machine with Solid Cylindrical Rotor".
AIEE, Trans., Vol. 56, 1937, pp.49-58.

84. AIEE SUBCOMMITTEE,
"First Report on Power System Stability".
AIEE, Trans., Vol. 56, 1937, pp.261-282.

85. C. CONCORDIA,
"Two-Reaction Theory of Synchronous Machines with Any Balanced Terminal Impedance".
AIEE, Trans., Vol. 56, 1937, pp.1124-1127.

86. Y.H. KU,
"Extension of 2-Reaction Theory to Multi-Phase Synchronous Machines".
AIEE, Trans., Vol. 56, 1937, pp.1197-1201.

87. C.F. WAGNER,
"Unsymmetrical Short Circuits on Water-Wheel Generators Under Capacitive Loading".
AIEE, Trans., Vol. 56, 1937, pp.1385-1395.

88. E.W. KIMBARK,
"Network Analyzer Solution of Multiple Unbalances".
AIEE, Trans., Vol. 56, 1937, pp.1476-1482.

89. H.P. KUEHNI and R.G. LORRAINE,
"A New A.C. Network Analyzer".
AIEE, Trans., Vol. 57, 1938, pp.67-73.

90. F.H. KIERSTEAD,
"Some Schemes of Current-Limiting-Reactor Application".
AIEE, Trans., Vol. 57, 1938, pp.272-280.

91. E. CLARKE, C.N. WEYGANDT and C. CONCORDIA,
"Over-Voltages Caused by Unbalanced Short Circuits - Effect of Amortisseur Windings".
AIEE, Trans., Vol. 57, 1938, pp.453-468.

92. C. CONCORDIA, S.B. CRARY and J.M. LYONS,
"Stability Characteristics of Turbine Generators".
AIEE, Trans., Vol. 57, 1938, pp.732-744.

93. H.C. STANLEY,
"An Analysis of the Induction Machine".
AIEE, Trans., Vol. 57, 1938, pp.751-757.

94. C.F. DALZIEL,
"Static Power Limits of Synchronous Machines".
AIEE, Trans., Vol. 58, 1939, pp.93-102.

95. R.B. GEORGE and B.B. BESSESEN,
"Generator Damper Windings at Wilson Dam".
AIEE, Trans., Vol. 58, 1939, pp.166-172.

96. W.K. BOICE, S.B. CRARY, G. KRON and L.W. THOMSON,
"The Direct-Acting Generator Voltage Regulator".
AIEE, Trans., Vol. 59, 1940, pp.149-157.

97. T.G. LE CLAIR,
"Arc-Furnace Loads on Long Transmission Lines".
AIEE, Trans., Vol. 59, 1940, pp.234-242.

98. M.M. LIWSCHITZ,
"Positive and Negative Damping in Synchronous Machines".
AIEE, Trans, Vol. 60, 1941, pp.210-213.

99. W.W. PARKER,
"The Modern A.C. Network Calculator".
AIEE, Trans., Vol. 60, 1941, pp.977-982.

100. G. KRON,
"Equivalent Circuits for the Hunting of Electrical Machinery".
AIEE, Trans., Vol. 61, 1942, pp.290-296.

101. W.E. ENNS,
"Method for A.C. Network Analysis Using Resistance Networks".
AIEE, Trans., Vol. 61, 1942, pp.875-880.

102. E.C. STARR and R.D. EVANS,
"Series Capacitors for Transmission Circuits".
AIEE, Trans., Vol. 61, 1942, pp.963-973.

103. B.M. JONES,
"Transmission Line, and System Problems in Supplying Large Electric-Arc Furnaces During Wartime".
AIEE, Trans., Vol. 62, 1943, pp.197-209.

104. W.E. ENNS,
"A New Simple Calculator of Load Flow in A.C. Networks".
AIEE, Trans., Vol. 62, 1943, pp.786-790.

105. C. CONCORDIA,
"Steady-State Stability of Synchronous Machines as Affected by Voltage Regulator Characteristics".
AIEE, Trans., Vol. 63, 1944, pp.215-220.

106. J.W. BUTLER, T.W. SCHROEDER and W. RIDGWAY,
"Capacitors, Condensers, and System Stability".
AIEE, Trans., Vol. 63, 1944, pp.1130-1138.

107. AIEE,
"American Institute of Electrical Engineers Test Code for Synchronous Machines".
No. 503, June 1945.

108. B. ADKINS,
"The Analysis of Hunting by Means of Vector Diagrams".
IEE, Journal, Vol. 93, 1946, pp.541-548.

109. E.D. TAYLOR,
"Utilization of Electrical Energy".
Universities Press Ltd., 2nd Edition, 1946.

110. H.A.P. LANGSTAFF, H.R. VAUGHAN and R.F. LAWRENCE,
"Application and Performance of Electronic Exciters for Large A.C. Generators".
AIEE, Trans., Vol. 65, 1946, pp.246-253.

111. J.D. RYDER and W.B. BOAST,
"A New Design for the A.C. Network Analyzer".
AIEE, Trans., Vol. 65, 1946, pp.674-679.

112. J.B. McCLURE, S.I. WHITTLESEY and M.E. HARTMAN,
"Modern Excitation Systems for Large Synchronous Machines".
AIEE, Trans., Vol. 65, 1946, pp.939-945.

113. B.V. HOARD,
"Characteristics of a 400-Mile 230 KV Series-Capacitor-Compensated Transmission System".
AIEE, Trans., Vol. 65, 1946, pp.1102-1114.

114. C.L. KILLGORE,
"Excitation Problems in Hydro-Electric Generators Supplying Long Transmission Lines".
AIEE, Trans., Vol. 66, 1947, pp.1277-1284.

115. W. WAGNER,
"Technical and Economic Aspects of the Transmission of Electrical Energy Over Long Distances".
IEE, Journal, Vol. 95, 1948, pp.340-351.

116. J.R. MORTLOCK,
"A Computer for Use in Power System Transient Stability Studies".
IEE, Journal, Vol. 95, 1948, pp.751-755.

117. E.L. MICHELSON and L.F. LISCHER,
"Generator Stability at Low Excitation".
AIEE, Trans., Vol. 67, 1948, pp.1-9.

118. C. CONCORDIA,
"Steady-State Stability of Synchronous Machines as Affected by Angle Regulator Characteristics".
AIEE, Trans., Vol. 67, Pt. I, 1948, pp.687-690.

119. J.M. COMLY, C.B. KELLEY, J.E. McCORMACK, H.W. PHILLIPS and T.W. SCHROEDER,
"Emergency Control of System Loads".
AIEE, Trans., Vol. 67, 1948, pp.1474-1483.

120. W.A. MORGAN, F.S. ROTHE and J.J. WINSNESS,
"An Improved A.C. Network Analyzer".
AIEE, Trans., Vol. 68, Pt. II, 1949, pp.891-897.

121. M.R. ROBERT,
"Micro-Machines and Micro Networks - Study of the Problems of Transient Stability by the Use of Models Similar Electromechanically to Existing Machines and Systems".
C.I.G.R.E., Paris, 1950, Paper No. 338.

122. G. LYON,
"Some Experience with a British A.C. Network Analyzer".
IEE, Proc., Vol. 97, Pt. II, 1950, pp.697-725.

123. R. RUDENBERG,
"Transient Performance of Electric Power Systems".
McGraw-Hill, 1950.

124. L.A. KILGORE and E.C. WHITNEY,
"Spring and Damping Coefficients of Synchronous Machines and Their Application".
AIEE, Trans., Vol. 69, Pt. I, 1950, pp.226-230.

125. "Electrical Transmission and Distribution Reference Book".
(Westinghouse Electrical and Manufacturing Col., 1950).

126. S.B. CRARY,
"Long-Distance Power Transmission".
AIEE, Trans., Vol. 69, Pt. II, 1950, pp.834-844.

127. A.L. WILLIAMS and E.L. KANOUSE,
"Power-System Planning in the City of Los Angeles".
AIEE, Trans., Vol. 69, Pt. II, 1950, pp.900-908.

128. C. CONCORDIA,
"Synchronous Machine Damping Torque at Low Speeds".
AIEE, Trans., Vol. 69, Pt. II, 1950, pp.1550-1553.

129. W.B. BOAST and J.D. RECTOR,
"An Electric Analogue Method for the Direct Determination of Power System Stability Swing Curves".
AIEE, Trans., Vol. 70, Pt. II, 1951, pp.1833-1836.

130. F.M. PORTER and C.P. ZIMMERMAN,
"Application of Shunt Capacitors at Transmission and Distribution Stations".
AIEE, Trans., Vol. 60, Pt. I, 1951, pp.112-120.

131. P.M. BLACK and L.F. LISCHER,
"The Application of a Series Capacitor to a Synchronous Condenser for Reducing Voltage Flicker".
AIEE, Trans., Vol. 70, Pt. I, 1951, pp.144-150.

132. W.E. ENNS,
"A Simple New Resistance Type A.C. Load Flow Board".
AIEE, Trans., Vol. 70, Pt. II, 1951, pp.1721-1726.

133. R.S. SEYMOUR and E.C. STARR,
"Economic Aspects of Series Capacitors in High-Voltage Transmission".
AIEE, Trans., Vol. 70, Pt. II, 1951, pp.1663-1670.

134. E.L. HARDER, J.E. BARKLE and R.W. FERGUSON,
"Series Capacitors During Faults and Reclosing".
AIEE, Trans., Vol. 70, Pt. II, 1951, pp.1627-1642.

135. Y.H. KU,
"Transient Analysis of Rotating Machines and Stationary Networks by Means of Rotating Reference Frames".
AIEE, Trans., Vol. 70, Pt. I, 1951, pp.943-957.

136. C. CONCORDIA,
"Synchronous Machine Damping and Synchronizing Torques".
AIEE, Trans., Vol. 70, Pt. I, 1951, pp.731-737.

137. J.R. MORTLOCK and M.W. HUMPHREY DAVIES,
"Power System Analysis".
Chapman and Hall, 1951.

138. J.M. BENNETT, F.V. DAKIN and U.G. KNIGHT,
"Digital Computers and Their Application to Some Electrical Engineering Problems".
C.I.G.R.E., Paris, 1952, Paper No. 304.

139. J.C. PRESCOTT,
"The Transient Stability of Alternators : A Graphical Solution of the Two-Machine Case".
IEE, Proc., Vol. 99, Pt. IV, 1952, pp. 367-371.

140. J.E. PARTON,
"A Note on the Equal-Area Stability Criterion".
IEE, Proc., Vol. 99, Pt. II, 1952, pp. 409-412.

141. W.G. HEFFRON and R.A. PHILLIPS,
"Effect of a Modern Amplidyne Voltage Regulator on Under-Excited Operation of Large Turbine Generators".
AIEE, Trans., Vol. 71, Pt. III, 1952, pp. 692-697.

142. S. KANEFF,
"A High-Frequency Simulator for the Analysis of Power Systems".
IEE, Proc., Vol. 100, Pt. II, 1953, pp. 405-416.

143. M.W. HUMPHREY DAVIES and G.R. SLEMON,
"Transformer Analogue Network Analyser".
IEE, Proc., Vol. 100, Pt. II, 1953, pp. 469-486.

144. V.G. EASTCOURT, C.H. HOLLEY, W.R. JOHNSON, P.H. LIGHT,
"Under-Excited Operation of Large Turbine Generators on Pacific Gas and Electric Company's System".
AIEE, Trans., Vol. 72, Pt. III, 1953, pp. 16-22.

145. L.L. FOUNTAIN, R.B. SQUIRES and W.A. HOPKIN,
"New Instrumentation of A.C. Network Calculator with Automatic Features".
AIEE, Trans., Vol. 72, Pt. III, 1953, pp. 368-375.

146. H.C. ANDERSON, H.O. SIMMONS and C.A. WOODROW,
"System Stability Limitations and Generator Loading".
AIEE, Trans., Vol. 72, Pt. III, 1953, pp. 406-423.

147. S.B. CRARY and L.E. SALINE,
"Location of Series Capacitors in High-Voltage Transmission Systems",
AIEE, Trans., Vol. 72, Pt. III, 1953, pp. 1140-1151.

148. D.F. SHANKLE, C.M. MURPHY, R.W. LONG and E.L. HARDER,
"Transient Stability Studies - I - Synchronous and Induction Machines".
AIEE, Trans., Vol. 73, Pt. IIIB, 1954, pp. 1463-1480.

149. R. ROBERT,
"Le Miroreseau Modele Dynamique de Reseaux".
Bull. Soc. Franc. Elect., Vol. 4, 1954, p. 67.

150. S. KANEFF,
"Dynamic Operation of an A.C. Network Analyzer".
IEE, Proc., Vol. 102, Pt. A, 1955, pp. 597-606.

151. J.H. FIELD,
"The Representation of Impedances on the Resistance Network Analyzer".
IEE, Proc., Vol. 102, Pt. A, 1955, pp. 823-827.

152. T.E. BROWN,
"The Electric Arc as a Circuit Element".
Journal Electro-Chemical Society, Vol. 102, 1955, pp. 27-37.

153. B.M. JONES,
"Electric Arc Furnaces - Problems and Solution in Power Supply".
Edison Elect. Institute Bulletin, Feb. 1951, pp. 39-46.

154. L.J. BUTTOLPH,
"Mercury Lamps - Light Made to Order".
Gen. Elect. Review, Vol. 58, No. 2, March 1955,

155. W.T. BROWN and W.J. CLOUES,
"Combination Load-Flow and Stability Equivalent for Power System Representation on A.C. Network Analyzers".
AIEE, Trans., Vol. 74, Pt. III, 1955, pp. 782-787.

156. P.J. SQUIRE,
"Operation at Low Frequency in Great Britain".
AIEE, Trans., Vol. 74, Pt. IIIB, 1955, pp.1647-1650.

157. A.S. LANGSDORF,
"Theory of Alternating Current Machinery".
McGraw-Hill, 2nd Edition, 1955.

158. H.K. MESSERLE and R.W. BRUCK,
"Steady-State Stability of Synchronous Generators as Affected by Regulators and Governors".
IEE, Proc., Vol. 103, Pt. C, 1956, pp.24-34.

159. H.K. MESSERLE,
"Relative Dynamic Stability of Large Synchronous Generators".
IEE, Proc., Vol. 103, Pt. C, 1956, pp.234-242.

160. C.H. HOFFMAN and M. LEBENBAUM,
"A Modern D.C. Network Analyzer".
AIEE, Trans., Vol. 75, Pt. III, 1956, pp.156-162.

161. J.B. WARD and H.W. HALE,
"Digital Computer Solution of Power-Flow Problems".
AIEE, Trans., Vol. 75, Pt. III, 1956, pp.398-404.

162. D.L. JOHNSON and J.B. WARD,
"The Solution of Power System Stability Problems by Means of Digital Computers".
AIEE, Trans., Vol. 75, Pt. III, 1956, pp.1321-1329.

163. E.W. KIMBARK,
"Power System Stability".
Vol. III, (Wiley - 1956).

164. C. ADAMSON and A.M.S. EL-SERAFI,
"Simulation of the Operation Impedances of Synchronous Machines on Network Analyzers".
AIEE, Trans., Vol. 76, Pt. III, 1957, pp.1373-1378.

165. A.S. ALDRED and P.A. DOYLE,
"Electronic-Analogue-Computer Study of Synchronous Machine Transient Stability".
IEE, Proc., Vol. 104, Pt. A, 1957, pp.152-160.

166. C. ADAMSON and A.M.S. EL-SERAFI,
"Simulation of the Transient Performance of Synchronous Machines on an A.C. Network Analyser".
IEE, Proc., Vol. 104, Pt. C, 1957, pp.323-331.

167. H.W. HARPER, T.R. MACON and A.F. SEDGWICK,
"Arc-Furnace Corrective Equipment Using a High Value of Buffer Reactance".
AIEE, Trans., Vol. 76, Pt. II, 1957, pp.74-80.

168. C. CONCORDIA, L.G. LEVOY and C.H. THOMAS,
"Selection of Buffer Reactors and Synchronous Condensers on Power Systems Supplying Arc-Furnace Loads".
AIEE, Trans., Vol. 76, Pt. II, pp.123-135.

169. AIEE SUBCOMMITTEE REPORT,
"Survey of Arc-Furnace Installations on Power Systems and Resulting Lamp Flicker".
AIEE, Trans., Vol. 76, Pt. II, 1957, pp.170-183.

170. D.S. BRERETON, D.G. LEWIS and C.C. YOUNG,
"Representation of Induction-Motor Loads During Power-System Stability Studies".
AIEE, Trans., Vol. 76, Pt. III, 1957, pp.451-461.

171. H.W. HALE and J.B. WARD,
"Digital Computation of Driving Point and Transfer Impedances".
AIEE, Trans., Vol. 76, Pt. III, 1957, pp.476-481.

172. K.A.E. KNOWLTON,
"Standard Handbook for Electrical Engineers".
McGraw Hill, 1957.

173. F. BUSEMAN and W. CASSON,
"Results of Full-Scale Stability Tests on British 132 KV Grid System".
IEE, Proc., Vol. 105, Pt. A, 1958, pp.347-362.

174. F.H. LAST, E. MILLS and N.D. NORRIS,
"Organization for Large-Scale Grid System Tests".
IEE, Proc., Vol. 105, Pt. A, 1958, pp.363-374.

175. A.S. ALDRED and G. SHACKSHAFT,
"The Effect of a Voltage Regulator on the Steady-State and Transient Stability of a Synchronous Generator".
IEE, Proc., Vol. 105, Pt. A, 1958, pp.420-427.

176. T.H. MASON, P.D. AYLETT and F.H. BIRCH,
"Turbo-Generator Performance Under Exceptional Operating Conditions".
IEE, Proc., Vol. 106, Pt. A, 1959, pp.357-380.

177. G.W. STAGG, A.F. GABRIELLE, D.R. MOORE and J.F. HOHENSTEIN,
"Calculation of Transient Stability Problems Using a High-Speed Digital Computer".
AIEE, Trans., Vol. 79, Pt. IIIA, 1959, pp.566-574.

178. E.C. WHITNEY, D.B. HOOVER and P.O. BOBO,
"An Electric Utility Brushless Excitation System".
AIEE, Trans., Vol. 78, Pt. IIIB, 1959, pp.1821-1826.

179. M.G. SAY,
"The Performance and Design of Alternating Current Machinery".
Pitman, 1959.

180. A.S. ALDRED and G. SHACKSHAFT,
"A Frequency-Response Method for the Predetermination of Synchronous-Machine Stability".
IEE, Proc., Vol. 107, Pt. C, 1960, pp.2-10.

181. J.C. PRESCOTT and A.K. EL-KHARASHI,
"The Performance of Displacement Governors Under Steady-State Conditions".
IEE, Proc., Vol. 107, Pt. A, 1960, pp.85-96.

182. J. RAVENSCROFT,
"The Determination of Electrical Characteristics of an Arc Furnace".
IEE, Proc., Vol. 108, Pt. A, 1960, pp.140-

183. R.N. SUDAN,
"Digital Computer Study of the Resynchronizing of a Turbo-Alternator".
AIEE, Trans., Vol. 79, Pt. III, 1950, pp.1120-1129.

184. H.E. BROWN, C.E. PERSON, L.K. KIRCHMAYER and C.W. STAGG, "Digital Calculation of 3-Phase Short Circuits by Matrix Method". AIEE, Trans., Vol. 79, Pt. III, 1960, pp.1277-1282.

185. P.P. GUPTA, and M.W. HUMPHREY DAVIES, "Digital Computers in Power System Analysis". IEE, Proc., Vol. 108, Pt. A, 1961, pp.383-404.

186. A.E. FITZGERALD and C. KINGSLEY, Jr., "Electric Machinery". McGraw-Hill, 2nd Edition, 1961.

187. R.V. SHEPHERD, "Synchronising and Damping Torque Coefficients of Synchronous Machines". AIEE, Trans., Vol. 80, Pt. III, 1961, pp.180-189.

188. S. KANEFF, "Some Experience with the Adelaide University Dynamic A.C. Network Analyzer". Proc. of 3rd International Conference on Analogue Computation (ETAN) Opatija, Sept. 1961, pp.419-427.

189. L.M. DOMERATZKY, A.S. RUBENSTEIN and M. TEMOSHOK, "A Static Excitation System for Industrial and Utility Steam-Turbine Generators". AIEE, Trans., Vol. 80, Pt. III, 1961, pp.1072-1077.

190. A. BRAMELLER and J.K. DENMEAD, "Some Improved Methods for Digital Network Analysis". IEE, Proc., Vol. 109, Pt. A, 1962, pp.109-116.

191. J.G. MILES, "Analysis of Overall Stability of Multi-Machine Power Systems". IEE, Proc., Vol. 109, Pt. A, 1962, pp.203-217.

192. B.J. CHALMERS, "Asynchronous Performance Characteristics of Turbo-Generators". IEE, Proc., Vol. 109, Pt. A, 1962, pp.301-308.

193. W.H. CROFT and R.H. HARTLEY, "Improving Transient Stability by Use of Dynamic Braking". AIEE, Trans., Vol. 81, Pt. III, 1962, pp.17-26.

194. H. COTTON,
"The Transmission and Distribution of Electrical Energy".
The English Universities Press, 3rd Edition, 1962.

195. S.B. CRARY,
"Power System Stability".
Vol. 11, (Wiley - 1962).

196. W.D. STEVENSON,
"Elements of Power System Analysis".
McGraw-Hill, 2nd Edition 1962.

197. G. SHACKSHAFT,
"General Purpose Turbo-Alternator Model".
IEE, Proc., Vol. 110, No. 4, 1963, pp. 703-713.

198. E.C. SCOT, W. CASSON, A. CHORLTON and J.H. BANKS,
"Multi-Generator Transient-Stability Performance Under Fault Conditions".
IEE, Proc., Vol. 110, No. 6, 1963, pp. 1051-1064.

199. P. BHARALI and B. ADKINS,
"Operational Impedances of Turbo-Alternators with Solid Rotors".
IEE, Proc., Vol. 110, No. 12, 1963, pp. 2185-2199.

200. W.D. HORSLEY,
"Turbo-Type Generators".
IEE, Proc., Vol. 110, No. 4, April 1963, pp. 695-702.

201. F.J. ASTON and J. WILSON,
"Planning the Development of the Electricity Supply Industry in New South Wales". Journal I.E.(Aust.), Vol. 36, Dec. 1964, pp. 295-308.

202. L. CLARK, G.A. CURTIS and R.O.M. POWELL,
"Capacitors in Relation to Transient Fluctuating and Distorting Loads".
IEE, Conf. Report Series No. 8, 1964, pp. 21-32.

203. J.M. COWAN and F.E. BROOKER,
"Connection of Power-Factor-Correction Capacitors to Electricity Supply Systems".
IEE, Conf. Report Series No. 8, 1964, pp. 33-38.

204. R.B. SHIPLEY, D.W. COLEMAN and H.J. HOLLEY,
"Power Circuit Representation for Digital Studies".
IEEE, Trans., on Power Apparatus and Systems, Vol. PAS-83, 1964, pp.376-380.

205. J. KEKELA and L. FIRESTONE,
"Under-Excited Operation of Generators".
IEEE, Trans., on Power Apparatus and Systems, Vol. PAS-83, 1964, pp.811-817.

206. B.G. GERAY and W.H. SCHIPPEL,
"Transient Stability of an Isolated Radial Power Network with Varied Load Division".
IEEE, Trans., on Power Apparatus and Systems, Vol. PAS-83, 1964, pp.964-970.

207. J.L. DINELEY and M.W. KENNEDY,
"Concept of Synchronous Generator Stability".
IEE, Proc., Vol. 111, No. 1, 1964, pp.95-97.

208. J.L. DINELEY and M.W. KENNEDY,
"Influence of Governors on Power-System Transient Stability".
IEE, Proc., Vol. 111, No. 1, 1964, pp.98-106.

209. J.L. DINELEY,
"Study of Power-System Transient Stability by a Combined Computer".
IEE, Proc., Vol. 111, No. 1, 1964, pp.107-114.

210. P.A.W. WALKER and A.S. ALDRED,
"Displacement Governing in a 2-machine System - A Hybrid Simulator Study".
IEE, Proc., Vol. 111, No. 2 1964, pp.325-334.

211. J.A. DEMBECKI,
"Thesis on the Automatic Control of Hydro and Thermal Generation on a Large Interconnected Power System".
Univ. of NSW, Dec. 1964.

212. B. ADKINS,
"The General Theory of Electrical Machines".
Chapman and Hall, 1964.

213. V.A. VENIKOV,
"Transient Phenomena in Electrical Power Systems".
Pergamon Press, 1964.

214. R.R. BOOTH,
"A Digital Model of a Multi-Machine Power System".
IE Aust., Elect. Eng. Transactions, Vol. EEI, No. 2, Sept. 1965, pp.67-74.

215. C.B. COOPER and E.D. HOWELLS,
"The Calculation of Power System Stability with Particular Reference to the Victorian System".
IE Aust., Elect. Eng. Transactions, Vol. EEI, No. 2, Sept. 1965, pp.75-84.

216. J.E. DAY and K.C. PARTON,
"Generalised Computer Program for Power-System Analysis".
IEE, Proc., Vol. 112, No. 12, 1965, pp.2261-2274.

217. H.A. PETERSON, D.K. REITAN and A.G. PHADKE,
"Parallel Operation of A.C. and D.C. Power Transmission".
IEEE, Trans. on Power Apparatus and Systems, Vol. PAS-84, 1965, pp.15-19.

218. R.D. BROWN and K.R. McCLYMONT,
"A Power System Swing Relay for Predicting Generation Instability".
IEEE, Trans. on Power Apparatus and Systems, Vol. PAS-84, 1965, pp.219-224.

219. H.E. LOKAY and R.L. BOLGER,
"Effect of Turbine-Generator Representation in System Stability Studies".
IEEE, Trans. on Power Apparatus and Systems, Vol. PAS-84, 1965, pp.933-942.

220. F.J. HUBERT and M.R. GENT,
"Half Wavelength Power Transmission Lines".
IEEE, Trans. on Power Apparatus and Systems, Vol. PAS-84, 1965, pp.963-974.

221. H.E. BROWN, H.H. HAPP, C.E. PERSON and C.C. YOUNG,
"Transient Stability Solution by an Impedance Matrix Method".
IEEE, Trans. on Power Apparatus and Systems, Vol. PAS-84, 1965, pp.1204-1214.

222. D.D. STEPHEN,
"Effect of System-Voltage Depressions on Large A.C. Motors".
IEE, Proc., Vol. 113, No. 3, 1966, pp.500-506.

223. J.F. ROOPER,
"Lighting for Commercial Buildings".
IEE, Journal, Electronics and Power, Aug. 1966.

224. R.A. HORE,
"Advanced Studies in Electrical Power System Design".
Chapman and Hall, 1966.

225. P.J. LAWRENSON and J.M. STEPHENSON,
"Note on Induction-Machine Performance With a Variable Frequency Supply".
IEE, Proc., Vol. 113, No. 10, 1966, pp.1617-1623.

226. H.A. PETERSON, P.C. KRAUSE, J.F. LUINI and C.H. THOMAS,
"An Analogue Computer Study of a Parallel A.C. and D.C. Power System".
IEEE, Trans., on Power Apparatus and Systems, Vol. PAS-85, 1966, pp.191-209.

227. H.A. PETERSON and P.C. KRAUSE,
"A Direct and Quadrature-Axis Representation of a Parallel A.C. and D.C. Power System".
IEEE, Trans. on Power Apparatus and Systems, Vol. PAS-85, 1966, pp.210-225.

228. T. MACHIDA,
"Improving Transient Stability of A.C. System by Joint Usage of D.C. System".
IEEE, Trans. on Power Apparatus and Systems, Vol. PAS-85, 1966, pp.226-232.

229. D.W. OLIVE,
"New Techniques for the Calculation of Dynamic Stability".
IEEE, Trans. on Power Apparatus and Systems, Vol. PAS-85, 1966, pp.767-777.

230. H.A. PETERSON and P.C. KRAUSE,
"Damping of Power Swings in a Parallel A.C. and D.C. System".
IEEE, Trans. on Power Apparatus and Systems, Vol.PAS-85,
1966, pp.1231-1239.

231. M.A. LAUGHTON,
"Matrix Analysis of Dynamic Stability in Synchronous Multi-Machine Systems".
IEE, Proc., Vol. 113, No. 2, 1966, pp.325-336.

232. P.G. KENDALL,
"Light Flicker in Relation to Power-System Voltage Fluctuation".
IEE, Proc., Vol. 113, No. 3, 1966, pp.471-479.

233. N.G. HINGORANI, J.L. HAY and R.E. CROSBIE,
"Dynamic Simulation of H.V.D.C. Transmission Systems on Digital Computers".
IEE, Proc., Vol. 113, No. 5, 1966, pp.793-809.

234. G.W. ALEXANDER, S.L. CORBIN and W.J. McNUTT,
"Influence of Design and Operating Practices on Excitation of Generator Step-Up Transformers".
IEEE, Trans. on Power Apparatus and Systems, Vol. PAS-85,
No. 8, 1966, pp.901-909.

235. G.E. GLESS,
"Direct Method of Liapunov Applied to Transient Power System Stability".
IEEE, Trans. on Power Apparatus and Systems, Vol.PAS-85,
1966, pp.159-168.

236. A.H. EL-ABIAD and K. NAGAPPAN,
"Transient Stability Regions of Multi-machine Power Systems".
IEEE, Trans. on Power Apparatus and Systems, Vol. PAS-85,
1966, pp.169-179.

237. H.M. ELLIS, J.E. HARDY, A.L. BLYTHE and J.W. SKOOGLUND,
"Dynamic Stability of the Peace River Transmission System".
IEEE, Trans. on Power Apparatus and Systems, Vol.PAS-85,
1966, pp.586-600.

238. I.R. SMITH and M.S. GARRIDO,
"Current Compounded Self-Excitation of Synchronous Motors".
IEE, Proc., Vol. 114, No. 2, 1967, pp.269-275.

239. B.J. KABRIEL,
"Optimisation of Alternator Voltage Regulators for Steady-State Stability Using Mitrovic Method".
IEE, Proc., Vol. 114, No. 6, 1967, pp.762-768.

240. J.M. UNDRILL,
"Power System Stability Studies by the Method of Liapunov :
I - State Space Approach to Synchronous Machine Modelling".
IEEE, Trans. on Power Apparatus and Systems, Vol.PAS-86, 1967, pp.791-801.

241. J.M. UNDRILL,
"Power System Stability Studies by the Method of Liapunov :
II - The Interconnection of Hydro Generating Sets".
IEEE, Trans. on Power Apparatus and Systems, Vol.PAS-86, 1967, pp.802-811.

242. D.N. EWART and F.P. DE MELLO,
"A Digital Computer Program for the Automatic Determination of Dynamic Stability Limits".
IEEE, Trans. on Power Apparatus and Systems, Vol.PAS-86, 1967, pp.867-875.

243. B.M. WEEDY,
"Electric Power Systems".
John-Wiley & Sons, 1967.

244. J.L. DINELY and A.V. MORRIS,
"Optimised Transient Stability from Excitation Control of Synchronous Generators".
IEEE PICA Conference Record, May 1967, pp.1-12.

245. D.W. OLIVE,
"Digital Simulation of Synchronous Machine Transients".
IEEE PICA Conference Record, May 1967, pp.13-20.

246. R.M. WEBLER and C.C. YOUNG,
"A Digital Computer Program for Predicting Dynamic Performance of Electric Power Systems".
IEEE PICA Conference Record, May 1967, pp. 21-30.

247. R.T. BYERLY, and D.G. RAMEY,
"Dynamic Simulation of Interconnected Systems".
IEEE. PICA Conference Record, May 1967, pp. 31-40.

248. J. BABA, S. HAYASHI, I. YAMADA, H. HANEDA, and F. ISHIGURO,
"Sensitivity Analysis of Power System Stability".
IEEE PICA Conference Record, May 1967, pp. 47-68.

249. K. PRABHASHANKAR and W. JANISCHEWSYJ,
"Digital Simulation of Multimachine Power Systems for Stability Studies".
IEEE, Trans. on Power Apparatus and Systems, Vol. PAS-87, No. 1, Jan. 1968, pp. 78-30.

250. S.L. SURANA and M.V. HARIHARAN,
"Transient Response and Transient Stability of Power Systems".
Proc. IEE, Vol. 115, No. 1, 1968, pp. 114-120.

251. P.L. DENDANO, A.N. KARAS, K.R. McCLYMONT and W. WATSON,
"Effect of High Speed Rectifier Excitation Systems on Generator Stability Limits".
IEEE, Trans. on Power Apparatus and Systems, Vol. PAS-87, No. 1, Jan 1968, pp. 190-201.

252. T.A. LIPO and P.C. KRAUSE,
"Stability Analysis for Variable Frequency Operation of Synchronous Machines".
IEEE, Trans. on Power Apparatus and Systems, Vol. PAS-87, No. 1, Jan 1968, pp. 227-234.

253. H.E. COLES,
"Dynamic Performance of a Turbo-Alternator Utilising 3-Term Governor Control and Voltage Regulation".
Proc. IEE, Vol. 115, No. 2, Feb. 1968, pp. 266-279.

254. R. M. SHIER and A. L. BLYTH,
"Field Tests of Dynamic Stability Using a Stabilizing Signal and Computer Program Verification".
IEEE, Trans. on Power Apparatus and Systems, Vol. PAS-87, No. 2, Feb. 1968, pp. 315-322.

255. J. M. UNDRILL,
"Dynamic Stability Calculations for an Arbitrary Number of Interconnected Synchronous Machines".
IEEE, Transaction, Vol. PAS-87, No. 3, 1968, pp. 835-844.

256. Y. WALLEH,
"Gradient Methods for Load Flow Problems".
IEEE, Trans. on Power Apparatus and Systems, Vol. PAS-87, No. 5, 1968, pp. 1314-1318.

257. W. A. MITTELSTADT,
"Four Methods of Power System Damping".
IEEE, Trans. on Power Apparatus and Systems, Vol. PAS-87, No. 5, 1968, pp. 1323-1329.

258. K. N. STANTON,
"Simulating the Dynamic Behaviour of Power Systems During Large Disturbances!'
A paper presented at IFAC Symposium on "System Dynamics and Automatic Control in Basic Industries", held in Sydney, 26-30 Aug. 1968.

Frequency-dependent dynamic representation of induction-motor loads

M. Y. Akhtar, B.Sc.(Eng.), B.E.

Synopsis

For comprehensive transient and dynamic stability studies, induction-motor loads have usually been represented by fixed shunt impedances at system nominal frequency. A method is proposed here which allows single induction motors or groups of induction motors to be considered as frequency-dependent and dynamic. If the necessary parameters of the motors are known and if computation effort is not a problem, accurate assessment can always be made for single machines or groups of machines but may involve lengthy calculations. Alternatively, an approximate, rapid method is presented which gives the change in active-power input to an induction motor or group of induction motors due to inertia and frequency-variation effects to within $\pm 2\%$ of the actual change for known power factor, inertia factor and full-load slip; and to within $\pm 5\%$ of the actual change when the assumed parameters are within the following limits: power factor within $\pm 5\%$; inertia factor within $\pm 10\%$ and full-load slip within $\pm 20\%$ (where the actual change in power has been assessed by the use of an equivalent circuit). The change in reactive power, as assessed, is within $\pm 20\%$ of actual change in reactive power. $\pm 5\%$ change in operating frequency has been considered. For simplicity, windage and friction losses have been taken as an integral part of the load supplied by the motor, and core losses have been assumed constant. These methods can be applied to power-system stability studies, as illustrated by an example.

List of symbols

P = active-power input
P_h = horsepower
n_1 = synchronous speed, rev/min
n_∞ = full-load speed, rev/min
n_0 = speed at the end of the interval, rev/min
n = instantaneous speed, rev/min
f_0 = base frequency
f = instantaneous frequency
s = instantaneous slip
s_∞ = full-load slip
s_1 = instantaneous slip at the beginning of interval
s_2 = slip at the end of the interval
α = slope of torque/slip and torque/speed characteristic
T_l = load torque
T = instantaneous motor torque
Δt = time interval
J = moment of inertia
ω_1 = synchronous angular velocity
ω = instantaneous angular velocity
ω_0 = angular velocity at the end of the interval
H = inertia factor
η = efficiency of the motor
m = number of phases
V = supply phase voltage
r_0 = resistance equivalent to no-load losses
r_1 = stator resistance
x_1 = stator reactance
r_2 = rotor resistance as referred to stator
x_2 = rotor reactance as referred to stator
x_3 = magnetising reactance
R, X = resistance and reactance equivalent to active- and reactive-power input to the motor, respectively, at a given supply voltage
I = current drawn by the motor
I_{0m} = magnetising current
R', X' = transmission-line resistance and reactance, respectively
V_r, I_r = receiving-end voltage and current, respectively
V_s, I_s = sending-end voltage-and current, respectively
ψ = phase angle between V_r and I_r
$\cos\phi$ = power factor of an induction motor
d, l = rotor diameter and length of an induction motor, respectively
B = specific magnetic loading, Wb/m^2
a_c = specific electric loading, A cond./m
K_w = winding factor
p = number of pairs of poles
γ_j = magnetising current as fraction of full-load current
ρ = density of the rotor material
i = current iteration
$i-1$ = preceding iteration to i

Paper 5520 P, first received 11th July and in revised form 4th December 1967
Mr. Akhtar is with the Department of Engineering Physics, Research School of Physical Sciences, Australian National University, Canberra ACT, Australia

1 Introduction

Load flow, stability studies and load surveys are periodically carried out, and load trends[11] are considered at various points in power systems at intervals by system planners so that future power demands can be met conveniently for the worst predictable conditions. At the detailed local levels of planning, rudimentary data for various types of loads are usually available. By considering various aspects, such as demand factor, diversity factors, efficiency and power factors of equipment, the active- and reactive-power demands can be ascertained for a particular time and for the worst conditions. Owing to lack of adequate information and convenient methods of assessment, induction-motor loads have previously been represented for power-system transient and dynamic stability studies in various ways, such as by

(*a*) constant shunt impedance at system nominal frequency, giving active and reactice powers directly proportional to the square of the terminal voltage
(*b*) constant-current sinks, giving active and reactive powers directly proportional to the terminal voltage
(*c*) nonlinear loads.

All of these representations treat the loads as static and independent of frequency, but they are, in fact, dynamic and frequency-dependent. It has usually been considered that the results obtained in this way are safe;[1] however, an example in Section 3 suggests that this belief may be erroneous.

In the case of important induction motors (such as pump motors in power stations), for which a great deal of information is available, representations in comprehensive computer programs have ranged from steady-state equivalent circuits, through approximate equations which give asymptotic behaviour, to exact equations derived from the circuit analysis of the machines,[8] and have taken account of varying terminal voltage and operating frequency.[5,10]

Induction motors contribute significantly to power-system loads, their input active and reactive powers depending upon the instantaneous magnitudes of the terminal voltage and operating frequency. In the past, the change in instantaneous speed of synchronous machines under disturbed conditions has been neglected, as it has been considered insignificant.[1] However, during electromechanical oscillations on power systems, the instantaneous frequency does change, and changes in system loads have been previously taken into account,[7] for example, by a system damping coefficient of 2. Further, the system frequency is a very powerful parameter available for adjustment by the power-system controller, but information regarding load variations with instantaneous frequency is not readily available.

From the point of view of economy, the system should be designed close to stability limits, and, from the operational viewpoint, knowledge of the true behaviour of the system is essential.

It is the aim of the paper to treat induction-motor loads as being dynamic and frequency-dependent for power-system stability studies. Two methods are presented, one being accurate and applicable to the case where parameters of the equivalent circuits of individual machines are known, the other being approximate, more rapid, and useful, irrespective of whether knowledge of motor equivalent-circuit parameters is or is not available. In the approximate method, full-load slip and inertia factor may be designated from typical representative values.

2 Dynamic and frequency-dependent representation

Full-load slip of induction motors normally varies from 5·5 to 1%, inertia factor varies from 0·1 to 0·3 and magnetising current varies from 50 to 20% of the full-load current for general-purpose induction motors, over a range of 1 to 1000hp, as shown in Tables 1 and 2 (which have been assembled from information provided by several manufacturers).

It has been verified in practice that the inertia-factor contribution of loads such as drilling, grinding, milling and spinning machines, fans, lathes, pumps, compressors etc. is quite significant, and at least equal to that of the driving motor. Installations with exceptionally high inertia factor, such as Ward Leonard–Illgner speed-control and large motors, fall under the category of important induction motors and should be considered separately.

Tests quoted, for example in Reference 2, can give some idea of load-torque variation with speed (otherwise the safest case is to treat the load torque as being constant). Load reductions due to frequency change assumed in Reference 7 indicate that $T \propto \omega^n$, where $n > 1$.

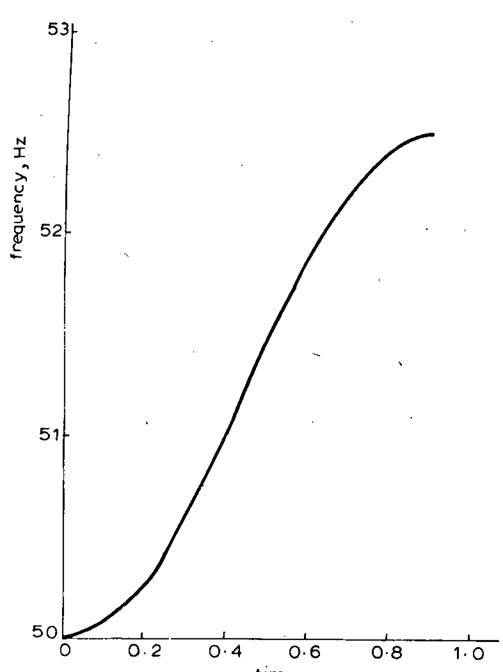

Fig. 1
Operating frequency against time at the motor terminals

2.1 Frequency range

To study the dynamic and frequency-dependent behaviour of induction motors, a frequency range of $50 \pm 2{\cdot}5$Hz has been selected. The 2·5Hz change has been distributed over 18 intervals, each of 0·05s, as shown in Fig. 1; the law of variation closely corresponds to the swing curves of synchronous machines under disturbed conditions. In practice, frequency variations are less, but these excursions will serve to compare the proposed approximate method with more precise calculations carried out using equivalent circuits.

2.2 Torque/slip and current/slip characteristics

In general, the equivalent circuit shown in Fig. 2 can be employed to determine the performance characteristics of an induction motor. Fig. 3 indicates the torque/slip and

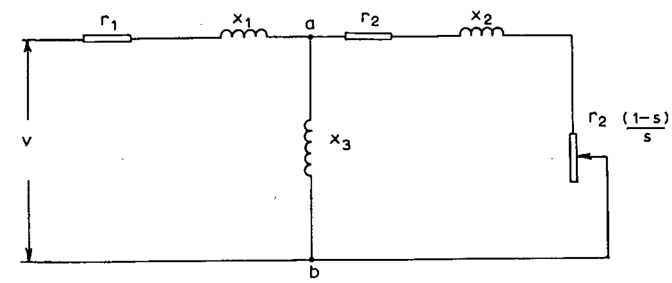

Fig. 2
Induction-motor equivalent circuit

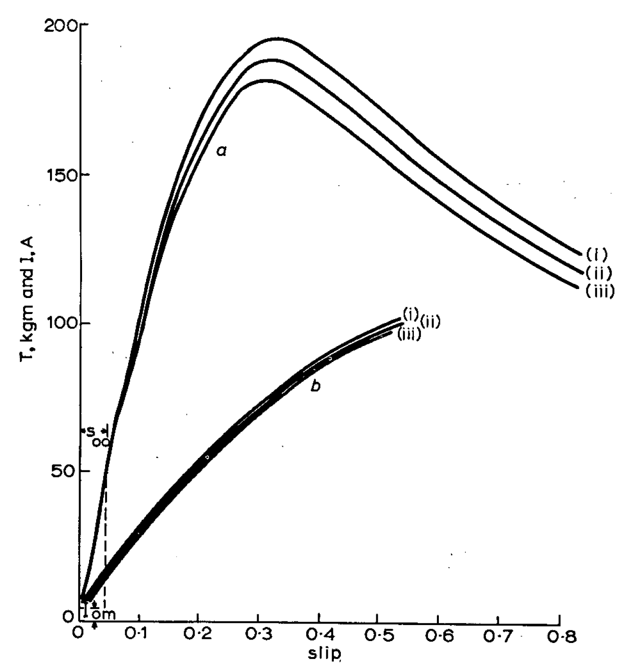

Fig. 3
Characteristics of 15hp squirrel-cage induction motor for various operating frequencies

a Torque against slip
b Stator current against slip
(i) 48·75Hz
(ii) 50·0Hz
(iii) 51·95Hz

stator current/slip characteristics for a 15hp squirrel-cage induction motor at various operating frequencies, when the terminal voltage is held constant. On examining Fig. 3, it is observed that the characteristics are linear to a good approximation over the working range of slip, and this property has already been employed for studying the natural oscillations of induction motors.[3] Eqn. 2 of Appendix 8.1 indicates that the slope of the torque/slip characteristics is inversely proportional to the operating frequency, at $s = 0$.

2.3 Representation with equivalent circuit

Fig. 4 indicates the torque/slip characteristics at various frequencies for a 15hp induction motor, when the terminal voltage is held constant. The characteristics are substantially linear over the working range; moreover, the part of the characteristic F′K′ is small. Considering the

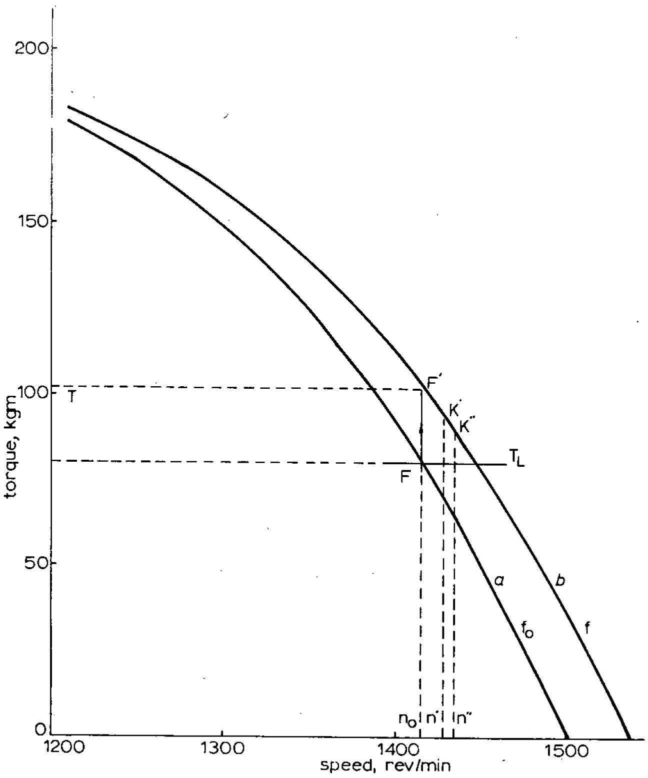

Fig. 4
Torque/speed characteristics of 15 hp squirrel-cage induction motor
Illustrating the effect of change in operating frequency

behaviour of the motor when the operating frequency is changed from f_0 to f, immediately the operating characteristic changes, i.e. for frequency f_0, the motor operates on characteristic a (at point F), under steady-state conditions. The time interval for this change in frequency has been taken as Δts. On changing the frequency from f_0 to f, the torque developed by the motor corresponds to the point F′. The motor accelerates and follows the path on the characteristic b,

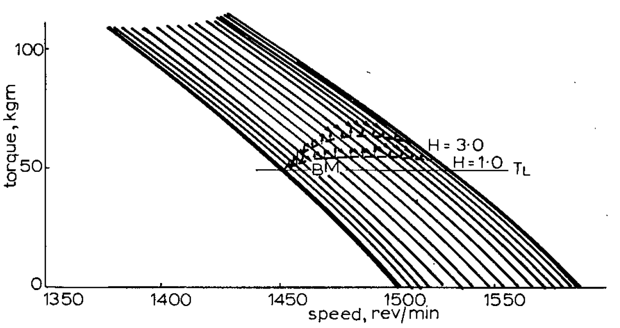

Fig. 5
Torque/speed characteristics of 15 hp squirrel-cage induction motor
Indicating the dynamic and frequency-dependent behaviour with different inertia factors when the load torque is constant and frequency varies from 50·0 to 52·5 Hz n 0·9s, as shown in Fig. 1

as shown. The final speed at the end of the time interval Δt depends on the interia factor of the machine. For higher values of inertia factor, the speed will change from n_0 to n', whereas for lower values it will change from n_0 to n''. Assuming that the F′K′ part of the torque/speed characteristic is linear, the equation of motion for the motor can be derived as in Appendix 8.4.

Following the steps indicated in Appendix 8.4, the dynamic and frequency-dependent behaviour of an induction motor can be studied for various values of inertia factor. The steps from (iii) to (xiii) are repeated for each step change in operating frequency. Curves, as shown in Figs. 7, 8a and b, have been obtained in this way.

2.4 Proposed approximate method for assessing active power

It is somewhat unlikely that comprehensive parameters on induction machines connected to a power system will be readily available; this raises the need to predict the various key parameters of induction motors. In an attempt to discover typical trends in parameters against motor ratings, Tables 1 and 2 have been assembled from information supplied by various manufacturers. Although individual motors of a given rating have parameters extending over relatively broad limits, an attempt has been made to determine average values. It will be seen later that these Tables are useful in practice, particularly when it is realised that a power system will normally supply thousands of different motors, and statistical factors will consequently apply.

Appendix 8.2 shows that inertia factor is approximately independent of the number of poles, and Appendix 8.3 indicates how equivalent parameters can be determined for a mixed group of induction motors, using information on parameters of individual machines, if known, or employing the values from Tables 1 and 2 (as being representative) in the more usual case in which all that is known about individual machines is horsepower rating and number of units.

Fig. 6 indicates the torque/slip characteristics of an induc-

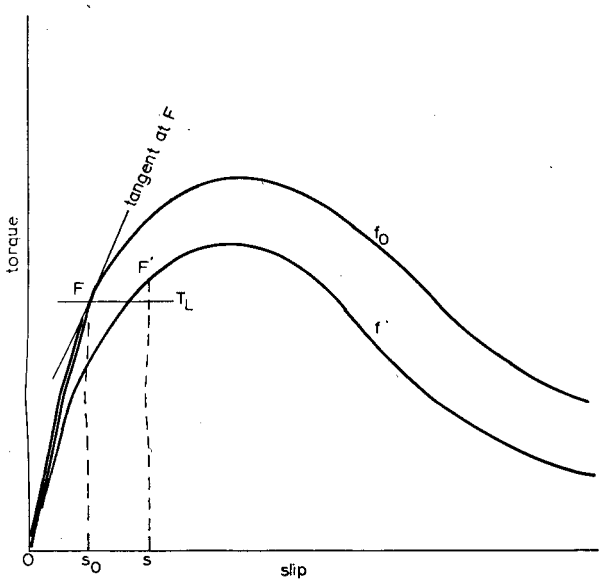

Fig. 6
Torque/slip characteristics
Indicating the slope used by the suggested approximate method

tion motor operating at the point F with slip s_0. When the operating frequency is changed from f_0 to f, the motor operates on a characteristic corresponding to f (it has been assumed that $f > f_0$). As already mentioned, the slope of the characteristic at $s = 0$ varies inversely with the operating frequency (as shown by eqn. 2), and the operating point F shifts to F′, having the instantaneous slip s. The motor accelerates and its slip falls, following the curve F′O in Fig. 6. The equation of motion can be derived as in Appendix 8.5.

Following the steps outlined in Appendix 8.5, the dynamic and frequency-dependent behaviour of an induction motor can be studied conveniently without the knowledge of equivalent circuit constants. The steps v and xi are repeated for each step change in instantaneous frequency; in this way, the appropriate curves in Fig. 7 have been obtained.

In the foregoing, the core losses have been taken into account by the efficiency of the motor, which has been assumed constant because its change is negligible.

Examination of Fig. 6 reveals that the slope of the torque/slip characteristic used is greater than the actual, and, from Fig. 7, it is observed that only 90% of the overall change in active power has been taken into account because of this fact. Two alternatives for improvement are:

(a) reduction of slope of the torque/slip characteristic
(b) increase of working slip.

Table 1

SHOWING VARIOUS TYPICAL INDUCTION-MOTOR PARAMETERS

Number	Horsepower	H	Full-load slip	Overall change at 51·25Hz		Full-load line current	Magnetising line current
				Active power	Reactive power		
		$\frac{\text{kWs}}{\text{kVA rating}}$	%	%	%	A	A
1	5s.r.	0·18	2·0	5·59	−1·62	7·5	3·97
2	7·5s.c.	0·113	5·3	4·44	−0·79	10·0	4·6
3	10s.c.	0·1	4·66	3·21	−0·76	13·5	6·1
4	10s.c.	0·12	2·3	2·93	1·38	13·5	4·6
5	10s.r.	0·284	1·67	10·61	1·35	14·5	5·8
6	15s.c.	0·106	2·32	2·74	1·76	20·5	6·1
7	15s.r.	0·172	3·0	4·77	0·27	21·5	10·15
8	20s.c.	0·12	3·33	3·65	0·047	26·5	9·7
9	20s.c.	0·14	1·86	2·88	1·08	26·5	9·36
10	20s.r.	0·2	3·7	6·26	4·01	27·5	10·0
11	25s.c.	0·134	4·0	4·38	2·30	32·0	9·5
12	30s.c.	0·18	2·38	3·12	8·85	40·5	10·5
13	40s.c.	0·175	1·5	2·80	1·73	54·0	15·4
14	40s.c.	0·24	2·66	3·55	1·04	52·5	18·5
15	40s.r.	0·38	1·28	7·28	2·75	55·0	19·71
16	50s.c.	0·144	1·51	2·58	1·12	71·0	26·5
17	50s.c.	0·2	2·66	5·26	1·95	64·0	19·5
18	50s.c.	0·217	1·33	3·33	1·13	64·5	21·5
19	60s.r.	0·157	2·8	4·32	2·26	80·0	28·4
20	75s.r.	0·137	2·3	3·37	0·68	102·5	42·7
21	75s.c.	0·218	1·35	3·36	2·96	103·0	29·5
22	100s.r.	0·153	2·4	3·82	2·21	147·0	45·8
23	100s.c.	0·22	2·13	4·65	2·62	125·0	23·5
24	200s.c.	0·25	1·46	5·64	6·25	136·0	32·5
25	200s.c.	0·3	1·87	7·62	11·25	250·0	51·8
26	250s.c.	0·25	1·33	4·11	6·08	40·0	8·07
27	450s.c.	0·28	1·48	5·36	8·66	71·0	12·1

Full load slip, inertia factors and overall changes in active and reactive powers at 51·25* Hz, as shown in Fig. 1 and expressed as percentage change per 2·5% change in frequency, when the load torque is constant

s.c. = squirrel-cage induction motor
s.r. = slipring induction motor

* Because there is maximum acceleration at this frequency during the whole change, as shown in Fig. 1

Table 2

SHOWING THE AVERAGE VALUES OF KEY FACTORS FOR A RANGE OF 1–1000HP INDUCTION MOTORS

Horsepower	1	2	4	10	20	40	100	200	400	1000
Inertia factor, $\frac{\text{kWs}}{\text{input kVA}}$	0·09	0·1	0·115	0·13	0·145	0·17	0·215	0·255	0·3	0·38
Full-load slip, %	5·8	4·7	3·75	2·9	2·4	2·0	1·7	1·5	1·5	1·35
Full-load power factor	0·78	0·8	0·83	0·86	0·88	0·89	0·896	0·9	0·91	0·915
Full-load efficiency, %	80·0	82·0	84·0	87·0	89·0	90·0	92·0	92·5	93·0	94·0
$\frac{\text{Magnetising current}}{\text{Full-load current}}$	0·63	0·54	0·46	0·38	0·33	0·28	0·25	0·23	0·22	0·2

Table 3

SHOWING THE EFFECT OF ERROR IN EQUIVALENT PARAMETERS ON ACTIVE-POWER INPUT TO GROUPS OF INDUCTION MOTORS AT 51·25 HZ INSTANTANEOUS FREQUENCY

Active-power input to 8175hp group	Assessed change as percentage of true change	Active power input to 3787·5hp group	Assessed change as percentage of true change	Remarks
MW	%	MW	%	
6·3410	—	2·8240	—	At 50Hz under steady-state conditions
6·5908	100	2·9466	100	Calculations by actual equivalent-circuit parameters
6·5859	98·43	2·9510	103·5	Calculations by approximate method with known parameters
6·5870	98·87	2·9470	100·32	Calculations by approximate method with assumed parameter as outlined in Appendix 8.3
6·5746	93·89	2·9389	93·71	Calculations by approximate method with 5% reduction in true equivalent power factor and 20% reduction in true equivalent slip
6·5986	103·53	2·9522	104·56	Calculations by approximate method with 10% increase in true equivalent inertia factor
6·5818	96·78	2·9410	95·43	Calculations by approximate method with 5% increase in true equivalent power factor
6·5940	101·68	2·9485	101·55	Calculations by approximate method with 10% increase in true equivalent inertia factor 20% increase in true equivalent slip and 5% reduction in true equivalent power factor

When treated as dynamic and frequency-dependent, for the frequency variations shown in Fig. 1

The first alternative depends upon the overall swing of the slip, which is determined by the inertia factor, whereas the second alternative changes the slope of the torque/slip curve

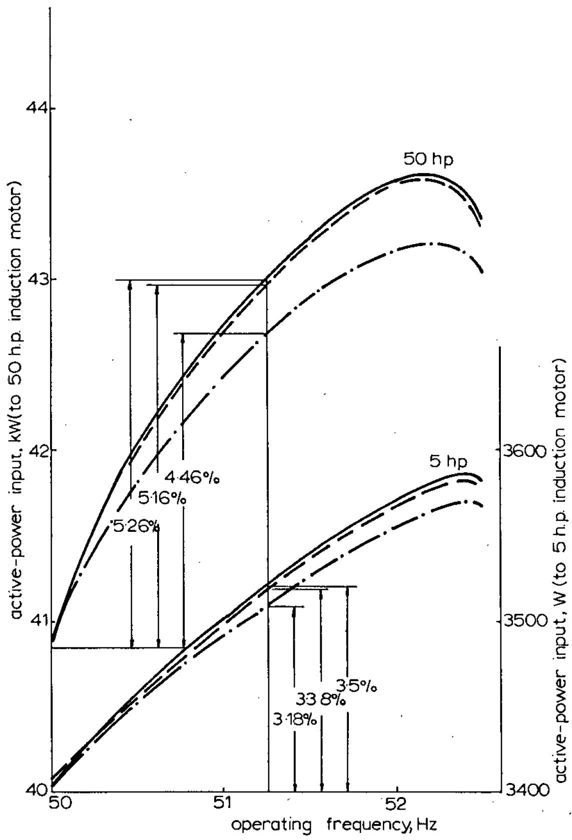

Fig. 7

Active-power input to 5 and 50 Hz squirrel-cage induction motors against frequency

For normal full-load slip and 40% increased slip
——— Active-power input by equivalent circuit
—·— Active-power input by suggested method with normal s
— — Active-power input by suggested method with increased s
% values indicate overall change in active-power input when treated as frequency-dependent and dynamic

and shifts the operating point to the right. Various values of working slips for different motors have been tried, and the results have indicated that a notional increase of 40% in overall working slip improves the assessment to within $\pm 2\%$ of the overall change in active power, as shown in Fig. 7. Consequently, in step (ii) of Appendix 8.5, $s_{\infty} = 1{\cdot}4 \times$ full-load slip.

Figs. 8*a* and *b* and Table 3 illustrate the magnitude of errors associated with this method of viewing groups of machines under variable-frequency conditions (as shown in Fig. 1). Using this approach, an equivalent motor of the total group rating can be obtained (as shown in Appendix 8.3), and equivalent induction-machine parameters are then available for comprehensive assessment of the power system, even when the only details available are the number of induction motors and their horsepower rating. It is clear from Figs. 8*a* and *b* and Table 3 that, acting on meagre information and employing the approximate method proposed, performance can be assessed within reasonable agreement of that possible using more detailed information and more exact methods.

This method has been used successfully in the study of frequency-dependent dynamic behaviour of groups of induction motors, calculations such as that in the example of Section 3 indicating that the method retains good accuracy.

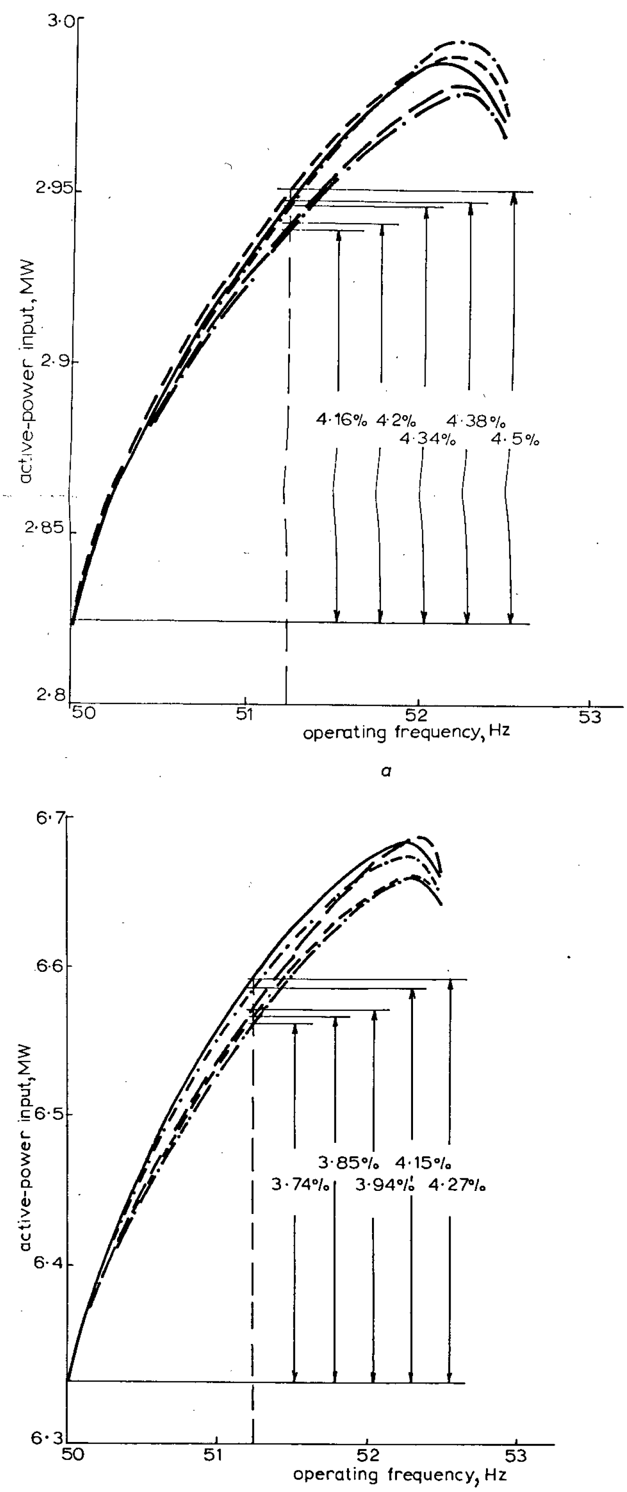

Fig. 8

Active-power input to groups of induction motors against instantaneous frequency

a Group of 3587·5 hp
—·—·—·— by equivalent circuit
——— approximate method with assumed parameters
- - - - - approximate method with known parameters
— — approximate method with 5% increase in power factor
—·— approximate method with 10% decrease in H

b Group of 8175 hp
——— by equivalent circuit
—·—·—·— by approximate method with assumed parameters
- - - - - by approximate method with known parameters
——— by approximate method with increase of 20% in slip and 10% in H
—·— by approximate method with decrease of 20% in slip and 10% in H

Percentage values indicate overall change in active power under different conditions when treated as frequency-dependent and dynamic

Details of groups

Rating	Number of motors	
	a	*b*
hp		
5	40	100
7·5	35	90
10	30	80
15	10	70
20	5	60
25	5	50
40	5	30
50	5	20
100	20	5

2.5 Assessment of reactive power

The total input reactive power is absorbed in the magnetising and leakage reactances. Considering the no-load approximate repressntation as shown in Fig. 9A, the part of the reactive power absorbed by this section is inversely proportional to the operating frequency. Fig. 9B indicates the equivalent circuit for the induction motor with the no-load section omitted. The total resistance component of the circuit depends upon the instantaneous slip of the induction motor and falls when the slip increases. If the operating frequency goes up, the instantaneous working slip rises and results in a reduction in overall resistance of the branch. As the reactance is frequency-dependent, the reactive power will go up under these conditions.

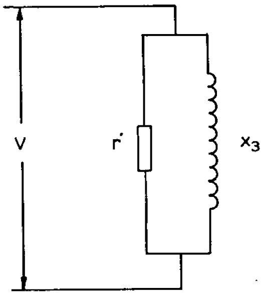

Fig. 9A
No-load section of induction-motor equivalent circuit

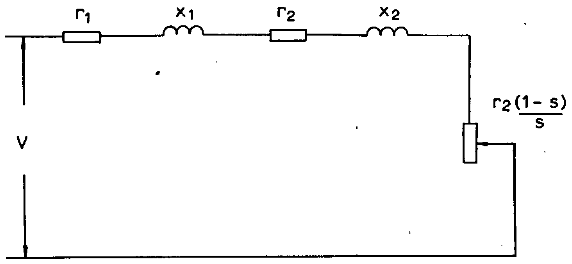

Fig. 9B
Induction-motor equivalent circuit (with no-load section omitted)

In the case of small motors, such as 1, 2, 5hp etc., the magnetising reactive power is usually predominant and results in a net reduction of overall reactive-power input under these conditions. On the other hand, the reactive power absorbed by the leakage reactance is predominant for large motors, such as 25, 50, 100hp etc., and results in a net increase of overall reactive power. However, it is very difficult to put a firm dividing line between small and large motors; e.g. two 50hp squirrel-cage induction motors supplied by the same manufacturer can behave differently with regard to reactive-power input, as shown in Fig. 10, where one machine clearly has more leakage reactance than the other.

The reactive-power input to an induction motor under disturbed conditions depends upon the following factors:

(*a*) output
(*b*) power factor
(*c*) slip
(*d*) ratio of stator leakage reactance to magnetising reactance
(*e*) ratio of rotor resistance to stator resistance.

Fig. 10 indicates the behaviour of reactive-power input to various types of motors against operating frequency.

Two alternative methods for considering reactive power are:

(i) Treat the reactive power as constant for a group of induction motors, because
  (*a*) such loads have a power factor ranging from 0·75 to 0·93; i.e. the ratio between active and reactive power varies from 1·1 to 2·5, and the change in reactive power has very little effect on the active-power demand as shown in Appendix 8.6
  (*b*) the overall change in reactive power is quite significantly less than that of active power, as shown in Fig. 10 and Table 1.

(ii) Treat the reactive power as variable.

With respect to (ii), Fig. 3 indicates the current drawn by the equivalent circuit against slip under steady-state conditions for various frequencies. From eqn. 4, $\partial I/\partial s$ at $s = 0$ is

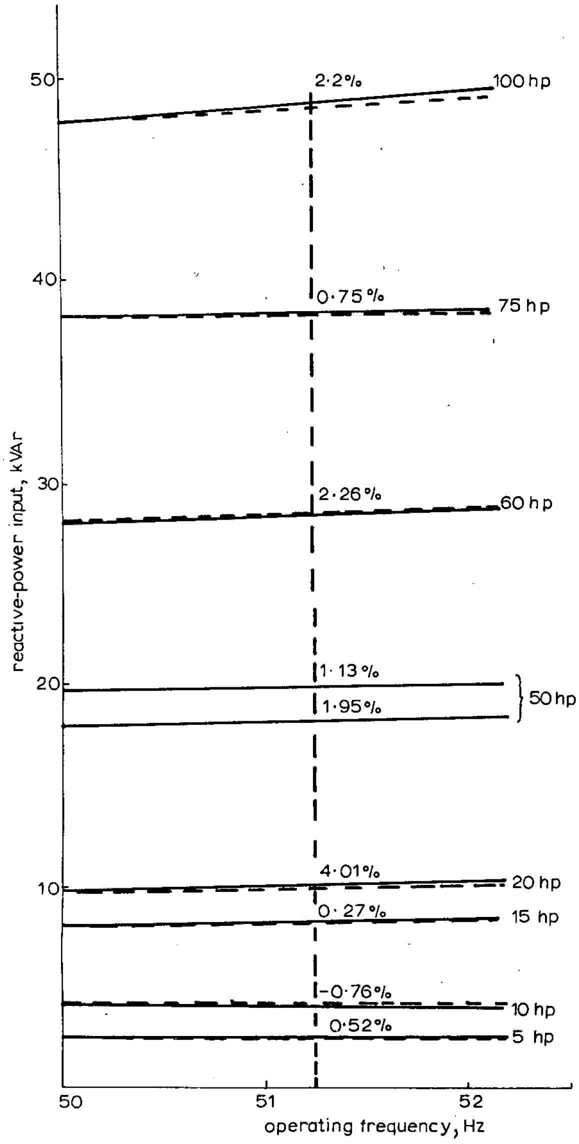

Fig. 10
Reactive-power input against operating frequency for various induction motors
——————— reactive power by equivalent circuit
- - - - - - - - - reactive power by approximate method
Percentage values indicate overall change in reactive power by equivalent circuit

independent of frequency and the characteristic is substantially linear within the full-load range, as shown; i.e. $I \propto s$, or $I = I_{0m} + Cs$, where C is a constant which depends upon the instantaneous operating frequency and is used as in Appendix 8.1. In this way, about 80% of the overall change in reactive power can be taken into account in the assessment, as indicated in Fig. 10.

3 Application to stability problems

The total instantaneous frequency at the load bus is taken as the total rate of change of phase angle of the bus voltage divided by 2π. To apply the suggested representations of induction-motor loads in transient and dynamic stability studies using a digital computer, the following approach is used here:

(*a*) Obtain an overall load balance under steady-state conditions, in conventional form.[1]
(*b*) Calculate the synchronous speed for the equivalent induction motors.
(*c*) Calculate the actual speed of the various equivalent motors, as $n_{00j} = n_{1j}(1 - s_{00j})$, where $s_{00j} = 1 \cdot 4$ (equivalent slip)$_j$ (Section 2.4).

(*d*) Calculate the various load torques.
(*e*) Calculate the core losses (represented by a fixed shunt resistance).
(*f*) Calculate the slopes of the torque/slip characteristics as

$$\alpha_j = \frac{T_{lj}}{s_{00j}}$$

(*g*) Determine the induction-motor currents for the induction-motor load as

$$I_j = \frac{(\text{induction motor MVA, p.u.})_j}{(\text{load bus voltage})_j}$$

(*h*) Determine the constants of the stator current equations as

$$C = \frac{I_j - I_{0mj}}{s_{00j}}$$

(*i*) Determine the equivalent shunt impedance for all the induction-motor loads.
(*j*) Apply the disturbance, and determine the initial conditions.
(*k*) Modify the slopes of torque/slip characteristics for all the load buses by eqn. 2 for the currently existing mean values of load bus frequencies.
(*l*) Modify the slopes of the current/slip characteristics for all the induction-motor loads by eqn. 5, for the currently appropriate value of load bus frequencies
(*m*) Calculate the coefficient A_j from the initial conditions at the beginning of the time interval Δt.
(*n*) Calculate the new instantaneous slips at the end of the time interval Δt by eqn. 3 or eqn. 34.
(*o*) Calculate the instantaneous torques developed by the equivalent induction motors at the end of the time interval Δt, as

$$T_{0j} = s_{0j}\alpha_j$$

(*p*) Calculate the instantaneous speed of the motors as

$$n_{0j} = n_{1j}(1 - s_{0j})$$

(*q*) Calculate the active-power input to the various equivalent motors as

$$P_j = \frac{T_{0j} 2\eta n_{0j}}{60\eta_j}$$

(*r*) Calculate the input current to the various equivalent motors at the end of the time interval Δt as

$$I_j = \left\{I_{0mj}\frac{f_0}{f_j} + C' s_{0j}\right\}\left\{\frac{\text{instantaneous bus voltage}}{\text{initial bus voltage}}\right\}_j$$

(*s*) Calculate the reactive-power input from current, active power and voltage.
(*t*) Represent each equivalent motor by its shunt impedance for the currently existing values of load bus voltages for the active and reactive powers obtained in steps (*q*) and (*s*).
(*u*) Calculate the driving-point and transfer admittances for the various synchronous machines.
(*v*) Calculate the instantaneous angular positions of the synchronous machines by solving their differential equations, for the time interval Δt (which is usually 0·05 s).
(*w*) Calculate the instantaneous load bus voltages and phase angles.
(*x*) Calculate the instantaneous frequency at each load bus and modify it with accelerating factor as

$$f_j^i = f_j^{i-1} + (f_j^i - f_j^{i-1}) \times \text{accelerating factor}$$

(*y*) Test for convergence of power angles of various synchronous machines to be within, say, 0·001°, and instantaneous load bus voltage and frequency to be within say 10^{-6}. If the test is not satisfied, go to step (*k*) and repeat.
(*z*) Write the final angular positions of the various synchronous machines.

The method outlined here proceeds towards a solution iteratively.

For an entirely convincing argument regarding the dynamic frequency-dependent behaviour of induction motors in power-system stability studies, the whole system should, of course, be represented accurately on a dynamic frequency-dependent basis. However this complete representation is deferred for consideration elsewhere. For purposes of the present discussion, the power system, except for the induction-motor loads, is represented at system nominal frequency. Consequently, any conclusions derived from this limited consideration are not necessarily valid to an accurate assessment of power systems, but serve to show the importance of considering induction motors on a dynamic and frequency-dependent basis.

A 4-machine problem[1] whose line diagram and circuit parameters are given in Fig. 11*a* is offered as illustrating the effects being considered. In this problem, an induction-motor load is included at bus 7 as a part of the existing 84 MW total load. Fig. 11*b* shows the swing curves for all four syn-

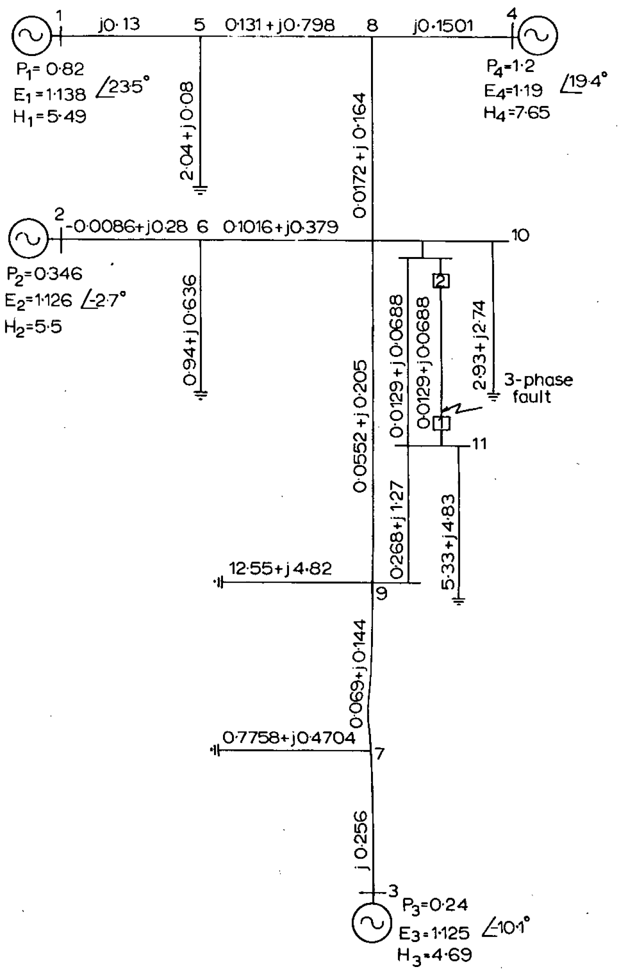

Fig. 11A

Line diagram on 100 MVA base of 4-machine power system for illustrating stability calculations

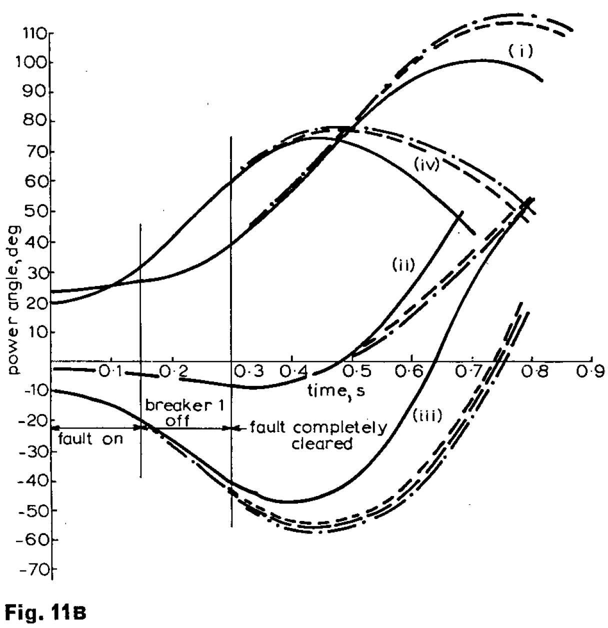

Fig. 11B

Swing curves for four machines when 14·3% of 84 MW load at bus 7 is represented as frequency-dependent and dynamic chronous machines assessed by conventional digital-computer programs (e.g. as in Reference 6), modified as indicated previously to take account of dynamic and frequency-dependent effects for the induction machines. The following cases have been plotted in Figs. 11*b* and *c*:

(i) considering the 84 MW load as passive
(ii) with 14·3% of the 84 MW (12 MW) treated as dynamic and frequency-dependent induction-motor load, being composed of small induction motors
(iii) with 40% of the 84 MW (33·6 MW) treated as in (ii).

It will be noticed that, whereas in case (ii) the system has been assessed as stable, but with less margin of stability than case (i), case (iii) is unstable. Indeed, with about 35% of the 84 MW load being treated as dynamic frequency-dependent induction-motor load, composed of small induction machines, the system just tends to instability.

In obtaining the results presented in Figs. 11*b* and *c*, adequate convergence occurred in 10 iterations when an accelerating factor of 1·35 was used for instantaneous frequency convergence (no effort has been made to optimise the time interval chosen in the example as the aim is merely to compare the various calculations).

Reasons for reduced margin of stability when the induction-motor loads are considered as dynamic and frequency-dependent include the existence of a lower assessed voltage after fault clearance than in the case of passive representation as shown in Fig. 11*d*. (The induction-motor load torque is assumed constant.)

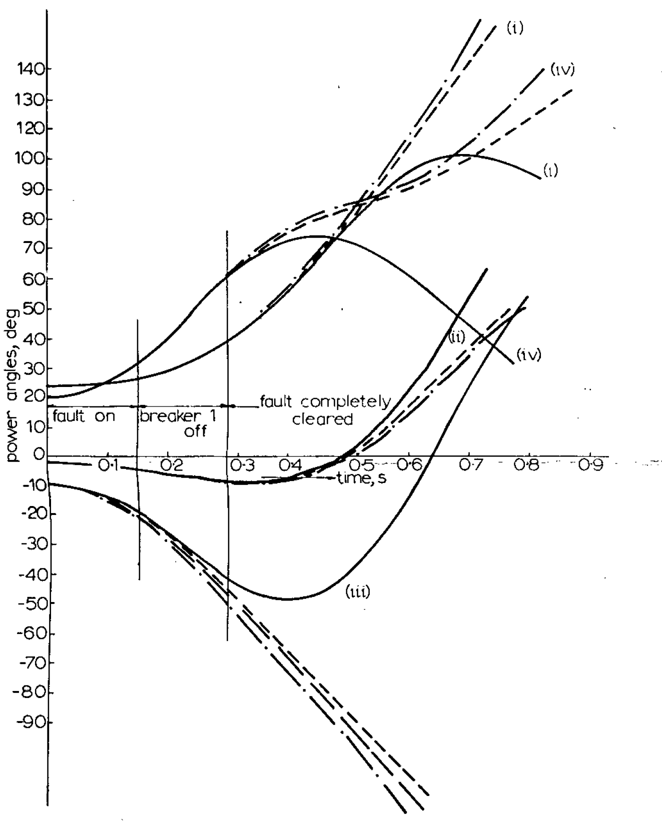

Fig. 11C
Swing curves for four machines when 40% of 84 MW load at bus 7 is represented as frequency-dependent and dynamic

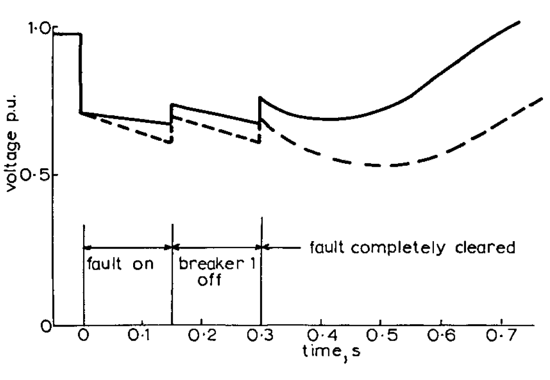

Fig. 11D
Terminal voltage at bus 7 when loads represented passively and 14·3% of 84 MW load at bus 7 is treated as frequency-dependent and dynamic

———— with passive loads
——·—— with equivalent circuits
— — — approximate method with assumed parameters
--------- approximate method with known parameters

4 Discussion

An object of the present work has been to be able to allocate induction-motor parameters (relying on conformity to type), so that this information may be useful to power-system planners to whom normally only the number of units and horsepower rating are known. By employing information from manufacturers and considerations as outlined in Appendix 8, Tables 1 and 2 have been found useful in allocating appropriate parameters. To test the order of accuracy implied by these methods, single machines and groups of machines have been studied with respect to their behaviour over assumed realistic power-system frequency excursions (as might be expected to be met during power-system electromechanical oscillations) by employing, on the one hand, accurate information and accurate method of computation, and on the other, assuming typical parameters and employing approximate methods of computation. Despite the fact that many assumptions have been made in the latter case, agreement between the two assessments (as shown in Figs. 7, 8*a* and *b*) appears reasonable. Because motor efficiencies follow a well defined pattern, active-power changes during transient conditions can be predicted considerably better than reactive-power changes, which depend on more diverse factors. Introduction of deliberate errors in appropriate parameters for the conditions of Figs. 8*a* and *b* and Table 3 gives results such that active-power changes are assessed by the approximate method of calculation to within ±5% of the true changes when the following factors have their stated limiting conditions:

(*a*) power factor within ±5% of true value
(*b*) inertia factor within ±10% of true value
(*c*) full-load slip within ±20% of true value.

Statistically, it is extremely unlikely that errors in assumed values for induction-motor parameters would be outside these tolerances, particularly on a system supplying large numbers of induction motors; results confirm this view. Single important induction machines whose parameters are known may, of course, be treated separately and accurately by using the methods proposed if the necessity arises.

Reactive power is influenced by many factors (Section 2.5). It is subject to greater errors in calculations, but changes in reactive power can normally be computed to within ±20% of the true value (Fig. 10), and further, as indicated in Appendix 8.6, change of reactive power has only a small effect on input active power.

A feature of the approximate method is the greatly reduced time for computations in relation to that required in the accurate method, as, in this latter case, each induction motor must be treated individually. In view of the reasonable degree of agreement between the two, the former method seems preferable in most cases.

To demonstrate the utility of dynamic frequency-dependent considerations of induction motors on power systems and the degree of accuracy attainable with the proposed approximate method of calculation with machine parameters assumed from typical values (in the absence of actual figures), the example of Section 3 has been presented. This shows clearly that the proposed approximate method is sufficiently accurate in relation to what can be achieved by employing true induction-motor parameter values. Furthermore, behaviour of the power system as assessed on the basis of frequency-dependent dynamic representation of induction machines differs markedly from an assessment based on passive representation of induction motors. Although no firm conclusions can be made regarding the true behaviour of the overall power system, as this has in all cases been represented in the normal fixed-frequency manner, the magnitude of the dynamic frequency-dependent effects has been highlighted, and the possible importance of representing the complete power system on a dynamic frequency-dependent basis has been underlined.

This work suggests that in other studies which have involved the behaviour of induction machines in dynamic stability studies, e.g. study of the Peace River scheme,[9] results might have differed significantly had dynamic frequency-dependent considerations been extended to all induction machines.

5 Conclusions

Methods have been suggested for treating induction motors on a dynamic frequency-dependent basis, and may be employed, respectively, in the presence or absence of knowledge regarding detailed induction-motor parameters. An approximate method, using assembled information on typical induction-motor properties, and valid even when all that is known about the induction motors on the power system is the number of units and their ratings, has been shown to be reasonably accurate and more rapid than an accurate assessment based on true induction-motor parameters.

The importance of dynamic frequency-dependent considerations for treating induction motors on power systems has been illustrated, and this, in turn, has suggested the possible need for assessing the whole power system on a dynamic frequency-dependent basis as a means to ensure closer agreement between calculated behaviour and true behaviour under disturbed conditions.

6 Acknowledgment

The author is indebted to S. Kaneff of the Department of Engineering Physics, Australian National University, for valuable discussions and guidance.

7 References

1 CRARY, S. B.: 'Power system stability', Vol. II (Wiley, 1962)
2 MORTLOCK, J. R., and HUMPHREY DAVIES, M. W.: 'Power system analysis' (Chapman and Hall, 1951)
3 RUDENBERG, R.: 'Transient performance of electric power systems' (McGraw-Hill, 1950)
4 SAY, M. G.: 'The performance and design of alternating current machines' (Pitman, 1959)
5 BRERETON, D. S., LEWIS, D. G., and YOUNG, C. C.: 'Representation of induction-motor loads during power-system stability studies', *Trans. Amer. Inst. Elect. Engrs.*, 1957, **76**, Pt. III, pp. 451–460
6 JOHNSON, D. L., and WARD, J. B.: 'The solution of power system stability problems by means of digital computers', *ibid.*, 1956, **75**, Pt. III, pp. 1321–29
7 LOCKAY, H. E., and BOLGER, R. L.: 'Effect of turbine-generator representation in system stability studies', *IEEE Trans.*, 1965, **PAS-84**, pp. 933–42
8 OLIVE, D. W.: 'New techniques for the calculation of dynamic stability', *ibid.*, 1966, **PAS-85**, pp. 767–777
9 ELLIS, H. M., HARDY, J. E., BLYTHE, A. L., and SKOOGLUND, J. W.: 'Dynamic stability study of Peace River scheme', *ibid.*, 1966, **PAS-85**, pp. 586–600
10 LAWRENSON, P. J., and STEPHENSON, J. M.: 'Note on induction motor performance with a variable-frequency supply', *Proc. IEE*, 1966, **113**, (10), pp. 1617–23
11 ASTON, F. M., and WILSON, J.: 'Planning the development of the electricity supply industry in New South Wales', *J. Instn. Engrs. Australia*, 1964, **36**, pp. 295–308

8 Appendix

8.1 Torque/slip and current/slip characteristics against frequency

Fig. 2 indicates the equivalent circuit of an induction motor. $R_1 + jX_1$ is the equivalent impedance of $r_1 + jx_1$ and

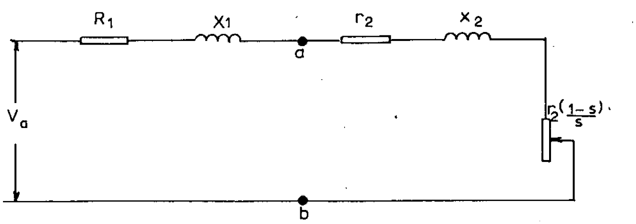

Fig. 12A
Equivalent circuit for Fig. 2 by Thévenin's theorem

x_3 in parallel, as shown in Fig. 12A. By applying Thévenin's theorem,

$$x_{11} = x_1 + x_3$$

$$V_a = V\frac{jx_3}{r_1 + jx_{11}}$$

and
$$T = \frac{mV_a^2\frac{r_2}{s}p}{2\pi f\left\{\left(R_1 + \frac{r_2}{s}\right)^2 + (X_1 + x_2)^2\left(\frac{f}{f_0}\right)\right\}} \text{ newton metre} \quad \ldots \quad (1)$$

From eqn. 1, the slope of the torque/slip characteristic at $s = 0$ is

$$\frac{\partial T}{\partial s} = \frac{mV_a^2 p}{2\pi f r_2} \quad \ldots \quad (2)$$

The current drawn by the motor is

$$I = \frac{V_a}{\sqrt{\left\{\left(R_1 + \frac{r_2}{s}\right)^2 + (X_1 + x_2)^2\left(\frac{f}{f_0}\right)^2\right\}}} \quad \ldots \quad (3)$$

From eqn. 3, the slope of the current/slip characteristic at $s = 0$ is

$$\frac{\partial I}{\partial s} = \frac{V_a}{r_2} \quad \ldots \quad (4)$$

Eqn. 4 indicates that $\partial I/\partial s$ is independent of the instantaneous operating frequency, at $s = 0$.

From the current/slip characteristic, $I = I_{0m} + Cs$, where the coefficient C is modified for instantaneous frequency as

$$C' = C\sqrt{\left\{\frac{R^2 + X^2}{R^2 + \left(\frac{f}{f_0}\right)^2 X^2}\right\}} \quad \ldots \quad (5)$$

and
$$I = I_{0m}\frac{f_0}{f} + C's$$

With the modified current and knowing the active power, the instantaneous reactive power can be calculated.

8.2 Effect of number of poles on inertia factor

From the design formula of an induction motor,[4]

$$\text{input apparent power} = \frac{1{\cdot}11 K_w \eta^2 B a_c d^2 l f_0}{\eta p \cos\phi} 10^{-3}\text{kVA} \quad \ldots \quad (6)$$

$$H = \frac{5{\cdot}48 \times 10^{-6} J n_1^2}{\text{rating in kilovoltamperes}} \text{ kWs/kVA} \quad \ldots \quad (7)$$

Assuming the rotor to be a solid cylinder,

$$J = \rho\frac{\eta d^2}{4} l \frac{d^2}{8} \text{ kgm}^2 \quad \ldots \quad (8)$$

or, from eqns. 6, 7 and 8,

$$H = K\frac{d^2 f_0}{B a_c p} \quad \ldots \quad (9)$$

where $K = 17{\cdot}7\rho\eta\cos\phi$

The diameter of the rotor depends upon the number of poles and the shape of poles, e.g. square or rectangular. In order to study the effect of number of poles on the inertia factor, assume square poles, which is the usual practice.

i.e. pole pitch = rotor length

or
$$l = \frac{nd}{2p}$$

Substituting for l in eqn. 6,

$$\text{input apparent power} \propto \frac{B a_c d^3 f_0}{p^2}$$

For fixed values of input apparent power, B, a_c and f_0,

$$\frac{d^3}{p^2} = \text{constant}$$

or $$d \propto p^{2/3} \quad . \quad . \quad . \quad . \quad (10)$$

substituting for d in eqn. 9,

$$H \propto \frac{p^{1/3}}{Ba_c} \quad . \quad . \quad . \quad . \quad (11)$$

Eqn. 11 indicates that the inertia factor will increase when the number of poles is increased for fixed values of specific magnetic and electric loading, which, in practice, depends on the $d:l$ ratio. However, because of the cube root, this increase is only a small one as the number of poles increases. From eqn. 11, there will be a reduction in inertia factor owing to increased values of B and a_c. Moreover, the inertia-factor contribution by other moving parts of the motor, such as the overhangs of the rotor winding, sliprings, shaft, cooling fan, pulley and the rotor end rings, will fall owing to reduced synchronous speed, which further reduces the overall inertia factor of the motor itself; and thus the inertia factor becomes approximately independent of the number of poles. In practice, for economic reasons of manufacturing, it is not always possible to have square poles, because the standard frame sizes will restrict the choice of rotor diameter, and consequently the inertia factor does not follow a definite law. The inertia-factor contribution of the load has been found to be at least equal to that of the driving motor, as pointed out earlier.

8.3 Assessment of equivalent parameters (full-load slip η, power factor H and I_{0m})

For an equivalent torque/slip characteristic, the overall slip for a group of induction motors is required. In Fig. 12B,

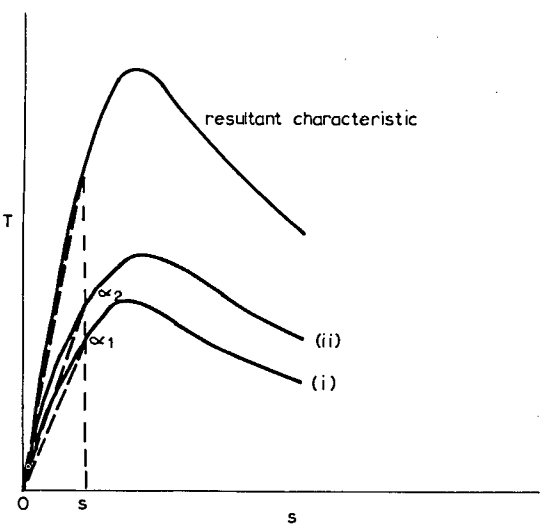

Fig. 12B
Resultant of two torque/slip characteristics

the torque/slip characteristics of two induction motors are shown as (i) and (ii). From the assumption of linearity,

$$T_1 = \alpha_1 s \text{ and } T_2 = \alpha_2 s$$

the resultant slip

$$s = \frac{T_1 + T_2}{\alpha_1 + \alpha_2} \quad . \quad . \quad . \quad . \quad (12)$$

$$T_j = \frac{746 \times 60 P_{hj}}{2\eta n_{1j}(1 - s_j)} \text{ newton metres} \quad . \quad . \quad . \quad . \quad (13)$$

For an equivalent motor, substitute eqn. 13 in 12,

$$s = \frac{\dfrac{P_{h1}}{n_{11}(1 - s_1)} + \dfrac{P_{h2}}{n_{12}(1 - s_2)}}{\dfrac{P_{h1}}{n_{11}(1 - s_1)s_1} + \dfrac{P_{h2}}{n_{12}(1 - s_2)s_2}} \quad . \quad . \quad . \quad . \quad (14)$$

For j types of motors with K_j quantities,

$$\text{equivalent slip (p.u.)} = \frac{\dfrac{K_1 P_{h1}}{n_{11}(1 - s_1)} + \dfrac{K_2 P_{h2}}{n_{12}(1 - s_2)} + \dots \dfrac{K_j P_{hj}}{n_{1j}(1 - s_j)}}{\dfrac{K_1 P_{h1}}{n_{11}(1 - s_1)s_1} + \dfrac{K_2 P_{h2}}{n_{12}(1 - s_2)s_2} + \dots \dfrac{K_j P_{hj}}{n_{1j}(1 - s_j)s_j}} \quad . \quad (15)$$

$$\text{equivalent efficiency} = \frac{\sum K_j P_{hj}}{\sum \dfrac{K_j P_{hj}}{\eta_j}} \quad . \quad . \quad . \quad . \quad (16)$$

$$\text{equivalent inertia factor} = \frac{\sum \dfrac{K_j P_{hj} H_j}{\eta_j \cos\phi_j}}{\sum \dfrac{K_j P_{hj}}{\eta_j \cos\phi_j}} \quad . \quad . \quad . \quad (17)$$

$$\text{equivalent power factor} = \frac{\sum \dfrac{K_j P_{hj}}{\eta_j}}{\sum \dfrac{K_j P_{hj}}{\eta_j \cos\phi_j}} \quad . \quad . \quad . \quad (18)$$

equivalent magnetising current (as fraction of full-load current)
$$= \frac{\sum \dfrac{K_j P_{hj} \gamma_j}{\cos\phi_j \eta_j}}{\sum \dfrac{K_j P_{hj}}{\cos\phi_j \eta_j}} \quad . \quad (19)$$

8.4 Study with equivalent circuit

From the assumption of linearity, i.e. $T = \alpha\omega$,

$$J\frac{d\omega}{dt} = \alpha\omega - T_l \quad . \quad . \quad . \quad . \quad (20)$$

(*a*) assuming T_l is constant,

$$\omega = \frac{T_l}{\alpha} + A \exp\left(\frac{\alpha}{J}\right)t \quad . \quad . \quad . \quad . \quad (21)$$

and $$A = \omega_0 - \frac{T_l}{\alpha}$$

From eqn. 21, the instantaneous angular speed is given by

$$\omega = \frac{T_l}{\alpha}\left\{1 - \exp\left(\frac{\alpha}{J}\right)t\right\} + \omega_0 \exp\left(\frac{\alpha}{J}\right)t \quad . \quad . \quad (22)$$

(*b*) Assuming $T_l = a\omega$, where a is a constant, eqn. 20 becomes

$$J\frac{d\omega}{dr} = \alpha\omega - a\omega \quad . \quad . \quad . \quad . \quad (23)$$

or $$\omega = A \exp\left(\frac{\alpha - a}{J}\right)t \quad . \quad . \quad . \quad . \quad (24)$$

and $$A = \omega_0$$

From eqn. 24, the instantaneous angular velocity of the motor,

$$\omega = \omega_0 \exp\left(\frac{\alpha - a}{J}\right)t \quad . \quad . \quad . \quad . \quad (25)$$

The instantaneous slope of the torque/speed characteristic may be determined by changing the speed slightly, e.g. by 0·01%, and determining the corresponding torque for the given instantaneous operating frequency.

In Fig. 5, the variations of torque developed by the motor at the end of each time interval are shown for various values of inertia factor. The instantaneous active-power input may be determined by the torque corresponding to points M, Q etc. from the following steps:

(i) Calculate the load torque for a given or assessed full-load slip s_{00} from the equivalent circuit.
(ii) Calculate the actual full-load speed for slip s_{00}.

(iii) Change the instantaneous frequency by one step, as mentioned earlier for the time interval of Δts (arbitrarily chosen here as 0·05 s).
(iv) Modify the equivalent-circuit reactances for the instantaneous frequency.
(v) Calculate the new synchronous speed.
(vi) Calculate the instantaneous slip at the beginning of the time interval Δt.
(vii) Determine the instantaneous torque developed by the motor corresponding to slip s from the equivalent circuit.
(viii) Determine the instantaneous slope of the torque/speed characteristic.
(ix) Determine the value of the coefficient A from the initial conditions at the beginning of the time interval Δt.
(x) Calculate the new instantaneous speed of the motor at the end of the time interval Δt from eqn. 22 or eqn. 25.
(xi) Calculate the instantaneous slip at the end of Δt, that is s_0.
(xii) Calculate the active- and reactive-power input to the equivalent circuit for slip s_0.
(xiii) Calculate the active-power input to the motor by adding core losses to the active power obtained for step (xii).

8.5 Study with proposed approximate method

From the assumption of linearity $T = \alpha s$, under steady-state conditions at the point F, $\alpha = \dfrac{T_l}{s_{00}}$.

$$s = \frac{\omega_1 - \omega}{\omega_1}$$

or
$$\frac{ds}{dt} = \frac{-1}{\omega_1}\frac{d\omega}{dt} \quad \ldots \quad (26)$$

and
$$J\frac{d\omega}{dt} = \alpha s - T_l$$

or
$$J(-\omega_1)\frac{ds}{dt} = \alpha s - T_l \quad \ldots \quad (27)$$

(a) Assuming T_l is constant, from eqn. 27, the instantaneous slip is obtained as

$$s = \frac{T_l}{\alpha} + A \exp\left(\frac{-\alpha}{J\omega_1}\right)t \quad \ldots \quad (28)$$

and
$$A = s_1 - \frac{T_l}{\alpha} \quad \ldots \quad (29)$$

The instantaneous slip (p.u.) of the motor is given by

$$s = \frac{T_l}{\alpha}\left\{1 - \exp\left(-\frac{\alpha}{J\omega_1}\right)t\right\} + s_1 \exp\left(-\frac{\alpha}{J\omega_1}\right)t \quad (30)$$

(b) Assuming $T_l = a\omega$, where a is a constant, eqn. 27 becomes

or
$$J(-\omega_1)\frac{ds}{dt} = \alpha s - a\omega_1 + a\omega_1 s \quad \ldots \quad (31)$$

or
$$s = \frac{a\omega_1}{\alpha + a\omega_1} + A \exp -\left(\frac{\alpha + a\omega_1}{J\omega_1}\right)t \quad \ldots \quad (32)$$

From eqn. 32,

$$A = s_1 - \frac{a\omega_1}{\alpha + a\omega_1} \quad \ldots \quad (33)$$

The instantaneous slip (p.u.) of the motor is given by

$$s = \frac{a\omega_1}{\alpha + a\omega_1}\left\{1 - \exp -\left(\frac{\alpha + a\omega_1}{J\omega_1}\right)t\right\} + s_1 \exp -\left(\frac{\alpha + a\omega_1}{J\omega_1}\right)t \quad (34)$$

In assessing the instantaneous active-power input to the motor, the following steps are involved:

(i) Calculate the synchronous speed of the motor for the specified number of poles.
(ii) Calculate the actual speed of the motor for a given or assumed full-load slip.
(iii) Calculate the load torque as

$$T_l = \frac{P_h 746\eta}{\omega_1(1 - s_{00})}$$

(iv) Calculate the slope of the torque/slip characteristic as

$$\alpha = \frac{T_l}{s_{00}}$$

(v) Change the frequency by one step as in Appendix 8.4.
(vi) Modify α by eqn. 2 for the instantaneous frequency.
(vii) Calculate the coefficient A and ω_1 for the instantaneous frequency from the initial conditions at the beginning of the time interval Δt from eqns. 29 and 33.
(viii) Calculate the new instantaneous slip at the end of the time interval Δt from eqn. 30 or eqn. 34.
(ix) Calculate the instantaneous torque developed by the motor at the end of Δt.
(x) Calculate the instantaneous speed of the motor at the end of Δt.
(xi) Calculate the active-power input to the motor as

$$P = \frac{T_0\omega_0}{\eta}$$

8.6 Effect of reactive power on active power

In order to see the effect of reactive-power variations on the active-power demand, an inductive load has been considered, as shown in Fig. 12c, supplied through a transmission line of impedance. $R' + jX'$ By using the approximate formula for the sending-end voltage,

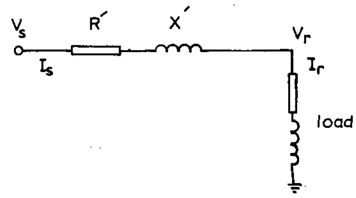

Fig. 12c
Inductive load supplied through a transmission line

$$V_s = V_r + I_r R' \cos\psi + I_r X' \sin\psi$$

Assuming I_r and V_r, the base current and voltage, respectively,

$$\frac{V_s}{V} = 1 + \underbrace{\frac{I_r R'}{V_r}\cos\psi}_{\mathrm{I}} + \underbrace{\frac{I_r X'}{V_r}\sin\psi}_{\mathrm{II}} \quad \ldots \quad (35)$$

For a fixed value of V_r, the reactive power at the receiving end is proportional to $I_r \sin\psi$. If this component falls, the sending-end voltage falls and results in a net reduction in the active-power demand at the sending end; i.e. assuming that per-unit resistance and reactance are 0·02 and 0·1, respectively. For 0·8 lagging power-factor load current of 1 p.u. at 1 p.u. voltage,

$$V_s = 1 + \underbrace{0{\cdot}02 \times 0{\cdot}8}_{\mathrm{I}} + \underbrace{0{\cdot}1 \times 0{\cdot}6}_{\mathrm{II}}$$
$$= 1{\cdot}076$$

For 1% change in reactive power at the receiving end, the term II in eqn. 35 is reduced by 1%, resulting in a 0·06% change in V_s, and the active-power demand is reduced approximately by 0·12%; whereas, for 0·9 lagging power-factor load, 1% reduction in reactive power at the receiving end will result in a 0·0872% reduction in the sending-end active-power demand.